Extending the design space of e-textile assistive Smart Environment applications

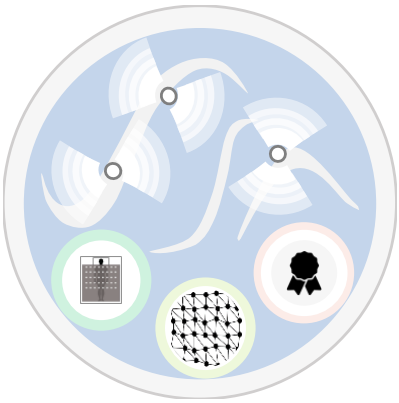

Vom Fachbereich Informatik
der Technischen Universität Darmstadt
genehmigte

DISSERTATION

zur Erlangung des akademischen Grades eines
Doktor-Ingenieurs (Dr.-Ing.)
von

M.Sc. Silvia Dorotheea Rus

geboren in Târgu Secuiesc, Rumänien

Referenten der Arbeit:	Prof. Dr. techn. Dr.-Ing. eh. Dieter W. Fellner Technische Universität Darmstadt
	Prof. Dr. Juan Carlos Augusto Middlesex University London
	Prof. Dr. Arjan Kuijper Technische Universität Darmstadt
Tag der Einreichung:	10/05/2021
Tag der mündlichen Prüfung:	30/06/2021

Darmstadt 2021

Rus, Silvia Dorotheea:
Extending the design space of e-textile assistive Smart Environment applications,
Darmstadt, Technische Universität Darmstadt,
Jahr der Veröffentlichung der Dissertation auf TUprints: 2021
Tag der mündlichen Prüfung: 30/06/2021

Erklärung zur Dissertation

Hiermit versichere ich die vorliegende Dissertation selbständig nur mit den angegebenen Quellen und Hilfsmitteln angefertigt zu haben. Alle Stellen, die aus Quellen entnommen wurden, sind als solche kenntlich gemacht. Diese Arbeit hat in gleicher oder ähnlicher Form noch keiner Prüfungsbehörde vorgelegen.

Darmstadt, den 10/05/2021 Silvia Dorotheea Rus

Abstract

The thriving field of Smart Environments has allowed computing devices to gain new capabilities and develop new interfaces, thus becoming more and more part of our lives. In many of these areas it is unthinkable to renounce to the assisting functionality such as e.g. comfort and safety functions during driving, safety functionality while working in an industrial plant, or self-optimization of daily activities with a Smartwatch.

Adults spend a lot of time on flexible surfaces such as in the office chair, in bed or in the car seat. These are crucial parts of our environments. Even though environments have become smarter with integrated computing gaining new capabilities and new interfaces, mostly rigid surfaces and objects have become smarter. In this thesis, I build on the advantages flexible and bendable surfaces have to offer and look into the creation process of assistive Smart Environment applications leveraging these surfaces. I have done this with three main contributions.

First, since most Smart Environment applications are built-in into rigid surfaces, I extend the body of knowledge by designing new assistive applications integrated in flexible surfaces such as comfortable chairs, beds, or any type of soft, flexible objects. These developed applications offer assistance e.g. through preventive functionality such as decubitus ulcer prevention while lying in bed, back pain prevention while sitting on a chair or emotion detection while detecting movements on a couch.

Second, I propose a new framework for the design process of flexible surface prototypes and its challenges of creating hardware prototypes in multiple iterations, using resources such as work time and material costs. I address this research challenge by creating a simulation framework which can be used to design applications with changing surface shape. In a first step I validate the simulation framework by building a real prototype and a simulated prototype and compare the results in terms of sensor amount and sensor placement. Furthermore, I use this developed simulation framework to analyse the influence it has on an application design if the developer is experienced or not.

Finally, since sensor capabilities play a major role during the design process, and humans come often in contact with surfaces made of fabric, I combine the integration advantages of fabric and those of capacitive proximity sensing electrodes. By conducting a multitude of capacitive proximity sensing measurements, I determine the performance of electrodes made by varying properties such as material, shape, size, pattern density, stitching type, or supporting fabric. I discuss the results from this performance evaluation and condense them into e-textile capacitive sensing electrode guidelines, applied exemplary on the use case of creating a bedsheet for breathing rate detection.

Zusammenfassung

Assistenzsysteme finden sich in den unterschiedlichsten unserer Lebensbereiche wieder. In einigen ist es schwer diese wegzudenken. Wir kommen mit ihnen unweigerlich in Berührung wie z.B. beim Autofahren, bei der Selbstoptimierung mit Hilfe der Smartwatch oder in industriellen Sicherheitsanwendungen. Sie unterstützen uns, um Komfort und Sicherheit zu bieten, durch die Beobachtung und die Kontrolle über die Situation – ggf. um unerwünschte Situationen vorzubeugen. In Deutschland verbringen Erwachsene etwa zwei Drittel ihres Tages im Bett, im Bürostuhl und im Auto - die Zeit zu Hause auf der Couch nicht mit eingerechnet. Während dieser Aktivitäten genießen wir den Komfort, den uns diese Orte bieten, insbesondere durch die weichen, anpassbaren und flexiblen Oberflächen.

Die Vorteile gekrümmter und flexibler Oberflächen finden sich in immer mehr Smarten Produkten und Anwendungen wieder, wie beispielsweise faltbare Handys, ausrollbare Fernsehen oder navigierende Jacken und Rucksäcke. Diese prominenten Beispiele aus Googles Project Jacquard wie die Levi's Jacke oder die smarten Rucksäcke von Saint Laurent und Samsonite demonstrieren, wie sich durch die zusätzliche Ausstattung von Textilien mit Sensoren, neue Möglichkeiten zur Interaktion und Bereicherung von Alltagsaktivitäten ergeben.

Die Ergonomie und Anpassbarkeit flexibler Oberflächen bieten uns maximalen Komfort und trotzdem rücken sie selten in den Fokus von Anwendungen in intelligenten Umgebungen - den Smart Environments. Einige Anwendungen nutzen die Vorteile flexibler Oberflächen, und manche statten feste Oberflächen aus, doch noch wenige nutzen die flexiblen Umgebungsoberflächen mit denen Menschen in Kontakt kommen, trotz der langen Zeit die wir uns damit umgeben. Dies rechtfertigt eine detailliertere Betrachtung und einen tieferen Einblick in den Prozess der Gestaltung von unauffälligen Assistenzanwendungen.

Diese Arbeit präsentiert Fortschritte in Bereich der flexiblen Smart Environments Anwendungen indem sie (1) durch neuartige Anwendungen das Spektrum der Assistenzanwendungen erweitert, (2) Entwicklern ein Tool zur Verfügung stellt um den Entwicklungsprozess auf der Ebene des Sensorlayouts zu unterstützen und (3) handlungsbefähigende Informationen bietet zur Integration von Sensoren mit den umgebenden Materialien.

Es gibt bislang sehr wenig Assistenzanwendungen, welche flexible Oberflächen zu intelligenten Umgebungen machen, also Flexible Smart Environments Anwendungen gestalten. Dementsprechend nutze ich dieses Potential und leiste durch folgende Beiträge eine deutliche Erweiterung des Anwendungsspektrums: (1) Dekubitus Prävention durch das Monitoring von Liegepositionen durch ein intelligentes Bettlaken, welches Liegepositionen erkennt [RGPK14, RGPK17], (2) Prävention von Rückenschmerzen durch die Erkennung von Sitzposen mittels eines intelligenten Stuhls [RBKK19b] und letztlich (3) eine Sitzposen und Emotionen erkennende Couch. Diese Beiträge beschreibe ich haupt-

sächlich in Kapitel 3. Weitere Anwendungen ziehen sich auch durch Kapitel 4 und 5 um die Anwendung dort vorgestellter Beiträge zu verdeutlichen: eine Liegepositionen erkennende Bettdecke, sowie eine ihre Form erkennende Jacke.

Assistenzanwendungen, oder Anwendungen im Bereich Mensch-Maschine-Interaktion, folgen in ihrer Entwicklung dem iterativen Prozess der Hardware- und Softwareanpassung ihrer Komponenten, um schlussendlich die erwünschte Funktionalität und die erwünschten Eigenschaften sicher zu stellen. Dieser iterative Entwicklungsprozess verbraucht viele Ressourcen wie Zeit und Arbeitskraft. In der Robotik sind bereits Simulationstools im Einsatz, welche die Ressourcennutzung optimieren. Auf ähnliche Weise können bei der Entwicklung von flexiblen Smart Environment Anwendungen solche Werkzeuge zum Einsatz kommen um Entwicklungszyklen zu verkürzen, insbesondere die kostenintensive Entwicklung von prototypischer Hardware. Zudem möchte man wissen wie gut ein System funktioniert bevor man die Hardware vollständig aufbaut und die Software dazu programmiert. Im Kapitel 4 adressiere ich diese Hürden durch folgende Beiträge: (1) die Entwicklung eines Simulationstools [RHvW*18], welches Hilfestellung leistet bei der Identifizierung der Anzahl von Sensoren und deren Platzierung um gezielte Entscheidungen zum Design der Anwendung zu treffen und (2) eine Untersuchung mit Hilfe des Simulationstools um herauszufinden inwiefern Expertise beim Entwicklungsprozess von flexiblen Smart Environment Anwendungen einen Vorteil bietet gegenüber der Anwendungsentwicklung mittels Intuition [RBKK19a].

Durch die Weiterentwicklung von Materialien eröffnen sich neue Möglichkeiten in der Sensortechnologie. Durch die Verschmelzung mit den Umgebungsmaterialien sind e-textiles besonders gut geeignet in der Umgebung des Menschen genutzt zu werden, sowie auch um Daten und Informationen zu gewinnen. Zudem können sie als Elektrode eines kapazitiven Sensors genutzt, die Präsenz von Menschen berührungslos, auf Annäherung erkennen. Die Integration von e-Textilien als Elektroden kapazitiver Sensoren in Stoffen bietet viele Herstellungsmöglichkeiten. Die strukturierte Untersuchung des Einflusses der verschiedenen Eigenschaften wurde noch nicht durchgeführt. Meine Beiträge in Kapitel 5 untersuchen die Leistungsfähigkeit der Elektroden abhängig vom Material, der Größe, der Form, des Nahtmusters, der Musterdichte, der Elastizität und der Art des Stützstoffes [RSBK15, RBKK19b]. Die Ergebnisse statten Entwickler mit einer Entscheidungsbasis aus, um für ihre Anwendung das geeignete Elektrodendesign zu gestalten.

Acknowledgements

For me writing this PhD thesis was a process. At the different stages I received support in different manners - enthusiasm, encouragements, guidance, discussions, and most importantly someone listening while I was sorting out my ideas.

I would like to express my gratitude towards Prof. Dieter W. Feller who challenged and guided me throughout my years at Fraunhofer IGD, keeping the bar of expectations high. I am very thankful that Prof. Juan Carlos Augusto agreed to evaluate this thesis. Prof. Arjan Kuijper has guided me by always asking the right question at the right time, always with constructive comments at hand, for which I am greatly thankful. He and many of my colleagues supported me actively throughout the paper writing process: Tobias Grosse-Puppendahl, Florian Kirchbuchner, Julian von Wilmsdorff, Martin Majewski, and Biying Fu. I thank my colleages for the great working atmosphere!

Reiner Wichert and Andreas Braun have persistently encouraged me from the beginning, when I was writing my first paper, until now. They have been a source of motivation the whole time. Thank you for that!

I am very grateful, that I had the opportunity to supervise many inspiring students writing their Bachelor's and Master's thesis. Their hard and diligent work considerably contributed to this thesis: Steffen Maus, Felix Hammacher, Patrick Schmitt, Nagarjun Manjunath, Dhanashree Joshi, Christian Gutjahr, Pinar Yakar, Stefan Helfmann, Zaki Ullah Chaudhry, Moritz Nottebaum, Romal Bijan, Luisa Dyroff, and Konstantin Strassheim.

My appreciation extends to all my friends for understanding my journey and their continuous encouragements. Finally, I thank my dear family, my parents for their wisdom, guidance, and their open ear whenever I needed it, my sister for her talent of putting things in another perspective and pushing me at times, and Zakaria for his never ending patience and encouragement.

Many thanks to all of you!

Contents

List of Figures

List of Tables

1. Introduction

"A smart environment is a small world where all kinds of smart devices are continuously working to make inhabitants' lives more comfortable" [CD04]. While the first term *smart* refers to intelligent and can be described as having the ability to autonomously acquire and apply information and knowledge, the second term, *environment*, refers to the surroundings of humans. This thesis brings into focus these two essential terms of the field of *Smart Environments*, for which the inhabitants and their comfort achieved by the assisting surrounding is of utmost importance.

The scientific field of *Smart Environments* has been thriving, fueled by advances in the fields of Electrical Engineering and Computer Science allowing for various capabilities of computing devices and interfaces to become part of our daily life. People are making use of these technologies and experience the limitations in terms of interaction and unobtrusiveness. To overcome these limitations, application designers are confronted with the challenge of adapting application design work-flows. It is imperative to design applications with a human-centred focus. The challenge is to combine these two main areas, such that unobtrusive, helpful systems, offering just the needed support are realized.

Unobtrusiveness is crucial, as Mark Weiser has put it in his famous article [Wei99]: "The most profound technologies are those that disappear. They weave themselves into the fabric of everyday life until they are indistinguishable from it." The goal is to seamlessly integrate sensing devices into the environment until they become a part of it. Since then, many applications were created. These are increasing the comfort of their users through equipping every-day objects with sensors, making them 'smart' e.g. smart watches, smart TVs, smart scales. What can be observed, is that most of these smart objects as part of a smart environment are rigid. They have sensors attached to them or integrated into them. However, surfaces with which users come in contact within their homes or their working environment are flexible, such as the cushion of the office chair, the couch, or the bed. This group of objects is less present, since seamlessly integrating sensors into them is a challenge. However, as sensing technologies evolve, objects which were initially rigid develop to a bendable or completely flexible form e.g. smartphones or large screen TVs. From the beginning of the TV, it has changed his form factor significantly, getting flatter and flatter and even getting curved and foldable like a poster [Ver]. These objects provide the possibility to integrate sensors into them, leveraging the flexibility and bendability of objects.

This thesis is built around two main paradigms. The first is that *advantages of flexible and bendable surfaces* must be exploited, in order to empower the Smart Environment with the ability to adequately assist its inhabitants. The second is that *principles to easily build and design applications* have to be adapted. Not only are there new technologies used to build these applications, but these technolo-

gies need to be explored in their functionality, the ability to seamlessly integrate as well by exploring possibilities of easily adapting the technology for different use cases.

1.1. Motivation

Assistive systems are widespread throughout different areas of our lives, In some of them it is hard to imagine the live without them. We come in touch with them during different activities such as while driving a car, self-monitoring through wearables such as smartwatches - towards the *Quantified Self* - or by being cared for by a robot. These assistive systems offer benefits and support through monitoring, controlling and therefore preventing undesired situations. While driving a car, the car has different functions such as parking assistance, the lane assist, speed limit detection, or emergency brake assist. These functions add comfort and safety, such that longer drives are possible in a safe manner. In contrast, smartwatches offer mostly comfort functions, such as reminders, call and messaging, activity detection or sensing of physiological parameters. Especially the activity detection offers a lot of functionalities such as step counting, sport type detection and sleep detection. These systems offer already good usability and are well integrated into the users' surroundings.

Adults in Germany spend on average 8 hours 25 min per day sleeping [Sta02], about 7 hours per working day working [Eur19] and about 1 hour commuting [Sta16]. Considering that roughly 50 % of the working population is working in offices, a significant number of people are spending their time at work sitting in the office chair, during commuting sitting in a car or train seat and at night sleeping in beds. This total of about about 16 hours and 25 minutes represents about two-thirds of a day, not counting the amount of time which we use media, where we mostly are sitting on a couch or chair.

These surfaces we come in contact with are built and adaptable to human use and maximize comfort. They have in common that they are bendable and flexible, offering us as much comfort as possible. Nonetheless, they are not at all in the focus when thinking of Smart Environment applications. Very few applications leverage these flexible surfaces. Examples are sensors attached to the body such as presented the works *iSkin* [WLB*15], *Tacttoo* [WGS18], *PhysioSkin* [NKK*20], or sensors attached to clothing such as *Zishi* [WTC*16] or *Project Jacquard* [PGF*16]. Other applications for Smart Environments equip rigid surfaces such as walls, bathtubs and furniture such as chairs and beds with sensors to enable interactions and human activity recognition [ZYH*18, WHBS16, HSH13, BFW15, DBM14]. While these are examples of smart applications worn on or around the body or integrated with rigid surfaces, the time spent surrounded by flexible surfaces justifies taking a deeper look at leveraging these and creating unobtrusive applications.

Capacitive sensors are very well suited to be integrated into materials since their sensing capability is not disturbed by hiding the sensor inside a non-conductive object. This capability makes them especially interesting for applications where humans interact with their environment and the sensors can be hidden behind materials or are an integrated part of the material itself.

The research in the area of shape changing interfaces is developing a lot, shown by the numerous applications around flexible objects, which are extended to serve as interfaces [SSH*17, WS17b].

However, flexible Smart Environment applications are scarce as presented in *Botanicus Interacticus* [PSLS12], where everyday objects like e.g. a plant's leaves are used as interaction interfaces or *RESi* creates textile interfaces such as an interactive area of a couch, which serves as remote control [PPP*18]. All these applications were specifically designed for a specific use case. In order to minimize effort when designing flexible Smart Environment applications portability of technology as well as fast prototyping are important. One would need a tool to support and be adapted to flexible Smart Environment applications. In the area of robotics, there are a few simulation tools available for creating applications, however, they are not suited for flexible use cases. Thus, a tool is needed to support and shorten the design process of flexible Smart Environment applications such as where to put the sensors, and how many sensors to use.

Additionally, to the factors such as number and location of sensors determined during the application design process, the properties of sensors are crucial. While new materials facilitate new sensing capabilities a multitude of properties has to be explored. This is also the case for e-textiles used as capacitive proximity sensing electrodes, especially since e-textiles are easily available for purchase and are especially suitable for flexible Smart Environment applications, e.g. in *FabriClick* where buttons are integrated into fabric by embroidering a 3D printed structure [GAGdR*20]. Knowledge regarding capacitive proximity sensing with e-textiles is limited, even though there are several existing applications especially in fashion and functional clothing where textile sensors are detecting postures or physiological parameters. Even though the use of e-textiles is widespread no structured analysis regarding proximity sensing performance exists.

1.2. Research Challenges

In the previous section I have outlined several gaps in the research around flexible Smart Environments applications. In order to fill-in some of these gaps, I identified three research challenges, which I address in this work. The challenges follow a top to bottom approach. The first research challenge starts from a high perspective, aiming to depict the potential of applications built-in into flexible surfaces. The second challenge is on the design process of flexible applications, addressing the need for tools to effectively design and build these types of applications. Finally, the third challenge investigates the suitability and performance of capacitive sensing electrodes for flexible Smart Environment applications. In the following, I will address and describe each research challenge in detail.

(1) New flexible Smart Environment applications: Developing assistive applications as part of flexible Smart Environments addresses a sedentary lifestyle, where we spend about two-thirds of a day sitting or lying, as well as our need for comfort and monitoring and preventing health related issues. Currently, most Smart Environment applications are built-in into rigid surfaces. Since we mostly prefer comfortable chairs, beds or any type of soft and flexible object, the first research challenge is the design of new assistive applications, leveraging these kinds of soft objects. These new applications show the potential in terms of a Smart Environment fully supporting humans - just enough to empower them.

(2) New design tools for flexible Smart Environment applications: Assistive applications, or applications in the field of HCI are generally designed by adapting hardware and software components to achieve the goals of a specific use case or set of use cases. This iterative design workflow of an application consumes resources in terms of time and money. In some fields, such as robotics, simulation tools which help minimize the effort of creating applications exist. Similarly, when developing flexible Smart Environment applications, such tools could be used to shorten the development cycles. Especially relevant is the costly development of hardware prototypes, which would need to be adjusted throughout the development cycles. A tool which would support the process of choosing the suitable number of sensors and their position in the environment would greatly advance the cause.

(3) Suitability and performance evaluation of e-textile capacitive electrodes: Capacitive sensing electrodes are especially well suited to be integrated into the humans surrounding environment. They sense their proximity and enable a plethora of applications from interaction to measuring health parameters. Even though capacitive sensors are very widespread through the ubiquitous use of smartphones, and the use of e-textiles as capacitive sensing electrodes picks up, there is a lack in knowledge around the performance influencing properties. By filling-in these gaps, the available e-textile creating techniques can be used appropriately, achieving the desired goal of balancing performance and costs.

1.3. Contributions

Following the research challenges presented in the previous section, in this section I describe how my contributions in this work address these research challenges. The field of flexible Smart Environment applications sets the context to my contributions: (1) new assistive applications; (2) a new design tool; (3) e-textile capacitive electrode performance evaluation, as illustrated in Figure 1.1. The contributions presented lead from a top view, at the level of uncovering new applications leveraging soft, flexible surfaces, to the middle level, where the design process of creating applications is supported by a sensor layout simulation tool, to the bottom level, where the specific sensor performance properties are evaluated.

(1) New flexible Smart Environment assistive applications: Humans spend two-third of their time sitting or lying on a chair, bed, or couch, which offer comfort through their soft and flexible surfaces. Most of the Smart Environment applications are embedded into rigid surfaces - ignoring the potential of applications embedded into flexible surfaces. This untapped potential has led me to creating several new assistive applications using these flexible surfaces and thus extending the design space of flexible Smart Environment assistive applications. This contribution comprises diverse prototypes in different application areas: (1) decubitus ulcer prevention by monitoring the bed posture through a bed sheet [RGPK14, RGPK17]; (2) back pain prevention by sitting posture monitoring and exercise tracking through a chair [RBKK19b]; (3) differentiating emotions through sensing movements on a couch [RBK17, RJBK18].

(2) New design tools for flexible Smart Environment applications: Similarly, as developing workflows and prototyping tools are needed to ensure the widespread application of emerging technologies

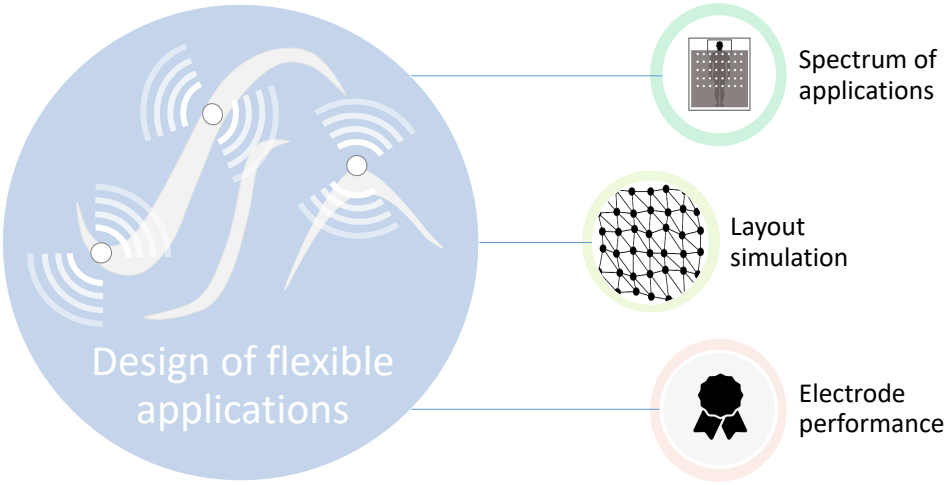

Figure 1.1.: Contributions to the field of flexible Smart Environment application design: (1) new flexible Smart Environment assistive applications; (2) new design tools for flexible Smart Environment application development; (3) performance evaluation of e-textile capacitive proximity sensing electrodes.

- flexible Smart Environment applications need these kinds of aiding tools, which help reduce the resources needed for the creation of different applications. Especially the iterative prototyping of hardware consumes resources such as development time and hardware costs. Thus, I have addressed this by contributing: (1) a simulation tool [RHvW*18], which aids in identifying the number and placement preferences for flexible Smart Environment applications, in order to ensure a specific functionality goal; (2) an investigation on whether human intuition versus human expertise results in better designs of flexible Smart Environment applications [RBKK19a].

(3) Suitability and performance evaluation of e-textile capacitive electrodes: New sensing capabilities are rendered possible by using materials with new capabilities. Such materials as e-textiles are especially well suited to be integrated into the sensing technology embedding materials. Thus, e-textiles are predetermined to be used while creating flexible Smart Environment applications. As there are many manufacturing possibilities for the electrode-material integration, the creation of these sensing and interactive surfaces has not been analysed in a structured way, with regards to the capacitive proximity sensing performance. My contributions regarding the performance evaluation in relation to electrode material, size, filling degree, stitching type, shapes, stretching, and support materials are filling-in the gaps around the performance influencing properties [RSBK15, RBKK19b]. This structured evaluation and the resulting findings support application developers in choosing the best suited electrode design for their capacitive proximity sensing application.

1.4. Structure of this work

After this initial introduction, motivation, presentation of research challenges and contributions, the rest of this work is organized in one chapter where the related works are presented, Chapter 2, and then three additional chapters, Chapters 3, 4, 5, corresponding to the three major research challenges and the according contributions presented.

CHAPTER 2 presents the essential background and related works. The background information focuses on capacitive proximity sensing, a technology which is applied in Chapter 3 and is focused on in Chapter 5, where the capacitive sensing electrode properties are evaluated. The related works present applications in the field of HCI from coarse grained to fine grained groups of applications, introducing tangible interfaces, shape changing interfaces, flexible applications in general, Smart Environment applications in general, and finally flexible Smart Environment applications.

CHAPTER 3 proposes possible assistive flexible Smart Environment applications. These leverage different technologies with a focus on capacitive proximity sensing, because it has the main advantage that it is easily embedded into materials and senses the presence of humans, which is especially good for assistive applications. These applications focus on the areas where humans spend a lot of time performing sedentary activities: (1) in bed, preventing skin ulcers by detecting the lying position; (2) sitting on the office chair, preventing back pain by supporting the user to include brakes and perform exercises on the chair; and (3) on the couch, by supporting relaxation through recognizing the emotional state by tracking lying and sitting positions.

CHAPTER 4 outlines the simulation framework for designing flexible Smart Environment applications with the focus of textile shape detection. This includes the description of the developed simulation framework, embedded in an application design workflow. This aiding tool is validated by comparing the outcome of the virtual application against the real-world prototypic implementation. The exemplary use case is the lying posture detection performed by integrating sensors in a bed cover. Furthermore, the role of intuition versus experience in application design is investigated by using the simulation framework. The designs of developers with various levels of experience are virtually evaluated.

CHAPTER 5 discusses the influencing properties on the performance of electrodes used for capacitive proximity sensing. After an initial evaluation of electrode materials and measurement modes, the performance of e-textiles in capacitive proximity sensing is discussed based on measurements performed with different influencing factor changes such as material, shape, size, pattern density or stitching type. These electrode measurements are compared and discussed. The findings are further consolidated on the exemplary use case of designing a bedsheet which can detect the breathing rate and the design of a sitting cushion for back pain prevention.

CHAPTER 6 concludes this work by summarizing the presented contributions and identifying potential areas of future research.

The three parts of the appendix include: a list of publications in Appendix A, a list of supervised Master and Bachelor theses in Appendix B, and a short CV in Appendix C.

2. Related Work

This chapter presents the background information and the relevant contributions from the state of the art of the topics handled by this thesis. First, I introduce the field of Smart Environment and assistive applications, starting from wearable applications to general assistive applications. Second, I focus on applications in the domain of HCI, which already use flexible surfaces. In these two parts I present applications using different sensor types and application domains, which lay the base to my own applications contributed in Chapter 3. In a third step, I collect the relevant work which addresses the application design process in general, which creates the basis for the contributions regarding the flexible Smart Environment application design work-flow presented in Chapter 4. Subsequently, I explain ground notions, which serve for better understanding the contributions of this thesis in Chapters 3 and 5. Finally, I will present the existing contributions on how to create and integrate capacitive sensing capabilities into flexible surfaces, showing the need of contributions presented in Chapter 5.

2.1. Smart Environments and assistive applications

The field of Human-Computer Interaction (HCI) is very vast. It includes a multitude of multidisciplinary research areas, which are concentrating on its different aspects e.g. sensorial experience, natural user interfaces, multimodal interaction, and ubiquitous computing. These research fields are overlapping and not neatly separable. They are being described using different keywords such as: Tangible User Interfaces, Wearables, Shape Changing Interfaces, Affective Computing, Smart Environments, Active and Healthy Living, Exergames, Natural Language Processing, Ambient Intelligence, etc.

In the context of this thesis most relevant is the research area of **Smart Environments**. The terms Smart Environments, Intelligent Environments, Ambient Intelligence or Assistive Technologies have in common that they refer to devices connected through a network, possibly interacting with a user, with the goal of supporting her to carry out daily activities [CD04]. These devices are usually part of the surrounding environment, embedded tightly into it e.g. Fisher et al. paint Smart Furniture as component of the Smart City [KMS*19]. This relevance of smart solutions, its drive towards ubiquity, and its early start towards market availability is presented by the state of the art described by Frischer et al. [FKM*20]. The direction of the evolution of this field is foreseen by Ben Shneiderman, who proposes in his recent work three ideas for Human-Centered Artificial Intelligence, which revolve around the balance between the level of automation and the level of human control, the shift from emulating humans to empowering them through their use of tool-like appliances and creating trustworthy systems throughout the different levels of governance [Shn20].

Due to the actual and multidisciplinary work in the field of Smart Environments, it is not possible to conclusively list all applications that are relevant to this work. Many of the applications are already collected by surveys, books or conference and journal publications such as CHI, IMWUT, Intelligent Environments, Ambient Intelligence, etc. However, in the following I will introduce relevant work from selected areas such as Physiological Aensing or Human Activity Recognition by describing exemplary applications in the domain of Smart Furniture or Wearables.

The field of **interaction with devices** has experienced a wast push by the widely adopted devices, which offer new capabilities, such as smartphones, smartwatches, virtual and augmented reality glasses, or smart speakers. The according interaction practices with the computing devices have been rethought and new alternative input methods created such that they are also accessible for people with motor impairments. For example, Cicek et al. have developed a head-tracking input mechanism for mobile devices using the front facing camera for which no calibration is needed [CDF*20]. For smartwatches, Klamka et al. have extended the limited input and output capabilities of the screen of the watch by extending the screen touch display to the strap of the watch [KHD20]. In some contexts user intent is explicitly required. Thus, Xiao et al. have proposed to use the gyroscopes of a smartphone to receive data by physically touching a emitting surface [XMH20].

Works of Yu-Chun Chen et al. and Perera et al. take the pure interaction with the device further by taking **the human and the context** in which the device is operated into account. Thus, interactions for Augmented Reality devices use the sensor data and context to reduce interaction ambiguities [Per20]. The suitability of an existing set of gestures for smart earpieces or augmented glasses is questioned by Chen et al. in order to uncover gesture design rationales and preferences [CLH*20]. In homes where the density of IoT devices is high e.g. smart lights, speakers, or mobile devices, the usage of voice as input is a natural modality. The devices are capable to interpret their context by detecting if they are targeted by a voice command or not. For this, they not only listen to the voice input, but additionally detect the direction from which the voice is coming [AKGH20]. Through this, a more intuitive speech interaction is created.

Not only the interaction with and the context of mobile devices are subject to new developments. **Capabilities of objects are extended** with the use of information and communication technology. Hence, Beruscha et al. have proposed and evaluated a multitude of input modalities for the interaction with a smart cooking pan in order to understand the preference of potential users with regard to interaction concepts [BMS20]. Objects are also created from scratch with touch sensing capabilities. Such examples are the 3D printed objects by Tejada et al. [TRBA20]. They print the objects by including tubes into the object, which lead from the surface to a central air-filled chamber where a pressure sensor is located. By touching the objects, the outlets of the tubes are blocked, resulting in characteristic air pressure patterns. Using machine learning techniques, different touch events can be pre-trained and reused every time the object is printed.

Starting from objects with new capabilities, **environments are also equipped with intelligent functionality** into Smart Environments. New alternative sensing options arise, which complement weaknesses of other sensing technologies, replacing them or fusing the information creating more robust systems. An example is an assisting system which determines the presence of humans in the room.

Common systems are based on motion sensors or cameras. Wilhelm et al. propose to leverage the monitoring of carbon dioxide levels in order to detect the presence or absence of multiple persons indoors [WJA20].

An especially interesting area of Smart Environment applications is **health monitoring**. Many of the existing works address health related issues such as sleep apnea, decubitus ulcers or physiological sensing. These applications mostly focus on **monitoring** the state the users find themselves in, by detecting their executed activities. In a second step the applications support the users by **preventing** undesired situations. I differentiate between location-bound and wearable systems. Wearable systems can be easily transported between locations and are usually worn close to the body, such as on clothing or on or even inside the body. In contrast, most location-bound systems are integrated into the surrounding environment of the users. Such common objects where users spend a lot of time are any type of seat, couch or bed, or even extending to parts of the room such as walls, sealing and floor. In the following, I will present some examples focusing on these environments.

Yousefi et al. have inspected especially decubitus ulcer prevention in hospital or home care settings, where patients are bound to the **bed** for long times. They use a pressure sensing mat, with very high resolution to track the lying posture of the bed occupant [OYF*11, YOF*11a]. A system of multiple units made of air-filled bladders are presented by Brush et al., which can adjust the pressure on its units by adjusting the degree of air and the tilt of the units [BBTR13]. Using this system Yousefi et al. implement a proof-of-concept system comprised of the pressure sensing mat in combination with the actuated modular air bladders mattress, which should serve as automatic decubitus ulcer prevention system [YOF*11b], see Figure 2.1. Similarly, Chang et al. created a sensing module based on capacitive proximity sensing. They place several modules underneath the mattress and detect the lying posture performing basic exercise tracking for rehabilitation [CCCY14].

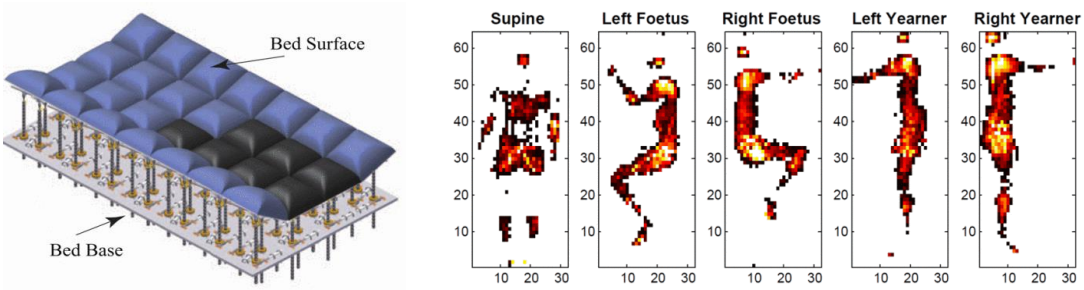

Figure 2.1.: Yousefi et al. aim at preventing decubitus ulcers by detecting pressure points and adjusting these using an bed surface of air bladders [YOF*11a, YOF*11b], ©2011 IEEE.

Chairs have also been in the focus of enhancing the environment with new capabilities. They mostly detect the sitting posture and vital signs and integrate different types of sensors into different parts of the chair. Martins et al. have similarly to Yousefi et al. equipped a chair with air bladders and pressure sensors in order to detect and correct the sitting posture by changing the amount of air in

the bladders [MLB*13]. Chairs, as well as wheelchairs, were equipped with force resistive pressure sensors. The goal was to detect the sitting posture [MLGF17, MKF*07]. From these chairs the level of interest and the level of activity of the occupant were detected [MP03]. Besides the pressure sensing chairs, which are quite accurate but costly [MLGF17], capacitive sensing was used in chairs as part of capacitive pressure sensors or for capacitive proximity sensing [BFMW15, BFW15, KLM08]. Braun et al. detected sitting postures and animated the users to do exercise during work breaks by attaching capacitive proximity sensing electrodes underneath the seat cushion, the armrests and in the backrest. *Proto-Chair* is a 3D printed morphing public space chair, with the goal to determine how chairs are used in public spaces [EYK*20]. By using an accelerometer and a gyroscope as well as a ultrasonic sensor, it detects sitting styles and the applied load to the chair.

The **couch** has been less in the focus of enhancements, compared to the works which equipped chairs and seats with sensors. Kivikunnas et al. have equipped a two-seat sofa with six foot, seat and backrest capacitive proximity sensors in form of metal foils underneath the cushions of the sofa [KSK*10]. Similarly, Grosse-Puppendahl et al. equipped a three-seat sofa with eight capacitive proximity sensors in seat, backrest and armrest [GPMB11]. Pohl et al. use the detected postures of the couch to control ambient lightning [PHK*15]. Heikkilä et al. envisage posture and activity tracking throughout the day by connecting furniture in a network composed of bed, couch and chair [HSK*13].

Besides Smart Furniture, **walls, floors, and ceilings** have also been subject to environment sensing. The main application areas are indoor localization and human activity recognition [ZSP*95a]. Indoor localization is especially targeted through pressure, capacitive and electric potential sensing systems integrated into floor tiles, the floor itself and the ceiling. Paradiso et al. have developed hexagonal pressure sensitive tiles, which are connected through a self-organizing network structure [RLFP04]. Capacitive proximity sensors were used by the floor tiles developed by Valtonen et al. [KVVV13]. They used special sensing and transmitting electrodes to assign the foot location to tiles and thus analyse the walking path. Using passive electric field sensing indoor localization was performed by a grid system integrated underneath a non-conductive floor [FKvW*17] or using a setup of six electrodes on the ceiling [GPDH*16]. A similar system to the grid electrodes underneath the floor was used to detect gait by using a capacitive pressure sensing grid inside a mat [MBBN05]. Zhang et al. have proposed a sensing wall composed of a mutual proximity sensing grid [ZYH*18]. It can detect touches and proximity of the user at close distances. By receiving the electromagnetic noise emitted by appliances, their usage and which type of appliance is used can be determined.

There are other fields of research with different denominations such as **Tangible Interaction** or **Shape-Changing Interfaces**. Each of these are dedicated to a main aspect, focusing on a specific perspective. In *Proxemic transitions*, the authors created a prototypical shape-changing table with interactive projections [GKP*17]. Gønbæk et al. define proxemic transitions as the process of changing the aspect of furniture. They design shape-changing furniture for informal workplace meetings, which intends to change the ways of collaboration in such a setting. Similarly, Perteneder et al. have proposed a **modular** set of smart furniture components. By snapping the individual building blocks together, a personalized piece of furniture is created and can be **flexibly adapted** to ones needs [PPL*20].

Another approach to create interactive objects and surfaces is to spray them with paint and add through this process the interactive aspect. Zhang et al. use electric field sensing to equip a wide variety of objects with touch sensing capabilities [ZLH17]. They spray or use a brush to coat objects with conductive material. Then they attach sending and receiving electrodes to the perimeter of the surface. By touching the object at a specific location, the electric field changes and the touch location can be detected. On a larger scale Wessely et al. create interactive surfaces by spraying functional inks with different layering techniques on **variable 3D geometries** [WSC*20]. They prepare cardboard stencils specifically adapted to the surfaces they spray and add microcontrollers in combination with conductive paint for interactivity.

Quickly reviewing the presented systems one can observe that both objects and the environment are provided with additionally functionality by adding sensing capability. In most examples, sensors are added to rigid surfaces or are hidden behind soft and flexible surfaces. The evolution of creating furniture which can change in shape and functionality offering different interaction capabilities to 3D objects, shows how relevant it is to be able to add functionality and interoperability to all kind of shapes and surfaces.

2.2. Flexible surfaces in HCI

In recent years the interest around the topic of flexible surfaces has risen. This can be also observed by the rising number of publications on and around e-textiles. Smart Clothing, Shape-Changing Interfaces, and other research areas such as Skin Interfaces are ubiquitously present. They guide the public view towards flexible surfaces such as textiles or skin, made possible by combining development of new materials and standard manufacturing methods. In the following, I will introduce relevant works showcasing different flexible materials with the focus on e-textile applications.

Flexible applications are built by integrating sensors into flexible materials, adding on top the sensor data processing and higher data processing and iterating throughout the process. Ideally, the integration is that complete that these electronic components are unobtrusive and not distinguishable from the material itself.

The integration of sensors into the flexible material can occur on different levels. Most of the existing applications are partially integrated, mostly integrated into the surface. This is due to the challenge that specific fabrication processes have to be created in order to embed sensors and material in such a way, that they cannot be distinguished from one another. One such challenge is the integration of the processing unit and the energy source used for the sensing operation. This challenge is not addressed by the topic of this thesis.

Flexible applications can be categorized further by considering the distance from the human body at which the sensors are placed. These can be placed on-body, can be worn close-by or be embedded in the environment. This thesis contributes mostly to applications in the environment and close to the body. In the following, a number of applications created on flexible surfaces at different distances from

the human body such as on skin, wearables, objects, and textiles, using a range of different sensing technologies are presented.

Most of the works focusing on **body-worn** systems offer comfort functionality through new ways of interaction or offer health related functions by monitoring physiological parameters. *SkinBot* is a wearable skin-climbing robot, which is capable of changing its position on the human body and thus capable to gather a wide range of body parameters [DHF*17]. By exchanging the sensing module, a variety of physiological parameters can be detected. Comparably, *Rovables* by Dementyev et al. presents small robots which are moving on clothes by magnetic wheels. They are autonomous and can be used to create a self-configuring interface for health sensing, decoration, interaction or displays [DKC*16, DHC*18, KAA*17]. On-body interaction combines aesthetics and functionality and is inspired by advances in material science such as **Epidermic Electronics** [YKL*13]. Kao et al. present skin-friendly tattoos. They offer different user interfaces such as touch input, output through thermochromic color and wireless communication through NFC by attaching gold-leaf **tattoos on the skin** [KHR*16, KJRC16]. Khan et al. propose a time-saving fabrication process for thin and stretchable circuits for soft interactive devices through inkjet printing [KRKS19]. This work is extended by Weigel et al. in which they leverage visual and spacial recall advantages of body landmarks [WNOS17]. The temporary tattoos they use are very elastic and can be strongly curved, offering interaction schemes such as touch, squeeze or bend and visual output. Very thin temporary tattoos are also proposed by Withana et al. [WGS18], used in virtual reality applications. Based on this work, Nittala et al present skin-worn multimodal physiological sensors by using a desktop inkjet printer and commercial materials to create ultra-thin skin-conformal electrode patches [NKK*20]. In combination with textiles they create a sports vest that tracks muscle movements and hearth rate. By attaching a temporary tattoo on the chest area the hearth rate variability is measured. The tattoo also serves as a button. By touching it, emotions are expressed by sending the signal of the live heartbeat.

Similarly, skin-adhesive techniques are used to attach wires as unobtrusively as possible to the surface of the human skin, adapting to its bends and stretches. Kao et al. propose to use zig-zag sewing techniques to manufacture on-skin wiring, demonstrating an lightweight finger tracking system [KBL18]. By incorporating circuitry through weaving directly into fabric they explore the advantages textiles offer in terms of patterns, layering and multi-material integration [SOD*20b, SOD*20a]. Choi et al. have also presented a tattoo-inspired fabrication of circuits on the body [CRK*20]. They propose to skip the step of printing the circuit using an inkjet printed, instead they created a wearable conductive-ink deposition machine. They demonstrate the printer by printing strain gauge sensors used for movement and posture detection. The resistance of the conductive paint printed to the body changes when it is being stretched or bent. Thus a curved back can be detected. When using the conductive ink as an electric connection to the human skin, the body capacitance can be sensed, and through its change when touching other objects or persons activities can be detected.

Other types of interfaces for the skin have been proposed by Hamdan et al. They use tiny springs attached to multi-layered stickers to create tactile patterns such as stretching, pressing, pulling, dragging, and expanding [HWV*19]. Using the abilities of a thermally reactive hydrogel, which is able to transition between soft and rigid states, Kao et al. proposes skin overlays for individualized foot

protection, skin armour or as carpal tunnel splint [KBKS18]. The eyelid has been also in the focus of Kao et al. as input and output interaction. They propose to use the chemical changing powders, applied as make-up on the lid, in order to reflect elevated levels of ultraviolet rays, ozone and carbon monoxide [KNRD17]. By using conductive thread within a multi-layer sticker, similar to the presented tattoos, eye-blinking is detected [LFC*20]. Very close to the body, but not glued on the body, Weigel et al. present *DeformWear*, a small input device, which can be placed at different body locations with high resolution pressure, shear and pinch deformation [WS17a].

Flexible objects which are equipped with sensors have also been part of numerous applications. Such as *FlexCase*, which is a flexible smartphone case combining flexible sensors and an e-paper display. This flip cover augments input and output capabilities of the phone such as grip sensing for mode-switching [RKP*16]. For generalized prototyping purposes with flexible, curved surfaces Dementyev et al. have developed *SensorTape*, which enables users to intuitively create applications with various sensing capabilities. Each sensing module is composed of a microcontroller and different sensors which are easily interconnectable and programmable. *PrintScreen* are flexible displays developed by Olberding et al., which are printed on flexible substrates and have unconventional shapes and can be bent, rolled, and folded [OWS14]. Folding and bending objects were created by Withana et al. They embed into thin objects printed circuits which detect the deformation [VS17a]. In *ObjectSkin* everyday objects are equipped with input and output capabilities by transferring printed electronics to the 3D object. Groeger et al. design the print in such a way that when transferring it using water-transfer the desired shape is achieved on the 3D surface [GS18]. In a similar manner, interactivity is added to 3D printed objects by adding conductive areas to curved geometry objects [GFWS19]. A laser cutter is used to very easily create interactive objects which are flexible. Specific patterns are cut into flat surfaces, such that the surface can adapt to bending and stretching. By adding conductive traces into the cut pattern, a flexible surface with sensing capabilities is created [GS19]. Through these stretchable circuits, applications such as interactive textiles or a stretchable 3D printed game controller were presented.

Not only conductive inks and 3D printed conductive materials are used to create interactive 3D deformable objects. By using conductive fabric and thread and exploiting the resistivity change with applied pressure interactive **textile interfaces** are created. *Zishi*, developed by Wang et al. and *Social Textiles*, developed by Kan et al. are two examples of textile wearables which offer functions such as rehabilitation support for the back posture or offer ice-breaking interaction possibilities [WTC*16, KFA*15]. Further, Enokibori et al. have created a vest with the role of a wearable spirometer or used e-textile to detect the bending angle of an arm [EIS*13, EM14]. For foot shape detection and dedicated shoe creation, Zhang et al. have created a stretch-flexible sock [ZCG*20]. Two textile pressure sensing systems are presented by Parzer et al.: one where two sensing surfaces are separated by a buffering surface [PSV*17, VPS18] and another system, where the buffering surface is not needed and the two orthogonal conductive surfaces are combined to one. Using the second technique has the advantage, that common manufacturing processes can be used to create the fabric. Using both techniques, the authors present different interactive prototypes in clothing such as pressure sensing socks or bending sensing sleeves [LPP*16, PSV*17], bags or furniture [PPB*16] or covers made of

resistive yarn used as pressure sensor [PPP*18]. Wu et al. present an antenna sewn out of conductive thread into fabric for touchless hand gesture detection [WQC*20]. In Project Jacquard, Poupyrev et al. present touch-sensitive textiles produced by standard manufacturing processes, which can be adapted in color, material, and thickness [PGF*16]. The conductive material is integrated into a biker jacket and backpacks. They offer the functionality to control ones smartphone and thus, assist the wearer to perform his daily activities.

Many different applications are created with e-textiles. Examples go so far as monitoring the digestion or the eating habits or creating embedded speakers. Baronetto et al. have presented a smart T-shirt with attached small microphones in the area of the abdomen. By listening to the digestion sounds the different digestion phases were differentiated with the final goal of digestion monitoring [BGF*20]. By using a wearable cap with integrated textile pressure sensors, the eating and snacking habits of persons are detected [ZL20]. With *Sonoflex*, Preindl et al. present flexible speakers embroidered exemplary into a jacket or in a beanie for notification purposes. They use an embroidery machine in combination with a thin wire to create the coils [PHP*20]. In order to create these smart textiles, many dedicated manufacturing steps are needed in combination with expert-knowledge. Klamka et al. present a rapid prototyping kit, which enables smart clothing designers to create the desired functionality more easily. For this, heat-activated adhesive materials are used which can be easily ironed-on to create custom interfaces [KDS20].

The plethora of applications is further extended by possibilities such as augmenting textiles with electrical functionality. By applying different manufacturing steps, using only readily available tools, textiles are enriched polymers applied in specific patterns enabling the dedicated creation of textiles with sensing capabilities [HPWT*20]. Using elastic therapeutic tape attached to the skin, the movement detection and touch interaction is possible. Another possibility to create smart textiles with dedicated functionality is to use stitching types to knit the desired patterns and ability into the material. Hofmann et al. have presented a fabrication tool, which generates the machine-knittable program [HMH20]

While smart clothing has been in the subject of many recent works, adding interactivity to objects or to measure physiological data or behavioural data to Smart Environments such as **Smart Furniture** is not less relevant. The textiles of which bedsheets and chairs are made of have been subject to fewer works. Liu et al. present a **bedsheet** which is capable of fine-grained pressure sensing and is flexible. It is based on e-textile material where yarn is coated with a polymer, achieving high resistivity. The bedsheet is composed of three layers: two layers of textile with conductive stripes and one e-textile polymer coated surface. By applying pressure on the two orthogonally overlapping conductive stripes, the resulting lying posture image is created [LXH*13, LHXS14]. They use this system for sleep stage detection, lying posture detection and rehabilitation exercise tracking [HLX*14]. Similarly, Onose et al. use smaller parts of textile to create pressure sensing surfaces for educational purposes, by training carers to understand where pressure applies to different body parts [OHEM18]. Their sensing system is created by crossing conductive fibers. By measuring the capacitance change only one textile layer is needed. Onose et al. also add this textile to certain pressure prone surfaces in clothing [OEM17].

In addition to beds, **chairs** were also equipped with force sensors and binary sensors made of conductive fabric, such as the lounge chair by Hurst et al. [HZAF05]. According to the time of day, and

detected sitting posture, the lounge chair provides feedback and alerts [FDZ*05]. Conductive fabric electrodes are placed on the armrests, where occupants would likely expose their skin, and were used to measure the hearth rate, like through an EKG [GSB14]. Additionally, strip force sensors were used to detect the respiration rate at the back of the chair.

2.3. Designing process of applications

The design process of application is described throughout the related work from different perspectives. Tränkler et al. have described a general sensing system design process, which is very close to the manufacturing process [TR15]. Zhang et al. present a paradigm on how to design sensing systems in the domain of health monitoring [ZA05]. Choosing an even more specific domain, Hesselmann et al. describe an iterative process for designing gesture-based interactive surfaces [HB10b]. Cherenack et al. describe the creation process of smart textiles in terms of hierarchy of a setup [CvP12], while Steimle et al. describe challenges and their fabrication pipeline for on-body sensors [NS16].

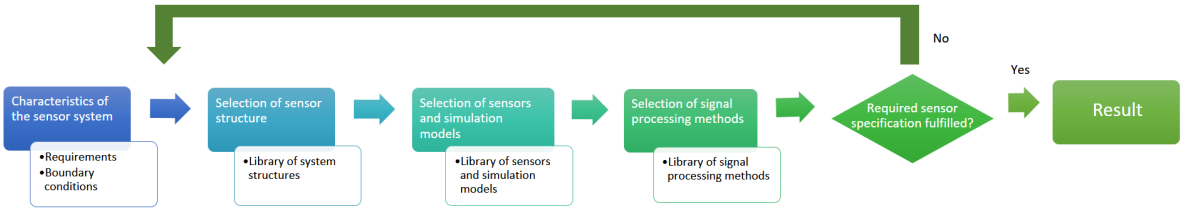

Figure 2.2.: Design concept for sensors and sensor systems after Tränkler et al. [TR15].

Figure 2.2 describes the sensor and sensor system design process presented by Tränkler et al. in four steps, where three of them are iteratively repeated. The design of a sensor system starts with the requirements collection and the boundary conditions. The specifications of the sensors system are deducted from these. The three next steps relate to the creation of the sensing system concept. Different sensing structures, sensors, simulation models and signal processing models can be selected. In the feasibility study rough system structures are evaluated and tested in their suitability. In the next step different technology aspects and signal processing methods are analysed through simulation towards the system performance. Finally, if the sensor system properties optimally suit the requirements and boundary conditions then the design process ends.

Zhang et al. consider the sensing systems they design to be "highly complex, comprising intertwined engineering, natural and human elements" [ZA05]. They see system design as steps towards controlling various uncertainty mechanisms such as lack of insight into the application problem, data capturing, experimental uncertainty and maximizing benefit vs. cost. Figure 2.3 (left) shows the paradigm for a health monitoring system with the seven influencing uncertainties directly affecting the choices regarding sensor type, sensor density, sensor location, communication and network architecture.

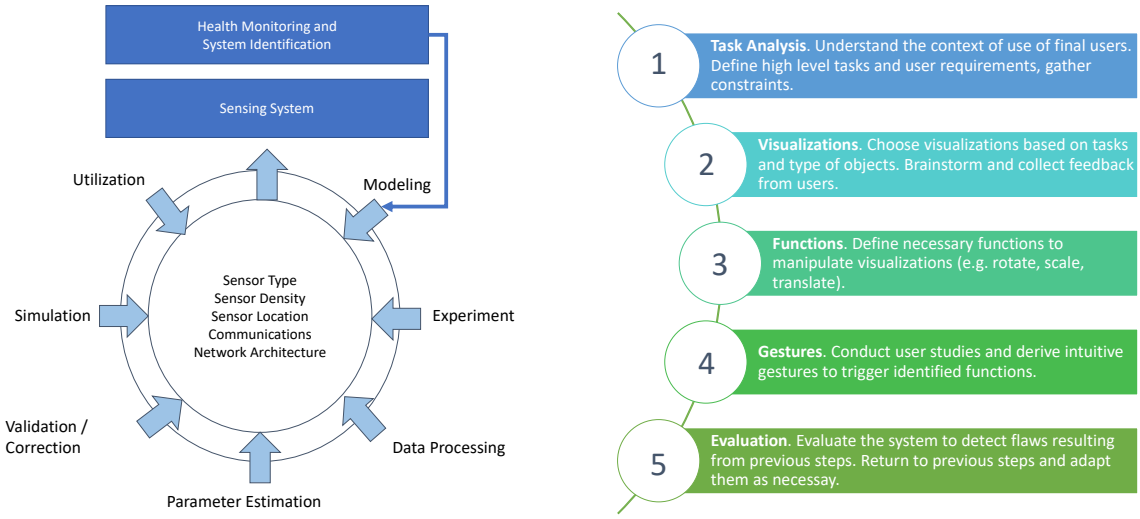

Figure 2.3.: Health sensor system design paradigm by Zhang et al. [ZA05], (left); Design concept for gesture-based interactive surfaces after Hesselmann et al. [HB10b], (right).

Figure 2.3 (right) shows a five-step process formalizing the design process of gesture-cased, visual interfaces for interactive surfaces. These are highly visual systems, which are controlled by touches or gestures on surfaces. The first step is the task analysis, which encompasses the formulation of the user's goal and defining the requirements and constraints. In a second step the technically suitable visualizations are chosen and gather feedback from final users. Usually the visualizations are not static. For this purpose, the needed functions to manipulate the visualizations are defined and derived in a user-centric process. These defined functions are triggered by gestures, which were defined through user studies. Finally, the complete system is evaluated in order to detect flaws. If one flaw is detected, the previous steps are repeated.

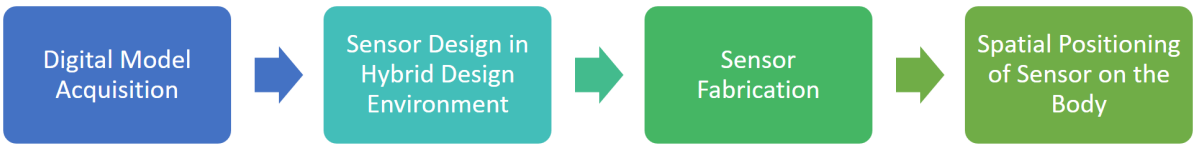

Figure 2.4.: Fabrication pipeline for on-body sensors by Steimle et al. [NS16].

Even more specifically, Steimle et al. have set up a workflow for the creation of on-body sensors [NS16]. Their work-flow is made of four steps: digital model acquisition, sensor design in hybrid design environment, sensor fabrication and spatial positioning of the sensor on the body. These steps are shown in Figure 2.4. The digital model acquisition refers to acquiring the individual body geometry. On this body part, the design of the interface can be directly sketched, and more intricate designs can be

performed on 3D digital models. After this hybrid design the sensor is created by automatically creating the masks for screen printing. Finally, the sensors are applied on the body. During these fabrication steps, several challenges have to be overcome such as a robust and accurate geometry acquisition, sketching and designing for different body characteristics and precise spatial positioning of the sensors.

These four different approaches of designing a sensor system have commonalities, meaning that the four step on-body sensor pipeline can be mapped to some of the steps presented in the design concept of Tränkler et al., e.g. the digital model acquisition serves to gather a set of boundary constraints, setting the characteristics of the sensor system. Equivalently, the task analysis from the design concept of the gesture-based interactive surface references the requirements, the constraints as well as the context of use. Most of these models also have in common, that they explicitly state that an iterative process is foreseen.

For the area of Smart Environments, or for Ambient Sensing, there are no specific design processes to be found to the best of my knowledge. Moreover, the general design approaches by Tränkler et al. and Zhang et al. can be applied to the specific field of smart environments, and a process can be created dedicated to technologies suitable for creating applications utilizing flexible surfaces.

2.4. Capacitive sensing and flexible surfaces

The applications presented in Section 2.2 show the variety and the relevance of applications in which humans interact with flexible surfaces or objects. Different kind of sensing principles are used such as acceleration, resistance, time of flight etc.

In this variety of sensing principles, electric field sensing, more specifically capacitive sensing, was used in multiple instances to add touch detection capabilities. This sensing principle offers multiple advantages in the possibilities to design flexible applications. Especially the ability to measure the human presence remotely, the possibility to separate the electrode from the sensor circuits as well as remaining hidden behind non-conductive surfaces facilitates many possible flexible applications.

In the following I will explain the working principle and the features of electrical field sensing. Subsequently, I will present how related works leverage capacitive sensing when creating applications using flexible surfaces. Finally, I present the works focusing on presenting guidelines on how to design capacitive sensing electrodes.

2.4.1. Capacitive sensing background

Disappearing in our environment and into devices we use every day, capacitive sensing has become ubiquitous. Embedded into touchscreens and touchpads we use them daily while operating laptops, phones or tables. Even more hidden, they surround us in form of buttons, such as in elevator buttons, or consumer electronics devices.

2.4.1.1. Capacitive sensing in nature

In nature the principle of detecting electrical potential changes developed in animals which were exposed to harsh environments [Hei77]. Such a limitation is for example the lack of sunlight which occurs in deep waters on in water in caves. There are species of fish, which have learned to sense the capacitive coupling to their environment by creating their own electric field [BLL06]. They produce electric signals with a specialized electric organ and sense it through the epidermal electroreceptor organs.

In Figure 2.5 the electric organ is placed at the back of the fish and the epidermal electroreceptor organs are distributed over almost the entire body surface. This electric system is involved in different behavioral functions: prey-hunting, passive electro-location, active electrolocation, species recognition, and intraspecific communication. Passive electrolocation is used by fish which do not have electric organs, however, are able to perceive electric fields through their electroreceptors. Thus, "sharks and ray can make well-aimed responses toward live prey, such as flatfish, buried in sand and invisible to the predator" [Nel05].

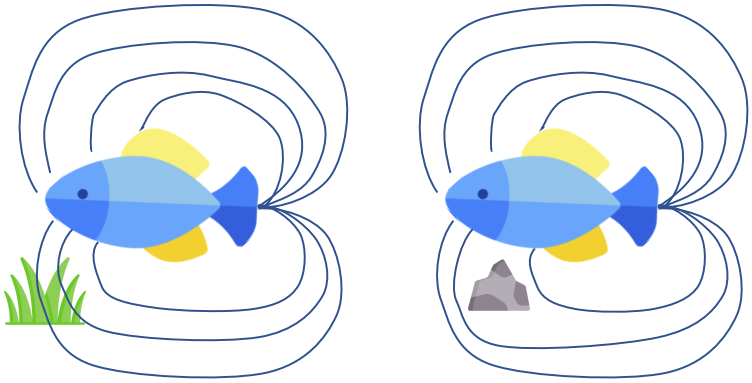

Figure 2.5.: Electric field distortions caused by water plants or rocks. Water plants are good conductors, thus electric field lines are dense. Rocks are isolators and reduce the electric field lines. [vdE99, Nel05], designed using resources from Flaticon.com.

For active electrolocation an electric organ discharge is performed. It is characterized by its voltage waveforms between the electrodes on the head and tail of the fish. "Objects are detected by analyzing the electric images which they project onto the animal's electroreceptive skin surface. Electric images depend on size, distance, shape, and material of objects and on the morphology of the electric organ and the fish's body" [vdE06].

2.4.1.2. Capacitive sensing in history

While animals have evolved organs for capacitive sensing for millions of years, human exploitation started about a hundred of years ago. Using a string electrometer (current measuring device) the motion of a beating hearth of a frog was analyzed by Cremer in 1907 [Cre07]. By placing the hearth between two capacitor plates, its capacitance change was observed while the hearth was moving. A few years later in 1920, Leon Theremin, a Russian physicist, invented the first electronic music instrument, the *Theremin*. It consists of two capacitive electrodes which create a field with the surrounding environment. When an interpreter disturbs the electric field by introducing his hands into the electric field between electrode and environment, the pitch and the volume are controlled. One of the electrodes is connected to a circuit influencing sound volume, while the other is connected to a circuit which changes the frequency of the sound [GM00]. When playing it, it is important to keep the body still, since by its larger size, it has a big influence on the measured capacitance.

Later, capacitive sensing gained a foothold in the area of engineering, used for application such as measuring distance, pressure, acceleration, force, etc. The break-through of capacitive sensors happened with the widespread use of smartphones. Their screen is made of a capacitive touch surface, a development of which the foundation was laid by engineers at CERN in 1973. They created a capacitive touch screen [BS73]. This was comprised of thin 80 μ wide conductors forming capacitors placed on a transparent substrate. The screen was manufactured with at that time standard printing techniques. The main innovation of this tablet is that it is capable to sense multiple contact points at a time, while it is also sensitive to the pressure executed on the surface of the tablet. The tablet was demonstrated controlling multiple virtual devices by use of templates placed over the tablet [LBS85].

These approaches gained much interest, and in 1995 Zimmermann et al. have introduced capacitive sensing into the area of HCI [ZSP*95a]. They proposed interaction with the environment which goes beyond touch sensing. A non-contact sensor was created by setting up an electric dipole field between an oscillating electrode and the ground to which it couples. Introducing a hand into this field disturbs it and makes at at the same time detectable. This way they created a person-sensing room and a finger pointing mouse, where the pointing finger does not need to be in contact with the screen.

2.4.1.3. Physical principles of capacitive sensing

A capacitor is generally composed of two electrodes separated by a dielectric material. The electrodes are usually referring to capacitor plates, however, they are conductive material which can come in various forms such as transparent foils, wires or conductive textile. The basic natural law to which capacitive sensing relates is Coulomb's law. It states that two charges Q_1 and Q_2 surrounded by dielectric material, separated by a distance d exert a force along the line connecting the charges. Depending on the sign of their charge the forces will attract or repel the charges.

$$F = \frac{Q_1 Q_2}{4\pi\varepsilon_0\varepsilon_r r^2}$$

The capacitance C measures the number of electrons, the charge Q when an electric potential V is applied to two electrodes [GPHC*17].

$$C = \frac{Q}{V}$$

The electric field E is the gradient of the voltage V. A current flows when an electric field is produced inside a material. This current is the result of adding the conduction current density J_c and the displacement current density J_d. The current density for conduction current is

$$J_c = \sigma E$$

where σ is the conductivity. In a good capacitor the dielectric material has a high resistance, thus the conduction current J_c is approximately zero. Due to this, the 'charge is transferred by a reorientation of polar molecules causing' a displacement current [Bax97].

$$J_d = \frac{\partial D}{\partial t} = \frac{\partial}{\partial t}(\varepsilon_0 \varepsilon_r E)$$

The direction of the displacement current is the same as of the electric field. And by applying Gauss' law, the 'total flow of charge due to displacement current through a surface is found by integrating D over that surface' [Bax97].

$$\Psi = \int_{surf} D ds$$

ds represents the elementary area and D the flux density normal to ds. This means that 'the total displacement of electric flux through any closed surface which encloses charges is equal to the amount of charges enclosed', since the alignment of the molecules to the electric field represents the displacement. The displacement charge Ψ is the total of the charges on the electrodes and the charge displaced in the polar molecules of a dielectric in the electric field.

For a parallel plate capacitor to which a voltage V is applied, the total flux Ψ is the amount charge which is proportional to the capacitance C and the applied voltage V.

$$\Psi = Q = CV$$

The 'total charge inside the surface is equal to the total displacement flux D times the area of the surface S ' [Bax97].

$$C = \frac{\varepsilon_0 \varepsilon_r S}{d}$$

2.4.1.4. Active vs. passive sensing techniques

Sensing techniques can be grouped into *active* or *passive* measurement techniques. The initial categories described by Zimmerman et al. have been extended by the current body of work towards the addition of passive sensing techniques [ZSP*95b]. However, most of the capacitive sensing systems are based on active sensing such as capacitive buttons or touchscreens.

The difference between active and passive capacitive sensing is that the active sensing systems must *actively* generate an electric field, while *passive* sensing systems use already existing electric fields, which are present or are generated in the environment [GPHC*17]. Such fields could be generated by electronic appliances, power lines or by users which generate fields by the triboelectric effect.

The advantages of passive systems are a lower power consumption and larger sensing distances. With larger sensing distances also the drawbacks become visible, since the sensors are more susceptible to any environment changes. A sensing system which has to generate an electric field and then measure will consume more power than a system which simply measures the voltage induced by a current.

Active capacitive sensors need to actively generate an as precise as possible constant current. This current flows through the resistance connected to the electrode, charging the electrode. An as precise timer as possible is needed to measure the time it takes to charge the electrode with the constant generated current.

In the case of a passive system a very small current is induced by bringing a charged object into the vicinity of the electrode. The electrode will charge itself with the opposite charge, resulting in a very small current. This current flows trough a very large resistance. The sensor measures the voltage drop over this large resistance.

The advantages and disadvantages of active and passive systems derive mostly from the possibilities given by the sensor setups. In theory a passive and an active system can have the same sensing range, since the principle of charged grounded objects coupling themselves to an electrode is the same. The measurement principle is different, and this brings the limitations. An active sensor needs multiple very precise components such as a precisely constant current and a precise timer. The passive sensor needs only a big resistance and a precise voltage measurement. Due to these differences the active capacitive sensors are designed such as to have less sensing range and the passive sensors can have larger sensing ranges. With larger sensing ranges and no possibility of measuring in a given direction, the sensor is susceptible to many environment changes, which is a disadvantage which has to be counted in, when designing a system.

2.4.1.5. Operating modes

In order to categorize into different sensing modes, the relation between the two components, the human body and the electrodes, needs to be analyzed. Figure 2.6 shows these two components and the capacitances between them. Depending on which of the capacitances is measured, different sensing modes can be defined. This lumped circuit model also highlights the fact that not only the electrodes and the human body influence the measurements, but that capacitances to the whole environment are built up, such as chairs, floor and have to be taken into account [SWD*98]. The conductivity of these objects plays an important role when in order to set up a sensing system which measures the intended interactions. The human body has a very good conductivity, being composed of a large percentage of water. By mostly standing on the ground, the human body is also very well coupled to the ground of the environment. Environmental objects such as tables, beds have a lower conductivity, making them less easy to detect.

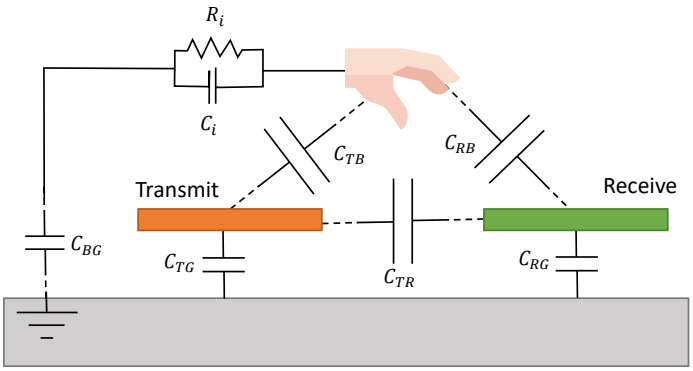

Figure 2.6.: Lumped circuit model showing the capacitance coupling not only to the desired measurement of the distance to the human body, but also the capacitance to the surrounding environment [GPHC*17], designed using resources from Flaticon.com.

The lumped circuit model, see Figure 2.6, shows a scenario where the distance to the electrodes T (transmit) and R (receive) of a human body part B is detected. The receiving electrode is optional and can be omitted. The two electrodes build up electric fields to their surroundings, resulting in the capacitances C_{TB}, C_{RB}, C_{TG}, C_{RG}, and C_{TR}. The capacitance C_{BG} represents the coupling of the human body to the ground and C_i and R_i represent the internal resistance and the internal capacitance of the human body. Generally, R_i is low and smaller than $1k\Omega$. The capacitances C_{TB} and C_{RB} are static capacitances which reflect the electrode coupling to the ground in a static setting. These capacitances are called *parasitic capacitance* and should be minimized since they can influence the sensitivity of the system. There are different electrode setups and measurement modes for capacitive proximity sensing.

Loading mode relies on a single electrode being charged and uncharged. This results in an oscillating field which is changed by moving a body part into the field. The body part absorbs some of the displacement current which flows to the ground. By changing the distance to the electrode, the amount of displacement current which flows to the ground changes C_{TB} and the sensor can detect the distance of the body part. This operation mode is the most widespread in the body of work and is often designated as *self-capacitance mode*. This is due to its simple setup. The loading mode uses only one electrode which serves as transmit and receive electrode at once. Since in most systems not only one capacitive sensor is needed, using one electrode per sensor is an advantage, making the system more clearly arranged. In passive capacitive sensing, there is no equivalent existing setup, since in passive sensing the electric field is only measured, meaning one single receiving electrode is needed at the sensing system.

In **shunt mode** two distinct electrodes are needed, a transmitting and a receiving electrode. With two electrodes there is a capacitive coupling between them, C_{TR}. When the human body gets closer to the receiving electrode, it shunts more of the displacement current between transmit and receive electrode away to the ground. In this manner, the proximity to the body part can be detected.

In active capacitive sensing it is most prominently used in capacitive touch screens or panels. A grid of electrodes is used to identify the location of the body part, such as on a touchpad of a laptop. In the case of a grid some of the wires are transmit electrodes and the others, overlaying the transmit electrodes are receiving electrodes. When the hand or finger of the touchpad user gets into the proximity of such a transmit-receive crossing, the capacitive coupling between the two wires is influenced by changing the capacitance. This measurement mode is also often designated as *mutual capacitance*. In passive capacitive sensing this is the most commonly used setup. The receiving electrode is part of the sensing system and the transmit electrode represents the environment generating the electric field.

Transmit mode and receive mode are similar to shunt mode. Both use two electrodes as in shunt mode. The difference is that in transmit mode the body is very close to the transmit electrode. Respectively in receive mode the body is very close to the receiving electrode. For each of these cases the capacitance between transmit electrode and body C_{TB} is much higher than the capacitance between receive electrode and body C_{RB} and the capacitance between transmit and receive electrode C_{TR}. Similarly, in receive mode the capacitance between receiver electrode and body C_{RB} is much higher than the capacitance between transmit electrode and body C_{TB} and the capacitance between transmit and receive electrode C_{TR}. Essentially in these measurement modes the body becomes an extension of one of the electrodes, the receive or the transmit electrode.

2.4.1.6. Limits of proximity detection

Our modern environments are equipped with many sources of electric fields, such as AC-powered instruments. These extraneous electric fields act as a source of noise to the electric fields, which the capacitive proximity detectors should measure.

In contrast to the ground in textbooks, the ground in real life is not a ‘perfectly conducting infinite plane’ [Bax97].

Shielding has the task to preserve a good Signal to Noise Ratio (SNR). In these constraints the signal is the electric field changes which we want to measure which are the result of a specific action, such as a body approaching. However, the capacitance is measured in all directions.

A good example is activity detection at a desk. We want to detect the hand movements on top of the desk. For this, capacitive sensors would be mounted underneath the tabletop of the desk. This would measure the movements on top of the desk, however, if a person sat down at that desk, the movements of the legs would exert a much more significant signal change that the arms on top of the desk. This results in the saturation of the detectable signal. The SNR would be very small, the hand movements not extractable from the signal. By shielding, using for example a shielding reference electrode, the electrode in the direction of the undesired signal, such as the legs, the signal strength of the desired signal can be detected.

‘The dielectric constant of dry air at $0C$ and 760 mm pressure is 1.000590, and that of gaseous water (steam) at $110C$ is 1.00785’ [Bax97]. This shows that the effects of temperature and humidity are minimal and can be considered to be neglected. However, it is still difficult to measure absolute

capacitance accurately since 'stray capacitances must be considered'. Shielding and grounding ensure that the variation of capacitance 'due to dielectric constant variation and fringe field can usually be ignored' [Bax97].

2.4.2. Capacitive sensing in flexible Smart Environments

Between people, their devices and conductive objects in the environment, capacitance continuously exists. The position and proximity of users can be computed resulting in a variety of applications. The limitations through noise and stray capacitive coupling may lead to ambiguous results. One of the challenges in the field of capacitive sensing is to enable flexible and stretchable applications [GPHC*17].

The integration of capacitive sensing, more specifically capacitive touch sensors into clothing was explored by Orth et al. in 1998, where they present a *Musical Jacket* with an embroidered keypad and a *Firefly Dress* where conductive fabric is used for power distribution [OPC98]. Baldwin et al. have used capacitive sensing through fabric integrated into a pair of trousers for gait analysis [BBR*15]. Singh et al. have used capacitive proximity sensing pads to create an accessible user interfaces through gestures [SNR*15]. The application domain of adding an touch interface to clothing is very prominent and has been subject to many works [HSP*08, HT13, PGF*16, SKBH18]. Capacitive touch sensing has been added all kinds of clothes such as belts [DHR15], trousers [DWHR17], shoes [PMBA04, HMBU15], gloves [HSP*08], jackets [PGF*16], shirts [HT13] etc.

Advancements in creating new materials through further embedding of conductive threads and yarns into fabric has facilitated a variety of applications and fabric interfaces. Examples are the integration of flexible circuits into regular fabric [OTKB19], or the creation of a braid with integrated conductive thread [OMPD*18, OSM20]. Using this braided e-textile cord, interaction schemes were investigated as casual discrete gestures. Pin-Sung et al. use a single thread for touch localization along this thread [KSW*20]. Further, Wu et al. have developed *ZebraSense*, a woven touch sensor, which can differentiate on which side it is touched. By integrating some conductive threads on one side and others on the other side, the textile is used as isolation and spacer in order to differentiate the side on which the direct touch is achieved [WFG*20]. Through layering of different conductive yarns, electrical circuits are directly woven into materials. Sun et al. explore possibilities for on-skin interfaces by weaving thermochromic displays or capacitive touch sensors [SOD*20b]. Skin interfaces, with capacitive touch capability are presented by Kao et al. [KHR*16]. They build skin-friendly temporary tattoos made of gold-leaf which are both functional and aesthetic. Similarly, in *Tacttoo* very thin, temporary tattoos enable tactile output and touch input when enriched with a PEDOT layer. The electrodes are created using screen printing and laser patterning [WGS18].

By leveraging the capacitive coupling between cloths and the wearer, information can be transmitted across the skin of the wearer. Wolling et al. propose to communicate by capacitive coupling, where the wearers' body transmits the signal from one unit to another through the body, the feedback from the second unit is transmitted through the conductive fabric connecting the two units [WSRVL17]. The conductive fabric has the advantage, that it can replace the usually erratic coupling to the environment ground.

Flexible, bendable 3D objects are often equipped with capacitive touch and sometimes capacitive proximity sensing capabilities. Pourjafarian et al. provide a prototyping technique to equip objects and fabrics with multi-touch input [PWPS19]. By attaching a grid with sending and receiving electrodes, using a shape which can adapt to curved objects, touch capabilities are added to drawings on paper, sleeves or other everyday objects. In the same grid layout, diamond shaped conductive fabric is attached to regular fabric using an iron-on adhesive. As a result, Wu et al. present table clothes or pockets which are able to detect conductive objects and classify which object it is [WTZ*20].

Printed electronics and flexible printed circuit boards can be used to create further touch or proximity sensing interfaces. Using printed circuits, smallest surfaces can be enhanced with interactive capabilities. *NailO* presents a sticker-like nail interface, which can detect gestures through capacitive touch sensing [KDPS15]. Arimatsu et al. use touch and proximity sensing capabilities for hand pose estimation for hand-held devices [AM20]. They use 62 electrodes to measure the proximity using loading mode. Designs of printed electrodes for hover and touch detection are presented by Withana et al. [WS17b]. Using flexible printed circuit stripes with a sensing and a receiving electrode, objects can be enhanced to sense their deformation. Through the bending, the capacitance changes between the sending and receiving stripe, resulting in a bending profile [SD20].

Objects are equipped with sensing capabilities beginning at the very first step of their creation. *Capricate* is a tool used to design 3D-printed objects with integrated capacitive touch capabilities [SKB*15]. These objects can be used as exemplary as personalized object for 2-factor authentication for screens of mobile devices [MSZ*20]. By creating and aligning conductive and non-conductive areas and a flexible infill pattern, different mechanisms such as pressing, squeezing, and bending of the object can be detected [SSH*17]. Takahashi et al. have combined the flexibility of textiles with 3D-printing and print textiles with similar flexibility and a set of woven patterns. By adding conductive material which form circuits and small electronics to the printed object, an interactive and flexible object can be created [TK19].

2.4.3. Properties of capacitive electrodes in flexible applications

In the book *Capacitive Sensors* by Larry Baxter capacitive sensing and electrode properties are described in order to guide the design process of capacitive electrodes [Bax97]. However, it does not address flexible, bendable capacitive electrodes. Smart Environments find their way into people's life, assisting them and making it more comfortable. Embedding sensing capabilities into deformable, bendable, flexible surfaces with which the people interact is thus an important feature.

To properly deploy capacitive sensing in real-life applications, one has to understand how to create them, such that they serve in a not obtrusive way, and the effects of deformation on the sensing capability is known.

The principles of capacitive sensing and some guidelines on how to design capacitive electrodes for printed circuit boards (PCB) are presented by Chan and Underwood [Cha08], Gu and Sterzik [GS13] and Gao [Gao13]. They describe capacitive sensing and especially capacitive touch sensing. Only Gao describes capacitive proximity sensing, presenting *GestIC* for gesture recognition in automotive, home

automation or game controllers. Most of the recommendations are unanimous. A summary addresses the placement of the electrodes, the suggested shapes and sizes and many PCB related design issues to increase robustness of the system. One of these factors is the placement of the ground plane and the location of the battery. The closer the ground plane is to the electrode, the smaller the percentage of change is when the object approaches. Thus, ground planes are hatched, such that they have only 25 % of the original surfaces. Another technique is to have a guard ring around the electrode. For proximity sensing, the ground plane and the guard ring can achieve directionality of the proximity sensing. The sensing range depends on the power as well. If the power source voltage increases, the range increases. It also increases directly proportional to the sensor size. The goal of the circuit design is to design a system with high signal-to-noise ratio (SNR) by keeping parasitic capacitances mall and reducing the influence of noise sources. Regarding the shape of the electrodes for capacitive touch, if the electrode size is small, thus pads in the shape of circles and squares are proposed for button areas. For large applications, Gao recommends using loops of any aspect ratio. However, the larger the trace width, the larger is the range of a proximity sensing system. He states that the shape of the electrode does not influence the effectiveness of the sensor, but rather the area of the conductor relative to the use. However, in the end, the design of a system is unique, constrained by physical restraints and aesthetic design limits.

The advanced in the area of printed electronics have led to a few works where the materials, the shape and the performance of the electrode is evaluated. Wei et al. have presented an inkjet printable capacitive proximity sensor on fabric [WTLT16]. They evaluated two factors: the filling pattern and the outer width of a loop. For the pattern filling, they compare an entirely filled electrode, a spiral filled electrode and a outline or loop electrode. Their results showed that even though the filled electrode has the maximum capacitance change, the loop and the spiral perform similarly. Therefore, their preferred design is the loop since less printing ink is required to print a loop and it still offers 90 % of the sensing range compared to the filled design.

For capacitive touch sensing mutual- and self-capacitance are most commonly used. Mutual capacitance was exemplary used by Götzelmann et al. in combination with 3D surfaces. For this purpose a grid of conductive traces is printed into the objects, enabling touch detection [GA16]. For proximity sensing, in most works the self-capacitance or loading mode is used. Research on the shape and arrangement of electrodes has been addressed by the diamond shaped grid. *Wall++* uses such a grid, to create an interactive wall tracking touch and gestures [ZYH*18]. The electrode pattern had to project an large electric field and to offer enough resolution for touch tracking. From the five patterns analysed (lines, stripes, half circles, diamond dot and circle dot), the diamond shapes were chosen, due to practicality reasons. The half circle, the circle dot and the diamond are otherwise equally well suited, according to their simulations. In the work of Aigner et al. different embroidering patterns are explored for resistive pressure sensors [APP*20]. They investigate five different space-filling pattern designs composed of two electrode traces: Interdigitated Electrodes, Boustrophendon Path, Meander, Fermat Spiral and the Hilbert Curve. They identified, that the sensing behaviour can be controlled by the pattern design, giving some parameters for adjustment.

Although flexible capacitive sensing is used in numerous fields, the existing research does not focus on the performance of capacitive sensing electrodes with regards to their various parameters such as material, shape, size, pattern, filling degree, stretch and substrate fabric.

3. Assistive applications for flexible Smart Environments

In this chapter I present assistive flexible Smart Environment applications developed by me. These applications using flexible surfaces represent my contributions to the first research challenge **New flexible Smart Environment applications**.

Throughout the following sections I will address different applications, which all have in common that they put the human in the center - offering assistance. All applications leverage surfaces which are not stiff, but can be bent and humans use them frequently during their daily activities such as sleeping, commuting, working in office, or watching TV from a couch, see Figure 3.1.

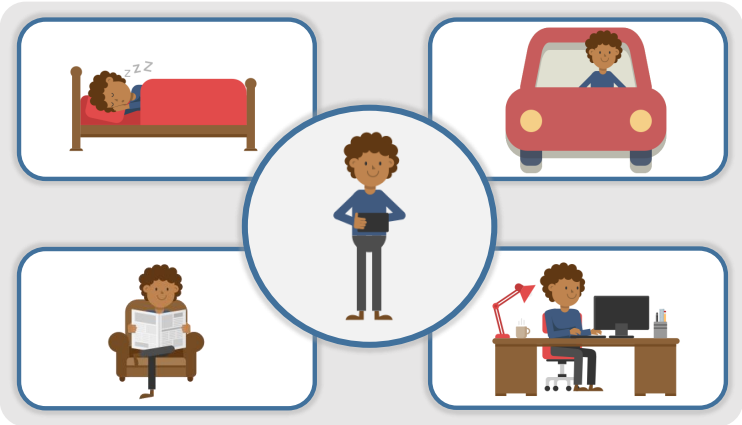

Figure 3.1.: Human centric assistance during Activities of Daily Living (ADL), ©CC-BY-SA 4.0, Black Man Sleeping in Bed Cartoon Vector.svg from Wikimedia Commons by Videoplasty.com.

Special interest is given to applications using the technology of capacitive proximity sensing, which facilitates ambient applications. The technology's main advantage is, that it enables the application designer to sense the presence of conductive objects or also body parts. Since humans are in the focus of assistive applications, this technology is well suited for assistive applications.

Section 3.1 presents an approach to support persons who must spend time in bed over a longer time - such as during rehabilitation. The application's focus is to prevent skin ulcers by detecting the lying position.

An office chair which supports the user throughout her day, is presented in Section 3.2. It prevents back pain and further diseases closely related to sitting still for a prolonged time by supporting the user to include brakes in forms of exercise on the chair.

Relaxation scenarios at home are supported by recognizing the lying and sitting position on a couch, as well as invoking the emotional state of mind from the user's movements. This work is presented in Sections 3.3 and 3.4.

The work presented in this chapter is an extended version of my papers, which will be introduced at the beginning of each section. In this chapter I introduce following scientific contributions:

- I provide a decubitus ulcer preventive system by creating a prototypical bed sheet, which can recognize bed postures and therefore infer pressure points.
- I create and compare different sitting cushion prototypes made of conductive textile material. By detecting 7 sitting postures and tracking exercises diseases such as backpain are prevented.
- I create a couch prototype, with which I explore the emotional state of the occupant through analyzing detected body movement.

3.1. Assistive bed posture monitoring

This section is based on my master's thesis [Rus13], my extended work presented in the two papers [RGPK14, RGPK17] and the bachelor's thesis of Steffen Maus [Mau14]. The authors referred later as "we" are Silvia Rus, Tobias Große-Puppendahl and Arjan Kuijper.

Enhancing the quality of care is an important factor in care facilities and home care. Many patients are affected by decubitus ulcers, also called pressure sore. This is a skin condition, caused by prolonged pressure on the skin on certain areas and can lead to severe injuries. According to the Center for Disease control and prevention 11 % of nursing home residents have pressure ulcers, from which the most common are stage two pressure ulcers, which describes skin braking open and injuries extending to deep layers of the skin [EPL04]. Best practice requires a caretaker to look after the bedridden person and change their position every one or two hours [fIiGuaPe13]. However, sometimes they patients may have already moved by themselves, or other caretakers have already done this.

We propose a technological solution that helps to determine these situations, notify the caretakers and provide decision support and appropriate actions to take. We envision a system, which might be used at home or in hospitals, where responsible personnel is on-site to react to the alarm of the system. The system monitors the bed posture changes of the bedridden person. The information of how long a person has been lying in a certain position can help the caregiver to decide which action to take next. For example, the bedridden person has been positioned during sleep to one lateral side. The caregiver will be presented with previous postures and the time the person spent in these poses. He can avoid

Table 3.1.: Comparison of our system with other capacitive solutions.

Reference	Measurement mode	Measurement points	Postures
Hamisu et al. [HB10a]	Self-capacitance	3	2
Braun et al. [DBM14]	Self-capacitance	4	Movement
Chang et al. [WCC14], [CCCY14]	Self-capacitance	320	
Rus et al. [RGPK14]	Mutual-capacitance	48	5

placing her back to the previous posture. This way harming the bedridden person is prevented by prohibiting that specific body parts will be exposed to higher pressure over longer time.

Capacitive sensing has found various applications in the field of smart environments. This variety is described by Braun et al. [BWKF15] and Grosse-Puppendahl et al. [GP15]. Detecting movements in bed with self-capacitance sensing, using 4 copper electrodes, has been the focus of Braun et al. [DBM14]. During sleep the pressure on the vertebral spine is an important indicator for the quality of sleep. This is achieved by Hamisu et al. [HB10a], differentiating if a person is lying or sitting upright in the bed, using capacitive sensors. The authors placed 3 electrodes underneath the mattress of a bed. When a person lies down, it activates a characteristic pattern of electrodes. The algorithm can then detect if a person is lying down or sitting. Chang et al. [WCC14], [CCCY14] presented the capacitive system FPCSM (Flexible Projected Capacitive-Sensing-Mattress). It is a flexible sheet placed on top of the mattress. It is based on 10 sensing units of 40 cm x 25 cm size which are composed of 32 sensors each, providing a total of 320 measurement points.

All these capacitive systems use the measurement mode of self-capacitance, meaning that one measurement point corresponds one sensor. Our proposed system [RGPK14] measures the mutual-capacitance, providing 48 measurement points while using only 8 sensors. Table 3.1 shows an overview of similar capacitive solutions. While most of them describe the used system, none of them have done a quantitative evaluation. Hamisu et al. are able to differentiate sitting and lying while Braun et al. concentrate on movements in the different sleeping phases. Chang et al. show only images of different lying positions and do not evaluate their system.

Different camera systems are used to acquire visual data. Diraco et al. make use of a [DLS13] a 3D Time of Flight (ToF) camera, Yu et al. [YRN*12] a common digital camera and Shotton et al. [SFC*11] a depth camera. These are designed mainly as fall-detection systems but can also identify a lying posture.

Accelerometers are used to detect bed postures like lateral left and right, supine and ventral. They are attached to the body on the sternum and on the right thigh [WBvO*12] or worn at the dominant wrist [BBV10]. Using accelerometers, a smart watch is used in [BHV13] to detect physical activity such as sleep detection.

The techniques presented above can be used independently to detect the bed posture, but systems using them in combination also exist, e.g. visual and capacitive sensing [Tes12], acceleration and

Table 3.2.: Comparison of resulting accuracy of our system compared to other solutions.

Reference	Sensor type	Measurement points	Pos.	Class.	Acc.
Liu et al. [LXH*14]	Pressure	8192	6	Sparse	82.9 %
Yousefi et al. [YOF*11a]	Pressure	2048	5	kNN	97.7 %
Hsia et al. [HLA*09]	Pressure	16	3	Bayes	100 %
Hsia et al. [HLA*09]	Pressure	56	6	SVM	83.3 %
Rus et al. [RGPK14]	Capacitive	48	5	J48	80.8 %
Rus et al.	**Capacitive**	**48**	**5**	**NN**	**90.5 %**

capacitive sensing [GPBB12], a combination of temperature, light, tilt and acceleration [VBKS08] or even RGB, depth camera and pressure [THFM15].

Using resistive and capacitive pressure sensors many approaches exist for detecting bed postures. For example, Liu et al. use a high-density sensor bed sheet for monitoring the patients' rehabilitation exercises [LHX*13, LXHA13, LXH*14]. It is composed of three layers where the top textile layer is coated with 64 conductive lines, the middle layer is an e-Textile material and the bottom textile layer is coated with 128 conductive lines, perpendicular to the first layer. At each intersection of the conductive lines a pressure sensor node is formed, leading to a total of 8192 pressure sensors. The mean of the achieved precision over all 6 selected postures is 83 %. An Under Mattress Bed Sensor (UMBS) is used by Walsh et al. to detect body movements [WM14]. The mattress is built by integrating a grid of 24 pressure sensors in a foam mat in the form of a band which is placed beneath the upper torso of the person lying in the bed. Similarly, pressure sensor arrays with a varying number of measurement points (72, 132, 48), form (stripes, pads), dimensions and placement are used in different setups [HLA*09, FMGK12, NAZW10].

On a dataset provided by Yousefi et al. [YOF*11a] with 2048 pressure sensors Ostadabbas et al. [OPNK14] achieved accuracies of 98.4 % for three main sleeping positions and an accuracy of 91.6 % for detecting 8 limbs lying on the back and 5 limbs in side sleeping positions.

Looking at the presented approaches using pressure sensors, one can observe that the detected positions are very different between the various deployments.

Table 3.2 shows a comparison of the existing systems implemented using pressure sensors and our proposed solution. The best result for the similar number of 5 evaluated bed postures is achieved by Yousefi et al. [YOF*11a]. They reach an accuracy of 97.7 %. However, they use 2048 measurement points, considerably more than we use in our system of 48 measurement points. Hsia et al. achieve 100 % for detecting three lying positions using 16 measurement points, but using 56 measurement points, they achieve an accuracy of 83.3 % for 6 lying positions. It is very hard to compare the different solutions because postures and metrics used are highly heterogeneous. Thus, no direct connection can be drawn between the number of measurement points and the achieved accuracy.

Applying different sensing modalities, multiple approaches have been developed, in order to realize a system, which detects bed postures. For example, camera-based visual data and capacitive pressure sensing are typically used. However, previous approaches require expensive hardware and are often not easy to deploy. Therefore, we propose an extremely easy to deploy and inexpensive to produce bed sheet. It is comparable to a large capacitive touchscreen and uses affordable hardware components.

We propose to apply mutual capacitance sensing to achieve this goal. Mutual capacitance sensing allows for a high number of measurements, which have positive influence on the recognition performance [SGB99]. Therefore, we place a grid of wire electrodes within the bed sheet and measure the proximity to the body. Measurements with mutual capacitance sensing require transmitter and receiver electrodes, one transmitter can have multiple receivers attributed to it. The data is subsequently evaluated using different machine-learning classification methods. The identified bed postures are displayed by a system which shows the bed postures over time.

3.1.1. Setup of smart bed sheet

This section presents the system overview of the hardware components of the bed sheet and its data processing. First, we give an overview of the system architecture and the different data processing steps in Figure 3.2. The three main components of the smart bed sheet are: the wired grid with the sensing unit, the evaluation boards to which the grid is connected, and the PC with the visualization and classification implementation. The wire grid is attached to the bed sheet. Each crossing of the wires represents a sensing node but only at the end of the vertical grid lines, 8 sensors are connected. The receiving evaluation board pre-processes the sensor data and forwards the data to the PC. Here the data is gathered, processed in order to classify the lying posture, which is subsequently visualized.

The two boards are named after their function. Hence, the TxBoard is used for transmitting the signal and the RxBoard is used to process the received information. It then sends the calculated value to the PC, using a USB connection, where the bed posture alarm program receives the data and performs the classification.

OpenCapSense [GPBB*13], is a capacitive sensing toolkit to enable the easy prototyping of capacitive systems. The toolkit has been published as an open-source project[1] and is inspired by CapToolKit [WKBS07]. Besides self-capacitance measurements, it also supports mutual-capacitance measurements, which were used for the measurements performed in this paper.

Besides a powerful floating-point microcontroller, OpenCapSense has eight capacitive sensing channels. They can be used for either transmitting or receiving a signal through an electrode. It is possible to build sensing arrays by connecting multiple evaluation boards via CAN-bus and synchronizing them. The board has a connection to the PC, which also serves as the power supply. Moreover, messages are passed to the computer through the on-board serial-to-USB interface. All these connection interfaces are shown in Figure 3.3.

[1] http://www.opencapsense.org

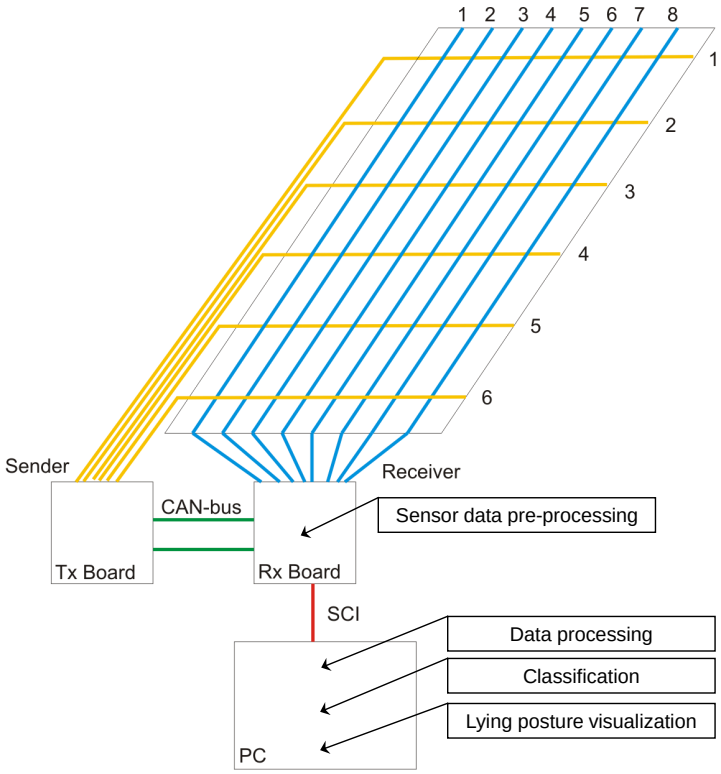

Figure 3.2.: Schematic overview of setup. Two OpenCapSense evaluation boards connected by a CAN-bus interface for synchronization. The transmitting board (TxBoard) sends out the signal through the electrodes while the receiving board (RxBoard) collects the data, processes it, and sends it to the PC.

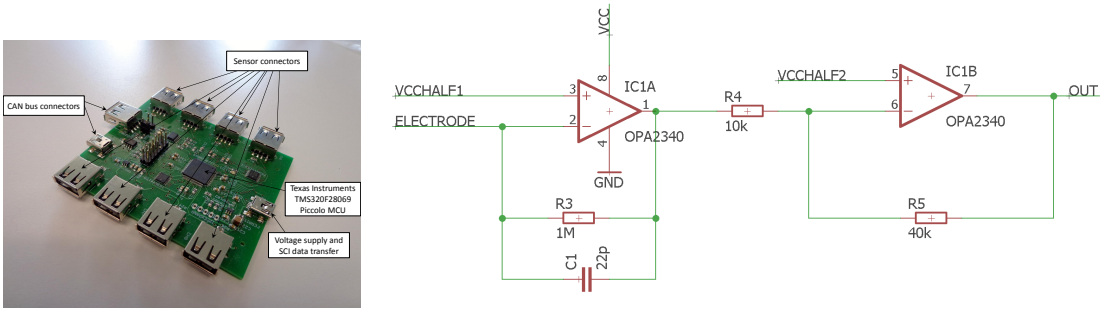

(a) OpenCapSense board

(b) Schematic of receiver

Figure 3.3.: Each receiving electrode is connected to a sensor with a transimpedance amplifier. The sensor amplifies the incoming displacement current from a transmitting electrode and amplifies it for further processing. [SGB99]

The board offers the functionality to generate signals, using a pulse-width-modulation. This allows the adjustment of the frequency of the transmitted signal. In our final bed sheet, we generated signals on six output ports, oscillating at a frequency of 7.3 kHz.

On the receiver side, dedicated hardware has been developed to evaluate the received signals based on the work of Smith et al. [SGB99]. The transmitted signals are received by an amplifier configuration displayed in Figure 3.3, which is similar to [SGB99]. The circuit is built of two stages, a transimpedance amplifier with a low pass filter, followed by an inverting amplifier with a gain of 4 ($G = 40k\Omega/10k\Omega$). The circuit of the low pass filter is built by adding a capacitor across the feedback resistor of the operational amplifier. The output voltage is passed to the ADC on the OpenCapSense board with a sampling rate of 100 kHz.

Hence, the total cost of the prototype setup needs to cover some copper wires, the receiving sensors, and the two OCS prototyping boards. The main advantages are due to the sensing material and the number of needed sensors. Due to the grid structure our prototype needs only 8 sensors which are composed of standard off-the-shelf components. An additional advantage is the flexibility of the system towards different bed sizes because the placement and the length of the wires which are embedded in the bed sheet is easily adjustable to different sizes of the bed.

The transmitting board starts its operation by setting the sending frequency and initializing the CAN-bus interface, the serial communication interface (SCI) and the output pins. The role of the transmitting board is to alternate the output sender pins on which the rectangular signal is sent. In order to achieve this, it listens for messages on the CAN bus, which indicate to start sending on a certain output pin. Starting the transmission, a square signal at 7.3 kHz is sent.

On the other end, the receiver board switches through all its receiving ports and subsequently sends the next expected sender port. For each measurement at the receiver, a window of 1024 values (the

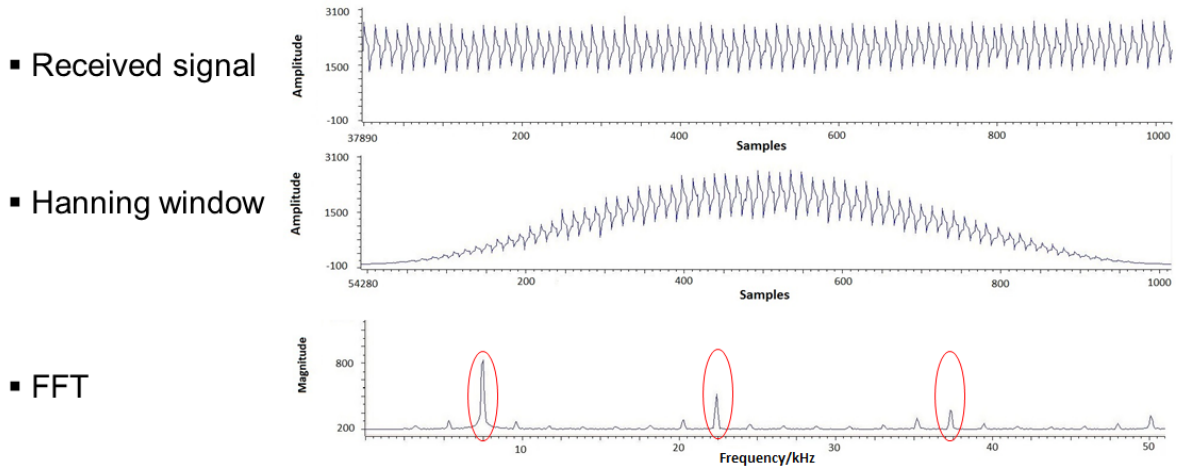

Figure 3.4.: The received signal is windowed and a Fourier Transform is applied on the signal. The resulting amplitudes of the magnitude of the FFT are added up resulting the sensed value.

size of the ADC buffer) is collected at once. Per capacitance measurement ten of these windows are collected.

3.1.2. Sensor data processing

As shown in Figure 3.4, the original signal is windowed, and the magnitude of the Fourier Transform is calculated. The peaks of the magnitude are summed up. For different frequencies of the sent rectangular signal, the peaks of the amplitude are placed differently. This way, operating the system using FDMA (Frequency Division Multiple Access) is possible by summing up the peaks in intervals which are specific for the expected frequency. This calculated value represents the sensed value transmitted to the PC through the SCI interface. The according sender and receiver information is added to the sent sensed value.

For each sender the sum of maxima of the magnitude of the Fourier Transform is calculated and the mean is determined over several sets of 10 windows. This mean value represents the intersection's capacitance which is sent to the PC for further processing, described in the following.

The sensed values are continuously received at the serial port using MATLAB, which supports real-time data acquisition on the serial port. In Figure 3.5, the sensed values for all receivers of sender 3 are displayed. Between measurement samples 15 and 31 a person was lying down in this area whereas all other measurement samples were taken while the bed was empty. For a single measurement point e.g. sender 3 and receiver 5 the raw data shows a rise of about 3000, from 3000 reaching 6000. This steep rise is due to the fact that a person was lying down on this sensor node. We observe that even in the empty state not all receivers share similar values. Furthermore, the difference between the empty bed

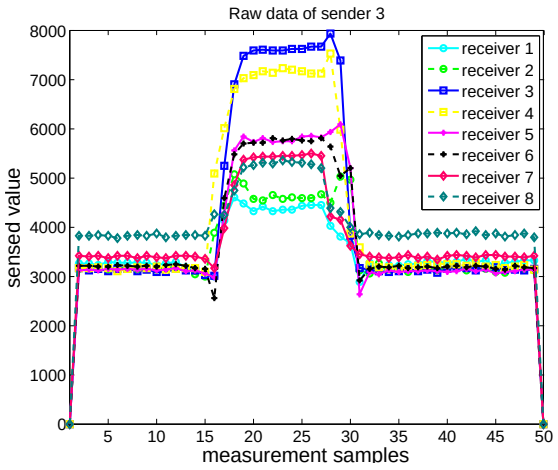

Figure 3.5.: Visualization of all eight receivers of sender 3

values and values obtained when a person lies down are different for each receiver. For receiver 3 the difference is around 4500 while the difference is approximately 3000 for receiver 5. In order to acquire comparable sensor values, normalization is required. For this, the system needs to be calibrated. This is achieved by detecting the sensed values of the empty bed and the values for a calibration object for all sensor nodes. Once the normalization is performed, the square root is applied on the data to boost smaller signals, in order to enhance detecting smaller objects. In Figure 3.6, we show the normalized 6x8 data in the top and in the bottom image the square rooted and twice interpolated data. We used a cubic interpolation.

We want to classify five lying postures, which will be detailed in Section 3.1.3. We consider two different classification approaches. We call the first feature-based classification and the second raw data classification. The feature-based classification uses the normalized and interpolated data as computation base, like depicted in the right image of Figure 3.6. The raw data classification is applied on the normalized 6x8 data, shown in the left image of Figure 3.6. For the feature-based approach we select and compute our own feature set. Both classification approaches are evaluated using the WEKA [2] framework. We evaluated the data using three different classification algorithms: the C4.5 decision tree implementation J48 [Qui14], the Support Vector Machine implementation libSVM [SV99] and the k=1 Nearest Neighbour implementation IB1 of WEKA with default settings [WL81]. We defined following classes: sitting on the bed, lying on the right or left side, lying on the stomach or back. Noise or movements in the region around the bed might lead to problems, that is why we also recorded a number of instances for an empty bed resulting in an additional class.

To detect lying postures, we create an image from the sensor values and apply image processing methods. This allows extracting features, such as mean or center of gravity. The center of gravity is computed as the maxima of the average of the row and the average of the column. To further refine the

[2] http://www.cs.waikato.ac.nz/ml/weka (date accessed: 2015-06-21)

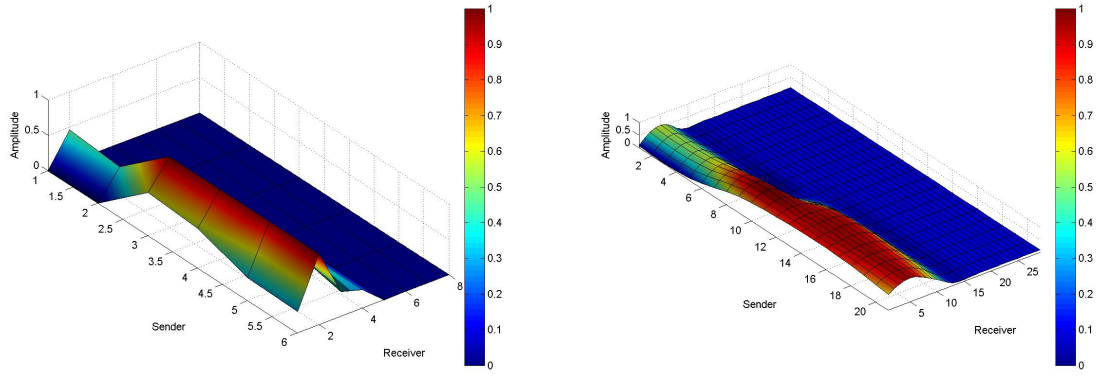

Figure 3.6.: 6x8 normalized data (left), interpolated data (right)

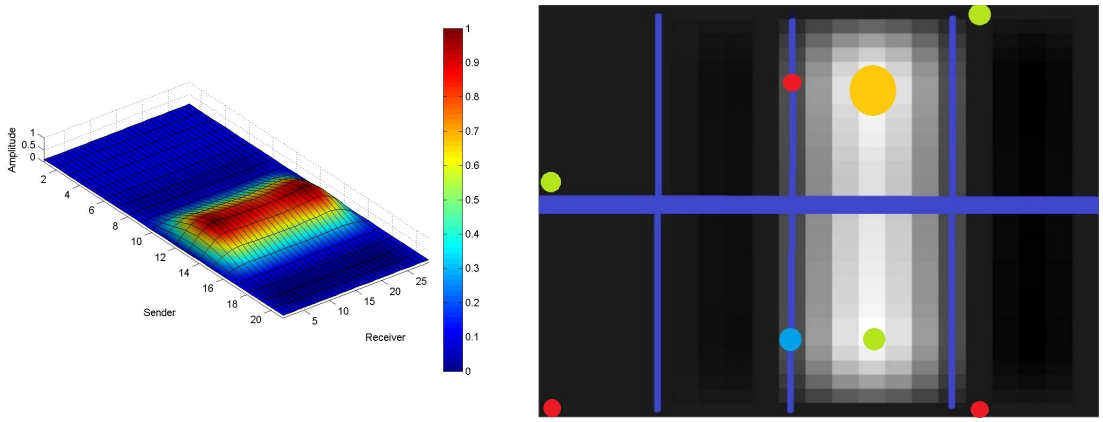

Figure 3.7.: Left and right images show a person sitting upright after lying down. The left image visualizes the normalized and interpolated values. The right image shows the 2D grayscale of the upper image slightly turned. It is divided into eight sections. For each, the center of gravity and the mean are calculated. Additionally, the center of gravity of the whole image is calculated.

Figure 3.8.: Prototype bed sheet with wired grid

results, the image is divided into 8 sections as shown in the bottom image of Figure 3.7. This image is created by computing the gray scale image of the top image and displaying it in 2D, proportional to a 6x8 matrix. The coloured dots represent the center of gravity calculated for each section, while the bigger yellow dot is the computed center of gravity of the whole image. Finally, we also add overall mean and center of gravity as features. This results in nine mean values and nine center of gravity values, leading to 18 features overall.

3.1.3. Evaluation setup

The goal of the experimental setup is to evaluate postures that are typical for the elderly, or persons who are bound to the bed. A possible use case for recognizing these postures is to support a caregiver in re-bedding patients. This is especially useful when persons sometimes have active and inactive phases. For example, in active phases, re-bedding can be avoided, while on the other hand, inactive phases may lead the caregiver to change the patient's bedding postures more frequently. However, there are numerous other application scenarios, like the *Quantified Self* trend, which describes the trend of taking measurements about the personal performance throughout the day, facilitating positive lifestyle behaviour changes. Those users could capture their own sleeping behaviour by recording postures throughout the night.

To realize the use cases mentioned above, our smart bed sheet needs to classify discrete user postures. Time spent in a specific posture can be recorded, to avoid long-term pressure on a specific body part. Therefore, the bed sheet was placed on an ordinary bed with a length of 2.0 m and a width of 0.8 m, as depicted in Figure 3.8. The bed sheet provides 48 measurement points, with eight horizontal and six vertical wires, a part of which is shown in Figure 3.8. In our first stage of the experiment, we asked 14 persons to lie down in the predefined postures shown in Figure 3.9. The test persons were only instructed by a few words, allowing them to carry out the postures as variable as possible. Figure 3.10 shows the weight and height distribution of the test persons. The height is recorded as the size in cm while the weight is recorded in 5 kg steps. For each test person we recorded 45 images of 6x8 sensing nodes per lying posture, resulting in 225 recordings for each person. For the raw data classification we

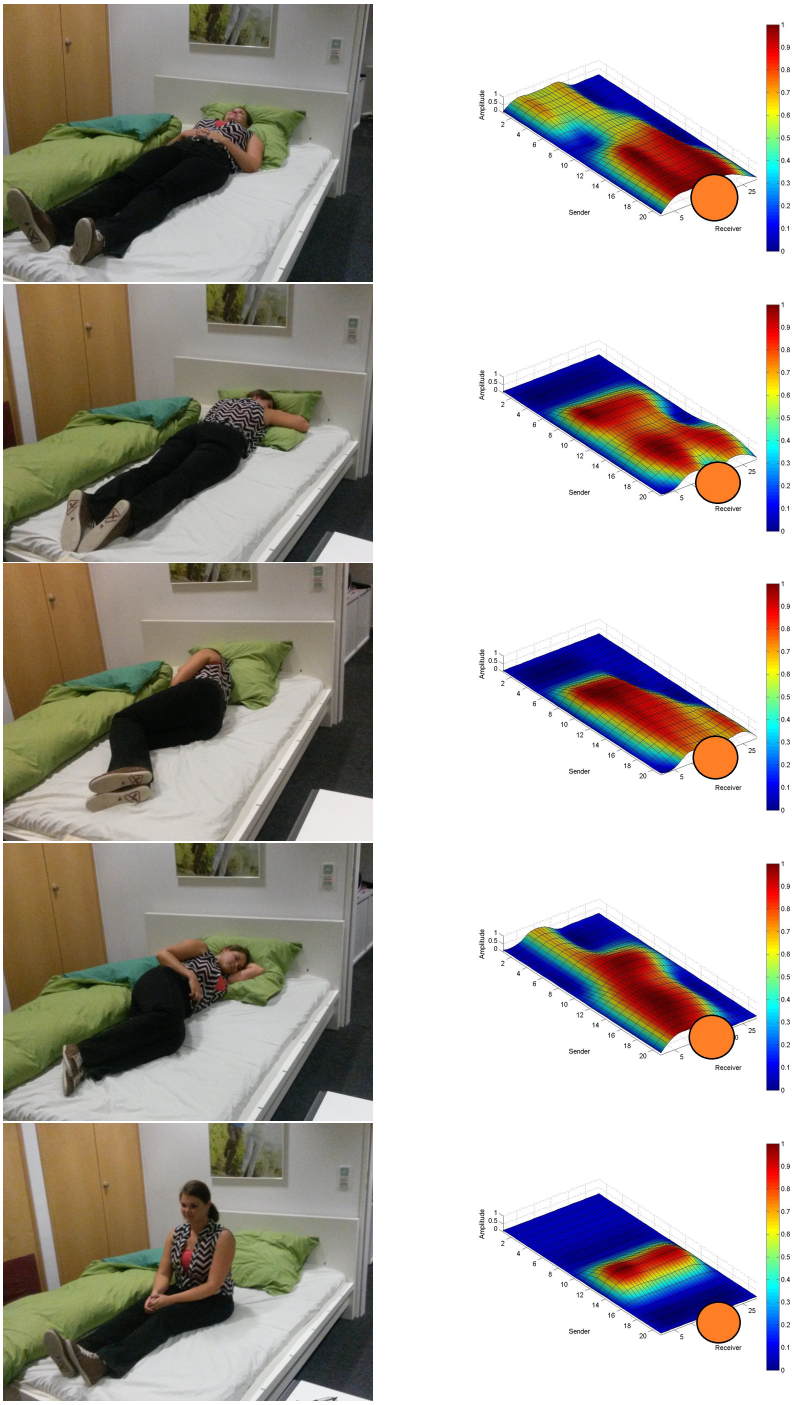

Figure 3.9.: Common bed postures used for the experiments and resulting visualization. The orange circle represents the direction of the head of the person lying down. Bed postures from top to bottom: lying on back, stomach, lateral right, lateral left and sitting on bed.

normalized the sensor data and use this to evaluate it. For the feature based classification, we calculated for each of the 225 recordings per user 18 features.

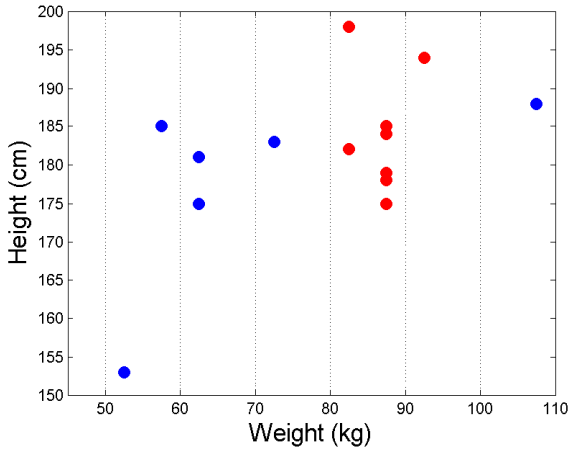

Figure 3.10.: Evaluation of subjects' weight and height diagram. The size is recorded in cm and the weight in 5 kg steps. The subset between 80-95 kg covers more than half of the set of test subjects.

3.1.4. Bed posture classification

For each posture, we recorded a set of 45 images, each with 48 measurement points. The 14 test persons carried out each posture, allowing them to vary between different interpretations for the specific posture.

For our preliminary results investigating the feature-based classification approach we divided the set of 14 test persons randomly in two. The first set of data of 7 persons was merged and used for training the C4.5 decision tree implementation J48 of WEKA. The second merged set of data of 7 persons was used for testing the recognition performance. Then, the training and test set were exchanged. In this way J48 led to a mean performance of 80.8 %.

After these first experiments, we quickly realized that the person's weight and height had much more influence on the classification performance than expected. It was very difficult to achieve a good recognition performance for persons with very different body sizes. The difference in sensor measurements of a heavy person (80 kg) compared to a light person (60 kg) for the same posture is depicted in Figure 3.11. Such examples show that features, which are invariant to body-size are very hard to find when the sensing area is a limiting factor. Investigating translation-invariant features was not necessary, since the bed's area was quite small and minor body translations did not have a big effect on the recognition performance.

Based on these observations, we decided to limit our next experiment on a set of eight persons whose weight and size is similar. We chose the interval between 80 and 95 kg, as depicted in Figure

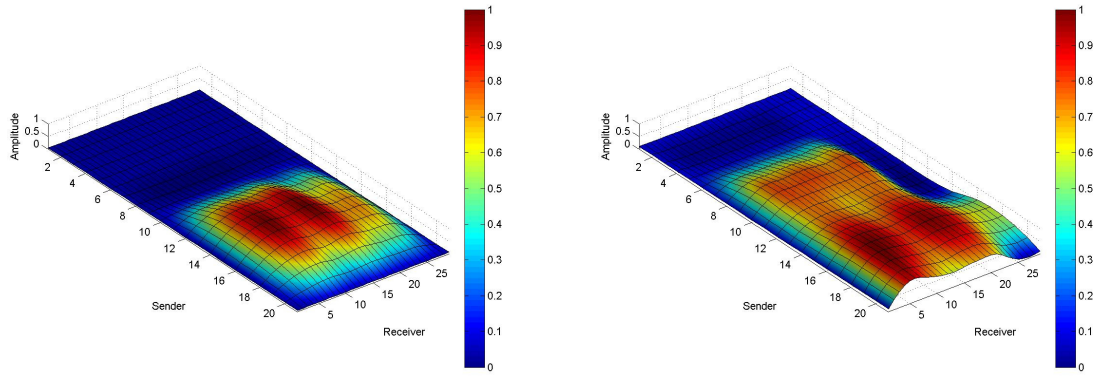

Figure 3.11.: Images of person with 60 kg (top image) and 80 kg (bottom image) sitting on the bed

Limited data set (80-95kg)						Overall data set						
a	b	c	d	e	f	a	b	c	d	e	f	← classified as
357	0	0	0	0	3	**568**	0	16	45	1	0	a = sitting
0	**327**	0	33	0	0	0	**530**	2	57	2	0	b = side right
0	0	**316**	44	0	0	0	0	**585**	0	45	0	c = side left
0	1	0	**359**	0	0	45	123	156	**306**	0	0	d = stomach
1	0	48	4	**307**	0	0	9	170	17	**434**	0	e = back
0	0	0	0	0	**360**	0	0	0	0	0	**630**	f = empty

Figure 3.12.: The classification performance depends highly on the person's body height and weight. Separating the test sets into persons with similar body properties, e.g. separating the persons by weight, leads to a much better performance in the data sets.

3.10. These 8 test persons were closest to each other regarding their weight and cover more than half of the number of test persons.

This set of 8 test persons, we randomly grouped them into two sets of 4 persons each. These sets were again used to train and test using J48. This led to an improved performance of 93.8 % overall accuracy.

The two resulting confusion matrices for both sets (14 persons set and 8 persons subset) are depicted in Figure 3.12. We observe the less dispersed confusion matrix of the smaller subset of 80-95 kg test persons. Evaluating the remaining dispersed set of test persons, dividing the 6 test persons into two groups of 3 test persons we repeated the evaluation. The resulting accuracy is 69.8 %. We conclude that our feature set, as well as the whole setup, depends strongly on body height and weight. In the future, the design of features that are more invariant to such circumstances is therefore a very important prospect to us.

The resulting decision trees of the subset of persons were also significantly smaller, having a depth of five levels, than the ones generated with the overall test set. These resulted in depths of seven or more levels.

The trees show that center-of-gravity features contribute significantly to the classification. With regard to the bed sheet's different sections, features from the sections in the middle of the bed are used more often in classification. On the other hand, sections representing data from the test persons' heads and feet are included less often in the decision trees. The reason can be seen in the in-homogeneous weight distribution on the mattress. The proximity to body parts has less influence on a mutual capacitance measurement than the deformation of the underlying mattress, caused by large pressure on a measurement point. As expected, the feature mean is used to decide between classes like *lying on stomach* and *lying on back*, where the weight in the corresponding regions is significantly different.

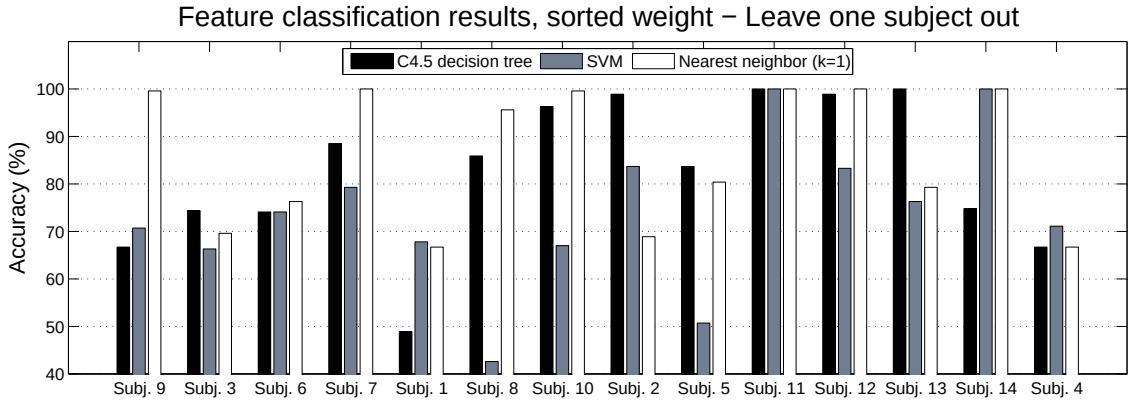

Figure 3.13.: Feature based classification results of leave one subject out evaluation.

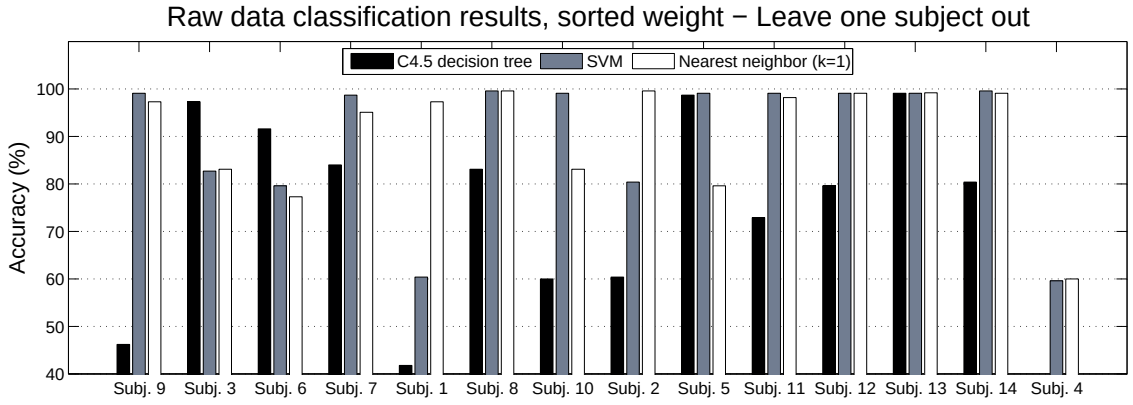

Figure 3.14.: Raw data classification results sorted in rising weight of the subjects. Leave one subject out evaluation.

Table 3.3.: Overview of classification results for feature and raw data based classification evaluated using J48, SVM, NN. The values are mean calculations from the Leave One Subject out evaluation of different test person subsets from Figure 3.14 and 3.13. We separated the data test person subsets whose weight is in and outside the weight interval 80-95kg.

	Dispersed subset Subj. {9,3,6,7,1,4}	Similar subset Subj.{8,10,2, 5,11,12,13,14}	Whole data set All Subj.
Preliminary feature J48	69.8	93.8	80.8
Feature J48	69.9	93.3	82.7
Feature SVM	71.5	75.4	73.8
Feature NN	79.8	90.5	85.9
Raw data J48	66.7	79.3	73.9
Raw data SVM	80	**96.9**	89.7
Raw data NN	**85**	94.7	**90.5**

For this classification using our own computed features, we can conclude that the classification performance currently depends highly on the test persons' body height and weight. The small bed size makes it hard for developers to design features that are invariant to these properties. Compared to the regions around a person's head and feet, the regions in the middle are more important for classification. An idea for future work is to increase the number of measurement points in the bed sheet's center region. This unequal sensing node distribution could lead to a better recognition performance.

In order to further evaluate the recognition performance of the feature-based approach, we conducted a Leave one Subject out evaluation. The data of a single person was used as test set, while the data of all the remaining 13 test persons was used for training. Figure 3.13 depicts the results of the J48, SVM and NN evaluation for each test person. To allow easier comparison, the test persons are ordered in increasing order of their weight. The mean accuracy per classification algorithm is: 82.7 % for J48, 73,8 % for SVM and 85.9 % for NN.

To further improve accuracy, we investigated the classification using only the raw data, which is the normalized data. For this, we conducted a Leave one Subject out evaluation of the 14 persons data set. We used 3 classification algorithm implementations of WEKA. Those are the same as for the dedicated feature classification: Nearest Neighbour (NN), Support Vector Machine (SVM) and C4.5 decision tree J48. The results are depicted in Figure 3.14. The mean accuracy per classification algorithm is: 73.9 % for J48, 89.7 % for SVM and 90.5 % for NN.

Table 3.3 resumes the recognition performances of all evaluations. The first row shows the results of the preliminary J48 feature classification, where the dispersed subset was separated into two sets of subjects 1,4,7 and 3,6,9 resulting in the weakest recognition performance of 69.8 %. Evaluating two subsets of the similar subset the recognition performance exceeds the overall performance of 80.8 % achieving 93.8 %. This is the second highest result in the column of the similar subset. For the next

tow evaluation groups, the feature or raw data classification, the mean accuracy of the subjects from the subset is calculated for each classification algorithm according to the results from the Leave one Subject Out evaluation. We observe the highest recognition of 96.9 % using SVM on the similar subset. However, the overall classification result of the raw data NN classification is better for each evaluated subset, achieving the highest overall recognition performance of 90.5 %. Having the highest possible coverage range of all subject sizes and weight is important for the bed posture recognition implementation, thus we chose to use the raw data NN evaluation. How this is implemented is described in the next Section 3.1.5.

3.1.5. Bed posture monitoring system

The goal of our work is to create a bed posture recognizing system that could be used in home care or hospitals. Caregivers could inform themselves on the patient's bedding history on a glance.

In this section the envisioned system implementation is described. The system shows multiple views. The goal of these views are to help the caregiver decide on the reliability of the current output of the system. To achieve this, the recognized posture history diagram is complemented by an indication of an uncertainty threshold.

The system offers three views. The first view, Figure 3.15, shows the processed data received from the bed sheet. Next to it the result of the NN classifier is shown. It is the best fit from the training data, that the classifier has found. Looking at this representation the caregiver can be assured and can check himself the similarity of the findings.

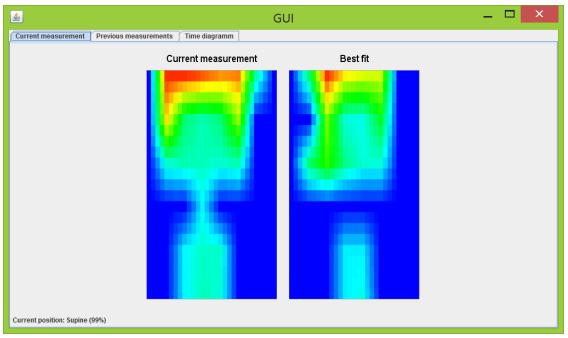

Figure 3.15.: Visualization of real-time data (left) and best matching result of classification (right).

The second view, Figure 3.16, depicts the last 10 detected lying postures and the time the bedded person spent in each of them. It allows to avoid repetition of postures.

Finally, Figure 3.17 shows the time frame of 24 hours. The different colors depict the detected lying position. The varying height of the bar in each time instance visualizes the certainty with which the system is sure that the detected bed posture is correct. This helps the caregiver on the one hand to have

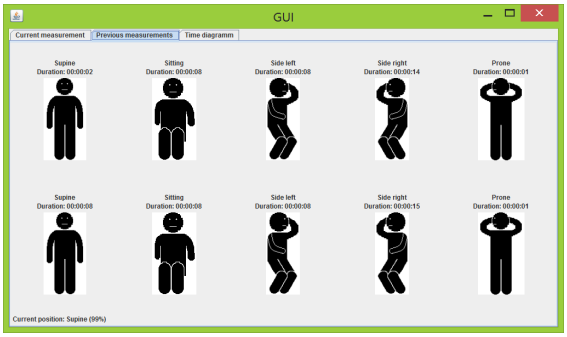

Figure 3.16.: History view of detected lying postures. The last 10 postures are shown.

confidence in the detection result of the classifier and on the other hand clarify eventual classification faults by consulting the patient.

This certainty value is calculated by looking into the classification process. The Nearest Neighbour (NN) classifier detects the distance to the nearest object as well as the distance to the nearest object of a different class. The uncertainty is the quotient of these two distances $d1/d2$. The greater the distance to the other class and the smaller the distance to the own class is the higher is the certainty. In order to reduce wrong classification, a class "uncertain pose" has been introduced. If the certainty of a result is not high enough the pose is classified as an "uncertain pose", reducing the level of wrong classification from 9.5 % to 1.9 %. This yields a correct classification in 80.3 % of the cases and in 17.8 % of the cases an "uncertain pose". In these circumstances, if the system recognizes a pose it is in 97.6 % of the cases correct.

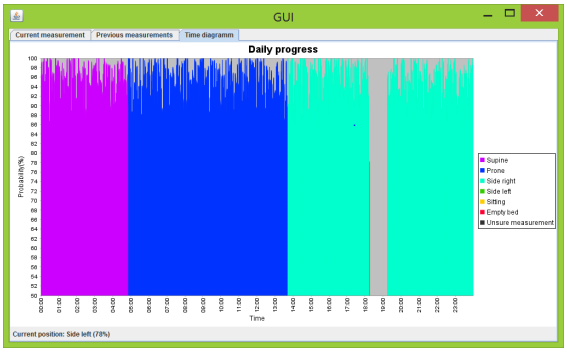

Figure 3.17.: 24 hour view of detected bed postures. The vertical value depicts the certainty of the classification result.

3.1.6. Summary

In Section 3.1 we presented a system of preventive nature, which is intended to alarm the caretaker which looks after a bedridden person and illustrate the current and previous lying postures. We evaluated a prototypical bed sheet, which can recognize bed postures and therefore infer pressure points. This can be applied for decubitus ulcer prevention in hospitals or at home. In contrast to previous work, the bed sheet is very affordable and easy to handle. It uses simple conductive wires, which are inexpensive and can be replaced without great effort. The prototype is composed of a wire electrode grid, where senders are placed horizontally to the bed posture and receivers are placed longitudinal to the bed. Measuring the mutual capacitance between these electrodes allows for the detection of the presence of human body parts. The received sensor data is treated like an image of 48 pixels. It is normalized, interpolated and features like the mean and the center of gravity are calculated for different regions of the image.

The evaluation with 14 participants using defined features resulted in a overall accuracy of 80.8 %, while the accuracy of a subset of taller test persons weighing between 80-95 kg resulted in an accuracy of 93.8 %. Better overall accuracy has been achieved using a NN classifier on the raw data, yielding an overall accuracy of 90.5 % compared to 80.8 %. We also introduce an uncertainty threshold. It is intended to help the caregiver decide, by illustrating how sure the system is of its findings. By using this threshold, the recognized bed posture is correct in 97.6 % of the cases.

For future iterations, the smart bed sheet can be improved in various areas. One of the challenges is the design of features that are more invariant to body height and weight. Furthermore, the influence of the calibration on the sensitivity of the bed sheet has to be investigated, in order to detect smaller body parts, like hands and feet. This could be achieved by improving the setup of the electrode grid. We could also investigate if for a small household, where the bed sheet could be able to identify persons just by lying down on the bed. Regarding the whole system, we need to evaluate the acceptance of such a system in home care or hospital settings, especially the aspect of using the uncertainty threshold.

Our goal is to support the prevention of decubitus ulcer by creating a lying posture recognizing system, based on mutual capacitance sensing, which we envision to be able to autonomously, not only alarm the caring personnel, but also move the bedridden person on its own.

3.2. Assistive chair: sitting posture detection

The application presented in this section is based on the work published in my paper "E-Textile Capacitive Electrodes: Fabric or Thread - Designing an E-Textile Cushion for Sitting Posture Detection" [RBKK19b]. The authors referred later on as "we" are Silvia Rus, Andreas Braun, Florian Kirchbuchner and Arjan Kuijper. Some parts of this work referring to specifics of electrode design are presented in Chapter 5 in Section 5.3.2. In this section we present the specifics regarding the creation of the application for back pain prevention.

Office workers often spend most of their working time seated in front of a screen. Many of them experience back pain, stiffness leading to long-term problems, impacting their quality of life. It is the most common form of chronic pain and is experienced as being the sixth biggest in terms of overall burden [HMB*14]. There are already mechanical methods to help prevent back pain such as ergonomic chairs, cushions, or stretching and exercises. Giving a user immediate feedback on his behaviour is helpful [Ban69], changing it, however, is not easy. The trend towards quantified self, where sensors eliminate the need of active monitoring shows that feedback from personalized data is very useful and acts as motivating force [Lup16].

Most smart furniture chairs integrate sensors into different parts of the chair. Common approaches use pressure sensors, capacitive proximity sensors or electrocardiogram electrodes [MLGF17,MLB*13, MKF*07, BFW15, BFMW15, GSB14]. Example applications track sitting poses, vital signs and support the user by tracking breathing and hearth rate or seating behaviour, improving sitting posture or triggering exercises during work. Systems where only the seat area is equipped with sensors, vary in number of sensors from 16 to about 2000. Tekscan and Sensimat are two commercial systems. Tekscan has developed Body Pressure Measurement System, a pressure sensing array which finds its application in beds, car seats or chairs [Tek]. Sensimat integrates 6 pressure sensors into a wheelchair cushion supporting the user in sitting correctly [Sen]. Xu et al. and Meyer et al. use E-textiles as capacitive pressure arrays to detect sitting postures [MAST10, XHA*13].

Capacitive proximity sensors are a valid approach in building smart furniture, as they sense the human body through non-conductive material. The sitting comfort of chairs is due to the soft, textile cushions.

In this work we evaluate conductive textiles attached to capacitive proximity sensors to detect some of the sitting postures, identified by the Global Posture Study [Ste]. To give design guidelines and define a minimal set of required material and sensors, we tested different sensor and textile electrode setups. We have built three prototypes with different textile electrode properties and tested their performance by detecting specified postures such as sitting upright, leaning back (the draw), leaning forward (the strunch), sit leaning back left and right (the smart lean). To test the performance, we evaluated the prototypes with a number of users, comparing single user vs. multi-user classification performance with various machine learning methods.

3.2.1. Setup of smart cushion

For fast prototyping purposes we use the OpenCapSense board capacitive proximity sensing and processing unit [GPBB*13]. The board forwards the sensor values via Bluetooth to a smartphone. The data is logged and can be evaluated against a trained classifier. the according application estimates the sitting posture and shows the user how much time she has spent in a given sitting posture.

For the first prototype we used a therapeutic wedge sitting cushion and for the second an orthopaedic thicker, softer cushion. Both were chosen such that sensors, processing board and battery could be fully integrated into the cushion, see Figure 3.18. The wedge cushion was able to include the needed hardware in a very compact way, but it takes getting used to sitting on such a cushion, even though it is

Figure 3.18.: First prototypes of Smart Cushion

intended to be used in correcting the back position during sitting. The thicker cushion was much thicker, offered lots of room for hardware integration, however it increased the sitting height considerably and did feel like a big addition on top of the sitting area of the chair.

These initial prototypes were equipped with a very basic setup by using four rectangular conductive textile electrodes. These covered most of the surface of the cushion. However, the variations in shape, placement and number of sensors could be improved. This process is described in detail in Chapter 5, Section 5.3.2. The final, the third cushion prototype is for ease of prototyping reasons a thin, flexible cover of synthetic leather attached to the sitting area of the chair, see Figure 3.19. The textile electrodes can be attached and removed from the synthetic leather cover. This emphasizes the ability to merge and integrate seamlessly into the ambient, in this case the sitting area of a chair.

By trying out different positions, we observed that there are areas which are more relevant when trying to detect the sitting poster. These are the areas close to the body, but not entirely covered while sitting. Two designs using 5 and 6 electrodes were the results of these trials. We evaluated these in a user study and concluded that the layout with 5 electrodes, performed better. 4 of the electrodes are shaped as triangles and one as a smaller trapeze. The triangle shaped electrodes are placed in the 4 corners of the chair. In the 2 corners in the front they have contact to the thighs. In the back, they control how much the person sitting is leaning towards the side of the sitting area. The 5th electrode is placed in the middle of the back of the sitting area, responding to the amount a person leans back and to the front.

Figure 3.19.: Seat cushion prototype with person sitting upright and leaning back

3.2.2. Sitting posture classification

We used this 5-electrode layout as basic layout for the further evaluation. As mentioned in Chapter 5, Section 5.3.2 the evaluation was created such that it could also detect the influence of electrode properties. To achieve this, different sitting postures were evaluated using different machine learning classifiers with a multi- and single-user evaluation. The participants were both male and female in equal parts. 20 persons participated at the evaluation. They executed five sitting postures: sit upright, lean back, lean front, sit left, sit right.

For each sitting posture, we recorded a set of 100 samples, each with 5 measurement points, corresponding to the number of sensors. The test persons were shown images of the intended sitting postures. Afterwards they carried out each posture. Additionally to the 5 postures, data was also gathered with the empty chair and a person standing in front of the chair. We observed small variations between the different postures. One participant repeated the evaluation 5 times in order to gather more data for a single-user evaluation.

The data was evaluated with 15 different classifiers and 3 additional parameter variations of SVM. We used the implementations from the WEKA machine learning [HFH*09] in a leave-one-subject-out cross-validation. The results are shown in Table 3.4.

From the multi-user data set we present the results of five test persons in order to ensure a comparable data amount in relation to the singe-user data amount. The highest values of the achieved accuracy is 97.1%. It was achieved for the single-user data. The difference of more than 15% in comparison to the highest value of the accuracy (78,6%) achieved in the case of the 5 participants multi-user evaluation is significant. The difference with regards to the 20 participants multi-user evaluation is much higher than

Table 3.4.: Evaluation results per electrode type

		fabric		spiral		perimeter	
		mean	max.	mean	max.	mean	max.
multi-user	accuracy	51.8	62.1	58.9	72.6	56.4	**78.6**
	f-measure	43.8	55.8	51.3	67.7	49.2	73.4
single-user	accuracy	81.3	91.4	89.6	97.1	88.9	**97.1**
	f-measure	76.8	89.1	86.7	96.2	86.3	96.2

anticipated. The reasons for this are mostly to interpersonal variations in the posture execution and the properties of the participants bodies.

Among the evaluated classifiers the WEKA implementation of K-nearest neighbours (IBk), Logistic Regression Trees (LMT), Naive Bayes Multinomial and Support Vector Machine (SMO, SMO with RBF kernel) perform best and result in the maximum classification results. Considering the overall mean performance per classifier Naive Bayes Multinomial performs best closely followed by Multilayer Perceptron and K-Nearest Neighbours (IBk).

3.2.3. Summary

In Section 3.2 I have described a cushion for detecting sitting postures by using capacitive proximity sensing. This seat cushion is equipped with capacitive proximity sensors which track the proximity and motion of the sitting user and distinguish up to 7 postures. Giving a user immediate feedback on the posture can facilitate healthier behaviour.

The electrodes were made of conductive textile materials such as conductive fabric and conductive thread. We have experimented and evaluated different electrode layouts and electrode materials and confirm the design indications by building different prototypes. These were evaluated with data collected from 20 users and 15 different classifiers. Our prototypes reached the highest single and multi-user accuracies of 97.1% and 78.6%. This indicates that the appropriate choice of material and classifier can lead to high accuracies but are reduced when considering more users. Future systems should account for that using calibration routines.

3.3. E-textile couch: posture detection

Application areas like healthcare and Smart Environments have greatly benefited from embedding sensors into every-day-objects, enabling for example sleep apnea detection. The application presented in this section is based on the work published in my paper "E-Textile Couch: Towards Smart Garments Integrated Furniture" [RBK17]. The authors referred later on as "we" are Silvia Rus, Andreas Braun and Arjan Kuijper.

The concept of self-aware materials [Dem16] and producing digital textiles at scale [PGF*16] enables to view our surrounding materials and surfaces differently, leveraging unexpected invisible ubiquitous interactivity [MBRS14b, MBRS14a]. To address these advances, we investigate how smart textiles can be seamlessly integrated within furniture and demonstrate this on the couch as our use case. The interactions between human and couch, create implications about the surrounding context, creating a self-aware object of every-day use.

Posture recognition has been subject of many works [XLW*16, EIS*13]. Especially in the area of Ambient Intelligence it is of utmost interest to know as much as possible about the human as interacting counterpart in the surrounding intelligent landscape, to which knowing the posture is an important contribution. In many works posture recognition has been attempted using different variations of smart textiles [WTC*16, ZSC*16]. Zhou et al. [ZSC*16] have built a sensing band which monitors gym exercises. They use textile pressure sensors in order to track leg activity during exercising. Focusing on posture monitoring Wang has interconnected smart garments with wearable electronics on a vest for rehabilitation purposes [WTC*16]. Few works have already partly integrated smart textiles into furniture. Braun et al. have created a chair to recognize poses and activities creating awareness of correct posture [BFW15]. The chair is endowed with capacitive sensors where one electrode integrated in the backrest woven through the mesh of the chair using conductive thread. Examples of furniture able to recognize the posture of the occupying human are bed, chair and couch. In the bed the sleeping posture is investigated by several works, where different types of unobtrusively placed sensors are used. For example Chang et al., Braun et al. and Rus et al. use capacitive sensors placed underneath the mattress, attached to the frame of the bed, respectively underneath the bed-sheet in order to detect sleeping postures, lying postures and prevent decubitus ulcers as a consequence [CCCY14, DBM14, RGPK14]. Liu et al. use capacitive pressure sensors in a high-density sensor bed sheet for monitoring the patients rehabilitation exercises [LXHA13].

First approaches of detecting seating postures have been made by Tan et al. using a pressure sensor mat [TSP01]. They classify 14 postures achieving more than 90 % accuracy per posture. Eight postures were identified by using pressure sensors endowed in an office chair created by Nazari et al. [SYS14]. Braun et al. have created several prototypes of sensing chairs by using capacitive sensing [BSF15, BFMW15]. One prototype is meant to support training micro-breaks in the office while another is a sensing system for car seats. The second one is based on 16 electrodes connected to capacitive sensors with the goal of identifying different properties of the driver, like e.g. drivers head posture.

Couches have been endowed with sensors several times, mostly using capacitive sensors. Kivikunnas et al. present a sofa equipped with six metal foil capacitive sensors analysing basic sensor data [KSK*10]. Grosse-Puppendahl et al. evaluate nine different postures with a couch equipped with 8 capacitive proximity sensors achieving 97 % precision and recall [GPMB11]. By creating a network of furniture composed of bed, couch, and chair Heikkilä et al. envisage posture and activity tracking throughout the day [HSK*13]. Even though, the couch has been also equipped with sensors only long-time evaluations with chair and bed have been reported. More recently, the couch has been used as a sensing device by Pohl et al. for context sensing in a living room, controlling ambient lightning,

Figure 3.20.: Couch endowed with eight textile electrodes.

music and tv [PHK*15]. The couch is equipped with six capacitive proximity sensors, evaluating eight postures with an achieved accuracy of 92.9 %.

Our contribution with this work, is to extend the usage of smart textiles from the on-body wearables to the seamlessly integrated ambient objects, like furniture. In this paper we cover an ordinary living room couch as our use case. We extend state of the art by analysing a set of several fine-grained postures which will contribute to adjusting the environment to the users' needs.

3.3.1. Prototype

The production of conductive textiles at large scale envisages that sensing electrodes will one day be fully integrated into the covering materials and thus into the production process of furniture. Following this chain of thought our interactive couch prototype is enhanced by placing eight textile electrodes on the surface of the couch, see Figure 3.20. We created the electrodes by using pieces of 15x16 cm^2 conductive fabric, sewing a loop of wire to the fabric using conductive thread and gluing it to pieces of ordinary couch cover. Details of this process are shown in Figure 3.21. This process ensures that the electrodes are isolated and utilize materials used for the production of an actual couch.

The electrodes are connected to sensors which are connected to a capacitive sensing prototyping board, the OpenCapSense board [GPBB*13]. The raw sensor data is collected and processed in order to extract the posture of a person on the couch.

We evaluated the couch by asking 15 test persons (2 female, 13 male) to execute 14 different sitting and lying postures: 12 sitting poses, of which 3 using the armrest of the couch (see Figure 3.22), and 2 lying postures. At all times there was only one person on the couch. Including the empty couch we

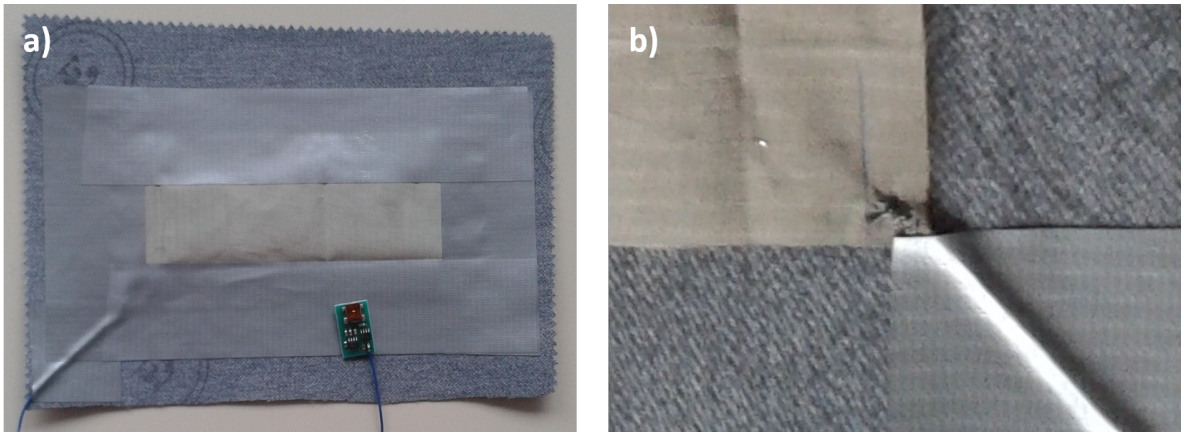

Figure 3.21.: a) Sensor and connected electrode made of conductive textile taped to regular couch cover sample. b) Sewn connection with conductive thread between textile and wire.

have evaluated 15 distinguished classes: empty couch; sitting upright, on right side; sitting on edge, on right side; sitting leaned back, on right side; sitting upright, on right side, using armrest in front; sitting leaned back, on right side, using armrest in front; sitting leaned back, on right side, using armrest at back; sitting upright, in the middle; sitting on edge, in the middle; sitting leaned back, in the middle; sitting upright, on left side; sitting on edge, on left side; sitting leaned back, on left side; lying down, head on right side; lying down, head on left side.

Figure 3.22.: a) Sitting upright; b) Sitting upright using armrest in front; c) Sitting leaned back using armrest in front; d) Sitting leaned back using armrest at back.

For each class we collected 30 data samples per sensor, which correspond to spending about 10 seconds in a given posture. The test persons were verbally instructed on how the posture should be executed. Only the desired position of the arm using the armrest has been marked at the position in front and back due to the more specific and smaller change in posture, harder to convey verbally.

We evaluated the data with leave-one-subject-out cross-validation using four different classifiers form the WEKA [HFH*09] framework. All classifiers were applied with their standard settings. The four classifiers are k-Nearest-Neighbours (kNN), naive Bayes, C4.5 decision tree (Weka J.48) and Support Vector Machine (SVM). At first, we applied them on the raw sensor data and subsequently on the normalized sensor data. In order to be able to compare the performance of conductive fabric electrodes with the performance of proximity capacitance measurements we selected the classes equivalent to the ones which were evaluated within the work of Pohl et al. [PHK*15]. These correspond to our classes $1-4$ and $11-15$.

3.3.2. Evaluation results

We have collected the raw data of 15 subjects and evaluated it with different classifiers. As input, we used the raw data, the per sensor normalized data and a subset of classes of the raw respectively the normalized data. The subset was chosen in order to compare the results of the fabric electrodes to the proximity sensing electrodes. The detailed results of the leave-one-subject-out cross-validation F-measure are shown in Figure 3.24. For each classifier we have calculated the overall accuracy and F-measure by compiling the mean of all leave-one-subject-out cross-validation results for the particular classifier. Table 3.5 shows an overview of the results.

Table 3.5.: Overview of classification results for C4.5, kNN, naive Bayes and SVM on different data sets.

	C4.5 decision tree		kNN		Naive Bayes		SVM	
Data	Acc.[%]	F-m.[%]	Acc.[%]	F-m.[%]	Acc.[%]	F-m.[%]	Acc.[%]	F-m.[%]
Raw	82.3	77.0	80.7	75.6	84.0	79.8	85.7	81.9
Normalized	89.1	86.0	88.9	86.2	87.2	84.1	**91.2**	**88.8**
Subset raw	83.3	78.9	87.5	83.9	89.7	87.0	90.45	88.1
Subset normalized	89.9	87.2	91.6	88.9	95.3	94.1	**95.5**	**94.1**

Comparing the overall results of the different classifiers, SVM produces the highest accuracy and F-measure. SVM performs on the normalized data an accuracy of 91.3 % and an F-measure of 88.8 %. On the subset of classes $1-4$ and $11-15$ SVM reaches even higher values of 95.5 % accuracy and 94.1 % F-measure.

These results outperform the results achieved by Pohl et al. [PHK*15]. Table 3.6 compares the accuracy achieved with the two classifiers kNN and naive Bayes which we used in common. For kNN our results were significantly better 91.6 % compared to 79.4 %. Pohl et al. achieved their best results with the naive Bayes classifier, reaching 92.9 % accuracy, whereas our prototype has achieved slightly more 95.3 % accuracy, only 0.2 % less than our overall best result of 95.5 % accuracy using SVM.

Grosse-Puppendahl et al. [GPMB11] have evaluated their prototype with a total of 9 classes. Six of these classes correspond to the classes evaluated using the current prototype. These classes are sitting

upright on left, middle and right side and lying down with the head on the right and the left side which correspond to classes 1, 2, 8, 11, 14, 15. The F-measure calculated from their precision and recall values of the individual classes is 97.5 % achieved using the RBF network. Selecting the same classes, using the current prototype, we achieve an F-measure of 99.8 %.

These results indicate, that using conductive textile electrodes reaches equally good results, slightly outperforming a system with electrodes placed under the couch cushions.

Table 3.6.: Performance comparison to related work.

	kNN	Naive Bayes	SVM
Pohl et al. [PHK*15]	79.4 %	92.9 %	-
Our work	91.6 %	95.3 %	95.5 %

The difference between the results of SVM on the normalized data and on the subset of normalized data is of 6 %. In order to find out, which of the classes cause the miss-classification, we inspected the confusion matrices of particular subjects. We chose to look at the subject with the lowest success rate, subject 4 (see Figure 3.23), and a middle success rate, subject 3. The confusion matrices indicate that classes sitting on the right, upright and on the edge were not differentiated at all for both test persons. Looking at the performance over all classes, in the case of subject 4 sitting upright and on edge were correctly identified, however differentiating between leaned back with arm in front and arm at the back were miss-classified as can be observed in Figure 3.23.

Subset of classes

a	b	c	d	e	f	g	h	i	<-- classified as
30	0	0	0	0	0	0	0	0	a = NONE
0	30	0	0	0	0	0	0	0	b = LEFT_UPRIGHT
0	0	30	0	0	0	0	0	0	c = LEFT_EDGE
0	0	0	30	0	0	0	0	0	d = LEFT_LEANBACK
0	0	0	0	30	0	0	0	0	e = RIGHT_UPRIGHT
0	0	0	0	30	0	0	0	0	f = RIGHT_EDGE
0	0	0	0	0	0	30	0	0	g = RIGHT_LEANBACK
0	0	0	0	0	0	0	30	0	h = LAY_HEAD_LEFT
0	0	0	0	0	0	0	0	30	i = LAY_HEAD_RIGHT

All classes

a	b	c	d	e	f	g	h	i	j	k	l	m	n	o	<-- classified as
30	0	0	0	0	0	0	0	0	0	0	0	0	0	0	a = NONE
0	30	0	0	0	0	0	0	0	0	0	0	0	0	0	b = LEFT_UPRIGHT
0	0	30	0	0	0	0	0	0	0	0	0	0	0	0	c = LEFT_EDGE
0	0	0	30	0	0	0	0	0	0	0	0	0	0	0	d = LEFT_LEANBACK
0	0	0	0	30	0	0	0	0	0	0	0	0	0	0	e = MID_UPRIGHT
0	0	0	0	0	30	0	0	0	0	0	0	0	0	0	f = MID_EDGE
0	0	0	0	0	0	30	0	0	0	0	0	0	0	0	g = MID_LEANBACK
0	0	0	0	0	0	0	30	0	0	0	0	0	0	0	h = RIGHT_UPRIGHT
0	0	0	0	0	0	0	30	0	0	0	0	0	0	0	i = RIGHT_EDGE
0	0	0	0	0	0	0	0	0	30	0	0	0	0	0	j = RIGHT_LEANBACK
0	0	0	0	0	0	0	0	0	0	30	0	0	0	0	k = RIGHT_UPRIGHT_ARMREST
0	0	0	0	0	0	0	0	0	0	0	30	0	0	0	l = RIGHT_LEANBACK_ARMRESTFRONT
0	0	0	0	0	0	0	0	0	0	0	30	0	0	0	m = RIGHT_LEANBACK_ARMRESTBACK
0	0	0	0	0	0	0	0	0	0	0	0	0	30	0	n = LAY_HEAD_LEFT
0	0	0	0	0	0	0	0	0	0	0	0	0	0	30	o = LAY_HEAD_RIGHT

Figure 3.23.: Confusion matrices of subject 4 for the subset and for all classes.

Taking only the miss-classification of sitting upright and on the edge on the right side, we could consider improving this by placing two electrodes on the sitting area, as has been done by Pohl et al. However, the fact that the two classes were correctly identified in the case of sitting on the left side and in the middle shows that it is possible to differentiate these poses in most of the cases. This means that one needs to consider a trade-off between the cost of using one or more additional sensors and accuracy.

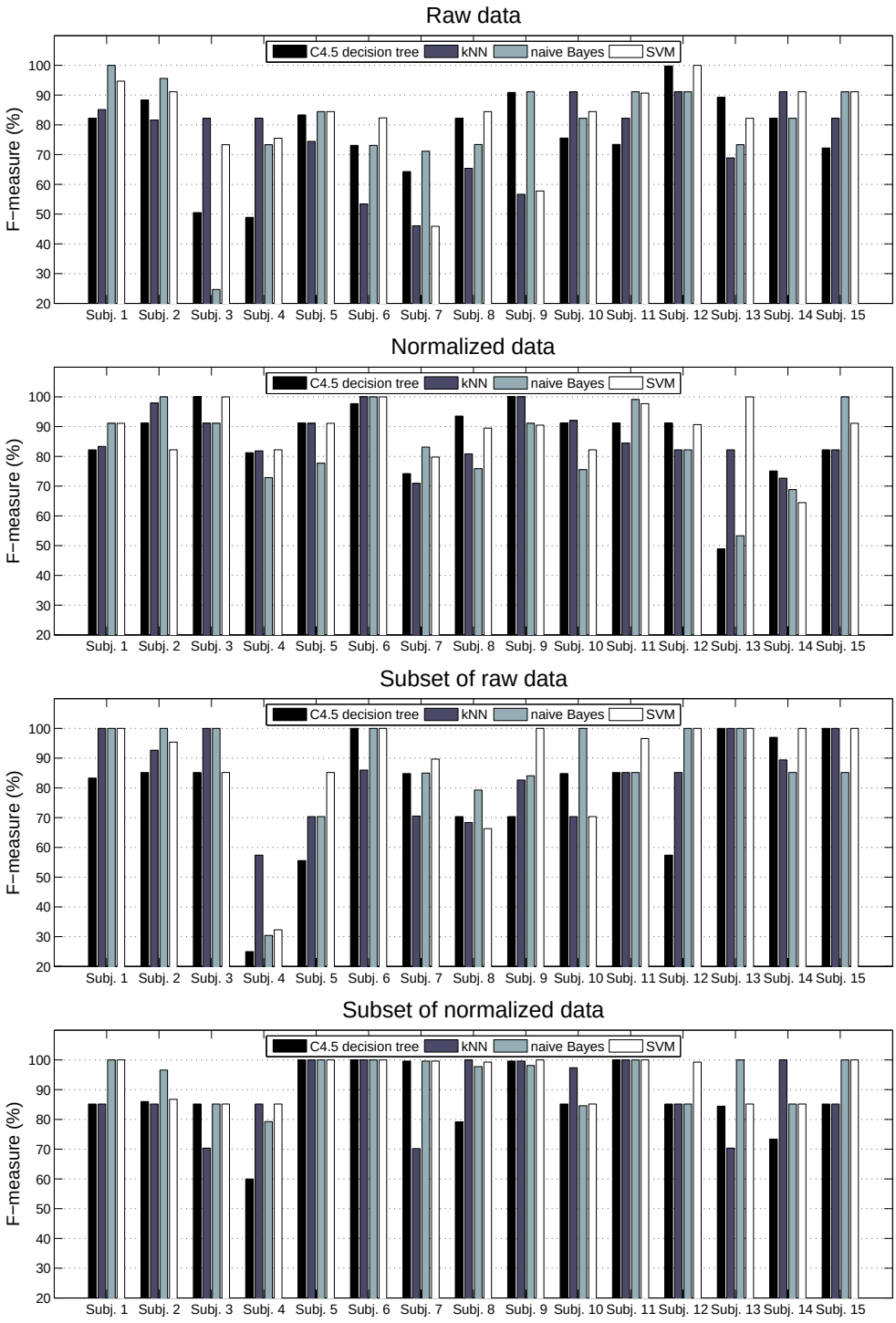

Figure 3.24.: F-measure of leave one subject out cross-valuation using different classifiers and on different data sets.

Regarding the placement of the arm, one single electrode does not seem to be enough to detect the position of the arm in a robust way. We are considering improving recognition rates with placing two electrodes on the armrest, one towards the front and one towards the back.

3.3.3. Summary

This section contributes to extending the usage of smart textiles from on-body wearables to seamless integration within ambient objects, like a couch. Conductive textiles used as capacitive electrodes yield as good results as capacitive proximity electrodes, slightly outperforming previous works.

The evaluation results show, that using conductive textile electrodes is equally suitable in order to detect postures. However, while attaching the textile electrodes to the couch cover, it became clear that integrating the electrodes with the couch cover has to be done by taking the design and shape of the couch into account. On a couch where three persons can sit down, but the sitting surface is made up of only two couch cushions one needs to consider the placement of the electrodes. Placing the electrodes underneath the couch cushion needs only one electrode to sense the user. Integrating the electrode into the cushion cover material would mean in the case of this couch to create two different electrodes, which could be connected to two sensors or connecting the two electrodes to one single sensor. Connecting multiple electrodes to one sensor could be used in order to increase the sensing area and would still send their signal to one single sensing unit. This approach could reduce conductive fabric material costs.

In order to be able to track a human skeleton motion model and measuring fine-grained postures there are a few steps to be considered: exploring conductive thread as electrodes, refining the placement of the electrodes and the number of electrodes needed. These concerns and further other concerns regarding the creation and the properties of conductive fabric and thread electrodes are further investigated in Chapters 4 and 5.

3.4. The emotion sensing couch

Our living environments are increasingly equipped with sensors and controlled devices that aim at supporting the inhabitants in their daily lives. Some of these sensors can be invisibly integrated into regular pieces of furniture to detect how humans act on or around those. The couch is a very frequent piece of furniture in the living room, often frequented while performing other activities, such as watching TV, reading books, or interacting with a smartphone. All of these actions can be a subject of affective human-computer interaction - based on the current emotional state, the content on the screens can be adjusted, or the lighting of the room to emphasize passages in a book, see Figure 3.25.

In this section I present such a couch, which aims to detect the occupant's emotions while protecting the privacy. This work is based on the paper "The Emotive Couch - Learning Emotions by Capacitively Sensed Movements" [RJBK18]. The authors are Silvia Rus, Dhanashree Joshi, Andreas Braun and Arjan Kuijper and are further referred by "we".

Over the years, research in emotion recognition has mainly focused on facial expressions, voice analysis and handwriting. Apart from these conventional methods, body movements, body postures and gestures or quality of movements can also be used to differentiate basic or fundamental emotions like happiness, anger, fear, sadness, or surprise. In case of fear, the body of a person contracts and muscles tighten, while in case of happiness, the muscles are more relaxed, and the body tends to occupy more space. Recognizing these emotions, based on presence and movement can improve the communication between human and machine in situations, where conventional methods of emotion recognition are impossible or undesired.

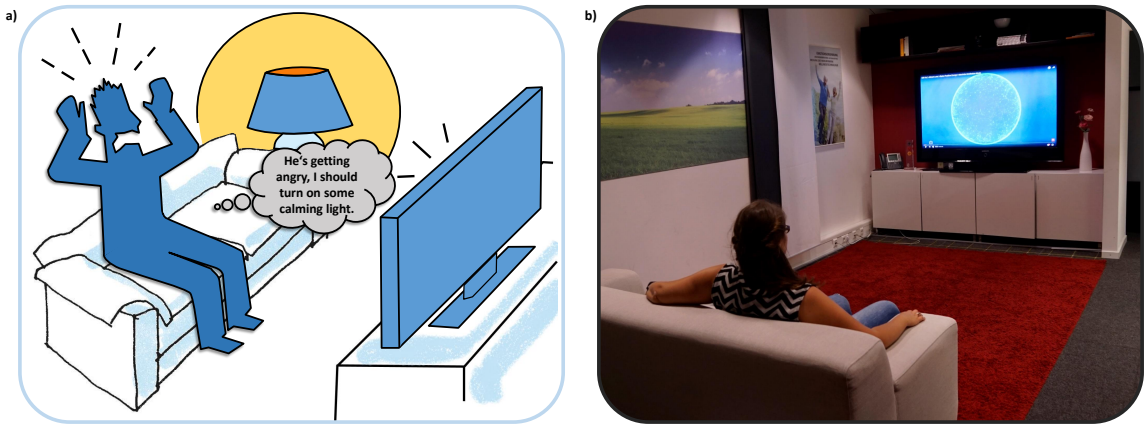

Figure 3.25.: (a) Based on emotional state the lightning of the room is adjusted. Invisible sensors in the couch sense the emotional movements and communicate with the lamp; (b) Living-room like Lab. The sensing couch is placed in front of a screen, creating a setting like watching a movie at home.

Ekman et al. have focused in 1978 for the first time on emotion recognition [EF78]. They found out that there is a basic set of emotions which humans universally understand independent of their cultural background. Emotion recognition is triggered by audio-visual signals abstracted and classified by the brain. These classes are decoded into emotions. The Facial Action Coding System (FACS) describes facial expressions according to the activated muscles. This system is largely used from psychologists in order to describe facial expressions. However, for emotion recognition not only mimic is used. There are a range of bodily signals which express emotions visually such as body posture or eye-to-eye gaze. Acoustically the frequency and the pitch of the voice are detected, next to other features. Bodily reactions mirror emotional states as well e.g. body temperature change, skin conductance, respiration, blood volume pressure, pupil size and heart rate [GCLF06].

Analysing speech for emotion recognition is not an easy task due to the complex configuration of parameters and feature selection [DPW96, LNP01]. Lee et al. reached an average accuracy of 76 % confirming results of Dellaert et al. at about 72 % mean accuracy. Hudlicka et al. state success rates for emotion recognition of about 63 % [Hud03]. More recently, Hasrul et al. present an overview of auditive emotion recognition with recognition rates between 41 and 96 %, where 96 % was reached classifying six emotions [HHY12].

Involuntary, according to our emotional arousal level, physiological signals show how our body prepares to react on the triggered emotion. The results in measuring physiological signals are comparable to human assessment reaching 81 % compared to 80-98 % by humans. Especially pupil size combined with gaze detection seems to lead to promising results [Hud03]. Multimodal physiological sensing has also been investigated. Picard et al. are detecting three different driving stress levels with 97 % accuracy. They are differentiating between happy and sad moods with 65-80 % accuracy [HP05, SYM*15].

Kleinsmith et al. have found that bodily expression is as effective as facial emotion detection. Body language might even convey emotions better, since it is harder to conceal emotions like with a "pokerface" [KBB13, BB16]. Furthermore, body postures also indicate what the reaction to the emotional stimulus might be. Initially, body postures were analysed from dance sequences [CMR*04] using cameras and depth cameras. Dance movements were later found to be overly expressive, not covering day-to-day activities. Thus, at first acted body movements were analysed, such as arm movements performing gestures like knocking or waving [PPBS01]. Later on the focus moved to more naturalistic movements in non-acted settings. Using depth cameras such as the Kinect, tracking acceleration, distances and angles between the 11 upper body joints, recognition rates of 90,8 % were achieved by Saha et al. for detection of five emotions [SDKJ14]. Camera systems work well when occlusion is not a problem and conditions such as lightning or background and viewing angle do not change too much. Wearables and sensors hidden in the environment are very well suited to ensure privacy since the identity of the user cannot be retrieved easily from video data [KSG*13].

While motion capture using wearables has been widely addressed [SSBB12], sensing body motion in ambient intelligence is not thoroughly explored. In previous work a multimodal system including a pressure sensing chair has been used to detect levels of interest and frustration of children [MP03, KBP07, DG09]. The chair was equipped with two matrices of pressure sensors, 2016 sensors arranged in a 42x48 grid, placed on the seating and leaning area. The chair reported nine pos-

tures of leaning forward, forward-to-left, forward-to-right, sitting upright, leaning back, back-to-left, back-to-right, sitting on the edge of the seat and slumping back. While determining three levels of interest, the system achieved 82.3 % for known test persons and 76.5 % for new test persons [MP03]. Using an additional camera, a pressure mouse and a skin conductance sensor the accuracy with which frustration was detected was overall 79 % [KBP07]. The accuracy rate for only posture detection was not reported, however the most discriminative features were found to be fidgets, velocity of head movements and the ratio of forward to backward postures.

In the past, this prominent role of the couch in our daily lives has been used to detect users and their posture [GPMB11] or even to express emotions using haptics, sound, and patterns [MBRS14a]. We present the Emotive Couch, which integrates sensors that track the proximity and motion of people on the couch. These capacitive proximity sensors detect changes in the electric field caused by the presence and motion of conductive objects, such as the human body [BWKF15]. The Emotive Couch uses flexible sensor electrodes that seamlessly integrate into the fabric of the couch [RSBK15].

3.4.1. Ambient affect sensing prototype

We challenge ourselves to achieve emotion recognition in an completely unobtrusive way, avoiding wearable sensors and ensuring a level of privacy which is more accepted as using cameras as sensing devices.

Body postures and movements are sensed using a couch equipped with eight capacitive proximity sensors [RBK17]. The sensors are distributed over the whole couch, minimizing the number of sensors needed to detect body postures. The sensing electrodes are flexible and are invisibly integrated into the couch cushion material. The postures which can be detected by the couch are leaning back, sitting upright, sitting on the edge, and lying down. When a person sits down on the left or right sitting area of the couch, three of the eight sensors are directly triggered. The nearby sensors also register slight changes due to their proximity sensing capability.

There are various systems which address establishing the link between emotions and movements. Movements are described from anatomical, directional and posture/movement point of view depending on the quality and type of movement. Coding systems are used to interpret and attribute the descriptions to specific emotions.

Since our system is able to detect movements and postures, we identified that the posture/movement description level is best suited for our work [FP14]. Different coding systems have been proposed to understand the bodily expressions of emotions based on postures and movements such as the Body Action and Posture Coding System (BAP). We use this coding system because it combines coding of both actions and postures. By checking how emotions are described in the BAP coding system we have selected which five emotions to detect.

Joy is described by various purposeless movements, jumping, dancing for joy, clapping of hands, stamping, head nods while laughing; during excessive laughter the whole body is thrown backwards and shakes or almost convulses; body and head are upright, arms are open generally above the head,

active movements. We chose to detect this emotion because most of these movements and postures imply whole body movement and less specific head or arm positions. In contrast *Sadness* is described by motionless or slow motions, head dropped on contracted chest, passive movements. With similar passive movements *Relaxation* is described by the whole body thrown backwards or sideways, arms open while seating and head backwards. Even tough *Sadness* and *Relaxation* are both described with passive movements, the body posture between them is expected to be different. When displaying *Interest*, the whole body is inclined forward, arms stretched out to the front, head straight, active or passive movements. *Anxiety* is characterized by short movement times and active movements.

These emotions are not only well suited because of their different characteristic body movement but are attributed to different quadrants of the Circumplex Model of Emotion which is used to place emotions in a 2D space with the dimensions pleasure and valence [PRP05]. The emotions in different quadrants are as far as possible from each other in order to be as different as possible in valence and pleasure, which eases the process of discriminating them.

3.4.2. Emotion detection study design

One of the major obstacles in evaluating emotion recognizing systems is to obtain non-verbal behavior which corresponds to realistic emotions. Carrying out experiments in the lab, a performer has to reproduce emotions by acting them.

Our lab is arranged like a living-room. As central part of the room, the couch is placed in front of a big screen a few meters away. This setting evokes very easily a feeling of watching a movie at home, see Figure 3.25b). We investigated emotion elicitation techniques which are suitable for this given setting. There are different methods to evoke emotions from a person in test laboratories. Such methods are imagination, repeating of phrases, music and film/videos.

We have researched emotion elicitation methods which correspond to our selected emotions. For eliciting *Joy, Sadness, Anxiety* we have selected videos, for *Relaxation* we play calm music and for *Interest* the user has to solve puzzles. We have chosen these elicitation methods because we think that these are most naturally suited for our living-room evaluation scenario. For *Joy* we show a compilation of funny baby videos. *Sadness* is meant to be induced by showing a scene from the movie "The Champ" which is generally approved to be a sad movie scene [GL95]. For *Anxiety* we chose a video of an individual performing parcours on top of a skyscraper. Calming images are accompanying music for *Relaxation*. For inducing *Interest* a few puzzles are shown with the task to search something in the image. Each activity lasts between 70 and 92 seconds.

Because acted and non-acted situations present different advantages [KBB13] we decided to try out both approaches, gathering body movements from elicited and from acted situations. For this, we have invited 15 test subjects (6 female, 9 male), aged 20-40 years into our lab. None of the test subjects had acting experience. Only one test person was allowed to enter the lab at a time. The experimenter was sitting in a different room. This assured the test person total privacy, in order to encourage natural reactions. After filling out some demographic information, the subjects were instructed to keep their mobile phones aside, in order to avoid disturbance. The test subject was instructed to sit on the right side

of the couch and watch the videos as though she would be at home. The lights of the lab were dimmed, and the videos started: first the video for *Anxiety*, followed by *Relaxation*, *Interest*, *Sadness* and *Joy*. The purpose of this order was to ease the transition between emotions. After each video, corresponding to a different emotion, lights were turned on and the user filled out a multiple-choice questionnaire, stating which of the presented emotions she felt during the last video and to which degree of intensity. This constituted *Round 1* of the experiment. After showing all videos, the experimenter explained to the subject, that the purpose of the experiment was to match motions to emotions. With this in mind the test subject was instructed to act all the emotions, supported by watching the videos a second time and by creating awareness of their movements by wearing a decoy sensing system. This constituted *Round 2*.

While the test subject was watching the videos and acting according to their emotions, the couch was providing eight values from the capacitive sensors. These eight sensor values are further on mentioned as raw sensor data. Additionally to the raw data, two features were computed. The first is the posture predicted by the couch and the second is the amount of movement.

We have evaluated the data using various combinations of features of which these two cases performed best: (1) raw sensor data; (2) all features: raw sensor data, movement, and posture. The data of the 15 test subjects was evaluated using leave-one-subject-out cross-validation. We used five classifiers to evaluate the data. We have evaluated the data by using Weka's implementation of C4.5 decision tree [Qui93]: J48, Weka's implementation of k-Nearest Neighbours [AKA91]: IBk, Weka's implementation of SVM using SMO [Pla98]: SMO, Weka's Naive Bayes classifier [JL95]: NaiveBayes and Weka's implementation of Random Forests trees [Bre01]: RandomForest. For each classifier we computed the average of the results of the 15 persons using leave-one-subject-out cross-validation.

3.4.3. Study results

The results of all evaluations are presented in Table 3.7. It shows accuracy and f-measures for different classifiers. *Round 1* denotes the part of the experiment where emotions are evoked and *Round 2* denotes the experiment where the subjects act the emotions. At first, we have computed results for two feature combinations considering all emotions. Subsequently we have considered a subset of emotions.

Comparing the overall results of different classifiers, Random Forest produces the highest accuracy and f-measure of 52.6 % and 48.4 % for five emotions in *Round 2*. For *Round 1* we achieved the highest accuracy of 43.6 % with SVM. Comparing the difference in accuracies between evoked and acted emotions from *Round 1* and *Round 2*, there is no notable improvement with differences of up to 3% for kNN (38.4% vs. 37.1%) , SVM (43.6% vs. 46.5%) and Naive Bayes (40.8% vs. 42.4%). However, for C4.5 Decision Tree (33.9% vs. 46.4%) and Random Forest (36.8 vs. 52.6%) there is a noteworthy difference of about 15%. The same pattern in difference between rounds is maintained in the results computed with all features.

During the experiments of our study, test persons mentioned the difficulty to act some of the emotions. Many participants reported that they managed to feel the emotions but did not know how to

Classifier	*Round*	*All emotions*				*Emotion subset*	
		Sensor Data		*All features*		*All features*	
		Acc (%)	*F-m (%)*	*Acc (%)*	*F-m (%)*	*Acc (%)*	*F-m (%)*
C4.5 Decision Tree	1	33.9	27.7	36.5	30.6	53.7	47.1
	2	46.6	40.6	45.2	40.7	66.4	61.5
kNN	1	38.4	31.0	38.0	32.5	56.3	48.1
	2	37.1	34.5	39.5	35.6	63.1	58.0
SVM	1	**43.6**	35.6	**42.0**	33.7	**62.2**	55.5
	2	46.5	39.7	48.3	40.1	**77.7**	73.0
Naive Bayes	1	40.8	31.5	40.5	30.5	54.5	45.5
	2	42.4	36.0	47.6	41.2	68.9	64.0
Random Forest	1	36.8	29.3	36.4	29.4	54.0	47.4
	2	**52.6**	48.4	**49.0**	43.9	68.6	63.4

Table 3.7.: Classification results of all emotions and a subset of emotions (Relaxation, Interest, Anxiety). All emotions are evaluated on two feature variations with raw sensor data only and combined with the features posture and movement.

manifest them. Especially with *Sadness* and *Joy* the test subjects mentioned that they were unable to translate those emotions into movements.

In order to find out which of the emotions causes miss-classification, we inspected the confusion matrices of multiple subjects. For the emotions *Sadness* and *Joy* almost all the instances are misclassified as *Anxiety*. By removing the two classes from the evaluation and evaluating the emotions *Relaxation, Interest* and *Anxiety* the accuracy increases by about 20 % reaching a maximum accuracy at 77.7 % in *Round 2* and 62.2 % in *Round 1*.

For three emotions, the probability of randomly picking the right class is at about 33 %. Having achieved a maximum average accuracy of 77.7 % is thus significant. Results indicate, that SVM could be a good general choice. Analysing individual results one can determine that for particular individuals, different classifiers reach the highest accuracies. Regarding evoked and acted emotions, the difference of 10-15 % between the two rounds shows that when acted, emotions classification results are better.

Our achieved results of 77.7 % for the emotions *Anxiety, Interest* and *Relaxation* are comparable with work of Mota et al. [MP03] and Kapoor et al. [KBP07]. Endowing a chair with a grid of 42x48 pressure sensors on the seating surface and on the backrest Mota et al. have investigated the level of interest. For three levels of interest they have achieved 82.3 % for test persons within the training set and 76.5 % for new data. Kapoor et al. have focused on detecting frustration. Complementary to the pressure sensitive chair used by Mota et al. their setup is equipped with a camera and a pressure sensing mouse. They achieved 79 % accuracy in detecting frustration. Due to the very different research questions it is hard

	Joy	Sadness	Relaxation	Interest	Anxiety
Effectiveness [%]	93	93	100	93	80

Table 3.8.: Effectiveness of evoking emotions using visual emotion elicitation methods

to compare the achieved accuracy for level of interest or frustration with detecting different emotions by means of ambient affect sensing.

The effectiveness of the videos which were used to evoke particular emotions was calculated by inspecting the sheets filled out by the participants during *Round 1* of the experiment. Table 3.8 shows with what percentage we achieved to convey the desired emotions. For *Anxiety* 80 % of participants found the video about parcours to evoke anxiety. In contrast 100 % of all participants found the music and the screen images to convey *Relaxation*. The emotions *Interest*, *Sadness* and *Joy* each achieved 93 %. These results show that we were successful in eliciting the intended emotions with an overall accuracy of 92 %. However, on some sheets of the participants the intended emotion was different from the perceived emotion. The perceived emotions may depend on many factors such as person's nature, his mindset during the experiment, his interests, etc. For example, the video showed for *Anxiety* can be perceived as interesting or can evoke joy if the person is adventurous. If a person looks for acting talent in a video, then she can find any video interesting.

During the experiment, the test subject was alone in the room. The experimenter was in other room with no line of sight thus the experimenter was unable to see the movements and postures that were taken by the test subjects. From the recorded data we observe a pattern between emotions and postures. For *Interest* most of the subjects were sitting on the edge of the couch while for *Relaxation* the subjects were sitting leaned back on the couch. These specific postures are responsible for the good results for the emotions *Interest* and *Relaxation*.

Movements of body parts like head, hands and shoulder play a major role in recognizing emotions. Because of the scarce placement of the capacitive sensors on the couch and the form of the couch, it is difficult to track the movements of head, shoulder, and hands. One way to overcome this without enhancing the couch is the use of wearable sensors. Another possibility would be to choose another kind of piece of furniture such as an armchair or a couch with a different form. If the couch would have a higher backrest or even a headrest one could track the head movements. By having sensors in the armrests arm and hand tracking would be possible.

3.4.4. Summary

In this section I presented a couch especially set up to measure emotional movements by sensing movements using capacitive sensors. The couch integrates capacitive sensors that track the proximity and motion of people. The couch gathers raw sensing data, posture, and movement data. It uses flexible electrodes which invisibly integrate into the cover material of the couch.

In a specifically designed study, we have gathered movement data from elicited and acted emotions of 15 participants. The sensed movements can be learned and linked to emotional states. For the classification of emotional states, we applied standard machine learning techniques and achieve 52.6 % accuracy for all 5 emotions *Joy, Sadness, Relaxation, Interest* and *Anxiety*. As expected, the results of the acted emotions were better compared to the elicited emotions. Analysing a subset of emotions *Relaxation, Interest* and *Anxiety* we have achieved results of 62.2 % for evoked emotions and 77.7 % accuracy for acted emotions.

I foresee a number of potential use cases for the Emotive Couch. The ability to assess emotion from motion can be used in applications for affective computing and beyond.

The data acquired from the Emotive Couch can be fused together with data from other devices that collect the affective state, such as cameras or wearables, to create a more complete picture of the users emotions, as well as increasing robustness and precision of the methods. This can also feed into a long-term assessment of changes in the users affective states that may be an indicator for mental disorders, such as depression.

The Emotive Couch can be used to personalize experiences based on the current affective states, particularly for applications that are performed on the couch. There could be selection or adaptation for multimedia playback, such as musical selection or movie loudness according to the current mood. When the system is linked to a home automation system this can be extended to control of the lighting situation.

The Emotive Couch can also be used in more engaged scenarios, such as interaction with smart phone or video games. The level of frustration while using the smart phone can be used by the current application to adapt their output in a beneficial way. The current affective state could also be used to adapt content, game play, and speed when playing a video game.

3.5. Conclusion

In this chapter, I presented contributions which feed into the first of the three research challenges *New flexible Smart Environment applications*. Through these contributions, I demonstrate that the untapped potential of embedding sensors into flexible surfaces is considerable and that it can be exploited. Thus, I present diverse prototypes from three different application areas.

The first area is the one of decubitus ulcer prevention [RGPK14, RGPK17]. I created a system based on a bed sheet that can be used in hospitals or at home, which alarms the caretaker looking after a bedridden person, if the person has spent too much time in a certain lying position. The prototype is composed of a wire electrode grid. Measuring the mutual capacitance between these electrodes allows for the detection of the presence of human body parts. The received sensor data is treated like an image of 48 pixels. After preprocessing and using machine learning, the bed sheet is able to recognize bed postures and therefore infer pressure points. The evaluation with 14 participants resulted in a overall accuracy of 80.8 %, with varying accuracy for different test person subsets achieving an accuracy of 93.8 %. The best overall accuracy has been achieved using a NN classifier on the raw data, yielding an

overall accuracy of 90.5 %. Compared to similar works, the bed sheet is affordable and easy to handle due to the wire grid, which allows for a high number of sensing points.

The second application area is back pain prevention by sitting posture monitoring and exercise tracking through a chair [RBKK19b]. Through different design iterations, I created a sitting cushion using 7 capacitive sensors with electrodes made of conductive textile materials that track the proximity and motion of the user. Even though previous works have achieved limited sitting posture detection, I extend the current body of knowledge by evaluating different e-textile electrode layouts. These were evaluated with data collected from 20 users and 15 different classifiers. The prototypes reached the highest single and multi-user accuracies of 97.1% and 78.6% demonstrating that the appropriate choice of material and classifier can lead to high accuracies.

The final application area to which I contribute in this research challenge, is differentiating emotions through sensing movements on a couch [RBK17, RJBK18]. I contribute a couch especially set up to measure emotion by interpreting measured movements. Through my work, I show that conductive textiles used as capacitive electrodes yield as good results as capacitive proximity copper electrodes when detecting lying postures, slightly outperforming previous works. I use the same setup to extend the sensing capabilities to motions from which I subsequently infer emotions. Initial results achieve 52.6 % accuracy for all 5 emotions *Joy, Sadness, Relaxation, Interest* and *Anxiety*. Different subsets of emotions *Relaxation, Interest* and *Anxiety* achieved results of 62.2 % for evoked emotions and 77.7 % accuracy for acted emotions.

While exploring the many possibilities to embed sensing into flexible surfaces and provide useful applications for their user, it is very motivating that high and very high accuracies could be reached. This shows that these systems are able to achieve their potential, once stable and seamless integration options of sensors into materials are possible. While I created these assistive applications using flexible materials, I encountered application design decisions I needed to take. This call to decide where to place sensors and how many are needed, led to the second research challenge, which I will address further throughout Chapter 4.

4. Simulation framework for designing flexible Smart Environment applications

Embedding sensors into fabrics can leverage substantial improvements in application areas like working safety, 3D modelling or healthcare, for example to recognize the risk of developing skin ulcers. In the previous chapter I have presented applications leveraging flexible surfaces, creating various assistive applications for Smart Environments. During the design process of these applications I have encountered the need to take different design decisions, such as where, which type of sensor and how many sensors should be placed. This led me to the second identified research challenge **New design tools for flexible Smart Environment**.

Finding a suitable setup and sensor combination for such a surface currently relies on the intuition of an application engineer.

I address this challenge by contributing in this chapter with: (1) an aiding tool for identifying the suitable number of sensors and layout, and (2) investigating the role of human intuition when designing a smart garment use case. In Section 4.1 I present the developed simulation framework. Its functionality is validated by comparing the simulated prototype with a real-world prototype for lying posture detection using a bed cover. In a second step, I use the validated simulation framework and investigate in Section 4.2 to which degree application designers can rely on intuition vs. expertise while creating an application with flexible surfaces.

The work in this chapter is an extended version of my papers [RHvW*18, RBKK19a] and the Master thesis of Felix Hammacher and Christian Gutjahr [Ham15, Gut17]. In this chapter we, the authors of these works, introduce following scientific contributions:

- We introduce a novel approach to simulate the application using flexible surfaces first and optimize the design to achieve better real-world implementations. In order to enable developers to easily prototype their shape-sensing scenario, we have implemented a framework that enables soft body simulation and virtual prototyping.
- We confirm the validity of our framework by comparing the simulated and real evaluation results of a virtual and a real-world prototype for the use case of lying posture detection.
- We investigate how well human intuition helps to design a smart garment application on flexible surfaces and to which extent sensor expertise plays a role in the design of these.

4.1. Prototyping applications for flexible surfaces through simulation

This Section is based on my paper "Prototyping Shape-Sensing Fabrics Through Physical Simulation" [RHvW*18] and the Master's Thesis of Felix Hammacher [Ham15]. The authors referred to as "we" are Silvia Rus, Felix Hammacher, Julian von Wilmsdorff, Andreas Braun, Tobias Große-Puppendahl, Florian Kirchbuchner and Arjan Kuijper.

The rapid development towards miniaturized sensors and bendable electronics has led to new concepts for shape-changing and shape-sensing devices [DMW*18, TKG*15, SJM13, KLMS11, RSL14]. Contrary to the traditional usage of cameras for shape-sensing, which suffer from occlusion, lack of mobility and lack of acceptance, sensors integrated into everyday materials can leverage fine-grained shape detection supported by developing bendable sensors [RGPK14, GSO*14, CLY10, SPM04, RKF*14]. One consequence of integrating sensors into everyday materials is the approach towards developing "Everything" as a Material, like Displays as a Material [SCHGP16], Microcontrollers as a Material [MJB*13] and Self-Aware Materials [Dem16] which are self-aware of their shape and deformation.

It is common to simulate prototypes in a virtual surrounding to see if the planned hard- and software is capable of fulfilling their desired purpose before they are built in real hardware [Ž08, ELDL11], especially in robotics research. Several robotic simulators have been implemented that integrate virtual sensors and use them together with other virtual robots [SM11]. Since robots are mostly made of rigid materials, none of the robotic simulators were found to be able to attach virtual sensors to soft materials, like fabrics and thus simulate our shape-sensing fabric. However, there are multiple existing shape-sensing fabrics approaches which we address in the following.

Flexible, self-sensing objects, which know their current shape and report their deformation have recently been in the focus of different works using technologies like piezoelectric, resistive and capacitive sensors [RKF*14, GSO*14, LGBV11, LRS*04]. An example of a self-sensing flexible surface is FlexSense, a piezoelectric transparent foil which can sense if it is bent. It is used as input foil for tablet interaction [RKF*14]. PrintSense is a similar approach for manipulation detection of flexible surfaces using capacitive sensing [GSO*14]. Resistive sensors enable the users of the PaperPhone to interact with its bendable corners [LGBV11]. Lorussi et al. create a piezoelectric sleeve which detects the arm bending [LRS*04]. All of these examples have as a goal to determine their shape and use this information for the use case at hand.

Additionally, there are a few approaches using inertia and magnetic sensors added on flexible surfaces, in order to determine their shape [DKP15, WTC*16, Wan16, HCG15, HN12, SSJLB14, HS08, HCG15]. The Three-Dimensional Capture Sheet measures its own shape only by using embedded inertia and magnetic sensors [HS08]. It produces a 3D-mesh without external devices, by attaching inertia sensors onto rigid links connected at their ends, forming a lattice structure. By determining the orientation of each attached sensor, the orientation of the corresponding link can be distinguished. The theory and a simulation of an exemplary 13x13 lattice structure shows the feasibility of using the orientation, measured via accelerometer and magnetic sensors, for shape reconstruction. However, only a small prototype with a 3x3 grid using 24 sensors, attached to the grid links, was realized.

MorphoShape consists of a rectangular piece of fabric embedding a 3x3 grid of inertia sensors [SSJLB14]. Although MorphoShape only uses 9 sensors (accelerometers and magnetometers), its reconstruction algorithm, based on curves, provides a realistic interpolation of the whole prototype. Hermanis et al. have developed two shape sensing prototypes [HN12, HCG15]. The first was comprised of a 4x4 acceleration sensor grid used for body posture recognition. The sensors were attached to clothing on the back. The second prototype was based on inertia sensors sewed into two layers of freely bendable fabrics. The 63 embedded sensors are aligned in a 9x7 grid.

In a similar manner Wang et al. have demonstrated Zishi, a wearable smart garment based on intertial measurement units monitoring the shape of the back of a person for rehabilitation purposes [WTC*16, Wan16]. Demetyev et al. have developed a cuttable SensorTape, where each sensor node has inertial, infrared, and light sensors gathered on a flexible substrate [DKP15]. Demonstrating the capability of their rapid prototyping they attach the tape to the back of the person, recording and displaying its deformation.

Having a flexible shape-sensing fabric use case, the engineer needs to decide on how to equip and distribute sensors across his shape-sensing surface. He has to try out different designs with solely his intuition to work with regarding type, number and placement of sensors. Even though supporting tools like simulators are well known in the robotics area they are only suited for rigid object simulation and not for flexible surface simulations [Ž08]. We close this gap by providing a tool for designing virtual prototypes for shape-sensing fabrics.

4.1.1. Simulation framework

Our proposed simulation framework offers tools to create and run a physical based simulation in real time. This simulation can not only contain physical objects interacting with each other, but also sensors attached to them. Instead of just being able to attach sensors to rigid bodies, like in most robotic simulators, sensors can also be attached to soft bodies. Thus, it enables a user to simulate the fabrics with embedded sensors.

4.1.1.1. Virtual sensors

The sensors currently included in the simulation framework are acceleration sensors and combined acceleration and magnetic sensors. The first ones only offer tilt sensing, the latter complete orientation sensing. Tilt sensing only measures the orientation of the sensor relative to earth's surface.

A 3-axis accelerometer measures it's acceleration in three local perpendicular axes. When left motionless, the accelerometer measures a fixed acceleration of 1 g (9.81 m/s^2) towards the earth center, due to the gravity of the earth. This gravity direction is used as axis to determine the tilt of the sensor relative to the earth frame. The tilt consists of the roll, the rotation around the earth-frame x-axis, and the pitch, the rotation around the earth frame y-axis of the sensor, as shown in Figure 4.1. They can be determined by calculating the angles between the reference Z_{earth}-axis and the local Z_{local}-axis of the sensor in the YZ- (roll) and the XZ-plane (pitch) respectively. The yaw, the rotation around the earth-

frame Z-axis, cannot be measured since the reference Z_{earth}-axis stands always perpendicular on the XY-plane and thus the angle between the Z_{earth} and Z_{local} is always zero. Furthermore, an accelerometer cannot distinguish between acceleration caused by gravity or by movement, thus it is not well suited for orientation measurements in non-linear motion.

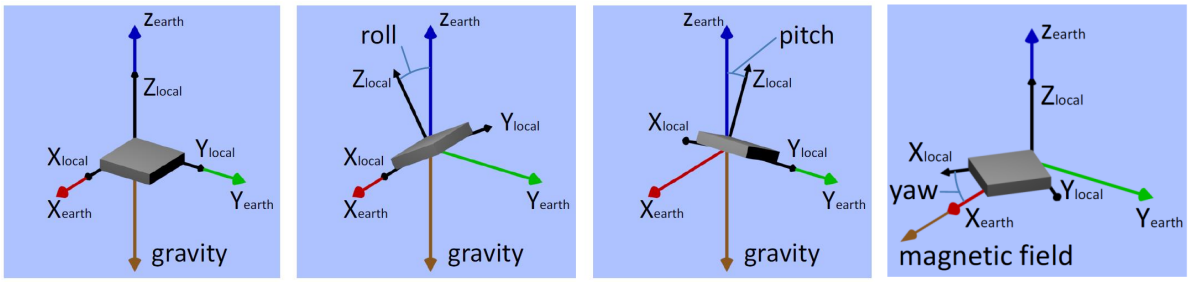

Figure 4.1.: Tilt sensing and orientation using an accelerometer-magnetometer combination [Ham15]

A 3-axis magnetometer measures the strength and direction of the magnetic field around it. If no other magnetic field is created, the only measurable one is the magnetic field of the earth pointing towards its magnetic north. Thus, the magnetometer can be used as a compass providing the direction towards magnetic north. In the right image of Figure4.1 the direction of the earth magnetic field is chosen to be aligned to the global X_{earth}-axis. By calculating the angle between the global X_{earth}-axis and the local X_{local}-axis in the XY-plane, the yaw of the sensor is determined.

Since both sensor types only provide a single reference vector, none of them alone can be used to calculate their complete orientation around all three global axes. Complete orientation sensing also includes knowledge of the cardinal direction the sensor points at. The sensor types offer different advantages and disadvantages for shape-sensing, shown in Table 4.1.

Table 4.1.: Advantages and disadvantages of different sensor types for shape-sensing fabrics

	Advantages	Disadvantages
Tilt sensing	• no calibration needed • cheap • software faster • less affected by wrinkles in fabric	• restricted to 90 degree bending • less precise if sensor grid yawed
Complete orientation	• no restriction due to bending • can handle yawed sensor grid • higher precision • better surface reconstruction possible	• more affected by wrinkles • calibration necessary • more expensive • software slower

4.1.1.2. Import realistic objects

The simulation framework is based on the bullet physics engine. This provides several types of objects: rigidbodies and softbodies. Rigidbodies are solid objects, which are not deformable. Their behaviour depends on many adjustable physical properties of the physics engine, such as friction and mas. Besides basic shapes such as spheres and cubes, the simulation framework provides the possibility to load OBJ files.

The fabrics in the simulation framework are represented by softbodies. These are soft structures, which can be deformed by external forces. These are directly applied on the nodes of the softbody mesh or as result of the impact with another object. A softbody consists of nodes connected by links. Depending on the configuration of the softbody 3-4 nodes connected by links form a face - a surface. The links act like springs, which exert force on the nodes. This force is defined by the link stretchability. By adding up the forces on the nodes, the impact on the whole softbody is calculated.

The number of nodes, and thus faces and links, depend on the resolution of the softbody. With an increasing number of nodes at the same expand of the softbody its resolution increases as well. A higher resolution provides more realistic behaviour, because the softbody can bend more freely. The collision detection between softbody and another collision object is also more accurate. Figure 4.2 shows the different accuracies of a softbody with 10 x 10 and 20 x 20 nodes in the same situation. Rising the resolution of the softbody leads to more calculations, what can prevent the simulation from running in soft real time.

Besides the possibility of using forces to interact directly with the nodes of a softbody, bullet provides the possibility to create anchors between nodes and rigidbodies. A softbody node connected to an anchor moves according to the rigidbody the anchor is attached to. A flag for example consists of a piece of fabric fixed to a flagpole. In the simulation the fabric is represented by a softbody, the flagpole by a rigidbody. By attaching the lower and the upper right node with an anchor to the rigidbody, the softbody follows the movement of the rigidbody like a real flag would. Anchors can be set and removed in the simulation-framework to help the user to create the desired scene.

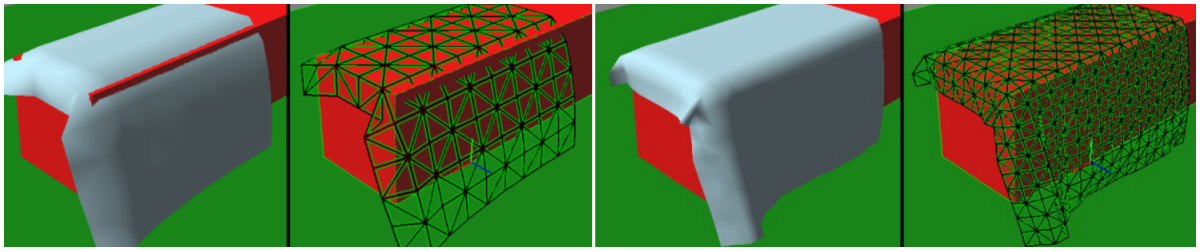

Figure 4.2.: Softbody with 10x10 and 20x20 resolution [Ham15]

In order to create scenes with realistic objects, complex meshes can be loaded. These meshes could be taken from databases or being custom created. A possibility is to use a depth camera to create a

high-resolution 3D shape of the object we want to import. In order to import this in the simulation framework, these shapes have to be transformed to meshes with lower resolution.

4.1.2. Simulation framework use case: sleeping posture recognition

The proposed simulation workflow, shown in Figure 4.3, eliminates the need for designing and building the hardware equipment. We introduce and evaluate a simulation framework for shape-sensing fabrics, which enables developers to investigate designs of applications prototypes, before any hardware installation. First, the application developer scans a several shape-sensing scenarios. With this representation, we provide the developer with a tool to estimate the desired level of accuracy, deciding on the trade-off between accuracy and number of sensors suitable for this use case. Finally, when the application developer is satisfied, the system can be implemented.

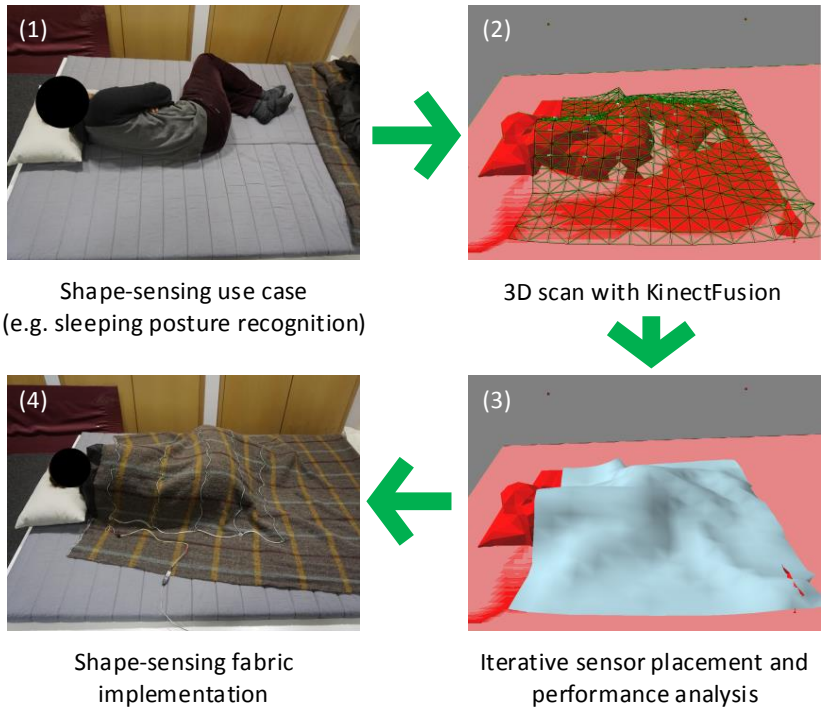

Figure 4.3.: Prototyping support of shape-sensing fabrics including simulation and refinement phase into workflow. First, we 3D-scan several scenarios e.g. sleeping posture recognition (1) to create a mesh representation (2). On this mesh, we place a virtual prototype of a shape-sensing fabric with simulated sensors (3). The classification performance is iteratively analysed, allowing the application developer to implement the best-performing shape-sensing fabric (4).

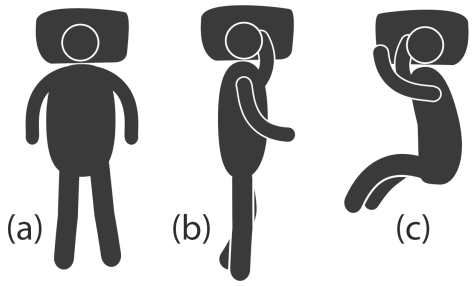

Figure 4.4.: Evaluated sleeping postures: (a) supine and prone; (b) straight left and right; (c) left and right fetal.

In order to show the workflow for simulation-aided prototyping of hardware and software, we choose sleeping posture recognition as application for shape-sensing fabrics. We cover a sleeping individual with a sensor embedded bed cover, which adapts to her body posture. The bed cover senses the shape of the person lying underneath and deduces her sleeping posture.

In this section we present the workflow, that supports planning the hardware for this specific use case like deciding on different dimensions of a prototype, the number of sensors and the sensor layout. This is achieved by creating a virtual prototype first. Subsequently, we describe the real prototype built according to its model, the virtual prototype. The description of the two prototypes, virtual and real-world prototype, is followed by a detailed comparison and evaluation in the validation section.

4.1.3. Creating a virtual prototype using the simulation framework

Our proposed simulation framework offers tools to create and run a physical based simulation in real time. This simulation can not only contain physical objects interacting with each other, but also sensors attached to them. Instead of just being able to attach sensors to rigid bodies, like in most robotic simulators, sensors can also be attached to soft bodies. Thus, it enables a user to simulate fabrics with embedded sensors. The sensors currently included in the simulation framework are acceleration sensors and combined acceleration and magnetic sensors.

Our shape-sensing fabric is comprised of a bed cover equipped with acceleration sensors. Before a hardware prototype is created, the simulation framework is used to test different sensor layouts which are suitable for the use case. The simulation framework provides a way to quickly generate sensor output for different virtual prototypes. Even huge amounts of sensors become manageable. Although a higher resolution of sensors leads to a more precise shape reconstruction, embedding more real sensors on a real prototype is very complex. To find the optimal solution for the trade-off between precision and complexity, the simulation framework is used. For this, we create the scene of the use case in the virtual environment of the simulation framework. The virtual bed cover consists of a soft body with 36 x 36 nodes and virtual sensors. Sensors can be attached to each of the nodes. This way, the behavior of the

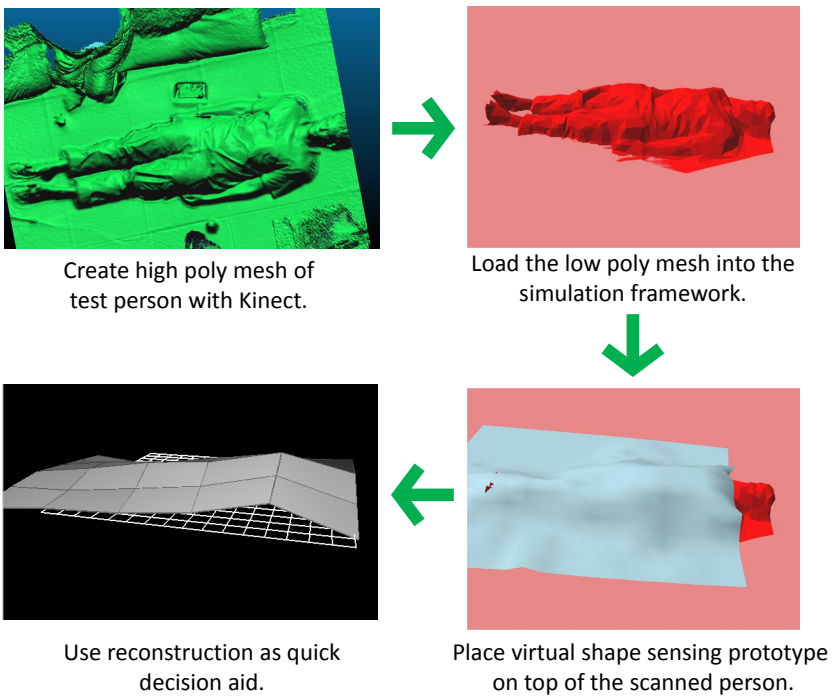

Figure 4.5.: Virtual prototyping workflow: the high-resolution mesh of a sleeping posture is created using a depth camera (upper left); this mesh is preprocessed creating a mesh of lower resolution, which is loaded into the simulation framework (upper right); the virtual bed cover equipped with sensors falls on the virtualization of the sleeping posture and delivers the according simulated sensor data (bottom right); the reconstruction of the surface calculated from the sensor data is displayed (bottom left).

soft body only slightly changes because of the weight of the attached sensors. Different resolutions of nodes instead would cause a different behavior of the bed cover.

For evaluating the analysed use case in the virtual area of the simulation framework, the ground truth of the use case has to be gathered and virtualysed. We have decided on detecting 6 common sleeping postures, depicted in Figure 4.4: lying on the back, on the stomach, on the left and on the right side with stretched legs and lying on the left and right side in foetus position. This ground truth is gathered by using a depth camera, in this case we used the Microsoft Kinect v2 and the free software KinectFusion. The outcome of this process, a raw high-resolution mesh of a test person is shown in Figure 4.5. After this initial 3D capture of a test person, all unnecessarily captured objects in the surrounding have to be eliminated. This is done be registering the persons 3D shapes against each other and cutting around the object of interest. The result from this process is a high-resolution mesh of the test person. In order to load this high-resolution mesh into the simulation framework, a lightweight low resolution mesh of

the test person has to be calculated. We chose to use Cloudcompare[1] for registration and Meshlab[2] for lowering the resolution of the 3D mesh. Finally, the lower resolution mesh is introduced in the simulation framework, shown in the upper right of Figure 4.5. In the bottom right, the mesh of the sleeping posture is covered by a soft body, the bed cover, which is equipped with the virtually modelled sensors. The sensors provide virtual sensor data of the softbody covering the 3D mesh of a sleeping posture. This data is passed to the classification algorithm where the sensor data is classified using a Support Vector Machine (SVM). Using the reconstruction algorithm, the reconstruction visualizes the sensed shape.

Initially, we have scanned two sets of sleeping postures from two test persons. We loaded the 3D shape data into the simulator using the process described in Figure 4.5. The next step was to decide on the positions of the sensors on the virtual bed cover - the layout. Due to resource limitation, the maximum number of available sensors was 40. Hence this number was used as a starting point. However, in the validation section we describe evaluation results in more detail, where the number of sensors varies and further adapts to our use case. For now, this number of 40 sensors was used to compare three different virtual layouts: one where the sensors were equally dispersed on the bed cover, one where the sensors cover the person underneath and one where the upper part of the body and the sides of the bed cover are occupied by sensors (see Figure 4.10. As a quick aid on deciding which layout was more suitable, we analyzed the reconstructed shape. The third layout showed the best recognizable shape for the human eye, hence we decided for the upper body covering layout. Even though, at this moment a human looking at the reconstructed image of the simulated sensor data was used to decide on the most suitable layout, further evaluations support this decision and are described in the validation section.

4.1.4. Creating the real-world prototype hardware and software

As a result of the virtual prototype simulation, the layout with the best results in detecting the sleeping posture was identified. This input is used to build a real-world prototype consisting of 40 sensors, arranged in a 5x8 grid. As shown in Figure 4.6, the extracted distances between the sensors from the simulated layout are 14 cm and 21 cm. These dimensions were chosen to cover a human torso using 40 sensors. The sensors are linked by three wires, two power lines and a bus-line for communication. The wires are sewn to the bed cover. Since the bed cover is deformed by every underlying object, the power lines as well as the bus-line have to withstand physical stress. In order to compensate for possible single point of failures in the links between the sensors, the links were built redundant on every side of the bed cover, as schematically depicted in Figure 4.6. The reason to not link each sensor to its neighbors is to preserve the flexibility of the bed cover.

Each sensor uses an accelerometer to detect its current orientation. The accelerometer is connected to an 8 MHz microcontroller via I^2C. The microcontroller transfers the data using the UART protocol. This was chosen in order to minimize wire-usage, as only one is required for transferring data.

[1] http://www.danielgm.net/cc/

[2] http://meshlab.sourceforge.net/

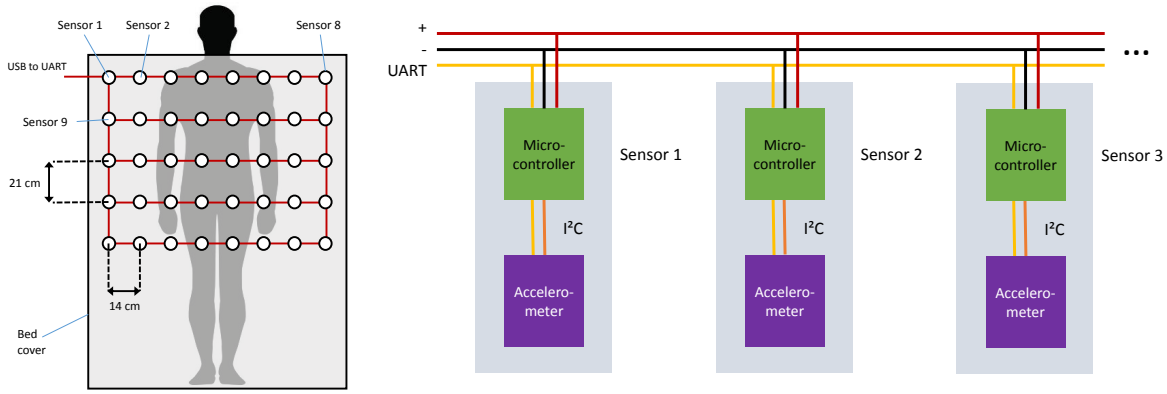

Figure 4.6.: Schematic of hardware implementation of posture recognizing bed cover. 40 sensors are aligned in a 5x8 grid, connected via bus and redundant power lines. Each accelerometer is connected to a microcontroller which communicates using the UART protocol. Dimensions and layout are outcome from the preliminary layout evaluation.

To transfer the data to a computer, we use a simple, yet fast protocol. Each sensor has a fixed, programmed address. The first sensor sends two start-bytes and the data of the accelerometer periodically in a fixed interval of time. The second sensor, as all other sensors, is counting the amount of data that was transferred over the bus. After the first sensor has sent all of its data, the byte-count of the sensor with address 2 will be $(sensoraddress - 1) * NumberOfBytesPerSensorData$. Then the second sensor starts transmitting. All other sensors follow the same procedure. The byte-count of all sensors is set to zero and the procedure is repeated if the start-byte, transmitted by sensor 1, is received. Using this method, all the 40 sensors can be read at a rate of more than 20 Hz.

4.1.5. Validation of simulation framework

We used the simulation framework for designing a virtual prototype for the exemplary use case of sleeping posture detection. Following its virtual model, we have built a hardware prototype. In order to validate the correct results of the simulation framework, the results of the evaluation of the virtual prototype will be compared against the results of the hardware prototype. Hence, in the following sections we will describe the evaluation setup used to gather data which will be used for comparing the simulated and the real prototype. We will further analyze in more detail the influence of the number and placement of sensors for this use case.

In order to compare the virtual and hardware prototype designed and built for sleeping posture detection, we asked 10 participants to carry out six different lying postures on a bed, depicted in Figure 4.4. The set of participants was predominantly male, with 8 male and 2 female participants. Each person repeated a lying posture twice. For each posture, we executed the steps shown in Figure 4.7.

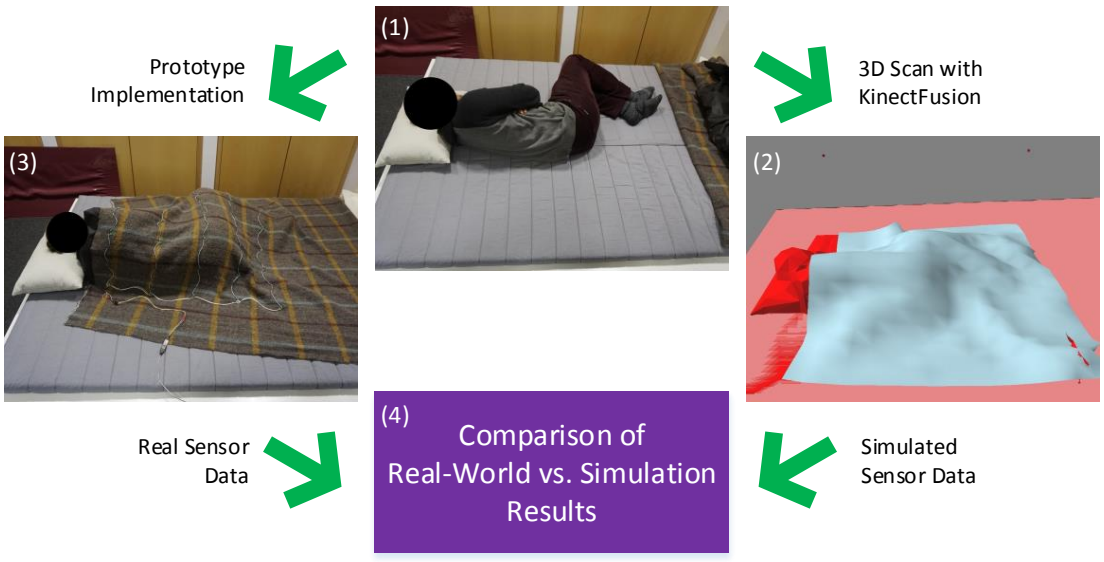

Figure 4.7.: Evaluation steps: (1) instruct test person to lie down; (2) the 3D shape of each posture is recorded and used in the simulation framework where the virtual prototype provides virtual sensor data; (3) the test person is covered with the real prototype gathering sensor data; (4) the real and the virtual sensor data are evaluated and compared.

First, we verbally instructed the participants to lie down in the different sleeping postures, not giving any further instructions. This assures highest resemblance to a natural setting. As a second step, we scanned the person in the sleeping posture using a depth camera. Next, we covered the person using the real-world prototype and gathered a sample of 500 sensor readings for each sensor. The whole process of scanning each of the six sleeping postures twice and gathering the sensor data using the real prototype lasted one hour per test person. The 3D shape of the test persons is used as input for the evaluation using the simulation framework. We have described the process of loading the 3D shape into the simulation framework, which is shown in Figure 4.5. Once the shape is loaded, the virtual bed cover hung on top of the shape is released and falls on the test person. Using this setup, for each sleeping posture virtual sensor data is collected.

As a result of the evaluation, we have collected sensor data corresponding to the sleeping postures from the real, as well as from the virtual prototype. To classify this data, we used Weka's implementation of the Support Vector Machine (SVM) classificator LibSVM with adjusted parameters (SVMType: nu-SVC, normalize: true).

For each sleeping posture we have recorded a set of 500 data samples per sensor. We calculate the mean value per sensor per sleeping posture. Joining the data of all the sleeping postures, we recorded 12 sleeping postures, two times six postures, per test person. As a final result, we have two data sets of the 10 test persons, one for the hardware prototype and one corresponding to the virtual prototype.

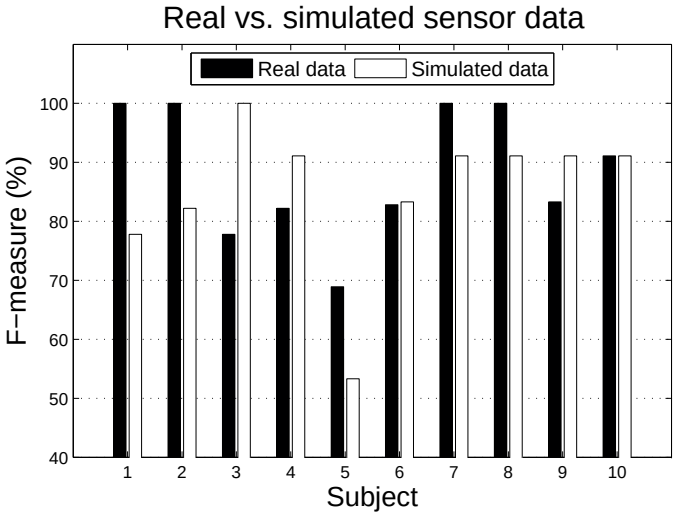

Figure 4.8.: Classification results of leave one subject out cross-validation of 10 test persons for real and simulated sensor data recorded by the hardware and virtual prototype for sleeping posture detection.

For each data set a leave one subject out cross-validation has been conducted, the results of which are shown in Figure 4.8. The Figure shows the resulting F-measure for each test person by evaluating

real and simulated data. We observe that the real and the simulated estimation are not far apart. The overall F-measure for the real data is 88.6 % and 85.2 % for the simulated data, resulting in a slightly more pessimistic F-measure of the simulated evaluation.

The small difference is caused by the slightly different execution of the simulated and the real evaluation. In the real evaluation we covered the test person with the bed cover. In the simulation the bed cover falls on the test person, causing the sensor node placement to be slightly different. Another influencing factor might be the parameters of the bed cover itself, which need to be set in the simulation framework. These slightly differ from the real bed cover.

4.1.6. Determining the optimal number of sensors and optimal sensor layout

In order to find out which number of sensors would be optimal for our application, the simulation framework can be used to easily equip the virtual prototype with simulated sensors. Hence, the simulated bed cover has been equipped with different numbers of sensors, ranging from 4 to 676. We distributed the sensors homogeneously in order to cover the full surface of the bed cover. The simulated sensor data has been recorded by letting the bed cover with different numbers of sensors fall on the 3D shape of the 10 test persons. The same evaluation process, mean calculation of F-measure of the leave one subject out cross-validation using SVM, results in the mean F-measures depicted in Figure 4.9.

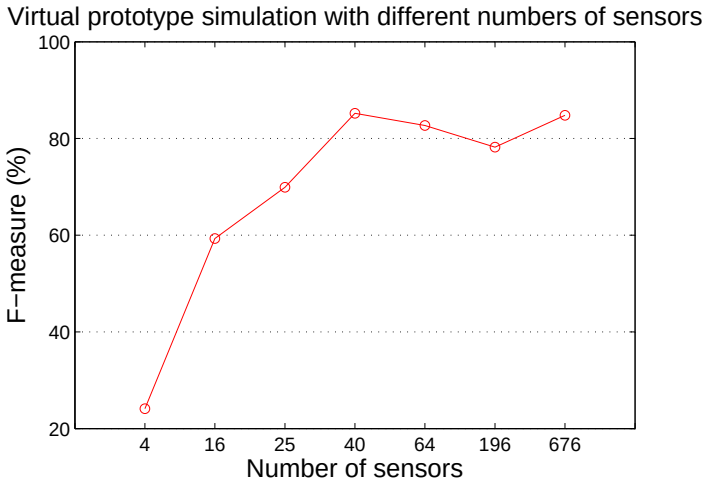

Figure 4.9.: Mean F-measure of total coverage layout with increasing number of sensors. Using the simulation framework up to 676 sensors are simulated on the prototype. The F-measure versus number of sensors trade-off is reached using 40 sensors.

We observe that in the interval of 4 to 40 sensors the highest F-measure gain is achieved, with its highest value at 40 sensors. Further increasing the sensor count to 64, 196 and 676 does not significantly

improve the results. Possible reasons might be that more sensors do not offer additional information that improves the feature selection. This is caused by the redundancy of information or because of over-fitting produced by sensors detecting small wrinkles in the bed cover. Hence, the simulation results confirm the trade-off between sensor count and improved F-measure as well as the decision of using the 5x8 grid of 40 sensors in the hardware implementation of the real prototype.

In a second step we compare different possible sensor layouts using the same sensor count of 40 sensors and evaluate these. Figure 4.10 shows the three evaluated sensor layouts. The left image of Figure 4.10 shows the equally distributed sensors covering the entire prototype. In the middle we see the 5x8 sensor grid in a more constrained area, covering the entire body of the test person. The third image at the right shows a combination of the previous two layouts covering the upper body and the sides of the bed cover. Underneath the images, the mean F-measure per layout is shown, reaching the highest value of 85.2 % with the upper body coverage layout.

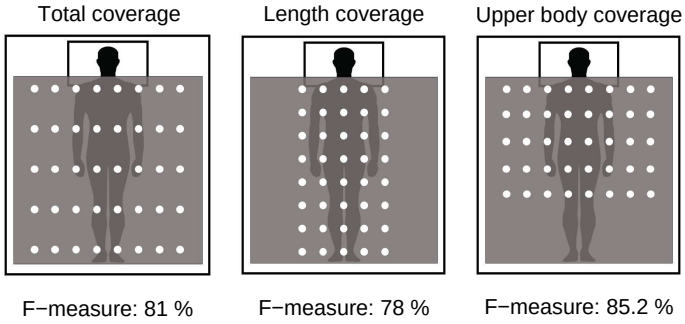

Figure 4.10.: Layout comparison of three different layout designs with 40 sensors evaluated using the simulation framework. The layout covering the upper body achieves the highest F-measure of 85.2 %.

In order to detect if some sensor data is still redundant, we consider the upper body coverage layout with a growing subset of sensors. The different sensor subsets are depicted in Figure 4.11. Additionally to these sensor layout subsets, Figure 4.12 shows the mean F-measure of the evaluation results. For each sensor layout subset, a leave one subject out cross-validation has been effectuated for real and simulated data. Both are depicted on the same graph. We observe that in general better results are achieved evaluating the real prototype. The simulation data shows a clear gain in F-measure at the layout using a subset of 14 sensors. The real data similarly shows a high slope at the layout using 14 sensors. The mean F-measure values at this point are 84.7 % for the real prototype and 80.4 % for the virtual prototype. Looking up the corresponding 14 sensor layout subset from Figure 4.11, we observe that it represents the minimum configuration covering the whole upper body of the test person as well as areas outside, where the bed cover lies on the bed.

We observe a second similar but smaller jump in F-measure by looking at the simulation data for the subset of 30 sensors. The real data mimics this small peak achieving the highest F-measure with 89.4 %. Looking at the corresponding layout subset with 30 sensors, we observe that the improvement

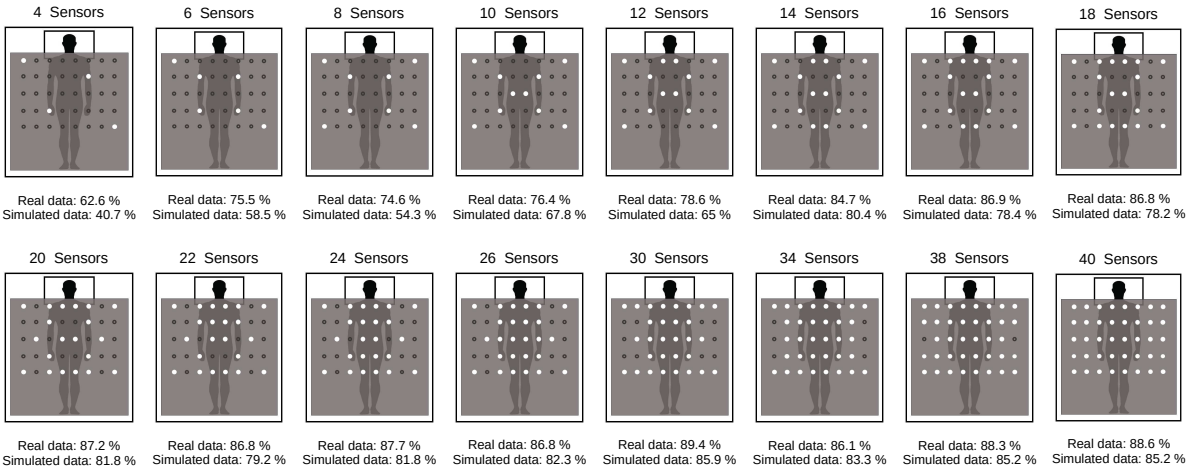

Figure 4.11.: F-measure of increasing sensor amount using upper body coverage layout with 40 sensors. For each sensor layout the mean F-measure is calculated by effectuating a leave one subject out cross-validation for simulated and real data.

of results is generated by adding sensors to the first and last line, covering the shoulders and legs as well as the area lying flat on the bed.

4.1.7. Summary

In Section 4.1 we presented a simulation framework for applications with flexible surfaces such as a shape-sensing fabric. Even before the hardware is available developers can start designing and virtually evaluating their prototype for their individual shape-sensing application.

We proposed and demonstrated the workflow of a prototype designing process with shape-sensing fabrics by virtually planning a sleeping posture detecting bed cover. According to its virtual model we have equipped a bed cover with 40 acceleration sensors and evaluated it with 10 different users. Comparing the F-measures of 85% for the virtual and 89% for the real-world implementation we validate our proposed simulation framework for shape-sensing fabrics. We show further advantages of the simulation framework in terms of analyzing optimization potentials in order to find the suitable trade-off point for the required application. To our knowledge there is no simulation framework which includes soft-body simulation and attaches virtual sensors to them. Through our simulation framework we were able to provide a decision basis for developers when they need to decide on the trade-off between number of sensors, sensor placement and achieved accuracy.

In Section 4.2 the general approach of the simulation framework is demonstrated by using this for planning further shape-sensing applications. Examples of such shape-sensing applications in the field of ambient intelligence could be intelligent clothing which reports on its status (in drawer, washing bin, coat hanger, coat hook, if it is worn correctly, etc.) or an intelligent furniture cover which would detect

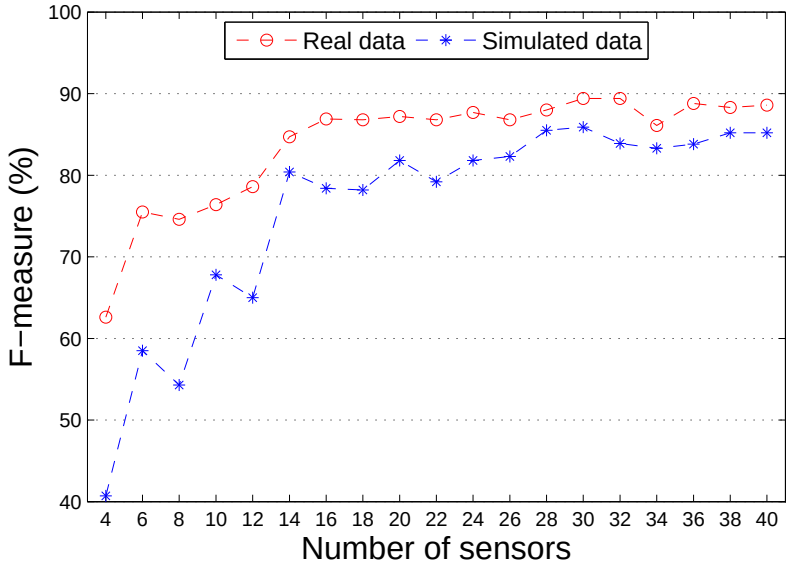

Figure 4.12.: F-measure of layout with increasing sensor number

on which furniture it is placed and provide the user with services such as posture detection, breathing frequency tracking, amount of movement.

4.2. Human intuition in designing flexible surface applications

This Section is based on my paper "Designing a Self-Aware Jacket Insights into Smart Garment's creation process" [RBKK19a] and the Master's Thesis of Christian Gutjahr [Gut17]. The authors referred to as "we" are Silvia Rus, Andreas Braun, Florian Kirchbuchner and Arjan Kuijper.

The use of smart garments has impacted different application areas. It has spread from fashion and Arts&Crafts, where it was used for achieving special effects in fashion shows which are unique like a piece of art, to areas such as rehabilitation or virtual reality where it was used for remote control [FHS17,FSH*18,Hom17,Sen17,Wan16,SPW07,PWB10]. These garments are enhanced by integrating flexible and stretchable electronics such as sensors and actuators which can be used to create different applications.

The question is how to deal with these new possibilities and how designers of such applications can deal with them. Do they have to have special training, is working experience with these materials needed or is the intuition of a person with basic background knowledge enough?

An example where smart garments are used on a daily basis is a biker jacket. Its functions range from controlling music, taking calls, getting navigation directions, notifying when the taxi is there to flashing brake lights and front lights [For18, PGF*16].

Research on smart garments has been concerned with creating different sensors which can be easily integrated into prototypes realizing different use cases. Initial textile sensor examples from Perner-Wilson *et al.* are bend, pressure, stretch, tilt and stroke sensors [PWB10]. Examples of smart garment use cases are Trainwear, from Zhou *et al.* which create a shirt for sports exercise recognition. [ZBF*17]. Voit *et al.* have created a textile authentication for wearables and a textile sleeve for public display interaction [VS17b, VPS18].

Smart Jackets were presented by Hutschenreuther, Google and Ford Smart Mobility [Hut17a,Hut17b, PGF*16, For18]. All of these jackets are intended for commuting by bike. Knitty-fi has started as a jacket with three knitted switch patches which were freely configurable. They fulfill specific programmable tasks, easing the day by day activities of people with impairments [Hut17a, Hut17b]. Ford Smart Mobility have developed LUMO, a smart jacket prototype for cyclists. Similarly to Levi's Jacquard jacket by Google, it assists the user's navigation by conveying directions by haptic cues, helps with taking calls and controlling the music player. Additional functions such as showing the directions using lights at the front and back or connection to commuter apps differentiate them from each other. Knitty-fi and LUMO are not on the market yet, while Levi's jacket can be already bought.

Most of the smart garment prototypes were created for a specific purpose and with a great deal of effort. To ease the process of creating e-textile prototypes Posch *et al.* have introduced new tools for electric textile making and Hamdan *et al.* have created an interactive system to support the user to easily create interactive embroidered prototypes [PF18, Pos17, HVB18]. These tools are of great help after the process of designing the electric textile project is finished.

Schneegass *et al.* have recognized this need for multiple application possibilities and created a multipurpose shirt, with many different textile sensors integrated into it. The wearer could set which functions of the shirt he wanted to use and create new applications for the given set of sensors [SHZ*15]. Further into this direction Dementyev *et al.* have proposed the vision of a fabric which is self-sensing. It would be equipped with sensors measuring stretch, the shape in 3D as well as temperature and proximity [Dem16].

With so many sensors integrated into the material is it economically and ecologically acceptable to use these resources?

The objectives of this research are to find out:

- how well human intuition helps to design a smart garment application and
- to which extent sensor expertise plays a role in the design of a smart garment application.

To answer these questions, we have collected a data set from test subjects which were presented with a smart garment use case. We created a simulation framework to transfer the collected data sets to the same smart garment use case. Then we have evaluated these results in toward answering our research objectives.

4.2.1. Design use case: the shape-sensing jacket

We want to investigate what the intuition is to design a system which fulfils a specific task. Throughout this section, we will call the person with such a task a system designer. When a system designer starts the design process, the question of how densely the sensors should be distributed, and which of them hold the key information to achieve the intended task is crucial for hardware optimization.

In order to gather insights into the intuition of system designers, we selected a smart garment use case. We assigned this use case to the system designers as a prototype design task. What we came up with is a jacket which knows its whereabouts and provides context information to the user. The jacket situations to detect are presented in Figure 5.34. As sensing units, the system designers have acceleration sensors at their disposal.

Figure 4.13.: Situations in which to detect the jacket: (a) on coat hanger; (b) over couch; (c) on coat hook; (d) over chair; (e) scrunched-up; (f) over table; (g) worn.

We selected this use case because of its potential. Use cases for such a jacket could be one-size clothes, like one-size-fits-all. By knowing the 3D shape the jacket could adjust itself to the body form of the wearer and to his level of comfort or preference of style. Other potential use cases could be to detect if a safety-vest is worn or not and if it is worn correctly.

To gather information on intuitive sensor layouts we first observed and discussed the designs of two system designers, which were experts in their field. They carried out the sensor placement practically. Later, we asked 18 participants for the theoretical placement of sensors in a survey. This facilitated the usage of more sensors. Also, the results could be captured more accurately.

The gathered sensor locations were used as input for the evaluation via the simulation framework described in Section 4.1. This tool enables the simulation of the different situations which the jacket should detect. The simulation framework allows to load a flexible surface, such as the bed cover used in the sleeping posture recognition use case from Section 4.1.2. For the shape-sensing jacket use case this is a rectangular piece of fabric, representing the jacket. By loading different 3D rigid objects into the simulation framework, the virtual jacket can be shaped into situations such the ones in Figure 5.34. The virtual jacket is equipped with accelerometer. This jacket situations are simulated by letting the sensor equipped textile fall on a table, on a chair, on a coat hook, etc. For variation purposes there were five different chairs, five coat hangers, five tables, etc.

4.2.2. Design process in practice

First, we asked two participants which are system designers with deep understanding of accelerometers to distribute up to ten sensors on a jacket in order to detect the situations presented in Figure 5.34. For this, a person wore the jacket and the system designers glued tags on the jacket where they would place the sensors, see Figure 4.14. Then, we transferred these positions from the jacket to positions on a grid. This grid corresponds to the sensor locations on the textile used in the simulation framework, our evaluation tool. By simulating the different situations, we gathered the sensor data and evaluated the created sensor position patterns using various classifiers from which we computed the maximum of the accuracies. For design (a) in Figure 4.14, the accuracy is 75.3 % and for design (b) the computed accuracy is 69 %.

Figure 4.14.: Final prototype designs by two knowledgeable system designers. Tags mark sensor placement on front and back of jacket.

The rationale behind the creation of design (a) was that each added sensor will contribute to differentiate between different situations. The upper sensor on the back could differentiate between *(coat hanger, coat hook, worn), (over couch, over chair)* and *over table*. The two lower sensors on the back were placed to differentiate between *over couch* and *over chair*. To differentiate between *coat hook* and *(coat hanger, worn)* one sensor was placed on the shoulder. The last sensor on the chest is intended to separate *coat hanger* from *worn*. For situation *scrunched-up* no specific sensor was placed since the jacket can be packed differently. This design used only five sensors and reached a maximum accuracy of 75.3 %.

Design (b) uses nine sensors. Similarly to (a), there are sensors placed on the back of the jacket in order to determine the curvature of the jacket, detecting *over couch, over chair, over table, scrunched-*

up. To detect the other situations *coat hanger, coat hook, worn* the sensors on the shoulders were added, one on each shoulder, on the front and also on the back. The achieved accuracy is 69 %.

This difference in accuracies shows us, that using more sensors does not necessarily mean that better results can be achieved. The placement of the sensors plays a key role in detecting the desired positions. This trade-off between the number of sensors and accuracy will be further investigated in the following.

4.2.3. Design process survey

In the second step, we interviewed 18 test subjects with the help of a questionnaire. The test subjects fulfilled the role of system designers implementing the already mentioned use case. The survey addresses our research questions by focusing on gathering initial information on the level of knowledge of the participants, providing the needed information to fulfill the given task, motivate and describe the task and propose the number of sensors to be distributed.

After providing some general information such as age, gender and educational background the participants are asked if they have already used accelerometers in previous projects. Subsequently, they were asked questions regarding their understanding of how accelerometers work. We proposed some aiding questions such as:

- What does an accelerometer measure?
- How can the accelerometer data be interpreted when there is no movement?
- How can the shape of a surface be computed from accelerometer data?

Upon their answers, they were able to self-evaluate their knowledge and mark on a scale from 1-5 (1-least, 5-most) their expertise. On the following pages, the answers to the previous self-evaluation aiding questions were provided with a detailed explanation. The goal was to provide every participant with the same knowledgebase regarding accelerometers.

In the next step of the form the participants were provided with the motivation of this work describing the task of detecting different situations of the jacket. They were instructed to distribute a certain number of sensors (from 4-50) on the grid drawn on a cloth, representing the worn jacket, see Figure 4.15. Due to simulation limitations, the sensors cannot be distributed on the arms. In the area of the neck on the front of the cloth there usually is a cut-out, thus sensors cannot be attached there either. Their task is to mark on the sheets of the form where they would place a given number of sensors {4, 6, 8, 10, 20, 30, 40, 50}.

4.2.4. Evaluation results

18 subjects participated in the survey. Nine of them are male and nine female. Five reported having used accelerometers in previous projects. The educational background ranges from Bachelor or Master of Computer Science, Electrical Engineering, Mathematics and Interactive Media Design, with a majority group of 12 participants whose educational background is Computer Science.

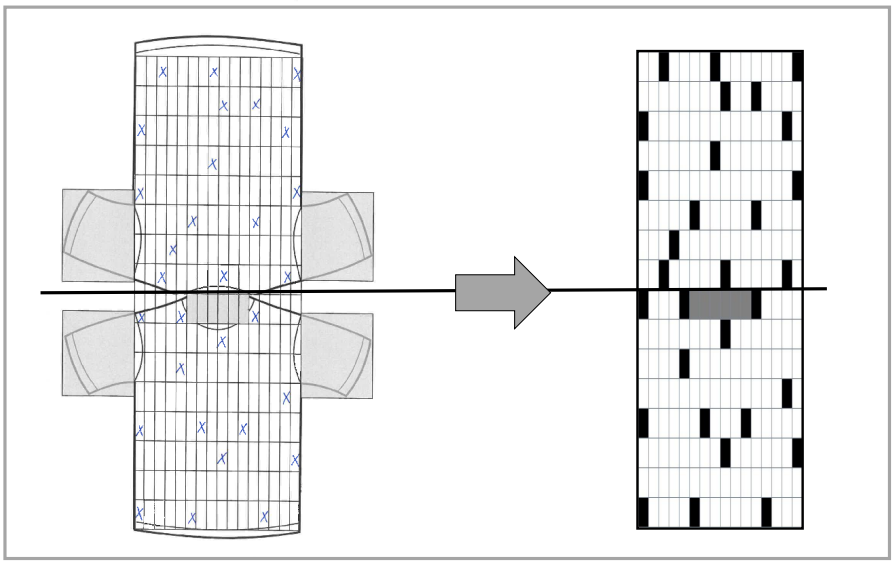

Figure 4.15.: Participants marked the sensor placement of a given number of sensors. We transferred the input to the simulated use case.

We transferred the input from the survey to a simulation framework. This simulation framework was built to evaluate different sensor setups. The executed simulation scenarios correspond to the situations shown in Figure 5.34. The framework has been developed because of the lack of a simulation tool, which is capable to attach sensors to soft-bodies. The reliability of the simulation framework has been confirmed by Rus et al. by comparing simulated prototypes with real world prototypes [RHvW*18]. The developed simulation framework is capable of attaching sensors to a soft-body, such as a textile. In the simulation, the sensor equipped soft-body is placed on a rigid-body such as a chair or a couch, corresponding to the situations from Figure 5.34.

Figure 4.16 shows a chair, the rigid-body used in our simulation, with the three instances of an orange soft-body. The sensor equipped garment is represented by a rectangular soft-body, equipped with sensors. This matches the grid used in the survey, see Figure 4.15. In the second representation of Figure 4.16 the garment is bent, in order to be as close as possible to the way e.g. a jacket would be placed on a chair. This preparation is necessary, such that the simulated garment can fall on the chair in the right position. After the simulated garment stopped moving, the virtual sensors measure their position and the data is stored. This data is used for the evaluation of the survey. Each situation depicted in Figure 5.34 is simulated five times using five different objects, such as five different chairs. On the soft-body, corresponding to the simulated garment, the maximum number of 256 sensors is attached. The data from all sensors is recorded. From this recorded data only the sensors chosen by the participants are used for the corresponding evaluation.

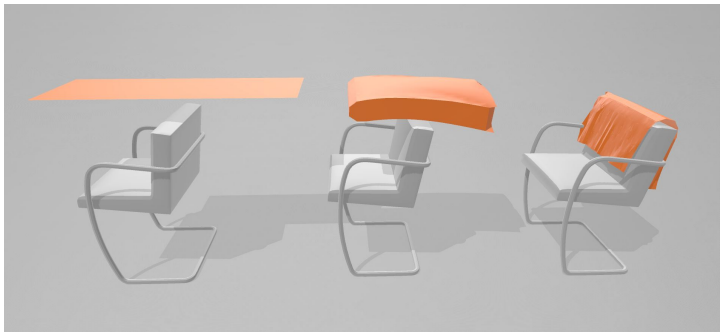

Figure 4.16.: Placement of virtual garment on chair in the simulation framework

The data was evaluated using a leave-one-subject-out cross-validation with five different classifiers and three additional parameter variations of Support Vector Machine (SVM). Leave-one-subject-out cross-validation was performed since we gathered sensor data using a simulated environment. The sensor data varies minimally due to the residual movement remaining when placing the sensor equipped soft-body on the objects such as the coat hanger or chair. By using k-fold cross-validation the classifiers get trained on data which is very similar to the test data, resulting in high accuracies. By using leave-one-subject-out cross-validation the system is tested on totally new test data, providing a better picture of the system performance. The classifiers used were the WEKA implementation of k-Nearest Neighbours (IBk), Decision Trees (J48), Naive Bayes, Random Forest, SVM and SVM with polynomial and RBF kernels. For each survey input, we noted the best performance independent of the classifier. We measure the best performance in terms of accuracy, which represents the percentage of test instances correctly classified. The overall results from the study are shown in Figure 4.17 and 4.18.

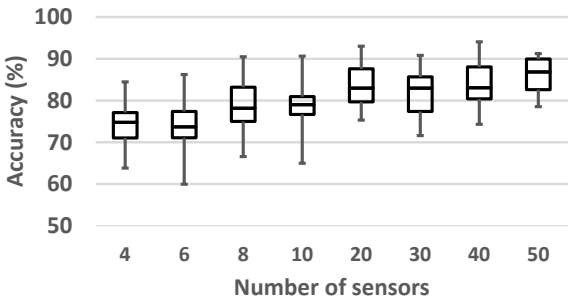

Figure 4.17.: Performance evaluation for different numbers of sensors.

From Figure 4.17 we observe that the accuracy rises the more sensors are used. However, not in a linear manner. A good result can be achieved by using eight sensors. A more robust result can be achieved by using 10 sensors. Here the median accuracy is 78,99 % (SD 6,06). If the number of sensors

rises, the quality of the results can be improved. However, the benefit is minimal. Using more sensors to reach a good result entails additional costs.

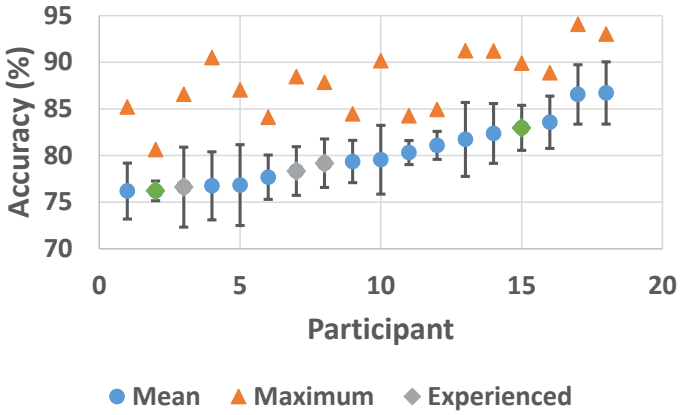

Figure 4.18.: Mean and maximum performance per survey participant. Participants with diamond shaped symbol have previously worked with accelerometers.

Compared with the results achieved by the two more experienced system designers, which created sensor layouts with 5 and 10 sensors with accuracies of 75.3 % and accordingly 69 %, the highest accuracies from the survey results for 4 and 10 sensors outperform the expert results. This indicates that special expertise in terms of having previously built wearable sensing devices does not result in best performing systems.

Figure 4.18 presents the maximum and mean performance per participant, sorted according to the mean performance. The achieved maximum accuracy is 94.06 % (SD 5,20) for a sensor setup with 40 sensors achieved by the second to last participant. The diamond shape represents participants which have previous knowledge in the field of accelerometers, such as experience by using accelerometers in previous projects. The green coloured diamond shapes of participant 2 and 15 represent the designs proposed by the two experts. The mean performance of the experienced participants places them in the first half of the participants. This indicates non-experienced test subjects can achieve better results in placing sensors by using their intuition than experienced test subjects.

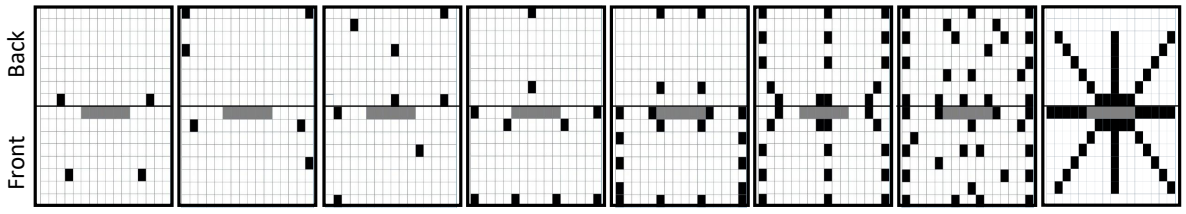

Figure 4.19.: Sensor layouts with best per sensor number performance.

The sensor layouts with the maximum accuracy per sensor are shown in Figure 4.19. These designs show that the area around the shoulders and on the edge of the textile are of high importance. Most of the designs have a symmetric component, whereas sensors are placed more asymmetrically towards the inner surface of the garment than on the edges.

4.2.5. Summary

In this section, we have investigated what role the human intuition has when designing a smart garment use case compared to designing a system by an experienced system designer. We proposed a novel smart garment use case in which a garment is equipped with accelerometers to detect different situations. To achieve this, we have gathered the input from experienced system designers in two hands-on sessions and through a survey with 18 participants. By evaluating the results with a specifically created simulation framework for this garment use case, we have found that special expertise does not provide an advantage, that good sensor layouts can be achieved by system designers with less or no experience. While technical knowledge does not play a significant role in the resulting performance, we observed that many participants intuitively create well-working patterns. Thus, rather intuitive sensor layouts achieve as good as and better results up to a maximum accuracy of 94% for 40 sensors.

Regarding the resources used for implementing this best performing sensor setup the trade-off between accuracy and invested resources is high. Compared to a sensor setup using 10 sensors (accuracy of 79%), one has to ask himself if the 4 times more used sensors give are worth the approx. 15% increase in accuracy. Depending on this preference the advisable number of sensors will vary.

As a next step, the optimal sensor layout could be calculated by evaluating the simulated sensor data. Principal Component Analysis could be used to identify important sensors and other optimization algorithms to address the sensor number vs. accuracy trade-off.

4.3. Conclusion

This chapter presented my contributions to the second research challenge *New design tools for flexible Smart Environment applications*. While creating assistive applications, certain design decisions need to be taken. I reduce the use of resources throughout the iterative work-flow by addressing the prototypical hardware iterations. For this, I contribute a simulation tool, which aids in identifying the number and placement preferences for flexible Smart Environment applications and a study on the relation between human intuition and expertise.

Section 4.1 presents the first contribution, namely understanding where sensors need to be placed and how many are needed to achieve the desired application functionality and accuracy. I contribute a simulation framework, which facilitates the creation of flexible applications [RHvW*18]. Since existing simulation tools only perform the simulation of rigid objects, I included a soft-body simulation with attached virtual sensors. Developers can create and evaluate their prototype virtually, even before the hardware is available. This workflow of virtually planning and subsequently implementing is

validated and demonstrated on the use case of designing a sleeping posture detecting bed cover. The built virtual and real prototypes, equipped with 40 acceleration sensors, have been evaluated with 10 different users, resulting in an f-measure of 85% for the virtual and 89% for the real-world implementation. The similar performance achieved by the real prototype and the virtual prototype validates the simulation framework. By varying the layout and number of active sensors, the optimization potential of the simulation framework is shown. For this use case of a posture detecting bed cover, one possible trade-off between application performance accuracy and desired costs in terms of integrated sensors is achieved by distributing 14 sensors throughout the surface of the bed cover while still achieving 84.7 % for the real prototype and 80.4 % for the virtual prototype.

My second contribution to this research challenge is the investigation on what role the human intuition has when designing a smart garment use case versus the expert knowledge used to design such a system by an experienced system designer [RBKK19a]. I use the developed simulation framework as a tool to compare the proposed designs for a smart garment which detects different situations. I gathered the designs through a survey with 18 participants and two hands-on sessions with experienced system designers. The result conveys that many participants intuitively create well-working patterns, and technical knowledge does not play a significant role. Thus, rather intuitive sensor layouts achieve as good as and better results up to a maximum accuracy of 94% for 40 sensors. Again, the simulation tool was used to evaluate the trade-off between the number of sensors and the system performance. Compared to a sensor setup using 10 sensors with an achieved accuracy of 79%, 4 times more sensors achieve an increase in accuracy of approx. 15%. Depending on the priorities of the developer of such a system, the minimum achieved accuracy and the cost trade-off can be thus computed.

In some situations it makes sense to settle for a trade-off with lower performance. In these situations, the performance could be increased by adding an additional sensing modality. One such modality could be a capacitive sensor. Capacitive electrodes in form of e-textile are especially well suited to be integrated into flexible Smart Environment applications. Even though their use is widespread in the field of Ubiquitous Computing and Human Computer Interaction, different manufacturing options are available, and subsequently capacitive electrode design decisions have to be taken. In Chapter 5 I address this research challenge of *Suitability and performance evaluation of e-textile capacitive electrodes* by offering a structured evaluation of various electrode properties for capacitive proximity sensing.

5. Properties of flexible capacitive proximity sensing electrodes

In the previous chapters, I have presented the possibilities and challenges flexible surfaces leverage in the domain of Smart Environments. I have created a number of new flexible assistive Smart Environment applications and extended the application design process by providing a tool enabling the evaluation of applications. Varying the number of sensors and their placement, trade-offs such as cost reduction and application performance can be determined. Increasing the performance can be achieved by multiple modalities. Adding capacitive sensing seems likely, due to the ability of human presence detection at a distance. Thus, capacitive sensing electrodes can be hidden in the environment. Based on this, the challenge of selecting the right electrode material, shape and size appears to be a fundamental factor in designing applications for flexible surfaces. The analysis of these properties will shape the content of this chapter.

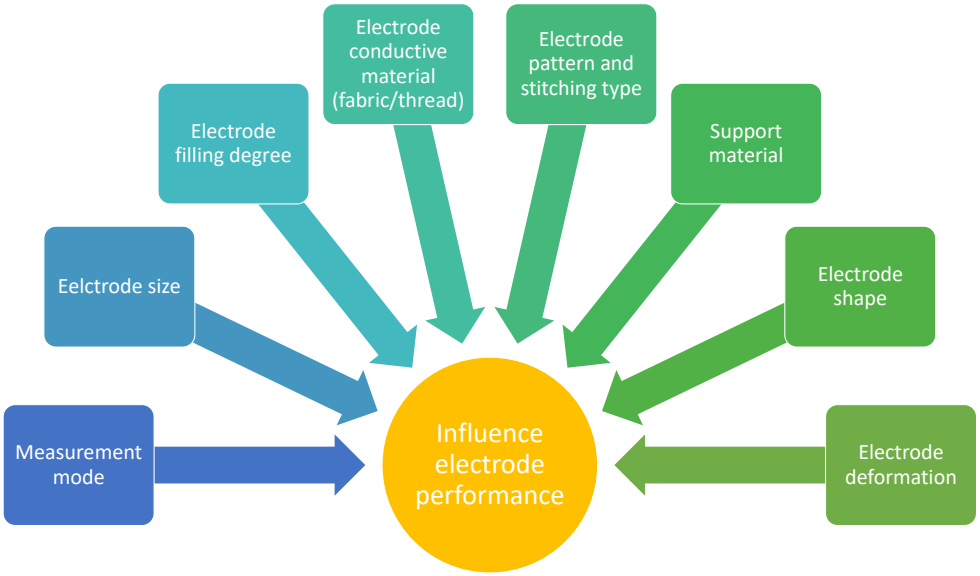

Figure 5.1.: Influencing factors of electrode performance and suitability for applications

First, I will compare different materials used as electrodes for capacitive proximity sensing. Electrode size will play a secondary role here. In the second part, I will focus on e-textile materials and

compare conductive fabric and conductive thread more into detail regarding shape, size and making. Based on the collected knowledge, I will conclude with a rationale on how to choose the proper/most suitable electrode for ones envisaged application, which I will exemplary apply in two use cases.

Figure 5.1 depicts influencing factors on capacitive electrodes in general with specific factors for the integration into materials which are flexible. The conductive material type itself plays a significant role. As described in Chapter 2 introducing capacitive sensing, there are several options available to be used not only in a rigid shape, but also materials which are deformable, such as stretchable and bendable.

Electrode shape, pattern, and pattern density are influencing factors which play a major role in the possibility to integrate the materials into everyday objects or the environment, in order to build useful applications. Moreover, when people, users of the application interact with these flexible and stretchable materials, the capacitive electrodes are deformed.

The work presented in this chapter is an extended version of the papers [RSBK15, RBKK19b] and Pinar Yakars bachelor's thesis [Yak19]. In this chapter we, the authors of these works, introduce following scientific contributions:

- We execute extensive measurements for five different materials using different setups. We provide measurements in self and mutual capacitance mode.
- We execute various measurements for e-textile materials with different variations of size, material, pattern density, shape and making such as support material and stitching types.
- We compare characteristics of the different materials and lead through the electrode choosing rationale by running-through the electrode creation process in two exemplary use cases.

5.1. Evaluation of electrode materials

Capacitive sensors in both touch and proximity varieties are becoming more common in many industrial and research applications. Each sensor requires one or more electrodes to create an electric field and measure changes thereof. The design and layout of those electrodes is crucial when designing applications and systems. It can influence range, detectable objects, or refresh rate. New materials, as well as advances in rapid prototyping technologies have vastly increased the potential range of applications using flexible capacitive sensors.

Existing applications show a variety of different materials used for building applications using capacitive sensors. For example, Singh et al. use clothing as input/control device [SNR*15]. They utilize conductive textile to build capacitive electrodes and integrate them into clothing. Equipping trousers with conductive textiles Baldwin et al. prevent falls by analysing the gait while walking [BBR*15]. By touching metal nibs in different areas of a belt Dobbelstein et al. control a head worn device or have a textile touchpad integrated in the fabric of the trousers' front pocket [DHR15, DWHR17]. Conductive paint is used by Teodorescu et al. to paint interdigital capacitive sensors on regular textile in order to detect specific movements of the arm by integrating the painted sensor into clothing [Teo13]. For the on-body interaction new, special materials have been developed, to fit to the requirements of not

harming the human body. Nearly all these applications are developed for capacitive touch interaction. Mostly the applications built into furniture exploit the biggest advantage of capacitive sensing of being unobtrusively mountable.

The multitude of applications presented here and in Section 2.4.2 shows how new materials find their way into capacitive sensing applications. However, most of them use a special electrode design and only cover capacitive touch. They don not evaluate properties such as the spatial resolution and the interaction range.

A few works also evaluate the influence shape and filling degree has on electrode performance. Chang et al. propose a circular electrode design composed of a guard ring and an electrode [WCC14]. The authors evaluate the influence of electrode area, shielding and of the gap between guard ring and electrode on the capacitance.

However, they did not evaluate the spatial resolution like it has been done By Grosse-Puppendhal et al. where different electrode materials like foil of polyethylene terephthalate (PET) coated with indium tin oxide (ITO) or PEDOT:PSS, conductive polymer are compared to different sizes of copper electrodes for distances up to 40 cm [GPBB*13].

Braun et al. evaluate capacitive proximity sensors in Smart Environments [BWKF15]. They focus on practical guidelines, gained in the design of various prototypes, but do not provide measurements of flexible materials or different measurement modes.

The measurement mode used is predominantly self capacitance, while applications which need to cover a larger surface like [ZYH*18] and [Rek02] and hence need more measurement nodes, explore the advantage mutual capacitance has to offer in terms of multiple measurement nodes.

The applications have been developed by trying out new materials and electrode layouts. Some capacitive sensing electrode guidelines have been presented in Section 2.4.3. However, a more quantitative approach might reveal qualities of the materials which will help developers to optimize the choice for the used materials for their application.

In order to enable developers to choose between available electrode materials, we further inspect by performing measurements, which of these are performing best in a capacitive proximity sensing scenario.

5.1.1. Measurement setup

The measurement setup utilized for measuring the performance of capacitive proximity sensing of different electrode materials is shown in Figure 5.2. The setup shows two electrodes: one on top - the reference electrode - and on the bottom multiple electrodes to evaluate made of different materials. The structure allows the upper reference electrode to adjust the distance to the electrode on the bottom. The reference electrode remains unchained throughout all measurements in the electrode materials measurement series. It is made of a copper plate of 10 x 16 cm, the same size as the evaluated electrodes. The chosen size is approximately the size of a hand palm. This simulates a hand getting closer to the electrode. The upper electrode is connected to ground, similar to how one is coupled to ground when

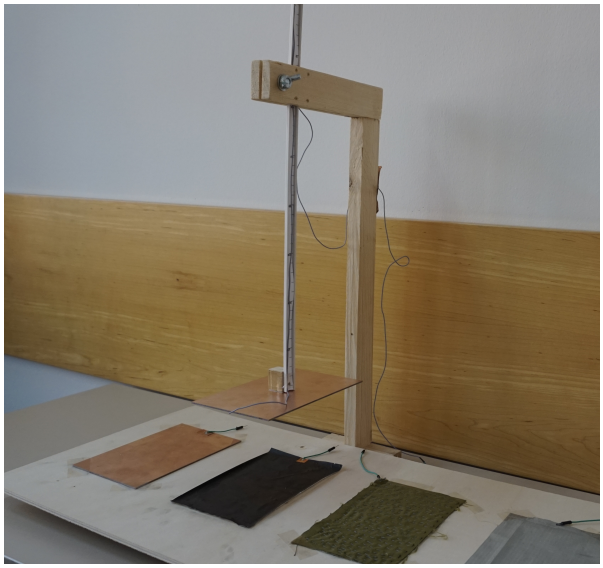

Figure 5.2.: Setup with measurement copper electrode adjusted at different distances in relation to various electrode materials

interacting through the hand with a capacitive electrode. During our measurements we also show measurement results with loosely grounded electrodes.

Depending on the size of the electrode the sensing distance can vary. Capacitive sensing distances up to 50 cm are achievable with acceptable electrode sizes. Hence, we have effectuated measurements up to distances of 50 cm.

We effectuate measurements in self capacitance and in mutual capacitance sensing mode. When measuring the self capacitance a single electrode is needed. This electrode is connected to a sensor which sends the sensed signal to an OpenCapSense evaluation board [GPBB*13].

For measuring the mutual capacitance, multiple sending and receiving electrodes are used. The sending electrodes send out a signal generated by the sending OpenCapSense board, while the two receiver electrodes are connected to two sensors, which are connected to the receiving OpenCapSense board. From there the values are further transmitted.

For each setup we used five different materials for the measurements. These materials are: copper (electrode and wires), conductive paint, conductive paint on fabric, conductive fabric and conductive thread. Figures 5.3 and 5.4 show the used electrodes in the different measurement modes.

For self capacitance measurements only one electrode is used to measure the capacitance. Therefore, we choose electrodes of the same size of 10 x 16 cm. Next to the copper electrode one can see in Figure 5.3 the black conductive paint, which we applied on paper and contacted using copper tape to a small piece of wire. To the right of the conductive paint, conductive thread is sewn into a green piece of fabric. The conductive thread is sewn in narrow s-lines with spacing of about 0.5 cm, in order to

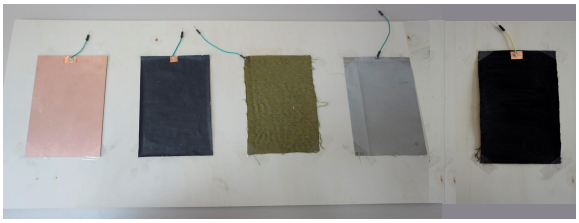

Figure 5.3.: Electrode material samples used in self capacitance measurement mode: (from left to right) copper electrode, conductive paint, conductive thread, conductive fabric, conductive paint on fabric.

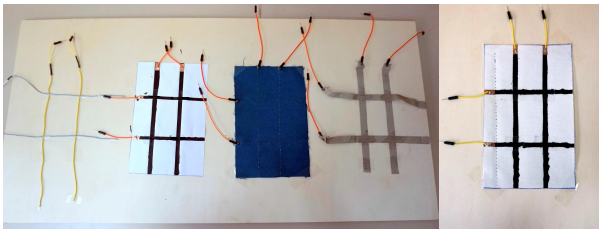

Figure 5.4.: Electrode material samples used in mutual capacitance measurement mode: (from left to right) copper wires, conductive paint, conductive thread, conductive fabric, conductive paint on fabric.

cover the whole surface of the electrode. Conductive thread is contacted by knotting the thread to the connecting wire. The fourth electrode material sample is conductive fabric, which is contacted using conductive thread which is sewn to the connector. We used the material Shieldex Zell-RS [1], widespread through retailers for electrical craftship. The last electrode is made of conductive paint like in the second sample but this time the used substrate is fabric. It is contacted using copper tape.

For the mutual capacitance measurement mode, one sending and one receiving electrode are needed. We use two sending and two receiving electrodes which are placed as a two times two grid. Instead of the copper electrode, wires are used. These are already isolated and can simply cross each other. For the other electrode setups 0.5 cm thick stripes of conductive paint and fabric have been used. After the horizontal electrodes have been placed, the crossing points were isolated using tape. Then the vertical electrodes have been added. In the case of conductive thread, the supporting fabric itself is used as isolation at the crossing points by sewing the receivers and the senders on top and on the bottom of the fabric. The contacting methods are the same as described for measuring the self capacitance.

We have effectuated three kinds of measurements, for both self and mutual capacitance measurement modes. First, we have used the measurement setup for distances of up to 50 cm. From 1-30 cm we measured in steps of 1 cm while from 30-50 cm we measured in steps of 2.5 cm. During these measurements the electrode simulating the hand was loosely coupled to the ground through the environment.

[1] https://www.shieldextrading.net/wp-content/uploads/2018/08/1500101130-Zell-RS.pdf

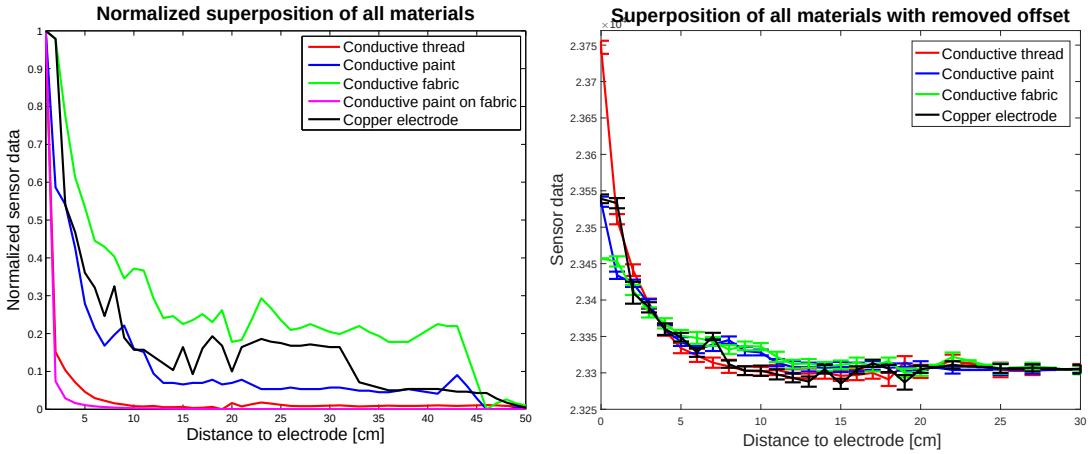

Figure 5.5.: Self capacitance measurement, loosely coupled to ground: (left) normalized mean; (right) superposed mean and standard deviation with removed offset.

Second, we connected the human hand simulating electrode to ground and measured the sensed value for distances up to 30 cm. This time we measured up to 15 cm in steps of 1 cm while from 15-30 cm we measured in steps of 2.5 cm. Additionally, we evaluated how the materials react to touch. For this the moving electrode has been placed on the different electrode materials with an isolating layer in-between. The touch measurement has been evaluated once without weight and once with a weight of 0.5 kg, to reflect the behaviour of pressing a button.

The resulting diagrams of the three measurement sets are presented in the following two sections 5.1.2, for the self capacitive measurement mode, and 5.1.3 for the mutual capacitance measurement mode.

5.1.2. Results of measurements for self capacitance measurement mode

Figure 5.5 shows on the right side the mean and standard deviation for distances of 1-30 cm of different materials, shifted to a common baseline. One can observe that the standard deviation is relatively high. Also, one can infer the deviations due to noise which lead to unusual drops and spikes in the signal. The influence of the environment noise is sensed because of the loose coupling to the ground.

In Figure 5.6 the moving electrode is grounded and yields a much smoother and constant signal throughout all electrode materials with very small standard deviations, see graphic on the right. For direct comparison we normalized the curves and show them in the left graphs of Figures 5.5 and 5.6.

From the left graph of Figure 5.5 showing the loosely coupled electrodes, one can infer that even due to much noise, the copper, conductive paint and conductive fabric electrodes have a better measurement of up to 12 cm. Conductive thread and paint on fabric have shown a different course with measurement

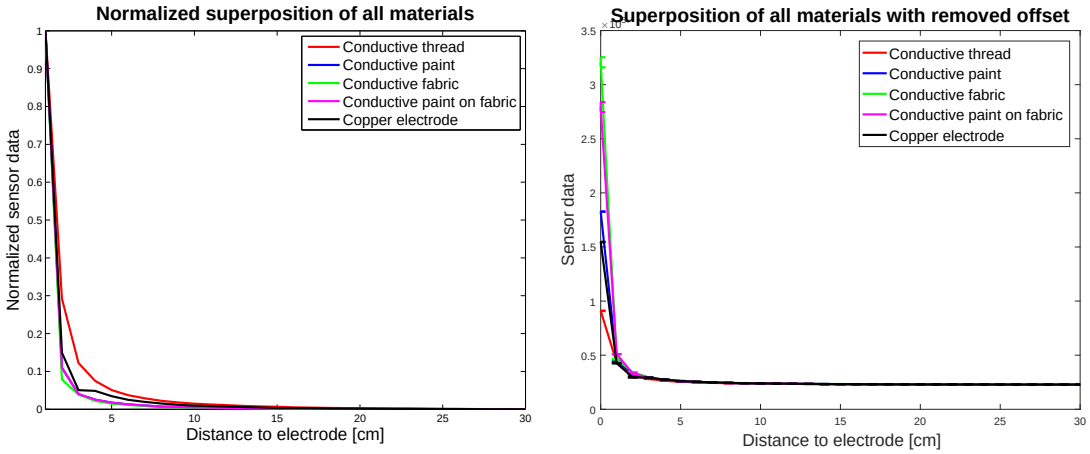

Figure 5.6.: Self capacitance measurement, grounded: (left) normalized mean; (right) superposed mean and standard deviation with removed offset.

ranges until around 5 cm. When looking at the raw data, shifted to a common baseline in Figure 5.5 in the right image, the conductive thread electrode shows the steepest slope, indicating a good differentiation of values for distances up to 10 cm.

In contrast, when grounding the moving electrode, the measurement ranges get closer together. At the distance of 0 cm the conductive fabric reaches the highest value, then the conductive paint on fabric, conductive paint, copper electrode and lastly the conductive thread. However, for the next measurement of 1 cm they all have a mean around the same value. The normalized view, in the left image of Figure 5.5 shows that all values of the electrodes take a very steep course, the conductive thread electrode with the least steep course.

In conclusion, using these measurement settings, there is no specific electrode material which clearly shows better properties. The noise, and the generally very high ground capacitance limits the sensitivity of the sensor.

5.1.3. Results of measurements for mutual capacitance measurement mode

Unlike the self capacitance the mutual capacitance measurements for two sender and two receiver electrodes yield four sensing nodes. Because we are using a single moving electrode centered over the four sensor nodes, these behave approximately the same. Figure 5.7 shows on the left the normalized values of the sender and receiver pair (1,1) and on the right the mean and standard deviation of each of them. We observe the very big standard deviation, which shows once again the influence of the noise (parasitic capacitance) of the environment when the electrode is coupled loosely to the ground.

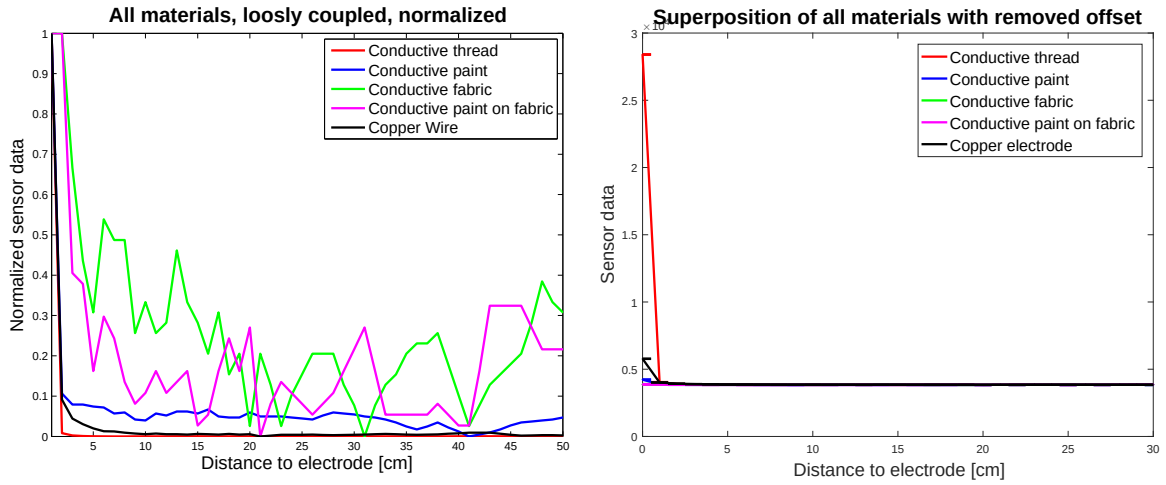

Figure 5.7.: Mutual capacitance measurements, loosely coupled to ground, sender-receiver pair (1,1): (left) normalized mean; (right) superposed mean and standard deviation with removed offset.

Grounding the moving electrode reveals the right graph from Figure 5.8. One can see that all materials show a smooth curve. At first, the measurements for the conductive paint electrode were very different from the graph of the conductive paint electrode on fabric. This led to the assumption, that the measurements were heavily noise prone. After repeating the measurements, the conductive paint on fabric and the conductive paint both showed nice characteristics. For mutual capacitance the surface between sender and receiver where the capacitance change is measured is very small - only at the crossing of the sender and receiver electrode. The noise can increase so much that the change in capacitance generated by the moving electrode can be to small and overruled by noise.

In mutual capacitance mode, it is very hard to infer a recommendation on which electrodes to use due to the strong influence of the noise for some electrode materials. However, from the right graph of Figure 5.7 one can infer that conductive thread, copper wire, conductive paint and conductive paint on fabric have a similar course. For conductive fabric the measured values are less steep and have a small standard deviation than compared to the conductive wire electrode or the conductive paint on fabric electrode.

5.1.4. Summary

Following our quantitative measurements, we are able to discuss a first set of factors influencing potential applications for flexible capacitive sensors. This discussion builds upon the results presented in Sections 5.1.2 and 5.1.3 where different electrode materials were investigated in settings using different measurement modes.

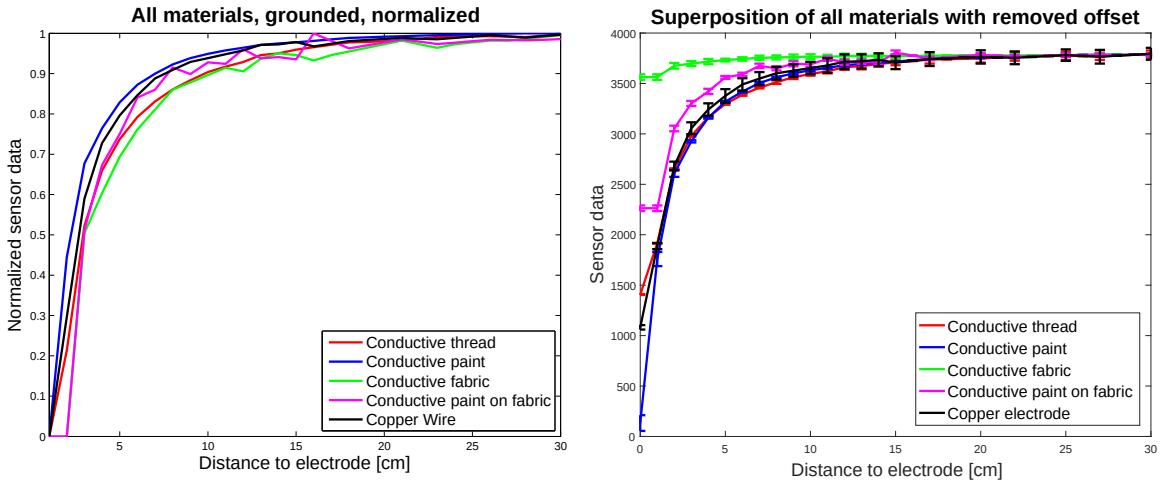

Figure 5.8.: Mutual capacitance measurements, grounded, sender-receiver pair (1,1): (left) normalized mean; (right) superposed mean and standard deviation with removed offset.

We compared self and mutual capacitance mode and got to the conclusion, that for applications which need to be robust and are surrounded by changing environmental properties it is advisable to choose the self capacitance mode over the mutual capacitance mode. This is because the parasitic capacitance is at some point so high that the small change in capacitance in mutual capacitance mode is not detectable anymore in comparison to the fluctuations in the noise. This leads us to the recommendation to prefer self capacitance measurement mode over mutual capacitance mode, especially when robustness is required, and the environmental conditions are prone to a lot of change.

However, by comparing the results in self and mutual capacitance mode of the different electrode materials, we infer that without the influence of noise all electrode materials would be equally well suitable for flexible capacitive sensor applications.

5.2. Efficiency of e-textiles in capacitive sensing

As e-textiles represent an emerging field and market attractiveness rises [Sul19], looking more deeply into capabilities of e-textile gives further indication on how to most effectively use them as part of applications. While designing an application using e-textile capacitive sensing electrodes, various questions need to be addressed: Which shape and size of electrodes should be used? Which material, conductive thread or fabric, should be used? Which pattern filling should be used? What kind of stitching should be used? And how do these characteristics influence an application?

In order to find answers to these questions, we create different electrodes with specific characteristics. The goal is to compare the different electrodes regarding the performance in a measurement setup

for capacitive proximity sensing. This is achieved by measuring the capacitance in an as noise-free environment as possible. The measurement device at choice is a capacitive proximity sensing measurement device where a reference electrode is lifted, and sensor values are gathered at different distances. This measurement device, called CapLiper (see Figure 5.9), has been developed by M. Majewski in his master's thesis [Maj17].

5.2.1. Measurement setup

To evaluate the performance of textile electrodes, as well as comparing textile electrodes to classic copper-based electrodes, a standardized method is needed. This method has to provide a similar environment across all evaluation runs. The assessment space has to be isolated from external influences, such as electric fields and electric noise. This isolation allows confidence regarding the measured values, as well as a higher resolution rating. To contain the influence of external noise throughout the evaluation trials, an effective shielding is needed. The used capacitive sensing board (OpenCapSense) offers an active shielding functionality. A connected conductive material acts as a barrier between unintended electrical influences from the outside of the CapLiper test chamber and the electrodes surface inside. To provide measurements under the same circumstances for all electrodes regarding electrode distance and noise minimization, a setup was created, composed of a mechatronic surrogate hand, a controller, and a data recording software. Figure 5.9 shows the measurement chamber, which serves as shield, the OpenCapSense board and the controller which moves the upper electrode, the surrogate hand. The size of the upper electrode is 5x5 cm. Inside the measurement chamber only one capacitive sensor is placed. It is connected through a wire to the evaluated electrode.

In order to evaluate textile electrodes, a system to hold the electrodes steady was developed. It is inspired by embroidery hoops. By 3D-printing such a hoop, an inner and an outer ring, which fit into each other, the textile on which the electrode is sewn can be fixed, like a fabric ready for embroidery. The electrode basic size is of 6x6 cm. The connection between electrode a capacitive sensor is done through a wire which is soldered at one end to the sensor pad, and at the other end is wrapped around and soldered to one side of a fabric snap. By attaching this side of the fabric snap to the corresponding second part, which is sewn to the electrode, the sensor is connected to the different measured electrodes.

Each electrode is placed in the measurement chamber and the upper reference electrode is moved up in steps of 1 cm. The arm moves up to a distance of 31 cm. After the arm moves up, the system stands still for 2 seconds until vibrations from the up movement have stopped. Then the data at each distance is recorded for about one minute.

5.2.2. Data processing

For each measured distance about 1470 sensor samples are gathered. Thus, during a lift from 0 to 31 cm more than 47000 data samples are gathered. For each distance, the mean and the standard deviation of the gathered sensor data are calculated. This is done for all three executions of the same measurement. For each distance, the median of the three means and the standard deviation are computed. The resulting

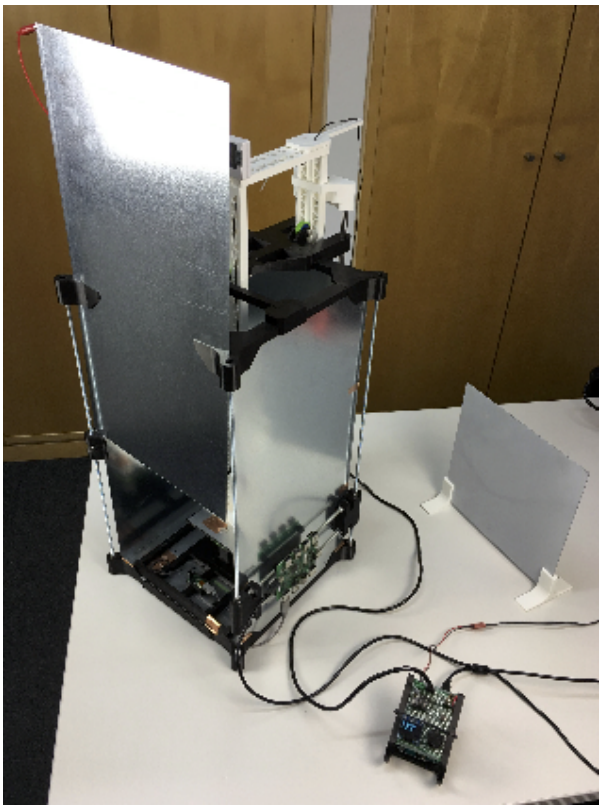

Figure 5.9.: Capacitive proximity sensing measurement device

values of mean and standard deviation are used throughout the following sections as basis for various computations displayed in various graphs.

The graphs computed have the goal of visualizing the performance of the compared electrode groups. The four graph types, see Figure 5.15, represent: raw sensor data shifted to a common baseline, normalization of the raw sensor data, the computed noise range (NR) of the raw sensor values and the signal to noise ratio (SNR) of the raw sensor values.

The raw sensor values are computed as mentioned by calculating the mean and standard deviation. By plotting these values, one can observe that the values follow the expected exponential curve, as mentioned in Chapter 2. These curves reach a plateau. When environment conditions such as temperature and humidity change, these plateaus are at different levels. To be able to more easily compare the electrodes, the curves with different plateau levels are brought to the same level, by shifting the curves with the difference. For this, the mean sensor value at the distance of 30 cm is taken as reference. All curves are shifted to the minimum of these values, thus to the lowest curve. The shape of the curves remains the same only their relative placement of the curves on the graphs is changed.

The normalization of the raw sensor data is computed by compiling the maximum and minimum sensor values for one electrode measurement set. The mean and standard deviation are normalized by mapping the data between the minimum and the maximum to the interval $[0,1]$. The formula used for this is:

$$normalizedvalue = (value - minimum)/(maximum - minimum)$$

Normalization is helpful in representing the data, due to the fact that the absolute values can shift under environmental condition changes. By normalizing the curves, comparisons are possible, by comparing the procedural gradients of the displayed sensor data.

The standard deviation is derived from the gathered raw sensor data. If the standard deviation is small, it indicates that different distances can be well distinguished. If the standard deviation is large, a distance cannot be detected with high precision. Finally, if the standard deviation is larger than the difference of the sensor values at the adjacent distances, the sensor values cannot be clearly assigned to a specific distance.

The Noise Range (NR) is a value computed on the base of the standard deviation 5.10. It shows the noise of the signal with reference to the distance. A maximum and minimum sensor value are calculated for each distance. By adding the standard deviation to the average sensor value of a specific distance the maximum value is computed. By subtracting the standard deviation, the minimum value for this distance is computed. Subsequently, the maximum and minimum values are projected onto the sensor values function. Finally, the height distance between both new function points is derived, which represents the NR value. The NR depends not only on the measured noise, represented by the standard deviation, but also on the steepness of the curve resulting from the sensor values. Furthermore, the NR value indicates the estimated distances of not uniquely identifiable distances for the given sensor value. Given this, a lower value of the NR at a given distance indicates a better performance of the electrode. By summing the NR values up for all distances, an overall NR for the electrode is computed, and used for the performance comparison evaluation.

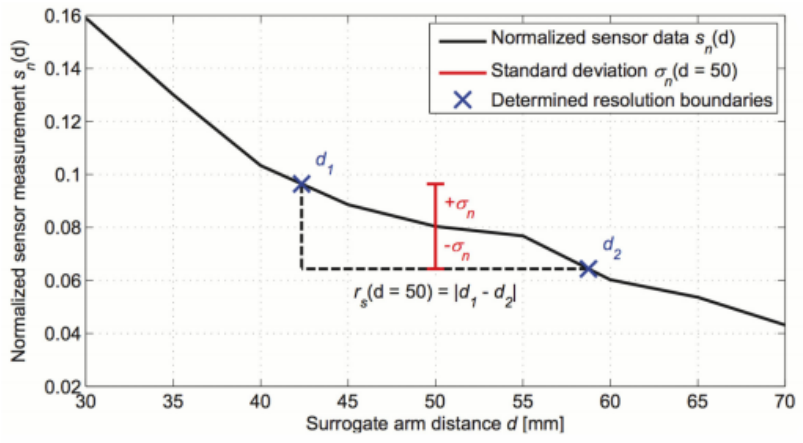

Figure 5.10.: Computation of Noise Range (NR) [GPBB*13]

The Signal to Noise Ratio (SNR) is a common measure in electrical and communication engineering to represent the quality of a signal. It expresses the level of the desired signal versus the level of background noise. It is defined as ratio of signal power to noise power. In this case, the meaningful input is the signal, the sensor values, at a given distance and the unwanted input is the noise, represented by the standard deviation. Thus, the formula applied for the SNR computation is:

$$SNR = \frac{\mu}{\sigma}$$

where μ is the mean at a given distance and σ is the standard deviation. Thus, the graphs displaying the SNR for various electrodes shows the quality of the signal throughout the measured distances.

These four views of the raw data, the normalized data, the NR and the SNR will be displayed throughout the comparison of different electrode groups presented in Section 5.2.3.

5.2.3. Evaluation measurement overview

As stated in Figure 5.1 the goal is to identify the performance of textile electrodes depending on different factors such as electrode material, pattern, pattern density and shape. The main focus in this section lies on electrodes fabricated from conductive textiles and conductive threads. These are more in detail the analysis of size of electrode, material of electrode, stretching deformation, pattern/filling of electrode, shape of electrode, support fabric, elasticity of e-textile fabric and stitching distance. An electrode in shape of a rectangle is used as reference electrode. All the other electrodes besides the electrodes from the electrode size comparison will be the same size as the reference electrode. Additionally, a control electrode, called placebo electrode is used for the general comparison. The placebo electrode is an electrode where only the connecting snap is sewn to the empty fabric electrode and the

wire is connected to the capacitive sensor. Through this, the performance with regards to a minimal electrode is compared.

Figure 5.11 shows the ensemble of electrodes used for the measurements. The numbers highlight different groups of electrodes compared more in detail throughout Sections 5.2.4 to 5.2.7. The electrode numerated with group 8 is the placebo electrode. It is shown also as part of group 7, however, it is used in all the proceeding electrode comparisons. The comparison of materials such as conductive textile and thread is performed from different perspectives and is represented in multiple groups such as in group 1, where different sizes of electrodes are compared, group 2, where stretching deformations are performed, group 3, where different types of conductive thread and different types conductive fabric are compared, as well as in group 5, where different filling degrees of the basic rectangle are compared. The measurements of group 1 are compared in Section 5.2.4. The comparison results of electrodes from group 5 are presented in Section 5.2.5. In Section 5.2.9 and 5.2.7 the comparison of different textiles and thread types are presented. Section 5.2.8 presents the stretching deformation comparison for conductive fabrics.

Since conductive thread offers the possibility to be easily added to existing fabrics, adding additional electronic functionality to the fabric, it is further evaluated more in detail. By using a sewing machine, thread can be sewn in different ways, for instance, using different stitching types. Also, various shapes can be easily created.

Figure 5.11 shows at the bottom the electrodes of group 7. These are sewn into different possible shapes. In order to compare only the variation given by the shape and eliminate the influence of the amount of material used to create the shapes, these shapes have the same perimeter, using thus the same amount of conductive material. The results of the shape comparison of electrodes are presented in Section 5.2.11.

Group 6 from Figure 5.11 shows the basic rectangle shape, sewn using different stitching types of the machine: narrow zigzag stitch and wide zigzag stitch. The results from the stitching type comparison are presented in Section 5.2.6.

Finally, group 4 shows three electrodes on which the reference shape of a rectangle was sewn. They are sewn in a similar manner, only that the material on which the conductive material is sewn on differs. Variations of different cotton, polyester compositions are used and a common material, such as synthetic leather. The results for this comparison of measurements are presented in Section 5.2.10.

Many more categories of comparison are possible. For example, the comparison of different shapes using conductive textile instead of conductive thread, or multiple filling patterns, adjusting also the density. There are many types of materials which are different material mixes, like the ones used in sportswear. It would be interesting to observe, if multiple properties identified with a good performance amplify the performance of the resulting electrode.

This initial set of comparing groups is meant as a basic start and should give an indication regarding the general performance tendency.

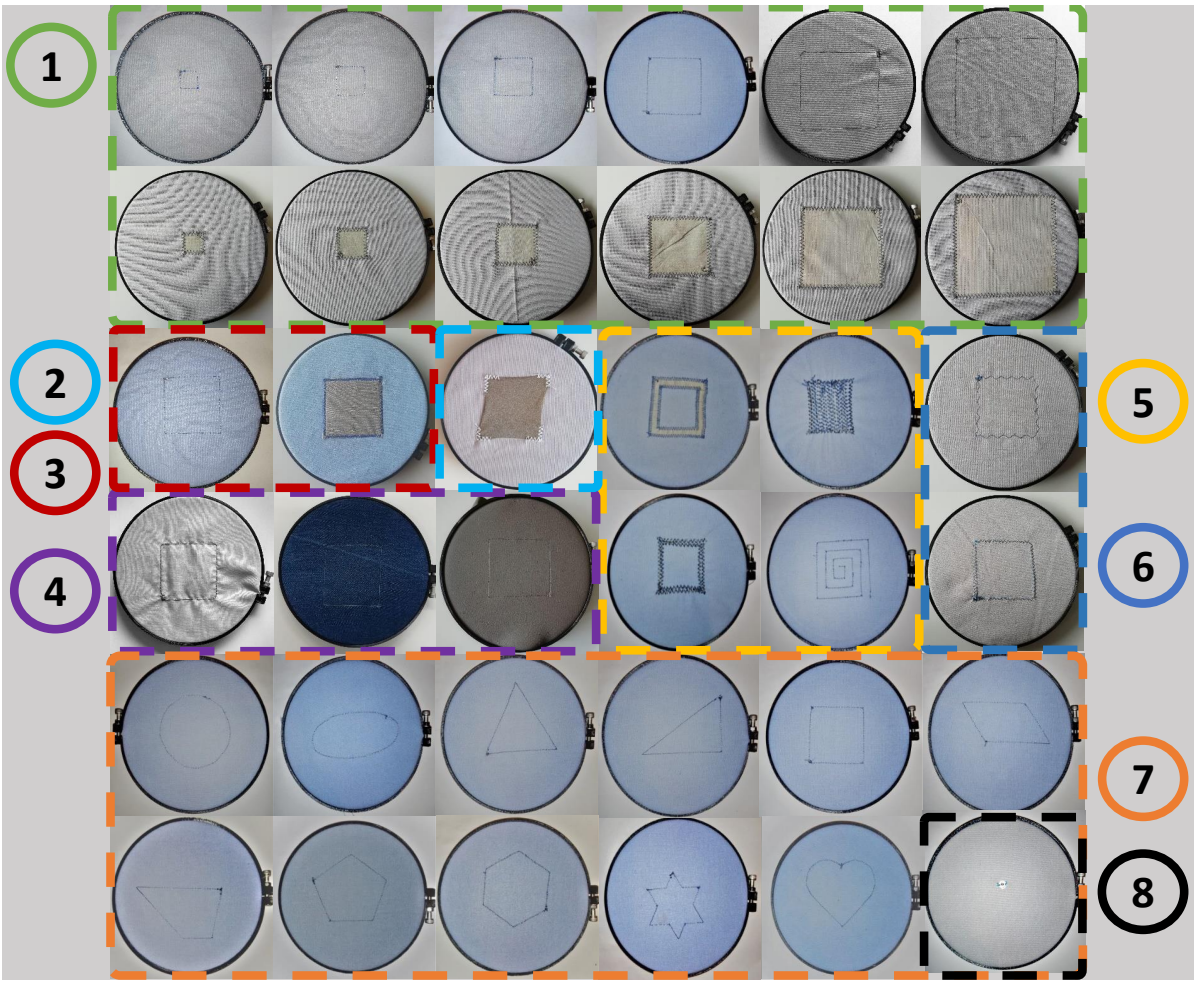

Figure 5.11.: Overview of electrode comparison groups: 1) size; 2) stretch deformation; 3) conductive thread and textile type; 4) support material; 5) filling degree; 6) stitching type; 7) shape; 8) placebo electrode;

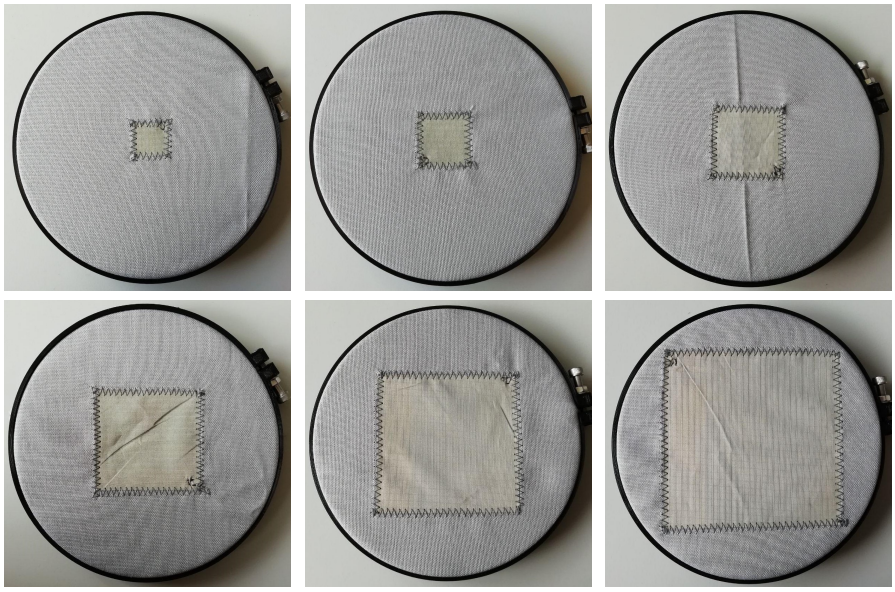

Figure 5.12.: Electrodes made of conductive textile rectangles of different sizes: 2, 3, 4, 6, 8 and 10 cm

5.2.4. Comparison of electrode size

In order to identify the influence of the electrode size, we use our reference shape of a rectangle and create a few electrodes with different sizes: 2x2 cm, 3x3 cm, 4x4 cm, 6x6 cm, 8x8 cm, 10x10 cm. They are created from both materials: conductive textile and conductive thread. The textile material used is the same as the one used in Section 5.1, *Zell-RS*. It is not stretchable and is woven in a ripstop manner. The thread used for sewing is conductive thread made of two conductive strands, *Adafruits Stainless Thin Conductive Thread*[2] (0.2 mm thick, 2 ply thread, 1.3 ohm per inch). It is widespread throughout the shops for electrical craftship. The created electrodes are shown in Figure 5.13 and 5.12.

The textile electrodes are created by cutting out pieces of conductive textile, in the desired size. They are subsequently machine-sewed to the supporting fabric. The thread used to sew the conductive material to the support material is regular thread. The snap for the connection with the wire and through that to the sensor, is sewn by hand using conductive thread on the reverse side of the fabric. The used supported fabric is 100% cotton, which is tightly woven, thus is not significantly stretchable.

The electrodes made of conductive thread are created by sewing the perimeter of the desired rectangle size. For this, a sewing machine was used equipped with a regular and a conductive thread. The rectangle is sewn in straight stitch on the setting "2" in stitch length. For the utilized sewing machine this represents a step length of 1.75 mm. The snap is sewn in a similar fashion as with all electrodes using conductive thread.

[2] https://www.adafruit.com/product/640

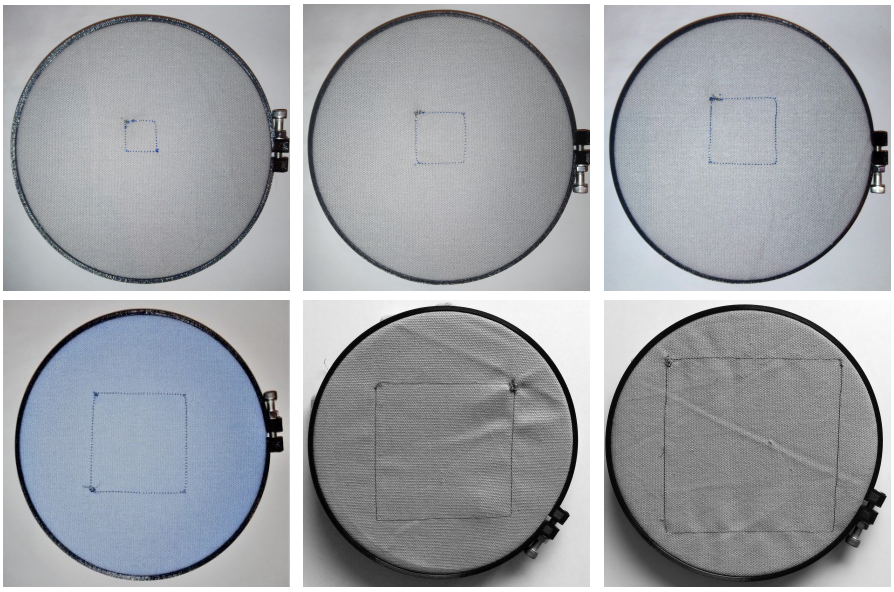

Figure 5.13.: Electrodes made of conductive thread rectangle perimeters of different sizes: 2, 3, 4, 6, 8 and 10 cm

The expected performance, for both conductive textile as well as conductive thread is derived from the basic formula of the capacitance, where the capacitance is proportional to the electrode area and inversely proportional to the distance between the capacitor plates, see Section 2.4.1.3 for more details.

$$C = \frac{\varepsilon_0 \varepsilon_r S}{d}$$

Thus, with the area of the textile electrodes rising from 2-10 cm the capacitance at a given distance should also be bigger as the electrode size increases.

Figure 5.14 shows the resulting values of the measurements of different sizes of conductive textile electrodes. The upper left diagram shows the raw shifted data. All curves were shifted to the common value they are converging to. The placebo electrode has the lowest values and then the values increase with increasing size of the electrode. This diagram confirms the expected behaviour in performance. By plotting the normalized curves, one can see that the slopes of the curves are very similar. Consulting the graph displaying the NR, it shows that the NR reaches values of 6 mm. Up until a distance of 200 mm the NR is low, and afterwards it increases. In contrast, looking at the graph displaying the SNR, the values of the noise are higher in the first 7 cm in relation to the sensor values, resulting in lower SNR. After the 7 cm the SNR of most electrodes is higher, indicating that the noise, in this case the standard deviation is smaller as at the beginning. The contrast between the good NR at the beginning and the worse SNR at the beginning do not indicate conflicting measures, they show that the NR does not solely depend on the standard deviation - the noise - but also on the slope of the curve, which for all electrodes

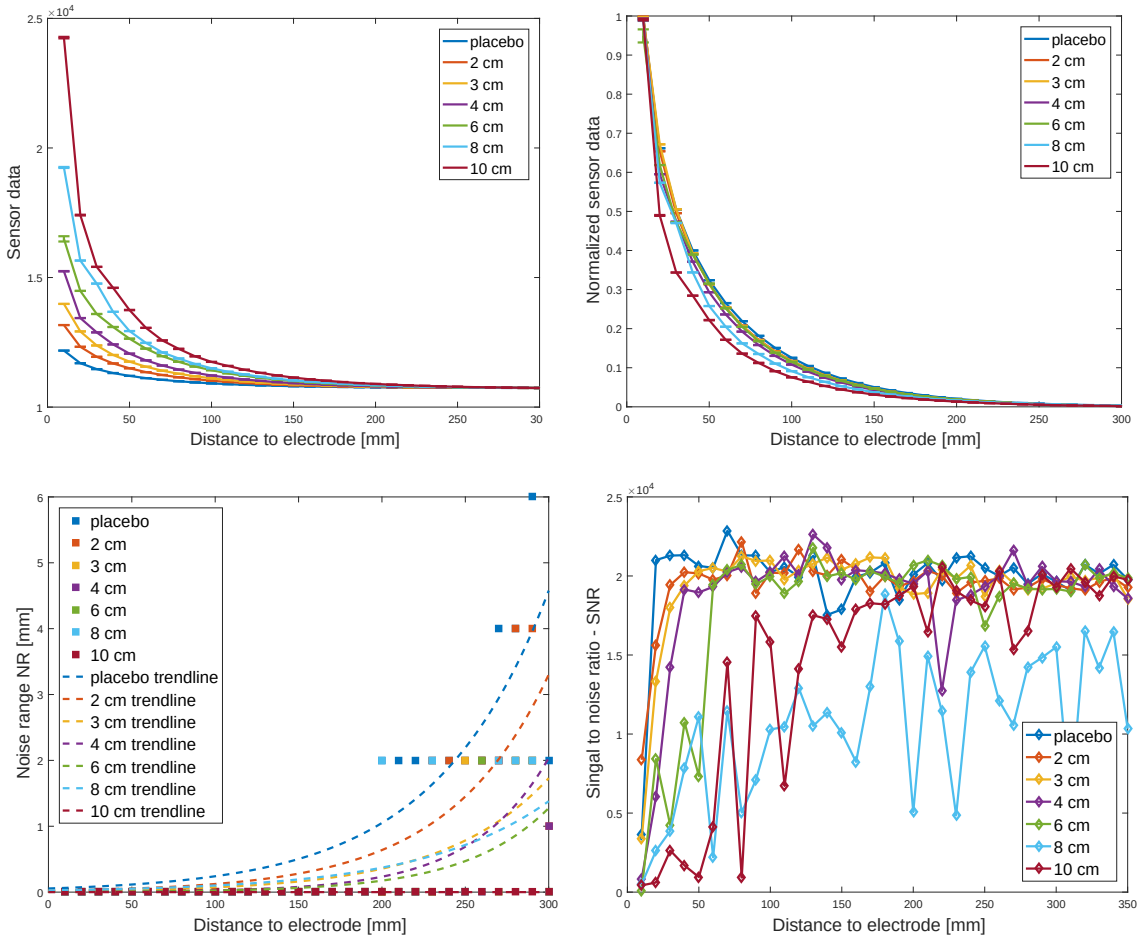

Figure 5.14.: Comparative graphs of conductive textile size comparison: shifted raw sensor data and standard deviation (top left); normalized sensor data (top right); Noise Range (bottom left); Signal-to-Noise Ratio (bottom right).

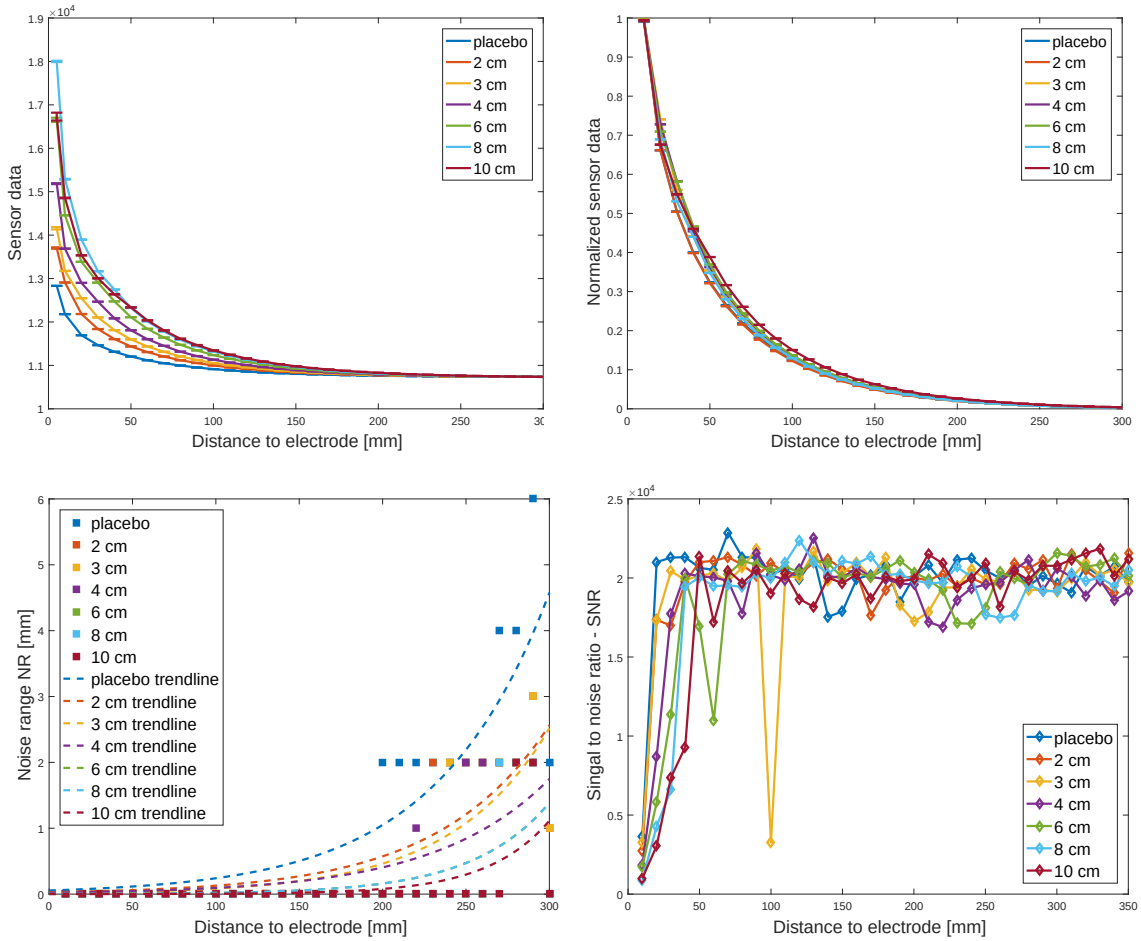

Figure 5.15.: Comparative graphs of conductive thread size comparison: shifted raw sensor data and standard deviation (top left); normalized sensor data (top right); Noise Range (bottom left); Singal-to-Noise Ratio (bottom right).

is very steep, especially for the 8 cm and 10 cm. Thus, the noise is not significantly high to influence the ability to discriminate between different distances.

Figure 5.15 shows the comparative graphs of rectangular electrodes made from conductive thread in different sizes. The graph on the top left represents the raw sensor data which is shifted. Similarly to the conductive textile electrodes, the smallest values at a given distance is achieved by the placebo electrode, with increasing values as the size of the electrode increases. The normalized graph on the top right shows that the curves have similar slopes. What can be observed is, that the behaviour observed at the distances of 1 cm for the conductive textile electrodes is not present anymore. Nonetheless, the values of the electrodes of sizes 6, 8 and 10 cm are very close together. This could be explained by the fact, that they are bigger as the reference electrode used for the measurements. In the NR view on the bottom left it still can be observed that the 10 cm electrode performs best in terms of NR. In contrast to to the conductive textile electrodes, the NR up until 20 cm is very low for all electrode sizes, indicating a good discrimination of distances. From 20 cm up, the NR starts to vary more, however it reaches a maximum at 6 mm, which indicates that even at a distance of 29 cm the distance of the electrode can be discerned. In practice a 6 mm NR means that an object at a distance of 29 cm could be confused with an object at 28.7 cm or at 29.3 cm. The SNR at close distances is small, indicating a higher standard deviation. After the distance of 7 cm, the SNR varies, but settles down, similarly as the behaviour of the SNR observed for the conductive textile electrodes.

Concluding, the two Figures 5.14 and 5.15 give an indication which the best performing electrode is in this group of size comparing electrodes. For both cases, the conductive textile and conductive thread, the largest electrodes have the smallest overall NR, thus the best performance. The overall NR of the conductive textile electrode of size 10 cm is 0 mm and the overall NR of the conductive thread electrode of size 10 cm is 4 mm - as also the trendlines indicate. The 2 cm electrodes have in contrast the highest overall NR besides the placebo electrode. This confirms the expected behaviour, supporting that a larger surface results in a higher detection range. These graphs show that this behaviour can be observed not only for surfaces of conductive material, but also applies to perimeters of rectangles made of conductive thread.

5.2.5. Comparison of filling degree of electrodes

In order to determine the trade-off between filling a surface completely with conductive material and keeping just the perimeter of the surface, we have varied the ways of filling these two shapes. Figure 5.16 shows in the top three images a rectangle filled with different variations, and in the bottom three images variations on perimeters of a rectangle. Through these variations the influence of the surface filling degree of the electrode is analysed. in addition to the sensing performance, the effort and material cost of creating these electrodes is also monitored, playing an important role in the feasibility of the electrode.

Figures 5.16a - 5.16c represent a rectangle with its surface filled by conductive textile, conductive thread densely stitched and conductive thread loosely stitched. Image 5.16a shows conductive textile cut to the reference rectangle shape. This electrode sample of a conductive textile rectangle of 6 cm side

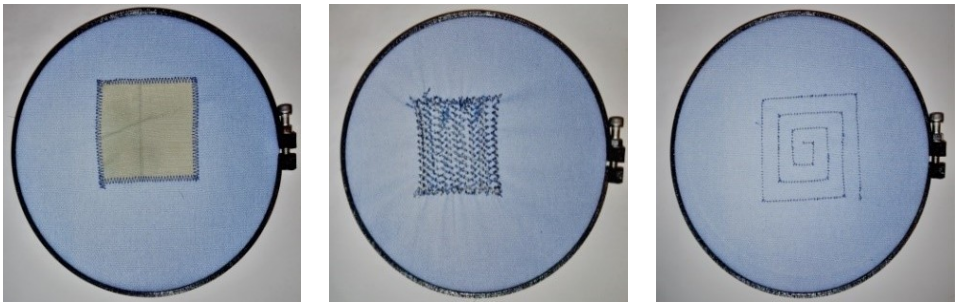

(a) textile filled (b) thread zigzag filled (c) thread spiral filled

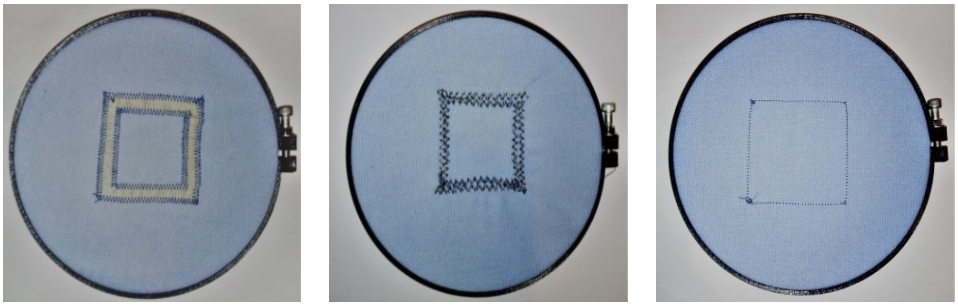

(d) textile perimeter (e) thread zigzag perimeter (f) thread perimeter

Figure 5.16.: Comparison of filling degree with textile and conductive thread

length is the same as the one used in the electrode size comparison. The electrode from Image 5.16d is made of the same conductive textile material. In Image 5.16b, the same 6 cm side length rectangle is filled by sewing conducting thread in a dense zigzag stitch. The same conductive thread is used throughout the other electrodes, as was used in the electrode size comparison. Image 5.16c shows a rectangle roughly filled using a spiral shape with a straight stitch. From Image 5.16a with the highest conductive material density on the surface, to Image 5.16c the density of the conductive material filling the surfaces diminishes.

These filled surfaces are compared against only the perimeter of the rectangle filled with conductive material. Thus, Image 5.16d shows a rectangle perimeter made of conductive textile. It has a width of 1 cm and has been cut out of the reference shape. This same area is filled with conductive thread sewn in a zigzag stitch, see Image 5.16e, and a straight conductive thread stitch in Image 5.16f. The electrode from Image 5.16f is the same as the conductive thread electrode used in the conductive thread size comparison, see Section 5.2.4.

The expected performance for this set of electrodes with varying filling degrees, realized by using conductive textile as well as conductive thread is derived from the same basic formula of the capacitance mentioned in Section 5.2.4. Thus, if we consider the surface of the electrodes to be only the surface where the supporting textile material is covered, the denser the surface is filled, the bigger the surface is.

Hence, the electrode loosely filled with a spiral made of conductive thread and the rectangle perimeter made of conductive textile are the surfaces with the lowest density and according surface. We expect that as density of conductive material increases, the capacitance at a given distance should also be bigger as the electrode surface density increases.

Figure 5.17 shows the results of the measurement sets from the six electrodes with different fill degree from Figure 5.16 plus the placebo electrode. The graph on the top left shows the raw data shifted to a common baseline. The smallest values are achieved by the placebo electrode. Next are the thread perimeter, thread spiral filled, thread zigzag filled at the same level as thread zigzag perimeter, then the textile perimeter and last the textile filled electrode. The normalized graph on the top right shows that the conductive textile electrodes have a slightly steeper slope at the beginning, while the electrodes from conductive thread have a very similar slope, which is close to the placebo slope. In the NR view on the bottom left can be observed that the conductive textile electrodes have the lowest NR and their trendlines are overlapping. Up until nearly the end also the thread spiral filled electrode has a very low NR, allowing for a good correlation of measured values to distance. Overlapping are also the thread zigzag filled and the thread zigzag perimeter electrodes. Finally, still with a distance to the placebo electrode the thread perimeter electrode has the highest NR. Overall, the NR is small, with a maximum of 6 mm. Similarly to the SNR of the electrode size comparisons, the SNR up to distances of roughly 7 cm are small, while after 7 cm the SNR varies with a few different spikes. However, this shows that the standard deviation at small distances is higher and plateaus afterward.

By observing the two variation of conductive textile, the filled rectangle and the rectangle perimeter of 1 cm in the raw data and the NR graphs, they are close together, or even overlapping. In the NR view they are equal, only the higher values from the raw sensor data graph differentiate them. The fact that they both perform so well indicates that electrode surfaces do not have to be fully covered. Creating an electrode out of a part of the surface of the same shape provides the same results by using less conductive material. Thus, when creating textiles in which the conductive part is embedded, not the whole surface has to be made of conductive material, the outer border of the same shape and size accomplishes similar results. Hence, costs could be reduced.

When considering only the NR, the thread spiral filled overlaps until the distance of 22 cm with the conductive textile electrodes. In the raw sensor data view, it has the second smallest values after the thread perimeter electrode. However, as the NR takes the slope and the standard deviation into account, it shows that it performs similarly well. One can very well correlate distance to sensor values.

In concordance with the filled and perimeter conductive textile electrodes, the filled and perimeter zigzag stitched electrodes have the same NR. They also have very similar raw sensor data values. This confirms that not the whole surface of a shape needs to be filled with conductive material, a thick perimeter performs similarly well.

Surprising from the NR view, is the difference in NR for the thread perimeter and the thread spiral filled electrode. The filled electrode performs in terms of NR at the level of the conductive textile electrodes. The zigzag stitch filled surface uses much more material as the spiral filled electrode. This observation contradicts the expected behaviour. Possible reasons could lie in the nature of the zigzag

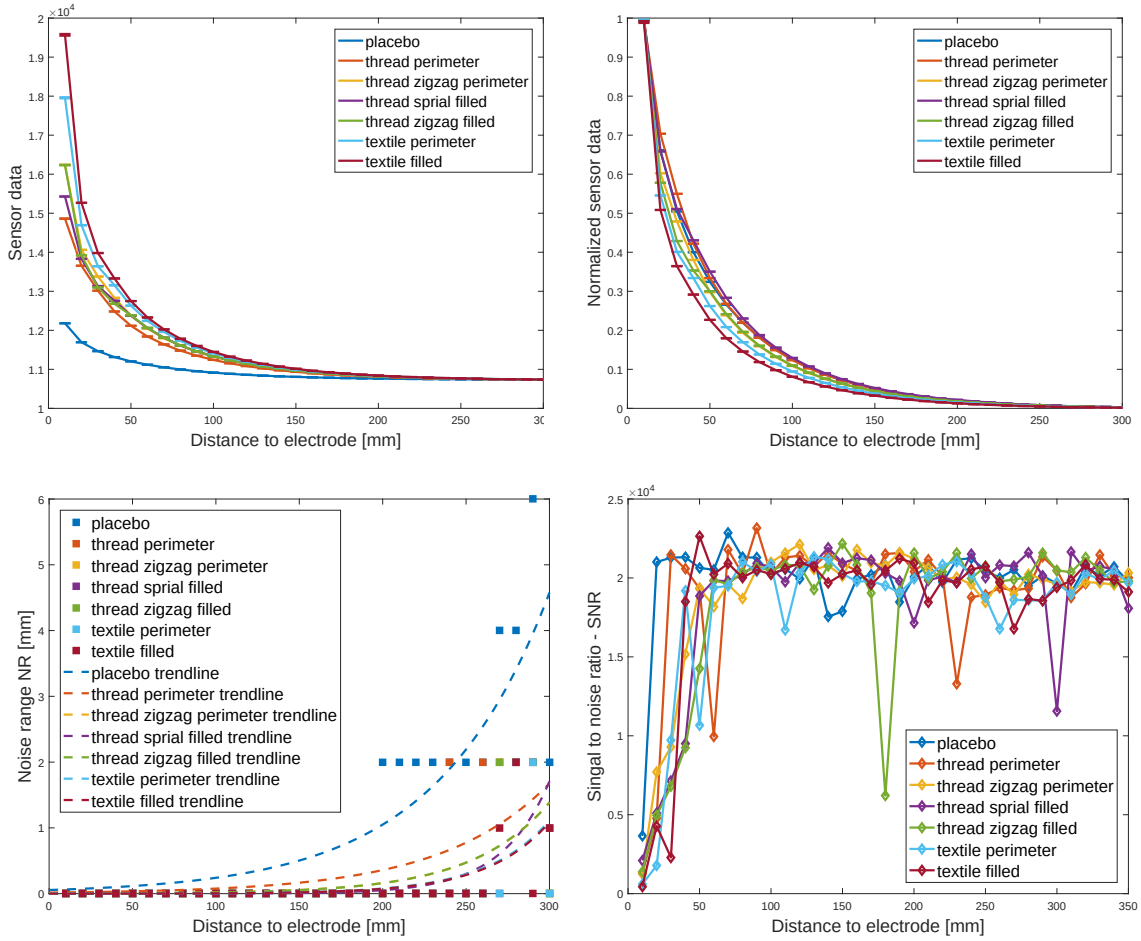

Figure 5.17.: Comparative graphs of electrode filling degree comparison: shifted raw sensor data and standard deviation (top left); normalized sensor data (top right); Noise Range (bottom left); Singal-to-Noise Ratio (bottom right).

stitch - having multiple edges, or by creating multiple connections between the threads - creating a whole surface, not like with the filled spiral one thread which does not connect to itself.

By summarizing the three compared filling degrees, when using conductive textile or conductive thread in a zigzag stitch, a thick perimeter of the same surface performs similarly well as the filled surface. However, in contrast a surface loosely filled with a spiral performs as good as the conductive textile and better than the zigzag stitched electrodes. When having to choose which filling degree one wants to use, a material optimizing choice would be the thicker border or a filled spiral. The filled spiral has the advantage, that the material is distributed over the whole surface and when interacting with the surface, e.g. by though, the possibility to touch the conductive part of the material is more likely.

5.2.6. Comparison of stitching types

In order to investigate the influence of different stitching types of conductive thread, we have used the most common stitching patterns on the reference rectangle shape. Figure 5.18 shows the three used stitching types: straight stitch, zigzag narrow stitch, and zigzag wide stitch, also known as multiple zigzag stitch. All electrodes were created using the same conductive thread type and using the same type of support material. The straight stitch is most common stitch, used the majority of the time. The zigzag stitches are used for sewing elastic materials which are able to stretch and the stitch need to also stretch. The wide zigzag stretch is used to finish the edges on a stretchy fabric, preventing puckering which might happen using the narrow zigzag stitch.

Indicators for the expected behaviour is on one side the general formula of the capacitance, where the capacitance is proportional to the electrode area and inversely proportional to the distance between the capacitor plates, see Section 2.4.1.3 for more details. However, the area and the amount of material does not vary to much in the case of different stitching types. A second indicator might be the higher amount of sharp edges for the zigzag stitches. The article of Madaan et. al state that sharp corners are more sensitive - at edges electrical field are focused [MK12]. The high amount of edges creates electric field lines straying in many different directions.

Figure 5.19 shows the results of the measurement sets of the three different stitching type electrodes and the placebo electrode. The graph on the top left shows the raw sensor data shifted to a common baseline. From the course of the curves the placebo electrode is on the bottom, followed by the straight stitch electrode and then the two zigzag electrodes are very close together. The narrow zigzag electrode has slightly higher values as the wide zigzag electrode. The normalized view of the sensor data only conveys a very similar steepness of the curves, the straight electrode is the least steep. When looking at the bottom left graph of the NR, the same order is kept as in the raw sensor data view. The two zigzag electrodes have an overlapping trendline with the same NR when adding it up. They are followed by the stitched electrode and at a certain distance by the placebo electrode. The SNR, in the bottom right graph, follows the already observed pattern, that the standard deviation is higher at the beginning of up to 4 cm and then plateaus with a few spikes of different electrodes.

Concluding, the zigzag stitched electrodes have the same overall NR, slightly higher than the straight stitch electrode. It was expected that due to more material being used by the zigzag stitching types these

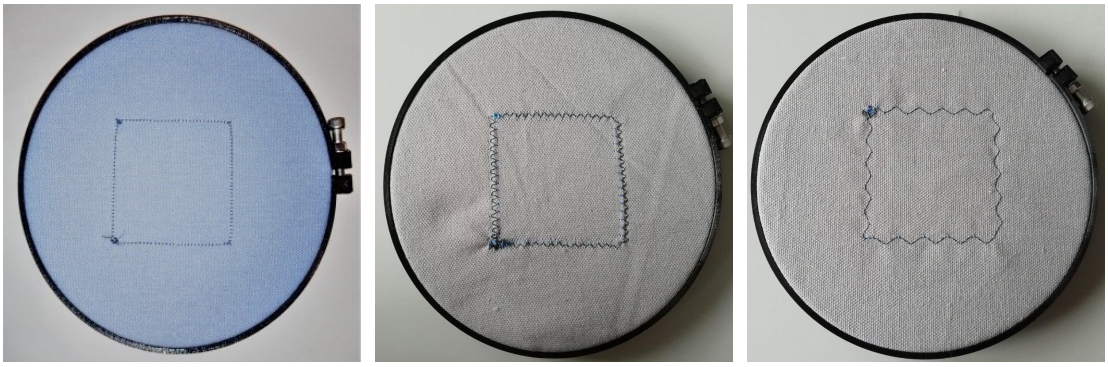

Figure 5.18.: Conductive thread rectangle with different stitching types: straight stitch, zigzag narrow stitch, zigzag wide stitch

result in higher sensor values. Since the narrow zigzag stitch is also very common it is a good choice if the pattern of the intended smart fabric pattern allows it. The fact that it has more edges does not seem to negatively impact the performance. However, if minimal use of conductive material is intended, then a straight stitch is also well suited.

5.2.7. Comparison of conductive textile type

Conductive textiles can be purchased in different variations. They are addressing different needs, such as e.g. the need to integrate interactive textiles into elastic materials. Thus, we have purchased additionally to the already used Shieldex Zell-RS[3] one variation of conductive elastic material Shieldex Medtex P130[4]and compared it against the previously used conductive fabric, as shown in Figure 5.20. The raw material of the conductive fabric is Nylon ripstop fabric, plated with silver and a surface resistivity of 0.02 Ohms. The elastic conductive fabrics raw material is a mixture of 78% Nylon and 22% Elastomer, plated with silver and a surface resistivity of on average 5 Ohm. It is stretchable in two directions. After cutting a rectangle of 6 cm side length, it was sewn to the support material with regular thread. The fabric was sewn in loose state, not stretched in any direction.

According to the base formula of the capacitance, see Section 2.4.1.3 for more details, the capacitance should be the same. Since the active surface is the same, the different conductivity of the materials could be an indicator on performance differences.

The resulting curves of the measurements are shown in Figure 5.21. The graphs in the left images shows the raw sensor data shifted to a common baseline. At the bottom is the curve of the placebo electrode and with some distance are the curves of the ripstop and elastic conductive textile partially overlapping.

[3]https://www.shieldextrading.net/wp-content/uploads/2018/08/1500101130-Zell-RS.pdf
[4]https://www.shieldextrading.net/wp-content/uploads/2018/08/1150902130-Medtex-P130.pdf

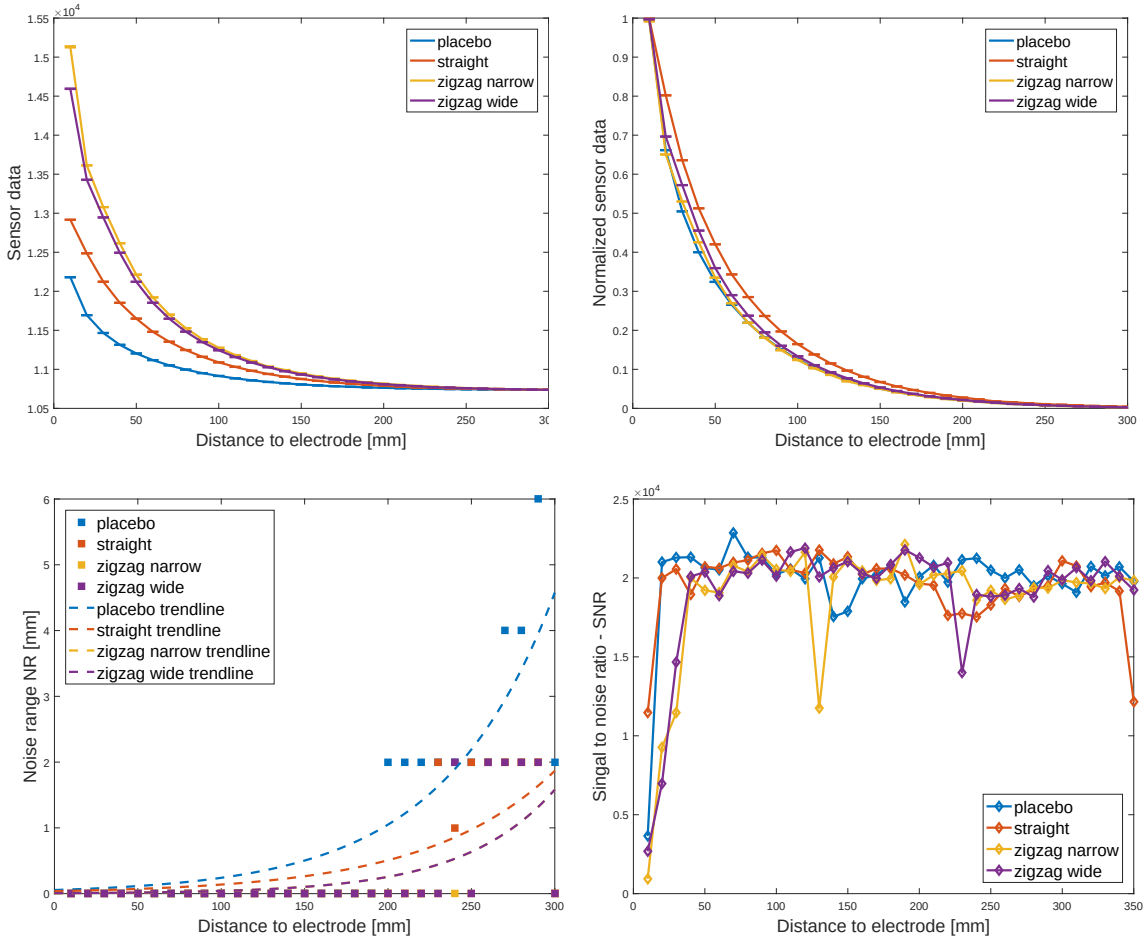

Figure 5.19.: Comparative graphs of stitching type comparison: shifted raw sensor data and standard deviation (top left); normalized sensor data (top right); Noise Range (bottom left); Singal-to-Noise Ratio (bottom right).

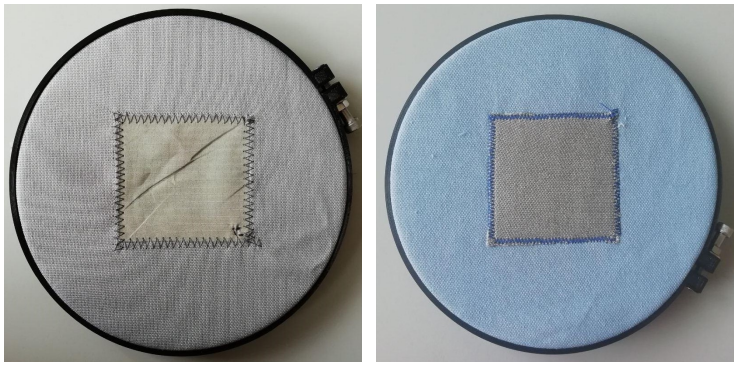

Figure 5.20.: Conductive textile rectangle with different material types: regular conductive textile ripstop, elastic conductive textile

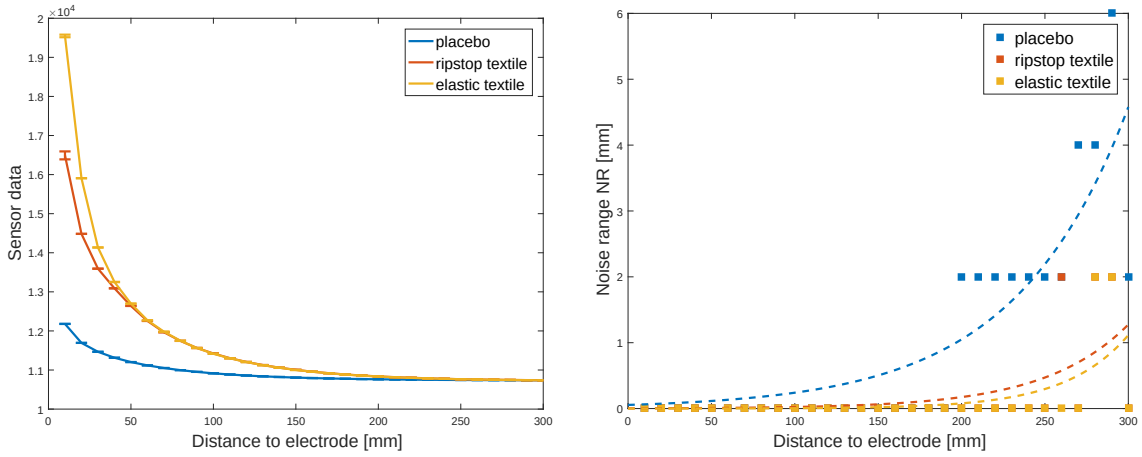

Figure 5.21.: Comparative graphs of conductive textile type comparison: shifted raw sensor data and standard deviation (left); Noise Range (right).

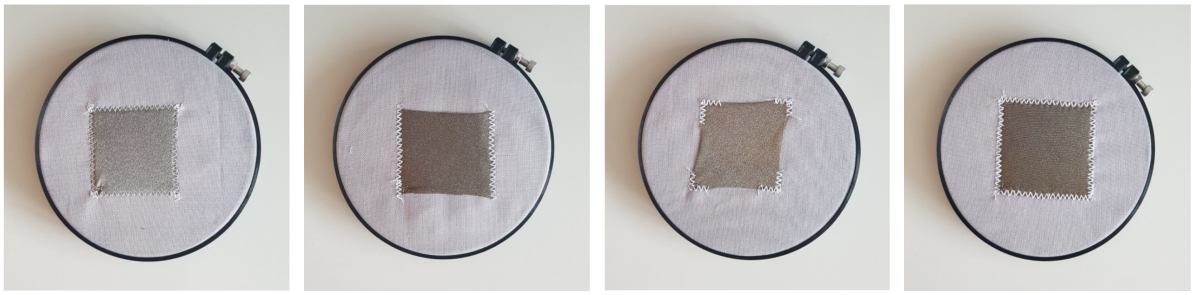

Figure 5.22.: Conductive elastic fabric stretched in different directions: reference rectangle shape, horizontally stretched electrode by 0.5 cm to the left and right side, diagonally stretched electrode by 0.5 cm to the upper right and lower left corner, electrode equally stretched by 0.5 cm in every direction

Consulting the graph shown on the right, the NR of the three electrodes are displayed. Up until distances of 27 cm the NR of the conductive fabrics is zero, just slightly rising towards the end to values of 2 mm. The smallest overall NR is achieved by the elastic textile electrode. It is however closely followed the ripstop textile.

Concluding, the graphs show that in a flat, unstretched setting the two conductive fabrics perform very similarly. However, since both perform similarly, the elastic material has the advantage that it is elastic and can adjust to surface strain. Secondly, the elastic conducive textile does not fray as much as the woven ripstop material.

5.2.8. Comparison of conductive textile stretch deformation

The same conductive elastic material (Shieldex Medtex P130) used in Section 5.2.7 is evaluated in this section towards the influence of stretching. Different stretching directions can be applied, stretching horizontally, stretching diagonally and stretching in both directions at the same time.

Figure 5.22 shows the reference shape of a rectangle not stretched, stretched in different directions and sewn to a not stretchable support material (the same as generally used). The stretching distance in each direction is of 0.5 cm. The electrodes support material was stretched by the embroidery hoop, such that it is flat and thus the material sewn to the surface stretches.

Since electrodes with bigger surface are expected to perform better than the ones with smaller surface, the expected behaviour for the stretched electrodes is, that the bigger the surface of the electrode is due to the stretch, the better the electrode performance.

Figure 5.23 shows the raw shifted data on the left, and on the right it shows the computed NR. The left diagram shows that the textile values are well differentiated from the values of the placebo electrode. However, the curves of the stretched and not stretched electrodes mostly overlap. The NR values of the

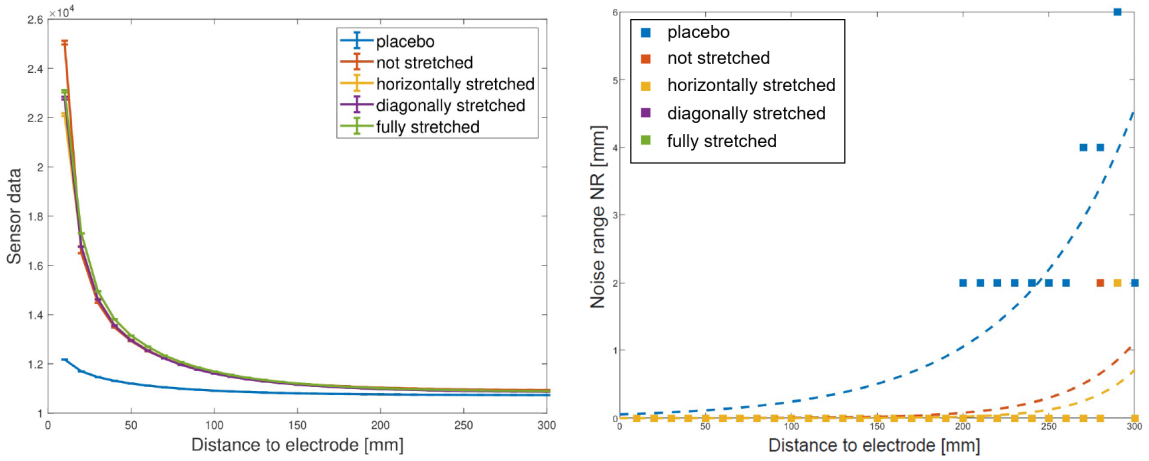

Figure 5.23.: Comparative graphs of stretched conductive elastic fabric comparison: shifted raw sensor data and standard deviation (left); Noise Range (right).

fabric are also very similar, with all the stretched variations overlapping. Up until a distance of 27 cm the NR is zero, when it rises firs in the not stretched fabric to 2 mm and then at 28 cm all stretched fabrics also reach a value of 2 mm.

In conclusion, this series of stretching measurements have not confirmed the expectations, of better performance of the stretched electrodes compared to the not stretched electrodes. Even though the NR of the stretched variations is smaller, it is very close to the not stretched electrode, indicating that stretching does not have a great influence, but if one would have to choose, the stretched electrodes perform slightly better in terms of NR.

5.2.9. Comparison of conductive thread type

Conductive thread can be purchased in different variations and has different properties. One main variation in the conductive thread that can be purchased is the number of thread strands which are twisted together to form the thread. The number of strands influences also the conductivity of the conductive thread. Thus, we compare two commonly available conductive threads with 2 and 3 strands, called 2ply and 3ply conductive thread. We use the 2ply and 3ply thread from Adafruit. Both are machine-sewable. Both threads are made of stainless steel. Due to the different number of strands the 2ply thread has a diameter of 0.2 mm, a resistance of 1.3 Ohm/Inch and a conduction current of up to 50 mA. The 3ply thread has a bigger diameter of 0.25 mm, a smaller resistance of 0.83 Ohm/Inch and a higher current of up to 100 mA. The evaluation is done similarly to the previous evaluations using the basic shape of a rectangle with the edge length of 6 cm.

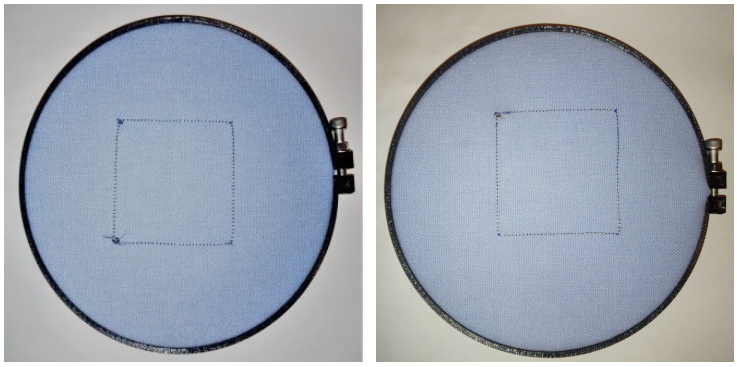

Figure 5.24.: Conductive thread with different thread types: 2ply (left); 3ply (right).

The expected behavior is, that the 3ply conductive thread performs better in measurements due to its smaller resistance which allows for higher capacitances. Additionally, it is expected, that the 3ply conductive thread is slightly more difficult to use when sewing with the sewing machine. This is because of the fibrous appearance and rough feel when touched.

Figure 5.25 shows on the left the raw sensor data shifted to a common baseline and on the right the values of the NR. The raw sensor values of the placebo electrode are overall the smallest, followed by the 2ply conductive thread and then the 3ply conductive thread. The overall NR of these electrodes show the electrodes in the same order, with the placebo electrode as highest NR, the 2ply electrode next, while the 3ply electrode shows the smallest overall NR. Up until a distance of 22 cm the electrodes have similar NRs. After this point the NR of the 3ply conductive thread has prevalently the smallest values with values of 2 mm from 27 to 9 cm.

As expected, the 3ply conductive thread has a better performance due to the smaller resistance and thereby better capacitive properties as the 2ply conductive thread. Additionally to the measurement performance, the ease of use is another important factor which needs mentioning. While creating the electrodes by using a sewing machine, one could observe due to the difference in diameter of the threads, that the 2ply conductive thread is easier to sew. The difference can be observed when sewing corners of electrode shapes. However, both can be used for sewing with the sewing machine.

5.2.10. Comparison of electrodes on different support materials

In order to inspect the possible influence of the support materials on capacitive electrodes, we sew the basic shape of a rectangle with the side length of 6 cm using the same 2ply conductive thread to four kind of support materials. Figure 5.26 shows the four general materials. They are samples of established materials used in everyday clothing and furniture. On the left, there is a tightly woven 100% cotton material. It is not stretchable and is used as a reference support material to all other measurements. Next to it, there is a mixed material of 65% polyester and 35% cotton. It is thinner as the cotton material but also not stretchable. The dark blue material, the third in Figure 5.26, is a

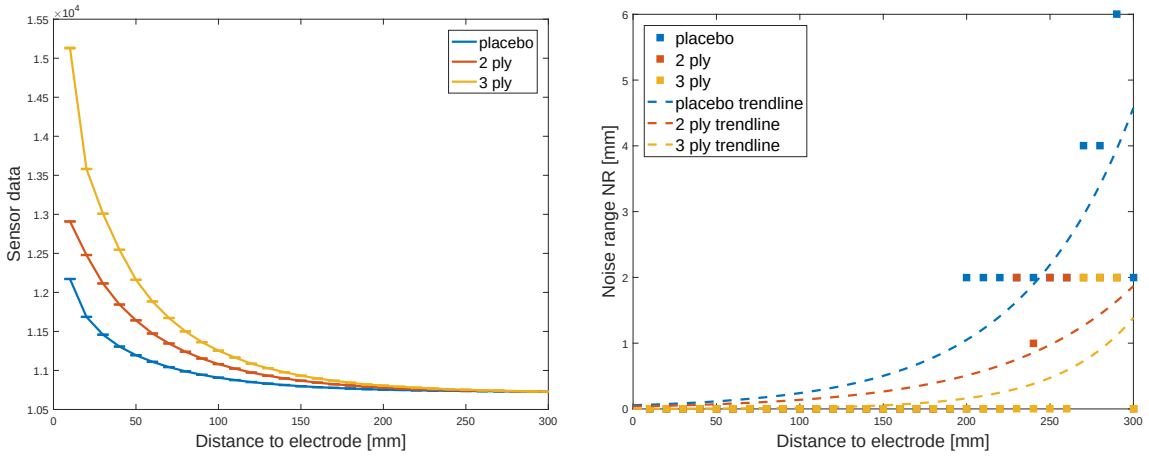

Figure 5.25.: Comparative graphs of conductive thread type comparison: shifted raw sensor data and standard deviation (left); Noise Range (right).

elastic material know from stretch jeans. It is a composed of a mixture of 84% cotton, 14% polyester and 2% elastane. It is tightly woven, thinner than the cotton material and thicker than the polyester material. Last, on the right of Figure 5.26, we show synthetic leather made of 100% polyurethane. It is the thickest material and in comparison to the stretch jeans material not stretchable. One is a more tightly woven jeans material made of cotton, while the other is a polyester material. [5]

Synthetic materials have generally a smaller resistivity as cotton material. Thus the expected behaviour for our different types of support materials is that the ones with less resistivity perform better than the ones with higher resistivity.

Figure 5.27 shows the curves of the measurement results of the support material comparison. In the left graphic the raw sensor data is displayed shifted to a common baseline. The placebo electrode is clearly distinguishable with the lowest values, followed by the material made of 100% cotton. Closer together, but with slightly increased values are the 65% polyester, the stretch jeans and synthetic leather with the highest values. The overall NR displayed in the graph on the right supports the findings of the raw sensor data. The overall NR of the material with 100% performs worse than the materials with some compound of synthetic fiber. Polymers have a poorer electrostatic isolating properties. Due to this the conductive thread can exchange with the polyester material more easily charges, which leads to a higher amount of charge, which leads to a higher capacity.

From this, one can conclude, that synthetic materials will positively influence the performance of the electrode. However, when a synthetic material would span as a top cover over multiple electrodes, it allows to exchange charges between the electrodes and can lead to less meaningful measurements

[5] https://www.uvex-safety.com/blog/electrostatic-discharge-capability-of-clothing-part-two-of-two/

Figure 5.26.: Conductive thread stitched to different support materials: 100% cotton, 65% polyester and cotton 35%, stretch jeans (84% cotton, 14% polyester, 2% elastane), synthetic leather (100% polyurethane)

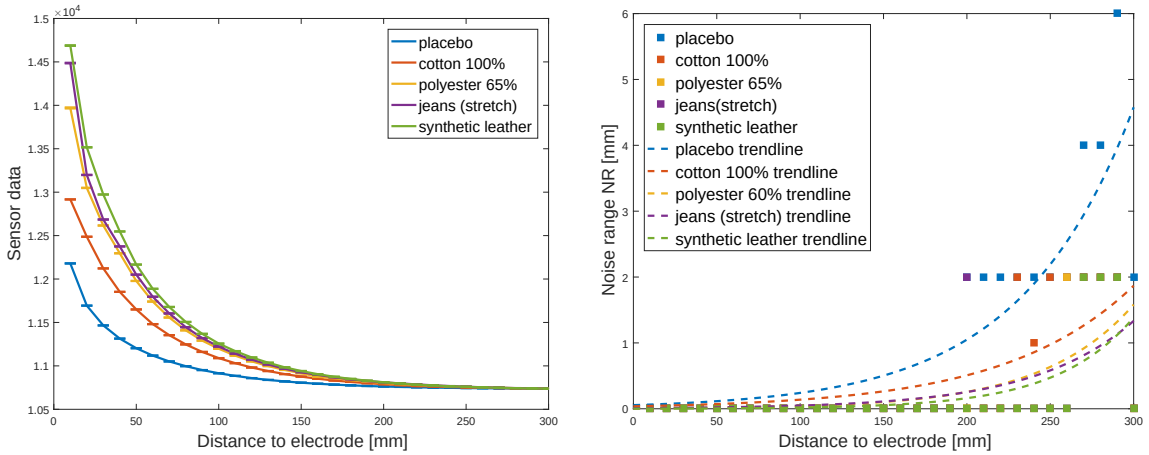

Figure 5.27.: Comparative graphs of support material comparison: shifted raw sensor data and standard deviation (left); Noise Range (right).

per sensor. Thus, materials prone to less electrostatic charging can have a isolating property, useful in multi-electrode systems.

5.2.11. Comparison of electrodes of different shapes

Using conductive thread, it is especially easy to create custom shapes of electrodes. One can simply stitch the thread into the material in the predefined form. Especially overlock sewing machines and highly specified industrial sewing machines are able to perform intricate patterns using a combination of different yarns.

In order to have some indication on whether different shapes, which can be sewn, influence the performance of a capacitive measurement, we selected various shapes, shown in Figure 5.28. To ensure comparability, the same amount of material should be used for all shapes and the same type of stitch. We stitched the perimeter of the different shapes. The size of the stitched shape is chosen such that the perimeter length of the shapes are equal. The length of the perimeter is 24 cm.

The same length of the shape perimeter excludes the factor of the varying amount of conductive material. Thus, the remaining expected factor which influences the performance is the amount of corners and acute angles. As the design guidelines for capacitive touch sensing area layouts suggest, a circle would be better than a square or a triangle [MK12]. The authors argue that edges are to be avoided, and acute angles even more. Thus, we expect the shapes with less edges, like the circle and the ellipse to perform well.

The results of the measurements of the 11 different shapes are shown in Figure 5.29. In the left image the shifted raw sensor value to a common baseline is shown. The placebo electrode is the only one separated from the bulk of the other 11 electrodes which have very similar behaviour. The graph on the right, shows the NR view for the different shapes. The circle followed by the ellipse are the shapes with the highest sensor values. These shapes are also among the smallest measured NR. The placebo electrode has as expected the largest overall NR.

Because these graphs with 12 curves and additional exponential trendlines are hard to read, we provide an additional graph, displaying the overall NR (sum of the NR at all distances). These values are shown in Figure 5.30.

Comparing the NRs the circle, ellipse, trapeze, rectangle, and pentagon perform best, followed by the triangles. These have an overall NR which is smaller than 10 mm. All the other shapes have a bigger NR but the placebo electrode has nearly double compared to the highest NR value of the electrodes. One can observe that there is no specific pattern regarding the number of edges. Circular shapes and shapes with fewer edges do not perform especially well in terms of NR. Next to the placebo electrode the hexagon, hexagram and parallelogram have a higher NR. This behaviour is not intuitive, since hexagon and pentagon are similar to circles, but have some edges. The influence of edges could be confirmed by the hexagrams NR, which is the highest of all shapes, with the highest number of edges. However, it is also contradicted by the NR of the heart, triangles and rectangle. From these measurements the

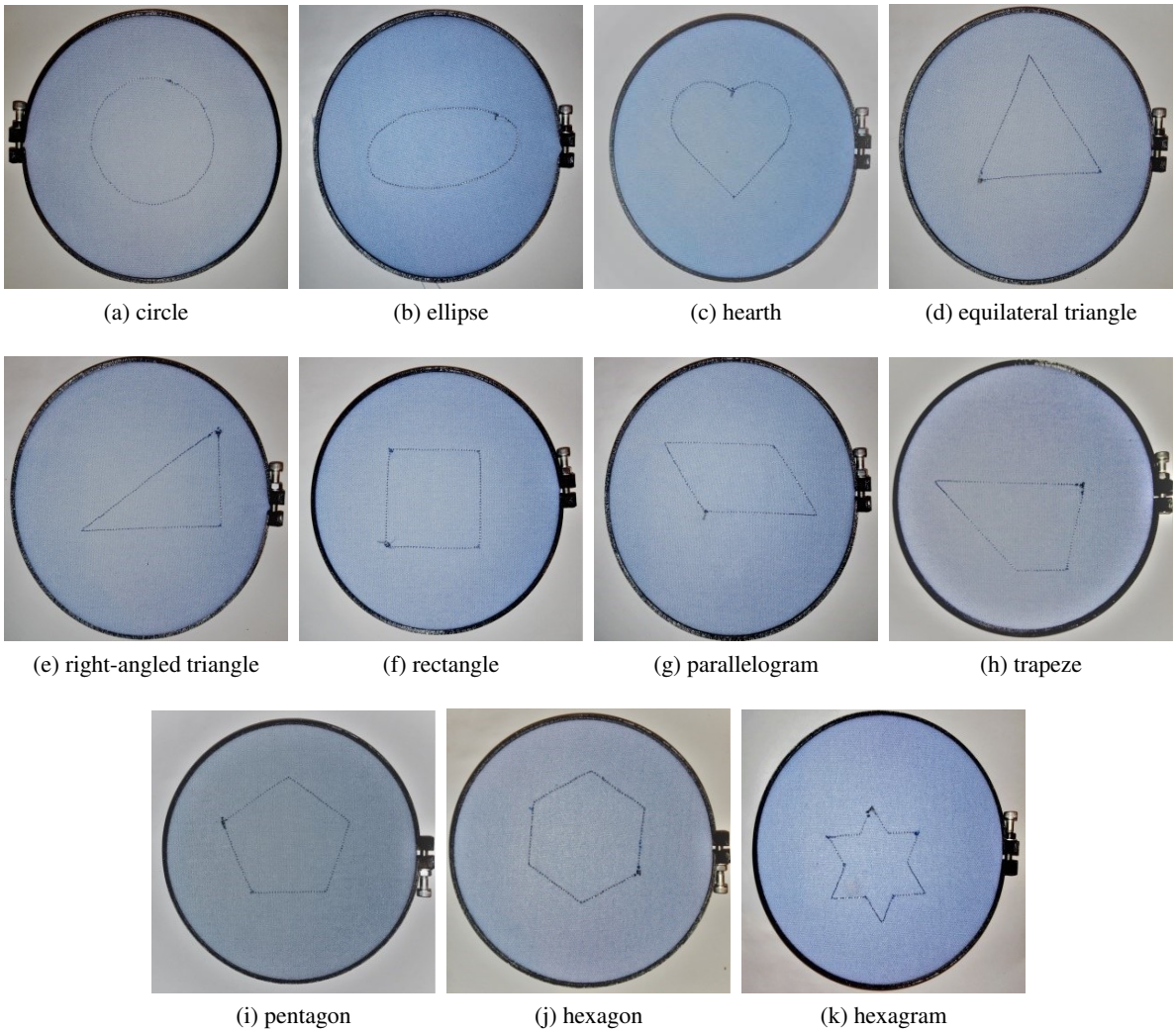

(a) circle (b) ellipse (c) hearth (d) equilateral triangle

(e) right-angled triangle (f) rectangle (g) parallelogram (h) trapeze

(i) pentagon (j) hexagon (k) hexagram

Figure 5.28.: Comparison of different electrode shapes of same perimeter length

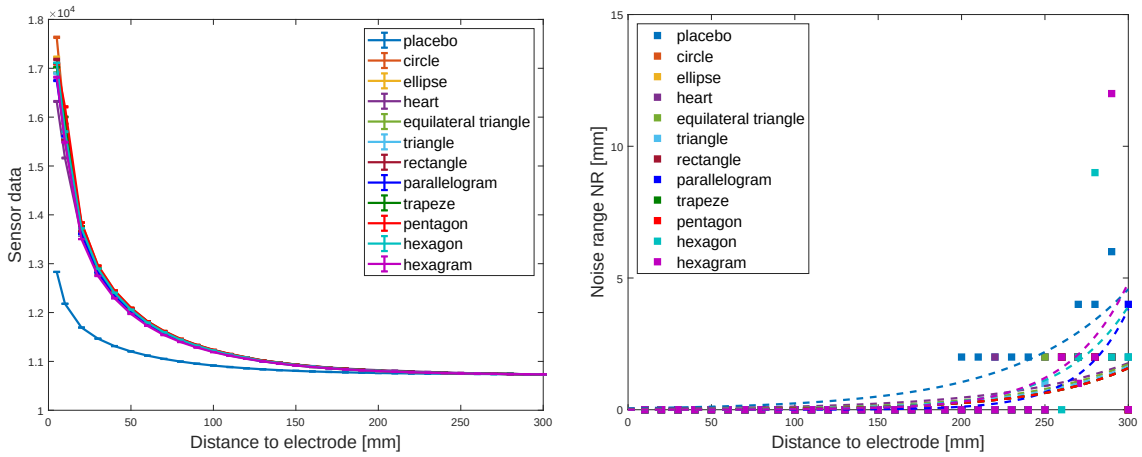

Figure 5.29.: Comparative graphs of shape comparison: shifted raw sensor data and standard deviation (left); Noise Range (right).

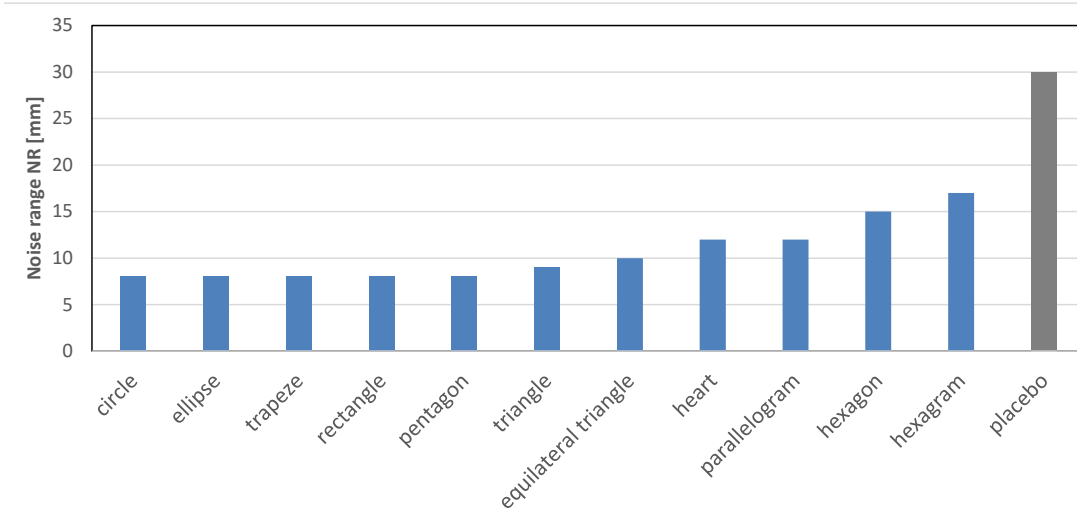

Figure 5.30.: Sum of Noise range (NR) comparison of different electrode shapes

indication to avoid shapes with corners can not be confirmed. At least, circular shapes as the ellipse and the circle are among the best performing shapes, confirming the expectation.

5.2.12. Electrode comparison results

From the electrode group comparisons performed in Sections 5.2.4 to5.2.11, we have in most cases identified a single best performing electrode. In case of the size of electrodes, the electrode with the largest size performs best in terms of NR. This is true for the electrode made of conductive textile, as well as for the electrode made of conductive thread. Thus, if one does not have a preference, fabric or thread can be chosen.

When comparing the results of how densely a surface needs to be covered in order to perform well, one can conclude that for conductive fabric only a perimeter of the area performs as well as covering the whole surface of the area. For conductive thread, only the shape of an area performs poorer than an area filled with a spiral of conductive thread. The conductive fabric perimeter and the conductive thread spiral perform comparably well.

If one decides to use conductive thread as capacitive electrode, one should prefer the variation of conductive thread with 3 strains, the 3ply conductive thread, since it performs better than the 2ply version. Nonetheless, it is harder to sew since it gets knotted very easily and the sewing machine gets blocked often.

The stitching types a sewing machine can perform are meant for different situations, such as using zigzag stitching for elastic materials. If one only compares the performance in terms of NR of straight vs. narrow and wide zigzag pattern, the zigzag patterns perform best, however, closely followed by the straight stitch.

Choosing between types of conductive fabric can depend on different factors. For capacitive electrodes, both, the elastic and the ripstop conductive fabric are performing in a similar way, with the elastic textile performing slightly better. Both materials are different in their intended usage, thus the suited material should be chosen for the desired application.

As the electrode properties influence the performance, the substrate, the supporting material to which the conductive thread or fabric electrode is sewn is an influencing factor. Generally, materials with parts of synthetic material perform better compared to cotton. Of the compared materials, synthetic leather, of 100% polyurethane performed best.

When using conductive thread, the shape of an electrode can be easily variated. We have evaluated a range of 11 shapes with the same perimeter length. The results show that the rectangle, circle and ellipse perform best in terms of smallest achieved NR.

In Figure 5.31 the best electrodes from the different groups are shown. These 8 electrodes are the 10 cm conductive textile, from the electrode size comparison, the conductive textile border and the conductive thread spiral filled shape from the filling density comparison, the 3ply conductive thread from the thread types comparison, the zigzag narrow stitch from the stitching types comparison, the elas-

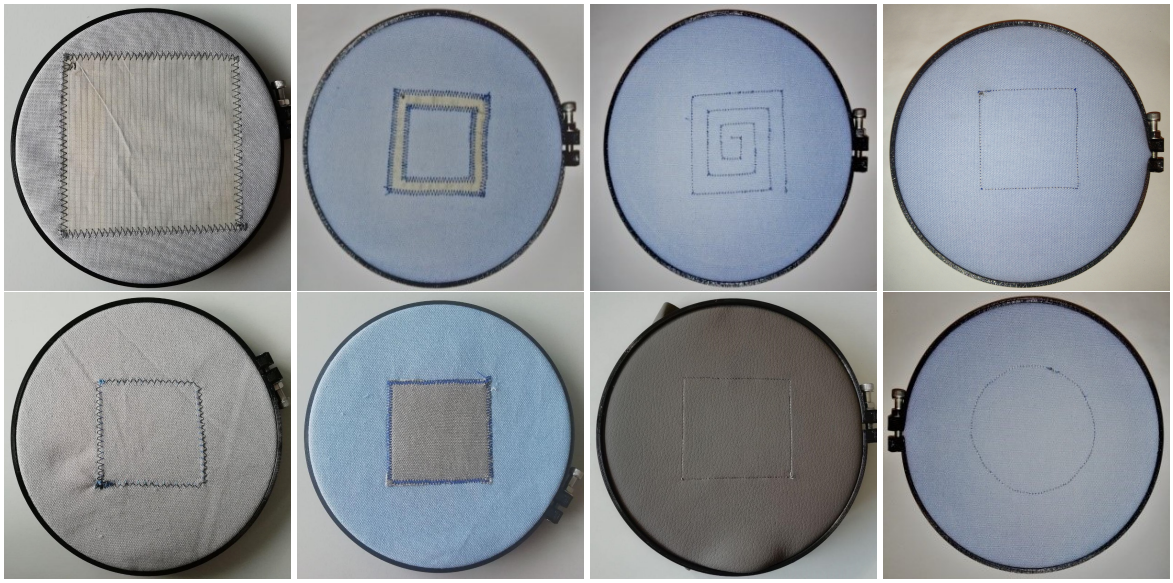

Figure 5.31.: Best electrodes from analysed categories: 10 cm electrode, textile perimeter, thread spiral filled, 3ply conductive thread, zigzag narrow stitch, elastic conductive textile, synthetic leather, circle.

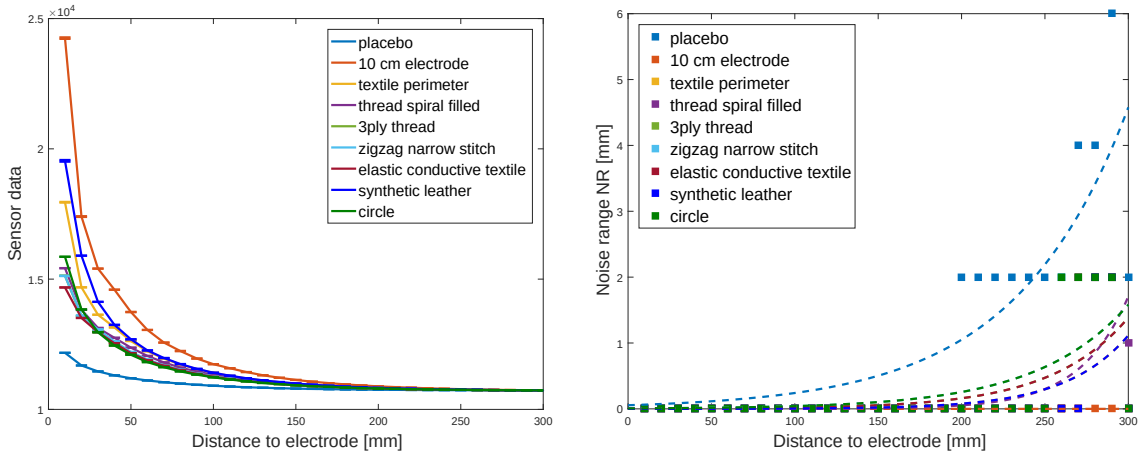

Figure 5.32.: Comparative graphs with best of electrodes from different groups: shifted raw sensor data and standard deviation (left); Noise Range (right).

tic conductive textile from the textile type comparison, the synthetic leather from the support material comparison and finally the conductive thread circle from the shape comparison.

When looking at the raw data, which is shifted to a common baseline, shown in the left image of Figure 5.32, one can observe that the 10 cm conductive textile electrode has the highest values, followed by the synthetic leather and the textile perimeter electrode. The other electrodes are very closely together, only the placebo electrode is separated. Looking at the NR display on the right image of Figure5.32, in a similar manner the 10 cm conductive textile electrodes performs best in terms of NR. At some distance the other electrodes are more or less grouped and at some considerable distance the placebo electrode creates the lower bound with the highest NR.

When looking into the other electrodes, which are close together, the closest ones to the conductive textile electrode are the textile perimeter and the synthetic leather support of the conductive thread electrode overlapping with a NR value of 4 mm. Next, with an overall NR of 5 mm, the conductive thread rectangle filled with a spiral is placed forth. The overall NR value of 6 mm is reached by the 3-ply conductive thread and the elastic conductive textile. On the top, the zigzag narrow stitch and the circle electrodes are overlapping with an overall NR value of 8 mm.

From the overall NR perspective, the best electrode is as expected the largest electrode, the conductive textile electrode with 10 cm edge length. However, if one wants to optimize conductive material or use other types of materials, more suited to the task or application, one can choose only a perimeter of the conductive fabric or use conductive thread on a material with high synthetic composition. Filling the shape with a loose spiral of conductive thread performs also very well.

5.3. Choosing the electrode design

As outlined in Section 5.1 there are many application areas in which flexible sensors can be applied. If we would like to use capacitive sensors in those domains, the choice of material and layout is crucial. Some of these aspects were already discussed in Chapter 4. In this chapter we already addressed questions regarding general setup of applications such as: Which sensors are right for my application? How many sensors are needed? Which layout should I choose? By asking similar questions associated to design factors specific for capacitive electrodes, the application designer can choose the optimal combination for their purpose.

What sensing range do I need?

Depending on the specific layout, flexible capacitive sensors are capable of detecting touch or proximity to a distance of 10 cm for the evaluated electrode size. Several competing technologies possess only touch detection capabilities. Accordingly, if a proximity detection is required in the specific use case, the designer can give priority to capacitive sensors.

What level of flexibility is required?

Certain applications require highly flexible sensors that can only be realized using some technologies. For other sensors it limits the design options. For example, high levels of bending can influence the conductivity of some materials. This limits the choice for applications using capacitive sensors.

Are capacitive sensors the right choice for my application?

The vast variety of materials, shapes, and modes to choose from, make capacitive sensors a powerful choice for applications. However, in many use cases this is not required or suitable. Capacitive sensors can only detect conductive objects and the presence of those. If we need information about other characteristics, such as color, other sensors are required.

How many sensors are needed?

This factor entirely depends on the use case. If we want to precisely measure the location of a small object, numerous small electrodes connected to sensors are required, e.g. small conductive thread patches that detect the presence of a finger for explicit interaction scenarios. For physiological measurements the size has to be adapted to the measured object. Detecting the breathing rate may require a large thread electrode near to the chest.

Which measurement mode should I choose?

The most notable advantage of shunt mode is the reduced number of required sensors in grid layouts. The mutual capacitance measurement is often chosen in touch screens. If we require similar levels of precision, using a grid and reduced number of sensors may be beneficial. For heterogeneous setups, using loading mode systems may be advantageous, since they do not require two electrodes in proximity.

What is the best electrode material?

Giving a definite answer on this is impossible, as the material and use case have to be chosen in accordance. Some instances may require specific properties, such as transparency. Our measurements have shown that all materials are good candidates for a large number of different use cases, as they equally combine high detection range and resolution. If possible, the best choice for a textile electrode is the largest possible electrode made of conductive fabric. If options with conductive thread are preferred, then filling a surface with a loose spiral or using synthetic fabrics as support/substrate material for conductive thread are good options.

In the following Sections 5.3.1 and 5.3.2, I address the system design process to develop two applications: a bed sheet with breathing rate detection capability and a sitting cushion back pain prevention by tracking the sitting behaviour. I presented the sitting cushion already in Section 3.2 of Chapter 3. During the design process of the sitting cushion I evaluate if the findings presented in Section 5.2 are confirmed by a finished system. I base the corresponding Section on my work described in [RBKK19b].

5.3.1. Designing a bed sheet for breathing rate detection

Depending on the use case one wants to implement, the findings from these previous measurements can be helpful in order to choose how to build a textile capacitive electrode. For example we take the use case of detecting the breathing rate while lying in bed. For this use case one can imagine creating

a bed sheet which has a textile capacitive electrode integrated with which the breathing rate can be detected. This electrode has to cover a wider area of the bed, since while asleep a person might move. The electrode should be big enough, that at any given time the person is lying on it. It has to be as wide as the distance between the shoulders and the belly button. The length should be the same as the width of the underlying mattress. This size would be enough to counter the movements of a sleeping person. One can decide how many sensors to use to cover this area. We decide to use a minimal hardware setup and thus use one single capacitive sensor with one single textile electrode. This electrode could be created using conductive fabric or conductive thread, or ultimately a mix of both.

Using conductive fabric, we could choose to use elastic material, since bedsheets usually span on the mattress and is thus better suited to use an elastic conductive fabric. Regarding the shape one could choose the ellipse, due to the available area on the mattress. The ellipse has proven to perform well for conductive thread. However, this ellipse would not have to be entirely filled, a perimeter of 1/6th of the covered surface length could be an option, provided the user reaches at all times a part of the electrode. This would be a viable solution for the breathing detection use case created with conductive fabric.

Using conductive thread allows for more variability and options. Thus, an electrode of conductive thread could be sewn directly on the bedsheet support material. The preferred conductive thread would be the 3ply conductive thread. It could be sewn in various shapes covering the sensing area. Using a ellipse as outline shape has proven to be a good choice for a minimal amount of material. Thus, for this use case the ellipse is the preferred choice. The spiral rectangle performed better than the simple perimeter of a rectangle. Transferring these results to the shape of an ellipse this would mean to have a spiral in shape of an ellipse. The space between the spiral lines could be of 1/6th of the width of the sensing area, ensuring that the person has contact to the electrode. Additionally, since synthetic materials perform better, one would prefer from a performance point of view, a material with higher percentage of synthetic materials, not a material made entirely of cotton.

Combining the two designs using conductive fabric could be a good option. However, it is not clear if the additional work would be worth it. Because of the ease of design and the material costs our recommendation is to use the conductive thread design. To finish the electrode, one needs to connect it to the sensor. The outer perimeter of the ellipse could be contacted to the sensor at the smallest distance from the electrode perimeter to the side of the mattress. This would ensure that the sensor does not disturb while sleeping.

5.3.2. Designing a sitting cushion for back pain prevention

We present the process of designing an E-Textile capacitive cushion. In Section 3.2 of Chapter 3 the application for back pain prevention is already described. In this Section, I describe the process of optimizing the design of the sitting cushion. Throughout the different cushion prototype versions the hardware setup remained the same.

What differentiates the prototypes, is the different setup of the electrodes. The experiments were conducted using the third type of cushion prototype, which is for ease of prototyping reasons a thin, flexible cover of the sitting area of a chair, see Figure 5.34.

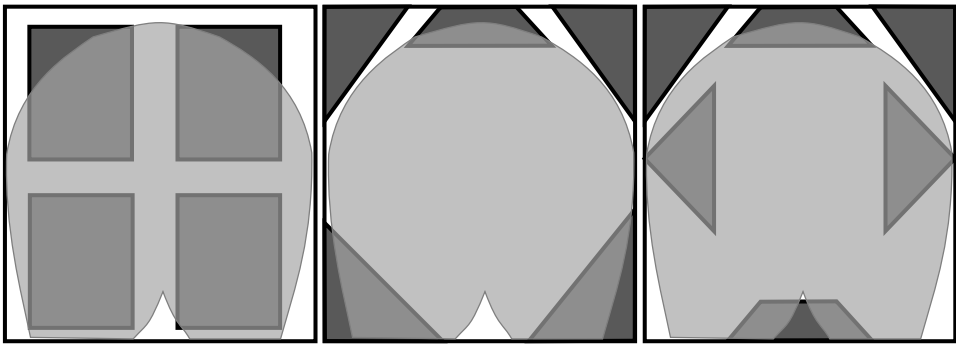

Figure 5.33.: Surface of sitting area covered when sitting on cushion layouts with 4, 5 and 6 capacitive sensing electrodes

Figure 5.34.: Seat cushion prototypes with three electrode types: conductive fabric, conductive thread, and spiral

The process of a person sitting down on a chair can be captured by different setups of electrodes in terms of shape, placement, and number of electrodes. When a user is sitting on the chair, most of the surface of the sitting area is covered, see Figure 5.33. For capacitive proximity sensing the relevant areas are those, where the sensor values change significantly during changes of sitting postures. These are the ones where the body of the person is in proximity to the electrodes. To analyze this we created prototypical electrode patches, inspired by the form of the areas not covered while sitting. We experimented with the placement and number of the patches. Resulting in two designs of 5 and 6 electrodes, chosen to detect as many sitting postures as possible.

From this shape and placement analysis we concluded that through experimentation and evaluation of different sensor layouts that the sensor layout with 5 electrodes performs best. In a second step we focused on the electrode itself.

Cushions need to be highly flexible. Since most of them are covered by some woven material, we chose textile conductive thread and fabric to be suitable for prototypes. These textile electrodes can

be made of different materials. We used conductive fabric and conductive thread [Shi, Ada18]. We evaluated both materials individually.

For this, we have created three different electrodes - before integrating textile electrodes directly into cushions covers. One electrode was made of conductive fabric, one where the shape perimeter is machine sewn with conductive thread and a third one where the shapes surface is filled by a spiral of conductive thread, see Figure 5.35. An additional fourth electrode, the placebo electrode, is an electrode with no conductive material connected to the sensor, just the connecting wire.

For each electrode we conducted measurements to measure the spatial resolution, derived as the inverse of the noise range at specific distances. We measured the capacitance change by repeating the measurements three times and collecting 100 samples per height level, in 1 cm steps up to 30 cm. The measurement device with the evaluated electrode and the measurement electrode connected to a moving spacer are depicted in Figure 5.35.

Figure 5.36 shows that the electrodes made of conductive thread perform slightly better overall than the conductive textile electrode, showing smaller Noise Range (NR) variations. From the distance of about 15 cm up the NR increases for the conductive thread perimeter electrode, with not as high variations in NR as the spiral conductive thread filled and the textile electrode. Starting from distances of 21 cm the NR of the conductive thread spiral electrode increases and starting at 24 cm the NR of the conductive textile increases reaching values higher than the placebo electrode. This indicates punctual noise. Due to this big NR variation the trendlines of the two conductive thread electrodes are lower and the conductive textile trendline depicting the overall NR slightly closer to the placebo electrode trendline.

In comparison, the best results were achieved in Section 5.2.5 by the conductive textile electrode. There the conductive thread electrodes performed worse. The spiral filled electrode performed slightly better than the thread perimeter electrode. In each measurement sets the conductive textile electrode shows much higher NR starting at the distance of 24 cm.

We aim at confirming the results obtained in Section 5.2 with regards to electrode layout and material through the evaluation of prototypes built following the design decisions. We integrated the three electrode types and the layout identified as best performing in prototype seat covers, as shown in Figure 5.34. We evaluate these with a multi- and single-user evaluation. For the evaluation we asked 20 participants (10 male, 10 female) to execute five postures: sit upright, lean back, lean front, sit left, sit right. For each posture we also gathered data for the empty chair and standing in front of it, resulting in a total of seven classes. For each posture we gathered 100 samples for 10 seconds. For the single-user evaluation one participant repeated the evaluation five times.

The data was evaluated using a leave-one-subject-out cross-validation with 15 different classifiers and three additional parameter variations of SVM, using the WEKA machine learning toolkit [HFH*09]. From the multi-user data set we present the results of five test persons, comparable to the amount of data of the single user data amount.

The mean and best classification results of both evaluations are shown in Table 5.1. We observe that the higher density of the conductive surface of the conductive fabric electrodes does not provide better

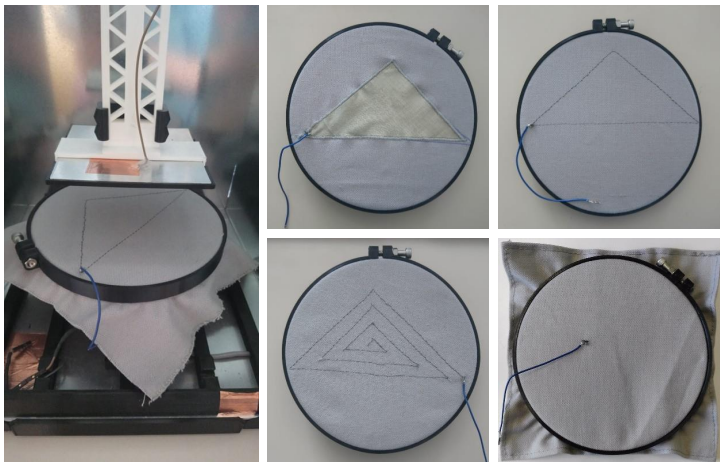

Figure 5.35.: Measurement device and compared electrode types: conductive textile, conductive thread perimeter, conductive thread spiral filled and placebo.

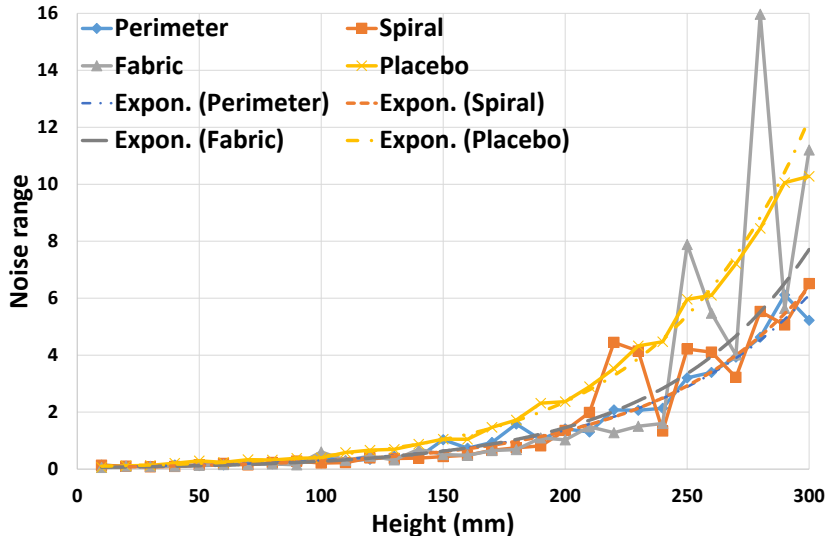

Figure 5.36.: Noise range comparison of electrode types: conductive textile, conductive thread perimeter, conductive thread spiral filled and placebo.

Table 5.1.: Evaluation results per electrode type

		fabric		spiral		perimeter	
		mean	max.	mean	max.	mean	max.
multi-user	accuracy	51.8	62.1	58.9	72.6	56.4	**78.6**
	f-measure	43.8	55.8	51.3	67.7	49.2	73.4
single-user	accuracy	81.3	91.4	89.6	97.1	88.9	**97.1**
	f-measure	76.8	89.1	86.7	96.2	86.3	96.2

results as one could have expected. Compared to conductive fabric, electrodes made of conductive threads outperform conductive fabric. However, the spiral layout of the electrode made of conductive thread performs on mean slightly better than just using conductive thread for the electrode perimeter. In contrast, the highest accuracy for the case of multi-users is reached by the electrodes with their perimeter made of conductive thread. In case of the single-user both electrodes made of conductive thread reach the maximum achieved accuracy. These findings show that electrodes with less material costs, such as conductive threads can achieve favorable results when used in applications.

Concluding, I can say that the conductive thread electrodes can be considered a good choice for e-textile electrodes. This is shown by both, the measurement setups in this section and in Section 5.2.5 as well as in the evaluation results of the sitting cushion application. The worse performance of the conductive textile than the conductive thread does not fall into line with the measurements from Section 5.2.5. However, it is consistent with the results from the prototype evaluation. This difference could derive from factors such as the fabrication or the shape of the electrode. In order to prove these one would need to be able to create electrodes even more uniformly and also evaluate the influence of shape for conductive textile electrodes.

5.4. Conclusion

In this chapter I have addressed the third research challenge *Suitability and performance evaluation of e-textile capacitive electrodes*. I have analysed a set of properties of capacitive electrodes such as electrode material and measurement mode, as for e-textiles in special I analysed properties such as electrode size, pattern density and making. These two analysed aspects feed their results into a rationale of creating capacitive electrodes. I have analysed the findings and used them as a design guideline in order to create electrodes in two exemplary use cases: a bed sheet for breathing rate detection and a cushion for back pain prevention.

Mostly copper electrodes in self capacitance mode is the go-to hardware setup of various applications where proximity sensing is used. Alternatives in terms of material are especially interesting for applications leveraging the flexible properties of objects and surfaces. There is a plethora of possible not very much explored materials. Also, mutual capacitance is a capacitive proximity measurement

mode which could be used as alternative with advantages already described in Section 2.4.1.5. By comparing self and mutual capacitance measurement modes the conclusion is that choosing which to use depends very much on the application. If it needs to be robust or is surrounded by a changing environment it is advisable to choose the self capacitance mode over the mutual capacitance mode for proximity sensing. This is due to the bigger influence of parasitic capacitance on mutual capacitance setups. When looking at different electrode materials, the electrodes are equally suitable for flexible capacitive applications.

Due to the ability of e-textiles to integrate easily into flexible surfaces, a special interest comes to conductive thread and fabric. Through measurements I have evaluated different properties such as the influence of size, pattern degree of filling, types of conductive thread and fabric, stretching deformation, different stitching types, support materials and shapes. The hypothesis that with increased size the performance increases is approved, in both cases of conductive fabric and conductive thread. When it comes to the density of conductive material on the electrode surface, the measurements indicate that a perimeter of fabric has similar performance as the whole surface of a rectangle. Interesting is also, that a perimeter of conductive thread, filled with a spiral is a viable and good option for an electrode made of conductive thread. When comparing stitching types, on a microscopic level, the zigzag stitch is preferable to the straight stitch. However, on a macroscopic level, in relation to the desired application straight and zigzag are both suitable. Similarly, when comparing 2ply versus 3ply conductive thread, the latter is better suited. But as with the conductive fabric type comparison between ripstop and elastic fabric, the fabric performs lightly better, however, in the end it depends on the needs of the application, and both are suitable choices. The same applies to the stretching deformation of an elastic fabric. The stretched materials performs slightly better. In terms of the material on which the conductive material is applied on, conductive thread on materials with high percentages of synthetic components in the fabric perform better than pure cotton. Finally, when looking at shapes, no certain answer can be provided regarding the number of edges of a shape. Thus, the recommendation to use less edges can not be broadly confirmed. The best performing shapes are the circle, ellipse, trapeze, rectangle, and pentagon.

In a final step, I presented application guidelines. By the example of two use cases I walk through the electrode creation rationale which integrates the findings relating the best performing electrodes. In the first use case the goal is to create a breathing rate detecting bed sheet. By going through the requirements of the application and applying the recommendations extracted from the previous sections, a final electrode is designed. The second use case serves to confirm that the findings from a measurement setup of electrodes reflect in the accuracy results of the application. For this use case the cushion for back pain prevention presented in Chapter 3 was created three times, each time with different electrode types.

Through my contributions in this chapter, I support application developers in choosing the best suited electrode design for their envisaged assistive application based on capacitive proximity sensing. They are going to be able to make informed decisions regarding their electrode design and thus provide us, the main beneficiaries of the assistive applications, with quickly developed, well performing systems.

6. Conclusions and Future Work

The topic addressed by this thesis, of extending the design space of assistive applications for flexible Smart Environments is highly relevant, as I showed in the related work in Chapter 2 and throughout Chapter 1 where I have presented the research challenges and outlined my contributions. The main goals I address through my contributions are to provide additions to the scientific field of assistive flexible applications, to enhance and ease the prototyping process and to offer design guidelines for flexible capacitive proximity sensing electrodes.

In this chapter, I summarize the contributions to the three main research challenges formulated in Section 1.2 and conclude by providing areas of promising future research in the field of flexible assistive Smart Environment applications.

6.1. Conclusions

The use of flexible surfaces in assistive applications, such as sensor equipped bed sheets, cushion covers, or cloths, aims at leveraging the comfort they offer to their users, and exploits the implicit closeness and thus the possibility of unobtrusive use. This work presented a set of new assistive applications in Chapter 3, a simulation tool supporting the application prototyping work-flow in Chapter 4 and e-textile capacitive sensing electrodes design guidelines in Chapter 5. All these components are intended to support the designing of sensor equipped flexible assistive Smart Environment applications. In the following, I will outline my contributions to each of the research challenges.

New flexible Smart Environment applications: The contributions to the first research challenge are presented in Chapter 3. This contribution materializes the untapped potential of sensors embedded into flexible surfaces. It comprises diverse prototypes from three different application areas. The first is the area of decubitus ulcer prevention [RGPK14, RGPK17]. I created a system based on a bed sheet, which can be used in hospitals or at home, and alarms the caretaker looking after a bedridden person, if the person has spent too much time in a certain position. The bed sheet is able to recognize bed postures and therefore infer pressure points. Compared to similar works, the bed sheet is affordable and easy to handle due to the wire grid in mutual capacitance measuring mode, which allows to have a high number of sensing points, at all wire crossings. The second application area is back pain prevention by sitting posture monitoring and exercise tracking through a chair [RBKK19b]. By giving the user feedback on his sitting posture, one can facilitate healthier behaviour. Through different design iterations, I created a seat that tracks the proximity and motion of the user. Even though previous works have achieved limited sitting posture detection, I extend the current body of knowledge by evaluating different e-

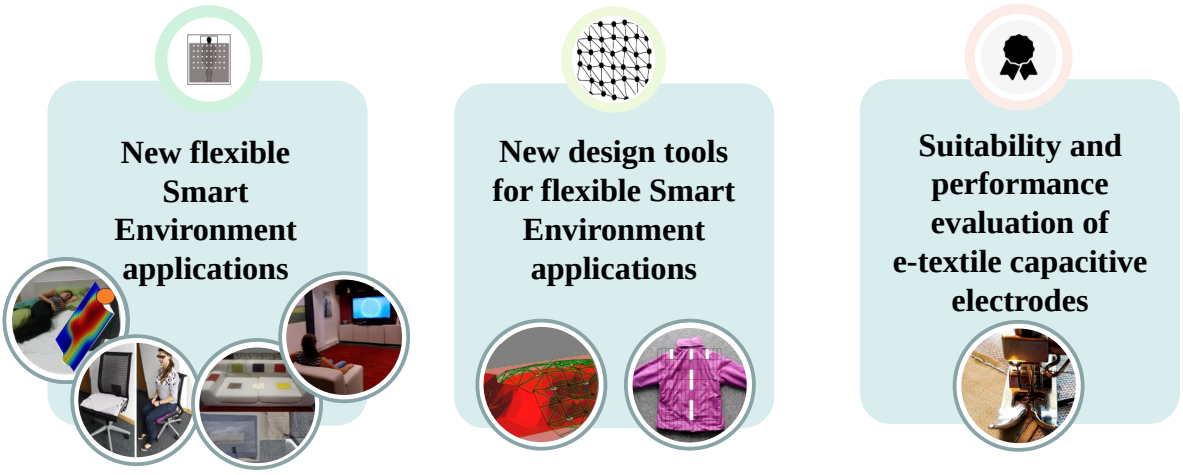

Figure 6.1.: Overview of contributions addressing the three research challenges.

textile electrode layouts and materials and compare the results by evaluating the designed prototypes in a user study. The final application area to which I contribute in relation to this research challenge, is differentiating emotions through sensing movements on a couch [RBK17, RJBK18]. I outline a couch specially set up to measure emotion by interpreting measured movements. Previous work has focused on user posture detection. By using conductive fabric as capacitive proximity sensing electrodes, I extend the sensing capabilities to motions from which I subsequently infer emotions.

Creating these applications, I explored flexible materials we use throughout our daily activities, and I not only created assistive systems which offer us comfort and health support functionalities, but which do this in an unobtrusive manner. While I created these assistive applications, I encountered application design decisions I needed to take, which have led to the next two research challenges.

New design tools for flexible Smart Environment applications: Chapter 4 contains my contributions to the second research challenge with relation to work-flows of designing applications using sensor-equipped flexible surfaces. I reduce the use of resources, such as time and hardware costs, by especially addressing the prototypical hardware iterations. For this, I contribute a simulation tool, which aids in identifying the number and placement preferences for flexible Smart Environment applications. Understanding where sensors need to be placed and how many are needed to achieve the desired application functionality and accuracy is vital information when designing any application. When designing applications for flexible surfaces, the appropriate aiding tools are needed. I contribute a simulation framework, which facilitates the creation of flexible applications such as shape-sensing applications [RHvW*18]. Existing works focus only on the simulation of rigid objects. I included soft-body simulation with attached virtual sensors and validated and demonstrated the work-flow by virtually planning and subsequently implementing a sleeping posture detecting bed cover. This process provides a decision basis for developer decisions regarding number of sensors, the sensor placement and achieved accuracy. My second contribution to this research challenge is the investigation on what

role the human intuition has when designing a smart garment use case, versus the expert knowledge used to design such a system by an experienced system designer [RBKK19a]. I used the simulation framework to compare the proposed designs from all study participants with the results from two hands-on sessions with experienced system designers. The outcome shows that many participants intuitively create well-working patterns.

Through these contributions, I closed the gap of the lacking support for the resource conserving creation of shape-changing applications. I also enable less experienced application and system designers to try out their designs and optimize them towards cost and performance, enabling a more efficient design process in general.

Suitability and performance evaluation of e-textile capacitive electrodes: My contributions to the third research challenge are contained in Chapter 5. E-textile materials are especially well suited to be integrated into various flexible assistive Smart Environment applications due to their flexibility and different manufacturing possibilities. In existing works, e-textiles find usage in many applications. However, the influence of varying manufacturing properties on the capacitive proximity sensing performance has not been analysed in a structured way. I contribute a performance evaluation of capacitive proximity sensing electrodes with different properties such as different material, size, filling degree, stitching type, shapes, stretching and support material [RSBK15, RBKK19b]. I compared different sizes of conductive thread perimeters and conductive fabric squares, as well as different types of conductive threads and conductive fabrics. For both materials, I also compared if the surface needed to be filled with conductive material, or if a loop would be enough. Additionally, I also investigated the influence of the support material type as well as its stretching influence. Creating electrodes from conductive thread offers an additional manufacturing dimension. Thus, I also contribute insights into the sensing performance of electrodes made with different stitching types or diverse shapes. Finally, I demonstrate the findings by contributing an electrode creation rationale with two examples a breath detecting bed sheet and a cushion for back pain prevention.

These contributions to this research challenge support applications developers in choosing the best suited electrode design for their capacitive proximity sensing application. By having performed the structured measurements, analysis, and comparison. The application designer can go through the electrode design constraints and choose step by step the preferred electrode properties, avoiding the creation of multiple electrode prototypes and thus allow for a quicker application design process.

In conclusion, the aforementioned contributions to the three identified research challenges enable the exploitation of flexible surfaces creating new assistive applications and enhancing the overall application design process by offering a tool for resource effective creation of prototypes as well as a design guideline for e-textile capacitive sensing electrode creation.

6.2. Future Work

As I have shown in Section 6.1 and throughout the related work in Section 2, the developments in the field of flexible Smart Environments are flourishing. Research areas such as Skin Interfaces, Shape

Changing Interfaces and Textile Interfaces are highly relevant, especially in the combination with material sciences, which allows for more leavened developments.

My current research was mostly focused on leveraging flexible surfaces such as textiles on furniture with which people come in contact in order to unobtrusively offer health assistance. In the future, I would like to explore from a technological point of view the combination of 3D-printing methods and flexible applications. On application level I would like to rest in the field of personal health and further focus on extending my work related to emotion detection and communication.

Personal health In my previous work I have created dedicated prototypes for assistive health applications. As mentioned throughout Chapter 3, there are several possibilities to enhance the different presented applications. Examples could be to enhance the grid setup used for the lying posture sensing bed sheet such that smaller body parts are detectable as well, and combine it with actuators able to autonomously change the position of the user. The proposed simulation framework could be extended to optimize the simulated hardware setup to find the suitable trade-off between the number of sensors and application accuracy. Overall, health applications profit if they can cover both aspects, generalization and individualization or personalization. In terms of generalization of hardware, I would like to create a system in the form of a textile cover, which is able to fit to all kinds of furniture and offer diverse services such as posture detection, physiological sensing and emotion detection. On the other hand, this textile cover would profit from person identification to cope with a small group of users and personalize its services.

Multimodal emotion detection and communication In my previous work I explored the unobtrusive detection of emotions by interpreting movements on furniture, see Section 3.4. By fusing physiological parameters such as breathing rate detected through the furniture and physiological parameters measured through available wearables, I want to improve the granularity and accuracy of detected emotions. Different modalities are used to detect emotions e.g. through brain-computer interfaces [SSA*20], smart-watches [CGJC19]. Not only detecting the emotions is of interest, but also communicating them to others or to machines, in order to be able to adapt to emotional variations [YAB19, EAYA*20, SSA*20, USL19]. From detecting and communicating emotions, I imagine that changing or influencing emotions is a next possible step. Controlling and changing ones emotions during every day activities [SMvB*20] could serve to enhance and emphasize our well-being [RM20] and performing ability [CGJC19, DMB*20].

Morphing 3D-printing Even though my previous work has not covered the area of 3D-printing, new printing materials and printing methods with the ability to create flexible and deformable objects have caught my interest. Examples are the foldable and unfoldable objects of daily use presented by Noma et al. [NNOK20], printing multi-material objects from one single filament [TPK20], spraying interactive displays on 3D-printed objects [HWM*20], printing biocompatible soft vibro-tactile actuators [FRS*20], or the fabrication of morphing lines into three-dimensional shapes through the use of thermoplastic material [WTC*19]. FabriClick by Goudswaard et al. and DefeXtiles by Forman et al. show how advances in 3D-printing can be leveraged in creating functional textiles [GAGdR*20, FDFI20]. These developments can be used to rethink functional furniture and create adaptable and personalized health services.

A. Publications and Talks

The thesis is partially based on the following publications:

A.1. Full Conference Papers

C. 11 **Rus, S.**, Nottebaum, M., Kuijper, A.: Person Re-Identification in a Car Seat: Comparison of Cosine Similarity and Triplet Loss based approaches on Capacitive Proximity Sensing data. In: Proceedings of the 14th ACM International Conference on PErvasive Technologies Related to Assistive Environments. ACM Digital Library (2021)

C. 10 **Rus, S.**, Helfmann, S., Kirchbuchner, F., Kuijper, A.: Designing smart home controls for elderly. In: Proceedings of the 13th ACM International Conference on PErvasive Technologies Related to Assistive Environments. ACM Digital Library (2020)

C. 9 **Rus, S.**, Braun, A., Kirchbuchner, F., Kuijper, A.: E-textile capacitive electrodes: Fabric or thread: designing an E-textile cushion for sitting posture detection. In: Proceedings of the 12th ACM International Conference on PErvasive Technologies Related to Assistive Environments. ACM Digital Library (2019)

C. 8 **Rus, S.**, Braun, A., Kirchbuchner, F., Kuijper, A.: Designing a self-aware jacket: insights into smart garment's creation process. In: Proceedings of the 12th ACM International Conference on PErvasive Technologies Related to Assistive Environments. ACM Digital Library (2019)

C. 7 **Rus, S.**, Hammacher, F., von Wilmsdorff, J., Braun, A., Grosse-Puppendahl, T., Kirchbuchner, F., Kuijper, A.: Prototyping Shape-Sensing Fabrics Through Physical Simulation. In: European Conference on Ambient Intelligence 2018. Lecture Notes in Computer Science. Springer (2018)

C. 6 **Rus, S.**, Joshi, D., Braun, A., Kuijper, A.: The Emotive Couch - Learning Emotions by Capacitively Sensed Movements. In: 9th International Conference on Ambient Systems, Networks and Technologies 2018. Procedia Computer Science. ScienceDirect (2018)

C. 5 **Rus, S.**, Braun, A., Kuijper, A.: E-Textile Couch: Towards Smart Garments Integrated Furniture. In: European Conference on Ambient Intelligence 2017. Lecture Notes in Computer Science. Springer (2017)

C. 4 Braun, A., **Rus, S.**, Kuijper, A.: Invisible Human Sensing in Smart Living Environments using Capacitive Sensors. In: 9. AAL-Kongress. Ambient Assisted Living. (2017)

C. 3 **Rus, S.**, Sahbaz, M., Braun, A., Kuijper, A.: Design factors for flexible capacitive sensors in ambient intelligence. In: European Conference on Ambient Intelligence 2015. Lecture Notes in Computer Science. Springer (2015)

C. 2 Covaci, A., Kramer, D., Augusto, J.C., **Rus, S.**, Braun, A.: Assessing Real World Imagery in Virtual Environments for People with Cognitive Disabilities. In: International Conference on Intelligent Environments 2015. IEEE (2015)

C. 1 **Rus, S.**, Grosse-Puppendahl, T., Kuijper, A.: Recognition of bed postures using mutual capacitance sensing. In: European Conference on Ambient Intelligence 2014. Lecture Notes in Computer Science. Springer (2014)
$\longrightarrow$ Best Paper Award

A.2. Journal Papers

J. 1 **Rus, S.**, Caliz, D., Braun, A., Engler, A., Schulze, E.: Assistive apps for activities of daily living supporting persons with Downś Syndrome. In: Journal of Ambient Intelligence and Smart Environments 9 (5)(2017) .

J. 2 **Rus, S.**, Grosse-Puppendahl, T., Kuijper, A.: Evaluating the recognition of bed postures using mutual capacitance sensing. In: Journal of Ambient Intelligence and Smart Environments 9 (1)(2017)

A.3. Short Papers

S. 1 **Rus, S.**, Braun, A.: Money Handling Training-Applications for Persons with Down Syndrome. In: Intelligent Environments, 2016 12th International Conference. IEEE (2016)
$\longrightarrow$ Best Short Paper Award

A.4. Workshop Papers

W. 1 Braun, A., Zander-Walz, S., Krepp, S., **Rus, S.**, Wichert, R., Kuijper, A.: CapTap: combining capacitive gesture recognition and acoustic touch detection. In: Proceedings of the 3rd International Workshop on Sensor-based Activity Recognition and Interaction 2016. ACM (2016)

B. Supervising Activities

The following list summarizes the student bachelor, diploma and master thesis supervised by the author. The results of these works were partially used as an input into the thesis.

B.1. Master's Thesis

6/2015 - 12/2015	Felix Hammacher (Technische Universität Darmstadt, Computer Science): Physical simulation- and reconstruction-framework for shape sensing fabrics.
1/2017 - 6/2017	Nagarjung Manjunath (Hochschule Bremen, Electrical Engineering) Simulation and validation of capacitive sensing on flexible and curved surfaces applied on sleeping breathing rate detection.
2/2017 - 8/2017	Dhanashree Joshi (Technische Universität Darmstadt, Computer Science): Emotion Detection By Evaluating Activities For Smart Home Appliances.
6/2017 - 1/2018	Christian Gutjahr (Technische Universität Darmstadt, Computer Science): Designing Self-Aware Textiles.
6/2018 - 1/2019	Stefan Helfmann (Technische Universität Darmstadt, Computer Science): Designing Smart Home Controls for Elderly.
11/2018 - 4/2019	Zaki Ullah Chaudhry (Technische Universität Darmstadt, Computer Science): Smart Furniture Cover: Designing a general purpose smart textile for supporting a healthy lifestyle.

B.2. Bachelor's Thesis

9/2014 - 11/2014	Steffen Maus (Technische Universität Darmstadt, Computer Science): Classification of Lying Postures using Capacitive Proximity Sensing.
11/2016 - 1/2017	Patrick Schmitt (Hochschule Darmstadt, Computer Science): Reporting on the effort of creating a Healthy Eating App for persons with Down Syndrome
6/2018 - 6/2019	Pinar Yakar (Hochschule Offenburg, Electrical Engineering): Breathing frequency and movement detection with e-textile capacitive sensing.
8/2019 - 1/2020	Moritz Nottebaum (Technische Universität Darmstadt, Computer Science): Person Re-identification in a Car Seat.

11/2019 - 5/2020	Konstantin Strassenheim (Technische Universität Darmstadt, Computer Science): Ambient breathing rate detection using capacitive sensors.
12/2019 - 6/2020	Romal Bijan (Technische Universität Darmstadt, Computer Science): Survey on designing capacitive sensing systems.
12/2019 - 9/2020	Luisa Dyroff (Technische Universität Darmstadt, Computer Science): Flexible Capacitive Sensors in different Materials and their Reaction to Deformation.

C. Curriculum Vitae

Personal Data

Name	Silvia Dorotheea Rus
Birth date	05.03.1987
Birth place	Târgu Secuiesc, Romania
Nationality	German and Romanian

Education

2011 – 2013	Master of Science in Electrical Engineering and Information Technology at Technical University Darmstadt, Germany
2008 – 20011	Bachelor of Science in Electrical Engineering and Information Technology at Technical University Darmstadt, Germany

Work Experience

Since 2013	Researcher, Smart Living and Biometric Technologies, Fraunhofer Institute for Computer Graphics Research IGD, Darmstadt, Germany.

Bibliography

[Ada18] ADAFRUIT: Stainless thin conductive thread - 2 ply, 2018. [Online; accessed 5 July 2018]. 138

[AKA91] AHA D. W., KIBLER D., ALBERT M. K.: Instance-based learning algorithms. *Machine Learning 6*, 1 (Jan 1991), 37–66. 65

[AKGH20] AHUJA K., KONG A., GOEL M., HARRISON C.: Direction-of-voice (dov) estimation for intuitive speech interaction with smart devices ecosystems. In *Proceedings of the 33rd Annual ACM Symposium on User Interface Software and Technology* (New York, NY, USA, 2020), UIST '20, Association for Computing Machinery, pp. 1121–1131. 10

[AM20] ARIMATSU K., MORI H.: Evaluation of machine learning techniques for hand pose estimation on handheld device with proximity sensor. In *Proceedings of the 2020 CHI Conference on Human Factors in Computing Systems* (New York, NY, USA, 2020), CHI '20, Association for Computing Machinery, pp. 1–13. 27

[APP*20] AIGNER R., POINTNER A., PREINDL T., PARZER P., HALLER M.: Embroidered resistive pressure sensors: A novel approach for textile interfaces. In *Proceedings of the 2020 CHI Conference on Human Factors in Computing Systems* (New York, NY, USA, 2020), CHI '20, Association for Computing Machinery, pp. 1–13. 28

[Ban69] BANDURA A.: Principles of behavior modification. *American Psychological Association* (1969). 50

[Bax97] BAXTER L. K.: Capacitive sensors. *Design and Applications* (1997). 22, 25, 26, 27

[BB16] BIANCHI-BERTHOUZE N.: The affective body argument in technology design. In *Proceedings of the International Working Conference on Advanced Visual Interfaces* (New York, NY, USA, 2016), AVI '16, ACM, pp. 3–6. 62

[BBR*15] BALDWIN R., BOBOVYCH S., ROBUCCI R., PATEL C., BANERJEE N.: Gait analysis for fall prediction using hierarchical textile-based capacitive sensor arrays. In *Proceedings of the 2015 Design, Automation & Test in Europe Conference & Exhibition* (San Jose, CA, USA, 2015), DATE '15, EDA Consortium, pp. 1293–1298. 26, 98

[BBTR13] BRUSH Z., BOWLING A., TADROS M., RUSSELL M.: Design and control of a smart bed for pressure ulcer prevention. In *2013 IEEE/ASME International Conference on Advanced Intelligent Mechatronics* (2013), pp. 1033–1038. 11

[BBV10] BORAZIO M., BLANKE U., VAN LAERHOVEN K.: Characterizing sleeping trends from postures. *International Symposium on Wearable Computers (ISWC) 2010* (Oct.

2010), 1–2. 33

[BFMW15] BRAUN A., FRANK S., MAJEWSKI M., WANG X.: Capseat: Capacitive proximity sensing for automotive activity recognition. In *Proceedings of the 7th International Conference on Automotive User Interfaces and Interactive Vehicular Applications* (New York, NY, USA, 2015), AutomotiveUI '15, ACM, pp. 225–232. 12, 50, 54

[BFW15] BRAUN A., FRANK S., WICHERT R.: The capacitive chair. In *Distributed, Ambient, and Pervasive Interactions* (Cham, 2015), Streitz N., Markopoulos P., (Eds.), Springer International Publishing, pp. 397–407. 4, 12, 50, 54

[BGF*20] BARONETTO A., GRAF L. S., FISCHER S., NEURATH M. F., AMFT O.: Gastrodigitalshirt: A smart shirt for digestion acoustics monitoring. In *Proceedings of the 2020 International Symposium on Wearable Computers* (New York, NY, USA, 2020), ISWC '20, Association for Computing Machinery, pp. 17–21. 16

[BHV13] BIEBER G., HAESCHER M., VAHL M.: Sensor requirements for activity recognition on smart watches. In *Proceedings of the 6th International Conference on PErvasive Technologies Related to Assistive Environments* (2013), PETRA '13, ACM, pp. 67:1–67:6. 33

[BLL06] BABINEAU D., LONGTIN A., LEWIS J. E.: Modeling the electric field of weakly electric fish. *Journal of Experimental Biology 209*, 18 (2006), 3636–3651. 20

[BMS20] BERUSCHA F., MUELLER K., SOHNKE T.: Eliciting tangible and gestural user interactions with and on a cooking pan. In *Proceedings of the Conference on Mensch Und Computer* (New York, NY, USA, 2020), MuC '20, Association for Computing Machinery, pp. 399–408. 10

[Bre01] BREIMAN L.: Random forests. *Machine Learning 45*, 1 (Oct 2001), 5–32. 65

[BS73] BECK F., STUMPE B.: *Two devices for operator interaction in the central control of the new CERN accelerator*. Tech. rep., CERN, 1973. 21

[BSF15] BRAUN A., SCHEMBRI I., FRANK S.: *ExerSeat - Sensor-Supported Exercise System for Ergonomic Microbreaks*. Ambient Intelligence: 12th European Conference, AmI 2015. Springer International Publishing, 2015, pp. 236–251. 54

[BWKF15] BRAUN A., WICHERT R., KUIJPER A., FELLNER D. W.: Capacitive proximity sensing in smart environments. *Journal of Ambient Intelligence and Smart Environments 7*, 4 (2015), 1–28. 33, 63, 99

[CCCY14] CHANG W.-Y., CHEN C.-C., CHANG C.-C., YANG C.-L.: An enhanced sensing application based on a flexible projected capacitive-sensing mattress. *Sensors (Basel, Switzerland) 14*, 4 (Jan. 2014), 6922–37. 11, 33, 54

[CD04] COOK D., DAS S. K.: *Smart environments: technology, protocols, and applications*, vol. 43. John Wiley & Sons, 2004. 3, 9

[CDF*20] CICEK M., DAVE A., FENG W., HUANG M. X., HAINES J. K., NICHOLS J.: Designing and evaluating head-based pointing on smartphones for people with motor im-

pairments. In *The 22nd International ACM SIGACCESS Conference on Computers and Accessibility* (New York, NY, USA, 2020), ASSETS '20, Association for Computing Machinery. 10

[CGJC19] COSTA J., GUIMBRETIÈRE F., JUNG M. F., CHOUDHURY T.: Boostmeup: Improving cognitive performance in the moment by unobtrusively regulating emotions with a smartwatch. *Proc. ACM Interact. Mob. Wearable Ubiquitous Technol. 3*, 2 (June 2019). 146

[Cha08] CHAN V.: Msp430 capacitive single-touch sensor design guide, 2008. 27

[CLH*20] CHEN Y.-C., LIAO C.-Y., HSU S.-W., HUANG D.-Y., CHEN B.-Y.: Exploring user defined gestures for ear-based interactions. *Proc. ACM Hum.-Comput. Interact. 4*, ISS (Nov. 2020). 10

[CLY10] CHENG M. Y., LIN C. L., YANG Y. J.: Tactile and shear stress sensing array using capacitive mechanisms with floating electrodes. *Proceedings of the IEEE International Conference on Micro Electro Mechanical Systems (MEMS) 2* (2010), 228–231. 72

[CMR*04] CAMURRI A., MAZZARINO B., RICCHETTI M., TIMMERS R., VOLPE G.: *Multimodal Analysis of Expressive Gesture in Music and Dance Performances*. Springer Berlin Heidelberg, Berlin, Heidelberg, 2004, pp. 20–39. 62

[Cre07] CREMER M.: *Ueber die Registrierung mechanischer Vorgänge auf elektrischem Wege, speziell mit Hilfe des Saitengalvanometers und Saitenelektrometers*. Lehmann, 1907. 21

[CRK*20] CHOI Y., RYU N., KIM M. J., DEMENTYEV A., BIANCHI A.: Bodyprinter: Fabricating circuits directly on the skin at arbitrary locations using a wearable compact plotter. In *Proceedings of the 33rd Annual ACM Symposium on User Interface Software and Technology* (New York, NY, USA, 2020), UIST '20, Association for Computing Machinery, pp. 554–564. 14

[CvP12] CHERENACK K., VAN PIETERSON L.: Smart textiles: Challenges and opportunities. *Journal of Applied Physics 112*, 9 (2012), 091301. 17

[DBM14] DJAKOW M., BRAUN A., MARINC A.: MoviBed - Sleep analysis using capacitive sensors. In *Lecture Notes in Computer Science* (2014), vol. 8516 LNCS, pp. 171–181. 4, 33, 54

[Dem16] DEMENTYEV A.: Towards self-aware materials. In *Proceedings of the TEI '16: Tenth International Conference on Tangible, Embedded, and Embodied Interaction* (New York, NY, USA, 2016), TEI '16, ACM, pp. 685–688. 54, 72, 87

[DG09] D'MELLO S., GRAESSER A.: Automatic detection of learner's affect from gross body language. *Applied Artificial Intelligence 23*, 2 (2009), 123–150. 62

[DHC*18] DEMENTYEV A., HERNANDEZ J., CHOI I., FOLLMER S., PARADISO J.: Epidermal robots: Wearable sensors that climb on the skin. *Proc. ACM Interact. Mob. Wearable Ubiquitous Technol. 2*, 3 (Sept. 2018). 14

[DHF*17] DEMENTYEV A., HERNANDEZ J., FOLLMER S., CHOI I., PARADISO J.: Skinbot: A wearable skin climbing robot. In *Adjunct Publication of the 30th Annual ACM Symposium on User Interface Software and Technology* (New York, NY, USA, 2017), UIST '17, ACM, pp. 5–6. 14

[DHR15] DOBBELSTEIN D., HOCK P., RUKZIO E.: Belt: An unobtrusive touch input device for head-worn displays. In *Proceedings of the 33rd Annual ACM Conference on Human Factors in Computing Systems* (New York, NY, USA, 2015), CHI '15, ACM, pp. 2135–2138. 26, 98

[DKC*16] DEMENTYEV A., KAO H.-L. C., CHOI I., AJILO D., XU M., PARADISO J. A., SCHMANDT C., FOLLMER S.: Rovables: Miniature on-body robots as mobile wearables. In *Proceedings of the 29th Annual Symposium on User Interface Software and Technology* (New York, NY, USA, 2016), UIST '16, ACM, pp. 111–120. 14

[DKP15] DEMENTYEV A., KAO H.-L. C., PARADISO J. A.: Sensortape: Modular and programmable 3d-aware dense sensor network on a tape. In *Proceedings of the 28th Annual ACM Symposium on User Interface Software and Technology* (New York, NY, USA, 2015), UIST '15, ACM, pp. 649–658. 72, 73

[DLS13] DIRACO G., LEONE A., SICILIANO P.: Human posture recognition with a time-of-flight 3D sensor for in-home applications. *Expert Systems with Applications 40*, 2 (Feb. 2013), 744–751. 33

[DMB*20] DMITRENKO D., MAGGIONI E., BRIANZA G., HOLTHAUSEN B. E., WALKER B. N., OBRIST M.: Caroma therapy: Pleasant scents promote safer driving, better mood, and improved well-being in angry drivers. In *Proceedings of the 2020 CHI Conference on Human Factors in Computing Systems* (New York, NY, USA, 2020), CHI '20, Association for Computing Machinery, pp. 1â€“13. 146

[DMW*18] DU J., MARKOPOULOS P., WANG Q., TOETERS M., GONG T.: Shapetex: Implementing shape-changing structures in fabric for wearable actuation. In *Proceedings of the Twelfth International Conference on Tangible, Embedded, and Embodied Interaction* (New York, NY, USA, 2018), TEI '18, ACM, pp. 166–176. 72

[DPW96] DELLAERT F., POLZIN T., WAIBEL A.: Recognizing emotion in speech. In *Proceeding of Fourth International Conference on Spoken Language Processing. ICSLP '96* (1996), vol. 3, IEEE, pp. 1970–1973. 62

[DWHR17] DOBBELSTEIN D., WINKLER C., HAAS G., RUKZIO E.: Pocketthumb: A wearable dual-sided touch interface for cursor-based control of smart-eyewear. *Proc. ACM Interact. Mob. Wearable Ubiquitous Technol. 1*, 2 (June 2017), 9:1–9:17. 26, 98

[EAYA*20] EL ALI A., YANG X., ANANTHANARAYAN S., RÖGGLA T., JANSEN J., HARTCHER-O'BRIEN J., JANSEN K., CESAR P.: Thermalwear: Exploring wearable on-chest thermal displays to augment voice messages with affect. In *Proceedings of the 2020 CHI Conference on Human Factors in Computing Systems* (New York, NY, USA, 2020), CHI '20, Association for Computing Machinery, pp. 1–14. 146

[EF78] EKMAN P., FRIESEN W.: Facial action coding system: a technique for the measurement of facial movement. *Palo Alto: Consulting Psychologists* (1978). 62

[EIS*13] ENOKIBORI Y., ITO Y., SUZUKI A., MIZUNO H., SHIMAKAMI Y., KAWABE T., MASE K.: Spirovest: An e-textile-based wearable spirometer with posture change adaptability. In *Proceedings of the 2013 ACM Conference on Pervasive and Ubiquitous Computing Adjunct Publication* (New York, NY, USA, 2013), UbiComp '13 Adjunct, ACM, pp. 203–206. 15, 54

[ELDL11] ECHEVERRIA G., LASSABE N., DEGROOTE A., LEMAIGNAN S.: Modular open robots simulation engine: MORSE. In *2011 IEEE International Conference on Robotics and Automation* (May 2011), IEEE, pp. 46–51. 72

[EM14] ENOKIBORI Y., MASE K.: Human joint angle estimation with an e-textile sensor. In *Proceedings of the 2014 ACM International Symposium on Wearable Computers* (New York, NY, USA, 2014), ISWC '14, Association for Computing Machinery, pp. 129–130. 15

[EPL04] EUNICE PARK-LEE C. C.: Pressure Ulcers Among Nursing Home Residents: United States, 2004 - National Center for Health Statistics, Data Briefs - Number 14 - February 2009, 2004. 32

[Eur19] EUROSTAT: Durchschnittliche Wochenarbeitszeit in Deutschland von 2009 bis 2018 nach Geschlecht, 2019. 4

[EYK*20] EGUCHI S., YAZAKI Y., KATO R., ARITA Y., MORIYA T., TANAKA H.: Proto-chair: Posture-sensing smart furniture with 3d-printed auxetics. In *Extended Abstracts of the 2020 CHI Conference on Human Factors in Computing Systems* (New York, NY, USA, 2020), CHI EA '20, Association for Computing Machinery, pp. 1–7. 12

[FDFI20] FORMAN J., DOGAN M. D., FORSYTHE H., ISHII H.: Defextiles: 3d printing quasi-woven fabric via under-extrusion. In *Proceedings of the 33rd Annual ACM Symposium on User Interface Software and Technology* (New York, NY, USA, 2020), UIST '20, Association for Computing Machinery, pp. 1222–1233. 146

[FDZ*05] FORLIZZI J., DISALVO C., ZIMMERMAN J., MUTLU B., HURST A.: The sensechair: The lounge chair as an intelligent assistive device for elders. In *Proceedings of the 2005 Conference on Designing for User EXperience* (New York, NY, USA, 2005), DUX '05, AIGA: American Institute of Graphic Arts, pp. 31–es. 17

[FHS17] FREIRE R., HONNET C., STROHMEIER P.: Second skin: An exploration of etextile stretch circuits on the body. In *Proceedings of the Eleventh International Conference on Tangible, Embedded, and Embodied Interaction* (New York, NY, USA, 2017), TEI '17, ACM, pp. 653–658. 86

[fIiGuaPe13] FÜR INNOVATIONEN IM GESUNDHEITSWESEN UND ANGEWANDTE PFLEGE-FORSCHUNG E.V. I.: Dekubitus - Immer noch ein Problem in der Pflege, 2003 - 2013. 32

[FKM*20] FRISCHER R., KREJCAR O., MARESOVA P., FADEYI O., SELAMAT A., KUCA K., TOMSONE S., TEIXEIRA J. P., MADUREIRA J., MELERO F. J.: Commercial ict smart solutions for the elderly: State of the art and future challenges in the smart furniture sector. *Electronics 9*, 1 (2020), 149. 9

[FKvW*17] FU B., KIRCHBUCHNER F., VON WILMSDORFF J., GROSSE-PUPPENDAHL T., BRAUN A., KUIJPER A.: Indoor localization based on passive electric field sensing. In *Ambient Intelligence* (Cham, 2017), Braun A., Wichert R., Maña A., (Eds.), Springer International Publishing, pp. 64–79. 12

[FMGK12] FOUBERT N., MCKEE A., GOUBRAN R., KNOEFEL F.: Lying and sitting posture recognition and transition detection using a pressure sensor array. In *Medical Measurements and Applications Proceedings (MeMeA), 2012 IEEE International Symposium on* (2012), pp. 1–6. 34

[For18] FORD MOTOR: Now that is a bright idea! cycling jacket prompts riders to turn, shows others when they do, 2018. Accessed: 2018-08-15. 87

[FP14] FOURATI N., PELACHAUD C.: Collection and characterization of emotional body behaviors. In *Proceedings of the 2014 International Workshop on Movement and Computing* (New York, NY, USA, 2014), MOCO '14, ACM, pp. 49:49–49:54. 63

[FRS*20] FANG L., RÖDDIGER T., SUN H., WILLENBACHER N., BEIGL M.: Flectile: 3d-printable soft actuators for wearable computing. In *Proceedings of the 2020 International Symposium on Wearable Computers* (New York, NY, USA, 2020), ISWC '20, Association for Computing Machinery, pp. 32–36. 146

[FSH*18] FREIRE R., STROHMEIER P., HONNET C., KNIBBE J., BRUECKNER S.: Designing etextiles for the body: Shape, volume 38; motion. In *Proceedings of the Twelfth International Conference on Tangible, Embedded, and Embodied Interaction* (New York, NY, USA, 2018), TEI '18, ACM, pp. 728–731. 86

[GA16] GÖTZELMANN T., ALTHAUS C.: Touchsurfacemodels: Capacitive sensing objects through 3d printers. In *Proceedings of the 9th ACM International Conference on PErvasive Technologies Related to Assistive Environments* (New York, NY, USA, 2016), PETRA '16, Association for Computing Machinery. 28

[GAGdR*20] GOUDSWAARD M., ABRAHAM A., GOVEIA DA ROCHA B., ANDERSEN K., LIANG R.-H.: Fabriclick: Interweaving pushbuttons into fabrics using 3d printing and digital embroidery. In *Proceedings of the 2020 ACM Designing Interactive Systems Conference* (New York, NY, USA, 2020), DIS '20, Association for Computing Machinery, pp. 379–393. 5, 146

[Gao13] GAO X.: Microchip capacitive proximity design guide. 27

[GCLF06] GARAY N., CEARRETA I., LÓPEZ J. M., FAJARDO I.: Assistive technology and affective mediation. *Human Technology: an Interdisciplinary Journal on Humans in ICT Environments* (2006). 62

[GFWS19] GROEGER D., FEICK M., WITHANA A., STEIMLE J.: Tactlets: Adding tactile feedback to 3d objects using custom printed controls. In *Proceedings of the 32nd Annual ACM Symposium on User Interface Software and Technology* (New York, NY, USA, 2019), UIST '19, Association for Computing Machinery, pp. 923–936. 15

[GKP*17] GRØNBÆK J. E., KORSGAARD H., PETERSEN M. G., BIRK M. H., KROGH P. G.: Proxemic transitions: Designing shape-changing furniture for informal meetings. In *Proceedings of the 2017 CHI Conference on Human Factors in Computing Systems* (New York, NY, USA, 2017), CHI '17, Association for Computing Machinery, pp. 7029–7041. 12

[GL95] GROSS J. J., LEVENSON R. W.: Emotion elicitation using films. *Cognition and Emotion 9*, 1 (1995), 87–108. 64

[GM00] GLINSKY A., MOOG B.: *Theremin: ether music and espionage*. University of Illinois Press, 2000. 21

[GP15] GROSSE-PUPPENDAHL T.: *Capacitive Sensing and Communication for Ubiquitous Interaction and Environmental Perception*. PhD thesis, TU Darmstadt, 2015. 33

[GPBB12] GROSSE-PUPPENDAHL T., BERLIN E., BORAZIO M.: Enhancing accelerometer-based activity recognition with capacitive proximity sensing. *Ambient Intelligence* (2012). 34

[GPBB*13] GROSSE-PUPPENDAHL T., BERGHOEFER Y., BRAUN A., WIMMER R., KUIJPER A.: Opencapsense: A rapid prototyping toolkit for pervasive interaction using capacitive sensing. In *2013 IEEE International Conference on Pervasive Computing and Communications (PerCom)* (2013), pp. 152–159. xvi, 35, 50, 55, 99, 100, 109

[GPDH*16] GROSSE-PUPPENDAHL T., DELLANGNOL X., HATZFELD C., FU B., KUPNIK M., KUIJPER A., HASTALL M. R., SCOTT J., GRUTESER M.: Platypus: Indoor localization and identification through sensing of electric potential changes in human bodies. In *Proceedings of the 14th Annual International Conference on Mobile Systems, Applications, and Services* (New York, NY, USA, 2016), MobiSys '16, Association for Computing Machinery, pp. 17–30. 12

[GPHC*17] GROSSE-PUPPENDAHL T., HOLZ C., COHN G., WIMMER R., BECHTOLD O., HODGES S., REYNOLDS M. S., SMITH J. R.: Finding common ground: A survey of capacitive sensing in human-computer interaction. In *Proceedings of the 2017 CHI Conference on Human Factors in Computing Systems* (New York, NY, USA, 2017), CHI '17, ACM, pp. 3293–3315. xiii, 22, 23, 24, 26

[GPMB11] GROSSE-PUPPENDAHL T., MARINC A., BRAUN A.: Classification of User Postures with Capacitive Proximity Sensors in AAL-Environments. In *Ambient Intelligence* (2011), Keyson D. V., Maher M. L., Streitz N., Cheok A., Augusto J. C., Wichert R., Englebienne G., Aghajan H., Kröse B. J. A., (Eds.), vol. 7040, Springer, pp. 314–323. 12, 54, 57, 63

[GS13] GU H., STERZIK C.: Capacitive touch hardware design guide, 2013. 27

[GS18] GROEGER D., STEIMLE J.: Objectskin: Augmenting everyday objects with hydroprinted touch sensors and displays. *Proc. ACM Interact. Mob. Wearable Ubiquitous Technol. 1*, 4 (Jan. 2018). 15

[GS19] GROEGER D., STEIMLE J.: Lasec: Instant fabrication of stretchable circuits using a laser cutter. In *Proceedings of the 2019 CHI Conference on Human Factors in Computing Systems* (New York, NY, USA, 2019), CHI '19, Association for Computing Machinery, pp. 1–14. 15

[GSB14] GRIFFITHS E., SAPONAS T. S., BRUSH A. J. B.: Health chair: Implicitly sensing heart and respiratory rate. In *Proceedings of the 2014 ACM International Joint Conference on Pervasive and Ubiquitous Computing* (New York, NY, USA, 2014), UbiComp '14, ACM, pp. 661–671. 17, 50

[GSO*14] GONG N.-W., STEIMLE J., OLBERDING S., HODGES S., GILLIAN N. E., KAWAHARA Y., PARADISO J. A.: Printsense: A versatile sensing technique to support multimodal flexible surface interaction. In *Proceedings of the SIGCHI Conference on Human Factors in Computing Systems* (New York, NY, USA, 2014), CHI '14, ACM, pp. 1407–1410. 72

[Gut17] GUTJAHR C.: Bringing self-aware textiles into the iot, 2017. 71, 86

[Ham15] HAMMACHER F.: Physical simulation- and reconstruction-framework for shape sensing fabrics, 2015. xiv, 71, 72, 74, 75

[HB10a] HAMISU P., BRAUN A.: Analyse des Schlafverhaltens durch kapazitive Sensorarrays zur Ermittlung der Wirbelsäulenbelastung. *Ambient Assisted Living-AAL* (2010). 33

[HB10b] HESSELMANN T., BOLL S.: Sciva: A design process for applications on interactive surfaces. In *ACM International Conference on Interactive Tabletops and Surfaces* (New York, NY, USA, 2010), ITS '10, Association for Computing Machinery, pp. 265–266. xiii, 17, 18

[HCG15] HERMANIS A., CACURS R., GREITANS M.: Shape sensing based on acceleration and magnetic sensor system. In *2015 IEEE International Symposium on Inertial Sensors and Systems (ISISS) Proceedings* (2015), pp. 1–2. 72, 73

[Hei77] HEILIGENBERG W.: *Principles of Electrolocation and Jamming Avoidance in Electric Fish: A Neuroethological Approach*. Studies of brain function. Springer-Verlag, 1977. 20

[HFH*09] HALL M., FRANK E., HOLMES G., PFAHRINGER B., REUTEMANN P., WITTEN I. H.: The weka data mining software: An update. *SIGKDD Explor. Newsl. 11*, 1 (Nov. 2009), 10–18. 52, 57, 138

[HHY12] HASRUL M. N., HARIHARAN M., YAACOB S.: Human affective (emotion) behaviour analysis using speech signals: A review. In *2012 International Conference on Biomedical Engineering (ICoBE)* (Feb 2012), pp. 217–222. 62

[HLA*09] HSIA C. C., LIOU K. J., AUNG A. P. W., FOO V., HUANG W., BISWAS J.: Analysis and comparison of sleeping posture classification methods using pressure sensitive bed system. *Conference proceedings : Annual International Conference of the IEEE Engineering in Medicine and Biology Society. 2009* (Jan. 2009), 6131–4. 34

[HLX*14] HUANG M., LIU J. J., XU W., ALSHURAFA N., ZHANG X., SARRAFZADEH M.: Using pressure map sequences for recognition of on bed rehabilitation exercises. *IEEE Journal of Biomedical and Health Informatics 18*, 2 (2014), 411–418. 16

[HMB*14] HOY D., MARCH L., BROOKS P., BLYTH F., WOOLF A., BAIN C., WILLIAMS G., SMITH E., VOS T., BARENDREGT J., MURRAY C., BURSTEIN R., BUCHBINDER R.: The global burden of low back pain: estimates from the global burden of disease 2010 study. *Annals of the Rheumatic Diseases 73*, 6 (2014), 968–974. 50

[HMBU15] HAESCHER M., MATTHIES D. J. C., BIEBER G., URBAN B.: Capwalk: A capacitive recognition of walking-based activities as a wearable assistive technology. In *Proceedings of the 8th ACM International Conference on PErvasive Technologies Related to Assistive Environments* (New York, NY, USA, 2015), PETRA '15, Association for Computing Machinery. 26

[HMH20] HOFMANN M., MANKOFF J., HUDSON S. E.: *KnitGIST: A Programming Synthesis Toolkit for Generating Functional Machine-Knitting Textures*. Association for Computing Machinery, New York, NY, USA, 2020, pp. 1234–1247. 16

[HN12] HERMANIS A., NESENBERGS K.: Grid shaped accelerometer network for surface shape recognition. *Proceedings of the Biennial Baltic Electronics Conference, BEC* (2012), 203–206. 72, 73

[Hom17] HOME R.: Smart Glove - Affordable Stroke Home Rehabilitation, 2017. Accessed: 2018-08-15. 86

[HP05] HEALEY J. A., PICARD R. W.: Detecting stress during real-world driving tasks using physiological sensors. *IEEE Transactions on Intelligent Transportation Systems 6*, 2 (June 2005), 156–166. 62

[HPWT*20] HONNET C., PERNER-WILSON H., TEYSSIER M., FRUCHARD B., STEIMLE J., BAPTISTA A. C., STROHMEIER P.: Polysense: Augmenting textiles with electrical functionality using in-situ polymerization. In *Proceedings of the 2020 CHI Conference on Human Factors in Computing Systems* (New York, NY, USA, 2020), CHI '20, Association for Computing Machinery, pp. 1–13. 16

[HS08] HOSHI T., SHINODA H.: 3D shape measuring sheet utilizing gravitational and geomagnetic fields. In *2008 SICE Annual Conference* (Aug. 2008), IEEE, pp. 915–920. 72

[HSH13] HIRAI S., SAKAKIBARA Y., HAYASHI H.: Enabling interactive bathroom entertainment using embedded touch sensors in the bathtub. In *Advances in Computer Entertainment* (Cham, 2013), Reidsma D., Katayose H., Nijholt A., (Eds.), Springer International

Publishing, pp. 544–547. 4

[HSK*13] HEIKKILÄ T., STRÖMMER E., KIVIKUNNAS S., JÄRVILUOMA M., KORKALAINEN M., KYLLÖNEN V., SARJANOJA E. M., PELTOMAA I.: Low intrusive ehealth monitoring: human posture and activity level detection with an intelligent furniture network. *IEEE Wireless Communications 20*, 4 (August 2013), 57–63. 12, 54

[HSP*08] HOLLEIS P., SCHMIDT A., PAASOVAARA S., PUIKKONEN A., HÄKKILÄ J.: Evaluating capacitive touch input on clothes. In *Proceedings of the 10th International Conference on Human Computer Interaction with Mobile Devices and Services* (New York, NY, USA, 2008), MobileHCI '08, Association for Computing Machinery, pp. 81–90. 26

[HT13] HAGAN M., TEODORESCU H.: Intelligent clothes with a network of painted sensors. In *2013 E-Health and Bioengineering Conference (EHB)* (2013), pp. 1–4. 26

[Hud03] HUDLICKA E.: To feel or not to feel: The role of affect in human-computer interaction. *International journal of human-computer studies 59*, 1-2 (jul 2003), 1–32. 62

[Hut17a] HUTSCHENREUTHER T.: Knitty-fi, 2017. Accessed: 2018-08-15. 87

[Hut17b] HUTSCHENREUTHER T.: Knitty-fi kleidung mit gestrickten schaltern und energieeffizienter, waschbarer elektronik. In *Silicon Saxony Arbeitskreis CPS* (Dresden, Germany, 2017), Silicon Saxony Arbeitskreis CPS. 87

[HVB18] HAMDAN N. A.-H., VOELKER S., BORCHERS J.: Sketch & stitch: Interactive embroidery for e-textiles. In *Proceedings of the 2018 CHI Conference on Human Factors in Computing Systems* (New York, NY, USA, 2018), CHI '18, ACM, pp. 82:1–82:13. 87

[HWM*20] HANTON O., WESSELY M., MUELLER S., FRASER M., ROUDAUT A.: Protospray: Combining 3d printing and spraying to create interactive displays with arbitrary shapes. In *Proceedings of the 2020 CHI Conference on Human Factors in Computing Systems* (New York, NY, USA, 2020), CHI '20, Association for Computing Machinery, pp. 1–13. 146

[HWV*19] HAMDAN N. A.-H., WAGNER A., VOELKER S., STEIMLE J., BORCHERS J.: Springlets: Expressive, flexible and silent on-skin tactile interfaces. In *Proceedings of the 2019 CHI Conference on Human Factors in Computing Systems* (New York, NY, USA, 2019), CHI '19, Association for Computing Machinery, pp. 1–14. 14

[HZAF05] HURST A., ZIMMERMAN J., ATKESON C., FORLIZZI J.: The sense lounger: Establishing a ubicomp beachhead in elders' homes. In *CHI '05 Extended Abstracts on Human Factors in Computing Systems* (New York, NY, USA, 2005), CHI EA '05, Association for Computing Machinery, pp. 1467–1470. 16

[JL95] JOHN G. H., LANGLEY P.: Estimating continuous distributions in bayesian classifiers. In *Eleventh Conference on Uncertainty in Artificial Intelligence* (San Mateo, 1995), Morgan Kaufmann, pp. 338–345. 65

[KAA*17] KAO H.-L. C., AJILO D., ANILIONYTE O., DEMENTYEV A., CHOI I., FOLLMER S., SCHMANDT C.: Exploring interactions and perceptions of kinetic wearables. In *Proceedings of the 2017 Conference on Designing Interactive Systems* (New York, NY, USA, 2017), DIS '17, Association for Computing Machinery, pp. 391–396. 14

[KBB13] KLEINSMITH A., BIANCHI-BERTHOUZE N.: Affective body expression perception and recognition: A survey. *IEEE Transactions on Affective Computing 4*, 1 (Jan 2013), 15–33. 62, 64

[KBKS18] KAO H.-L. C., BAMFORTH M., KIM D., SCHMANDT C.: Skinmorph: Texture-tunable on-skin interface through thin, programmable gel. In *Proceedings of the 2018 ACM International Symposium on Wearable Computers* (New York, NY, USA, 2018), ISWC '18, Association for Computing Machinery, pp. 196–203. 15

[KBL18] KAO H.-L. C., BEDRI A., LYONS K.: Skinwire: Fabricating a self-contained on-skin pcb for the hand. *Proc. ACM Interact. Mob. Wearable Ubiquitous Technol. 2*, 3 (Sept. 2018). 14

[KBP07] KAPOOR A., BURLESON W., PICARD R. W.: Automatic prediction of frustration. *International Journal of Human-Computer Studies 65*, 8 (2007), 724 – 736. 62, 63, 66

[KDPS15] KAO H.-L. C., DEMENTYEV A., PARADISO J. A., SCHMANDT C.: Nailo: Fingernails as an input surface. In *Proceedings of the 33rd Annual ACM Conference on Human Factors in Computing Systems* (New York, NY, USA, 2015), CHI '15, Association for Computing Machinery, pp. 3015–3018. 27

[KDS20] KLAMKA K., DACHSELT R., STEIMLE J.: Rapid iron-on user interfaces: Hands-on fabrication of interactive textile prototypes. In *Proceedings of the 2020 CHI Conference on Human Factors in Computing Systems* (New York, NY, USA, 2020), CHI '20, Association for Computing Machinery, pp. 1–14. 16

[KFA*15] KAN V., FUJII K., AMORES J., ZHU JIN C. L., MAES P., ISHII H.: Social textiles: Social affordances and icebreaking interactions through wearable social messaging. In *Proceedings of the Ninth International Conference on Tangible, Embedded, and Embodied Interaction* (New York, NY, USA, 2015), TEI '15, ACM, pp. 619–624. 15

[KHD20] KLAMKA K., HORAK T., DACHSELT R.: Watch+strap: Extending smartwatches with interactive strapdisplays. In *Proceedings of the 2020 CHI Conference on Human Factors in Computing Systems* (New York, NY, USA, 2020), CHI '20, Association for Computing Machinery, pp. 1–15. 10

[KHR*16] KAO H.-L. C., HOLZ C., ROSEWAY A., CALVO A., SCHMANDT C.: Duoskin: Rapidly prototyping on-skin user interfaces using skin-friendly materials. In *Proceedings of the 2016 ACM International Symposium on Wearable Computers* (New York, NY, USA, 2016), ISWC '16, Association for Computing Machinery, pp. 16–23. 14, 26

[KJRC16] KAO H.-L. C., JOHNS P., ROSEWAY A., CZERWINSKI M.: Tattio: Fabrication of aesthetic and functional temporary tattoos. In *Proceedings of the 2016 CHI Conference*

Extended Abstracts on Human Factors in Computing Systems (New York, NY, USA, 2016), CHI EA '16, Association for Computing Machinery, pp. 3699–3702. 14

[KLM08] KNIGHT H., LEE J., MA H.: Chair alarm for patient fall prevention based on gesture recognition and interactivity. In *2008 30th Annual International Conference of the IEEE Engineering in Medicine and Biology Society* (2008), pp. 3698–3701. 12

[KLMS11] KHALILBEIGI M., LISSERMANN R., MÜHLHÄUSER M., STEIMLE J.: Xpaaand. In *Proceedings of the 2011 annual conference on Human factors in computing systems - CHI '11* (New York, New York, USA, May 2011), ACM Press, p. 2729. 72

[KMS*19] KREJCAR O., MARESOVA P., SELAMAT A., MELERO F. J., BARAKOVIC S., HUSIC J. B., HERRERA-VIEDMA E., FRISCHER R., KUCA K.: Smart furniture as a component of a smart city definition based on key technologies specification. *IEEE Access 7* (2019), 94822–94839. 9

[KNRD17] KAO C. H.-L., NGUYEN B., ROSEWAY A., DICKEY M.: Earthtones: Chemical sensing powders to detect and display environmental hazards through color variation. In *Proceedings of the 2017 CHI Conference Extended Abstracts on Human Factors in Computing Systems* (New York, NY, USA, 2017), CHI EA '17, Association for Computing Machinery, pp. 872–883. 15

[KRKS19] KHAN A., ROO J. S., KRAUS T., STEIMLE J.: Soft inkjet circuits: Rapid multimaterial fabrication of soft circuits using a commodity inkjet printer. In *Proceedings of the 32nd Annual ACM Symposium on User Interface Software and Technology* (New York, NY, USA, 2019), UIST '19, Association for Computing Machinery, pp. 341–354. 14

[KSG*13] KARG M., SAMADANI A.-A., GORBET R., KUHNLENZ K., HOEY J., KULIC D.: Body Movements for Affective Expression: A Survey of Automatic Recognition and Generation. *IEEE Transactions on Affective Computing 4*, 4 (oct 2013), 341–359. 62

[KSK*10] KIVIKUNNAS S., STRÖMMER E., KORKALAINEN M., HEIKKILÄ T., HAVERINEN M.: Sensing sofa and its ubiquitous use. In *2010 International Conference on Information and Communication Technology Convergence (ICTC)* (Nov 2010), pp. 559–562. 12, 54

[KSW*20] KU P.-S., SHAO Q., WU T.-Y., GONG J., ZHU Z., ZHOU X., YANG X.-D.: Threadsense: Locating touch on an extremely thin interactive thread. In *Proceedings of the 2020 CHI Conference on Human Factors in Computing Systems* (New York, NY, USA, 2020), CHI '20, Association for Computing Machinery, pp. 1–12. 26

[KVVV13] KIVIMÄKI T., VUORELA T., VALTONEN M., VANHALA J.: Reliability of the tiletrack capacitive user tracking system in smart home environment. In *ICT 2013* (2013), pp. 1–5. 12

[LBS85] LEE S., BUXTON W., SMITH K. C.: A multi-touch three dimensional touch-sensitive tablet. In *Proceedings of the SIGCHI Conference on Human Factors in Computing*

Systems (New York, NY, USA, 1985), CHI '85, ACM, pp. 21–25. 21

[LFC*20] LUO E., FU R., CHU A., VEGA K., KAO H.-L. C.: Eslucent: An eyelid interface for detecting eye blinking. In *Proceedings of the 2020 International Symposium on Wearable Computers* (New York, NY, USA, 2020), ISWC '20, Association for Computing Machinery, pp. 58–62. 15

[LGBV11] LAHEY B., GIROUARD A., BURLESON W., VERTEGAAL R.: Paperphone: Understanding the use of bend gestures in mobile devices with flexible electronic paper displays. In *Proceedings of the SIGCHI Conference on Human Factors in Computing Systems* (New York, NY, USA, 2011), CHI '11, ACM, pp. 1303–1312. 72

[LHX*13] LIU J. J., HUANG M.-C., XU W., ALSHURAFA N., SARRAFZADEH M.: On-bed monitoring for range of motion exercises with a pressure sensitive bedsheet. *2013 IEEE International Conference on Body Sensor Networks*, c (May 2013), 1–6. 34

[LHXS14] LIU J. J., HUANG M., XU W., SARRAFZADEH M.: Bodypart localization for pressure ulcer prevention. In *2014 36th Annual International Conference of the IEEE Engineering in Medicine and Biology Society* (2014), pp. 766–769. 16

[LNP01] LEE C., NARAYANAN S., PIERACCINI R.: Recognition of negative emotions from the speech signal. In *IEEE Workshop on Automatic Speech Recognition and Understanding, 2001. ASRU '01.* (2001), IEEE, pp. 240–243. 62

[LPP*16] LEONG J., PARZER P., PERTENEDER F., BABIC T., RENDL C., VOGL A., EGGER H., OLWAL A., HALLER M.: Procover: Sensory augmentation of prosthetic limbs using smart textile covers. In *Proceedings of the 29th Annual Symposium on User Interface Software and Technology* (New York, NY, USA, 2016), UIST '16, Association for Computing Machinery, pp. 335–346. 15

[LRS*04] LORUSSI F., ROCCHIA W., SCILINGO E. P., TOGNETTI A., ROSSI D. D.: Wearable, redundant fabric-based sensor arrays for reconstruction of body segment posture. *IEEE Sensors Journal 4*, 6 (Dec 2004), 807–818. 72

[Lup16] LUPTON D.: *The quantified self - A sociology of self-tracking*. John Wiley & Sons, 2016. 50

[LXH*13] LIU J. J., XU W., HUANG M., ALSHURAFA N., SARRAFZADEH M., RAUT N., YADEGAR B.: A dense pressure sensitive bedsheet design for unobtrusive sleep posture monitoring. In *2013 IEEE International Conference on Pervasive Computing and Communications (PerCom)* (2013), pp. 207–215. 16

[LXH*14] LIU J. J., XU W., HUANG M.-C., ALSHURAFA N., SARRAFZADEH M., RAUT N., YADEGAR B.: Sleep posture analysis using a dense pressure sensitive bedsheet. *Pervasive and Mobile Computing 10, Part A*, 0 (2014), 34 – 50. 34

[LXHA13] LIU J. J., XU W., HUANG M.-C., ALSHURAFA N.: A Dense Pressure Sensitive Bedsheet Design for Unobtrusive Sleep Posture Monitoring. 206–214. 34, 54

[Maj17] MAJEWSKI M.: 3d-printed electrodes for electric field sensing technologies, 2017. 106

[MAST10] MEYER J., ARNRICH B., SCHUMM J., TROSTER G.: Design and modeling of a textile pressure sensor for sitting posture classification. *IEEE Sensors Journal 10*, 8 (Aug 2010), 1391–1398. 50

[Mau14] MAUS B.-T. V. S. M.: Klassifizierung von Liegepositionen mittels kapazitiver Näherungssensorik. 32

[MBBN05] MIDDLETON L., BUSS A. A., BAZIN A., NIXON M. S.: A floor sensor system for gait recognition. In *Fourth IEEE Workshop on Automatic Identification Advanced Technologies (AutoID'05)* (2005), pp. 171–176. 12

[MBRS14a] MENNICKEN S., BRUSH A. J. B., ROSEWAY A., SCOTT J.: Exploring interactive furniture with emotocouch. In *Proceedings of the 2014 ACM International Joint Conference on Pervasive and Ubiquitous Computing: Adjunct Publication* (New York, NY, USA, 2014), UbiComp '14 Adjunct, ACM, pp. 307–310. 54, 63

[MBRS14b] MENNICKEN S., BRUSH A. J. B., ROSEWAY A., SCOTT J.: Finding roles for interactive furniture in homes with emotocouch. In *Proceedings of the 2014 ACM International Joint Conference on Pervasive and Ubiquitous Computing: Adjunct Publication* (New York, NY, USA, 2014), UbiComp '14 Adjunct, ACM, pp. 923–930. 54

[MJB*13] MELLIS D. A., JACOBY S., BUECHLEY L., PERNER-WILSON H., QI J.: Microcontrollers as material: Crafting circuits with paper, conductive ink, electronic components, and an "untoolkit". In *Proceedings of the 7th International Conference on Tangible, Embedded and Embodied Interaction* (New York, NY, USA, 2013), TEI '13, ACM, pp. 83–90. 72

[MK12] MADAAN P., KAUR P.: Capacitive sensing made easy, part 2: Design guidelines. *EE Times Apr 16* (2012). 120, 129

[MKF*07] MUTLU B., KRAUSE A., FORLIZZI J., GUESTRIN C., HODGINS J.: Robust, low-cost, non-intrusive sensing and recognition of seated postures. In *Proceedings of the 20th Annual ACM Symposium on User Interface Software and Technology* (New York, NY, USA, 2007), UIST '07, ACM, pp. 149–158. 12, 50

[MLB*13] MARTINS L., LUCENA R., BELO J., SANTOS M., QUARESMA C., JESUS A. P., VIEIRA P.: Intelligent chair sensor. In *Engineering Applications of Neural Networks* (Berlin, Heidelberg, 2013), Iliadis L., Papadopoulos H., Jayne C., (Eds.), Springer Berlin Heidelberg, pp. 182–191. 12, 50

[MLGF17] MA C., LI W., GRAVINA R., FORTINO G.: Posture detection based on smart cushion for wheelchair users. *Sensors 17*, 4 (2017). 12, 50

[MP03] MOTA S., PICARD R. W.: Automated posture analysis for detecting learner's interest level. In *2003 Conference on Computer Vision and Pattern Recognition Workshop* (June 2003), vol. 5, pp. 49–49. 12, 62, 63, 66

[MSZ*20] MARKY K., SCHMITZ M., ZIMMERMANN V., HERBERS M., KUNZE K., MÜHLHÄUSER M.: 3d-auth: Two-factor authentication with personalized 3d-printed

items. In *Proceedings of the 2020 CHI Conference on Human Factors in Computing Systems* (New York, NY, USA, 2020), CHI '20, Association for Computing Machinery, pp. 1–12. 27

[NAZW10] NI H., ABDULRAZAK B., ZHANG D., WU S.: Unobtrusive sleep posture detection for elder-care in smart home. In *Aging Friendly Technology for Health and Independence*. Springer, 2010, pp. 67–75. 34

[Nel05] NELSON M. E.: Target detection, image analysis, and modeling. In *Electroreception*. Springer, 2005, pp. 290–317. xiii, 20

[NKK*20] NITTALA A. S., KHAN A., KRUTTWIG K., KRAUS T., STEIMLE J.: Physioskin: Rapid fabrication of skin-conformal physiological interfaces. In *Proceedings of the 2020 CHI Conference on Human Factors in Computing Systems* (New York, NY, USA, 2020), CHI '20, Association for Computing Machinery, pp. 1–10. 4, 14

[NNOK20] NOMA Y., NARUMI K., OKUYA F., KAWAHARA Y.: Pop-up print: Rapidly 3d printing mechanically reversible objects in the folded state. In *Proceedings of the 33rd Annual ACM Symposium on User Interface Software and Technology* (New York, NY, USA, 2020), UIST '20, Association for Computing Machinery, pp. 58–70. 146

[NS16] NITTALA A. S., STEIMLE J.: Digital fabrication pipeline for on-body sensors: Design goals and challenges. In *Proceedings of the 2016 ACM International Joint Conference on Pervasive and Ubiquitous Computing: Adjunct* (New York, NY, USA, 2016), UbiComp '16, Association for Computing Machinery, pp. 950–953. xiii, 17, 18

[OEM17] ONOSE R., ENOKIBORI Y., MASE K.: Garment vs. bed-sheet sensors: To deal with pressure dispersion cushion use in pressure ulcer prevention. In *Proceedings of the 2017 ACM International Joint Conference on Pervasive and Ubiquitous Computing and Proceedings of the 2017 ACM International Symposium on Wearable Computers* (New York, NY, USA, 2017), UbiComp '17, Association for Computing Machinery, pp. 169–172. 16

[OHEM18] ONOSE R., HARASAWA Y., ENOKIBORI Y., MASE K.: Textile sensor-based visualization to enhance skills to understand the body-pressure distribution for pressure ulcer prevention. In *Proceedings of the 2018 ACM International Joint Conference and 2018 International Symposium on Pervasive and Ubiquitous Computing and Wearable Computers* (New York, NY, USA, 2018), UbiComp '18, Association for Computing Machinery, pp. 194–197. 16

[OMPD*18] OLWAL A., MOELLER J., PRIEST-DORMAN G., STARNER T., CARROLL B.: I/O Braid: Scalable Touch-Sensitive Lighted Cords Using Spiraling, Repeating Sensing Textiles and Fiber Optics. In *Proceedings of the 31st Annual ACM Symposium on User Interface Software and Technology* (New York, NY, USA, 2018), UIST '18, Association for Computing Machinery, pp. 485–497. 26

[OPC98] ORTH M., POST R., COOPER E.: Fabric computing interfaces. In *CHI 98 Conference Summary on Human Factors in Computing Systems* (New York, NY, USA, 1998), CHI

'98, Association for Computing Machinery, pp. 331–332. 26

[OPNK14] OSTADABBAS S., POUYAN M., NOURANI M., KEHTARNAVAZ N.: In-bed posture classification and limb identification. In *Biomedical Circuits and Systems Conference (BioCAS), 2014 IEEE* (2014), pp. 133–136. 34

[OSM20] OLWAL A., STARNER T., MAININI G.: E-textile microinteractions: Augmenting twist with flick, slide and grasp gestures for soft electronics. In *Proceedings of the 2020 CHI Conference on Human Factors in Computing Systems* (New York, NY, USA, 2020), CHI '20, Association for Computing Machinery, pp. 1–13. 26

[OTKB19] OJUROYE O. O., TORAH R. N., KOMOLAFE A. O., BEEBY S. P.: Embedded capacitive proximity and touch sensing flexible circuit system for electronic textile and wearable systems. *IEEE Sensors Journal 19*, 16 (2019), 6975–6985. 26

[OWS14] OLBERDING S., WESSELY M., STEIMLE J.: Printscreen: Fabricating highly customizable thin-film touch-displays. In *Proceedings of the 27th Annual ACM Symposium on User Interface Software and Technology* (New York, NY, USA, 2014), UIST '14, ACM, pp. 281–290. 15

[OYF*11] OSTADABBAS S., YOUSEFI R., FAEZIPOUR M., NOURANI M., POMPEO M.: Pressure ulcer prevention: An efficient turning schedule for bed-bound patients. In *2011 IEEE/NIH Life Science Systems and Applications Workshop (LiSSA)* (2011), pp. 159–162. 11

[Per20] PERERA M.: Personalised human device interaction through context aware augmented reality. In *Proceedings of the 2020 International Conference on Multimodal Interaction* (New York, NY, USA, 2020), ICMI '20, Association for Computing Machinery, pp. 723–727. 10

[PF18] POSCH I., FITZPATRICK G.: Integrating textile materials with electronic making: Creating new tools and practices. In *Proceedings of the Twelfth International Conference on Tangible, Embedded, and Embodied Interaction* (New York, NY, USA, 2018), TEI '18, ACM, pp. 158–165. 87

[PGF*16] POUPYREV I., GONG N.-W., FUKUHARA S., KARAGOZLER M. E., SCHWESIG C., ROBINSON K. E.: Project jacquard: Interactive digital textiles at scale. In *Proceedings of the 2016 CHI Conference on Human Factors in Computing Systems* (New York, NY, USA, 2016), CHI '16, ACM, pp. 4216–4227. 4, 16, 26, 54, 87

[PHK*15] POHL H., HETTIG M., KARRAS O., ÖTZTÜRK H., ROHS M.: Capcouch: Home control with a posture-sensing couch. In *Adjunct Proceedings of the 2015 ACM International Joint Conference on Pervasive and Ubiquitous Computing and Proceedings of the 2015 ACM International Symposium on Wearable Computers* (New York, NY, USA, 2015), UbiComp/ISWC'15 Adjunct, ACM, pp. 229–232. 12, 55, 57, 58

[PHP*20] PREINDL T., HONNET C., POINTNER A., AIGNER R., PARADISO J. A., HALLER M.: Sonoflex: Embroidered speakers without permanent magnets. In *Proceedings of*

the 33rd Annual ACM Symposium on User Interface Software and Technology (New York, NY, USA, 2020), UIST '20, Association for Computing Machinery, pp. 675–685. 16

[Pla98] PLATT J.: Fast training of support vector machines using sequential minimal optimization. In *Advances in Kernel Methods - Support Vector Learning*, Schoelkopf B., Burges C., Smola A., (Eds.). MIT Press, 1998, pp. 43–55]. 65

[PMBA04] PARADISO J. A., MORRIS S. J., BENBASAT A. Y., ASMUSSEN E.: Interactive therapy with instrumented footwear. In *CHI '04 Extended Abstracts on Human Factors in Computing Systems* (New York, NY, USA, 2004), CHI EA '04, Association for Computing Machinery, pp. 1341–1343. 26

[Pos17] POSCH I.: Crafting tools for textile electronic making. In *Proceedings of the 2017 CHI Conference Extended Abstracts on Human Factors in Computing Systems* (New York, NY, USA, 2017), CHI EA '17, ACM, pp. 409–412. 87

[PPB*16] PARZER P., PROBST K., BABIC T., RENDL C., VOGL A., OLWAL A., HALLER M.: Flextiles: A flexible, stretchable, formable, pressure-sensitive, tactile input sensor. In *Proceedings of the 2016 CHI Conference Extended Abstracts on Human Factors in Computing Systems* (New York, NY, USA, 2016), CHI EA '16, Association for Computing Machinery, pp. 3754–3757. 15

[PPBS01] POLLICK F. E., PATERSON H. M., BRUDERLIN A., SANFORD A. J.: Perceiving affect from arm movement. *Cognition 82*, 2 (2001), B51 – B61. 62

[PPL*20] PERTENEDER F., PROBST K., LEONG J., GASSLER S., RENDL C., PARZER P., FLUCH K., GAHLEITNER S., FOLLMER S., KOIKE H., HALLER M.: Foxels: Build your own smart furniture. In *Proceedings of the Fourteenth International Conference on Tangible, Embedded, and Embodied Interaction* (New York, NY, USA, 2020), TEI '20, Association for Computing Machinery, pp. 111–122. 12

[PPP*18] PARZER P., PERTENEDER F., PROBST K., RENDL C., LEONG J., SCHUETZ S., VOGL A., SCHWOEDIAUER R., KALTENBRUNNER M., BAUER S., HALLER M.: Resi: A highly flexible, pressure-sensitive, imperceptible textile interface based on resistive yarns. In *Proceedings of the 31st Annual ACM Symposium on User Interface Software and Technology* (New York, NY, USA, 2018), UIST '18, Association for Computing Machinery, pp. 745–756. 5, 16

[PRP05] POSNER J., RUSSELL J. A., PETERSON B. S.: The circumplex model of affect: An integrative approach to affective neuroscience, cognitive development, and psychopathology. *Development and psychopathology 17*, 03 (2005), 715–734. 64

[PSLS12] POUPYREV I., SCHOESSLER P., LOH J., SATO M.: Botanicus interacticus: Interactive plants technology. In *ACM SIGGRAPH 2012 Emerging Technologies* (New York, NY, USA, 2012), SIGGRAPH '12, Association for Computing Machinery. 5

[PSV*17] PARZER P., SHARMA A., VOGL A., STEIMLE J., OLWAL A., HALLER M.: Smartsleeve: Real-time sensing of surface and deformation gestures on flexible, interactive textiles, using a hybrid gesture detection pipeline. In *Proceedings of the 30th Annual ACM Symposium on User Interface Software and Technology* (New York, NY, USA, 2017), UIST '17, Association for Computing Machinery, pp. 565–577. 15

[PWB10] PERNER-WILSON H., BUECHLEY L.: Making textile sensors from scratch. In *Proceedings of the Fourth International Conference on Tangible, Embedded, and Embodied Interaction* (New York, NY, USA, 2010), TEI '10, ACM, pp. 349–352. 86, 87

[PWPS19] POURJAFARIAN N., WITHANA A., PARADISO J. A., STEIMLE J.: Multi-touch kit: A do-it-yourself technique for capacitive multi-touch sensing using a commodity microcontroller. In *Proceedings of the 32nd Annual ACM Symposium on User Interface Software and Technology* (New York, NY, USA, 2019), UIST '19, Association for Computing Machinery, pp. 1071–1083. 27

[Qui93] QUINLAN R.: *C4.5: Programs for Machine Learning*. Morgan Kaufmann Publishers, San Mateo, CA, 1993. 65

[Qui14] QUINLAN J. R.: *C4. 5: programs for machine learning*. Elsevier, 2014. 39

[RBK17] RUS S., BRAUN A., KUIJPER A.: E-textile couch: Towards smart garments integrated furniture. In *Ambient Intelligence* (Cham, 2017), Braun A., Wichert R., Maña A., (Eds.), Springer International Publishing, pp. 214–224. 6, 53, 63, 69, 144

[RBKK19a] RUS S., BRAUN A., KIRCHBUCHNER F., KUIJPER A.: Designing a self-aware jacket: Insights into smart garments creation process. In *Proceedings of the 12th ACM International Conference on PErvasive Technologies Related to Assistive Environments* (New York, NY, USA, 2019), PETRA '19, Association for Computing Machinery, pp. 53–58. vi, 7, 71, 86, 95, 145

[RBKK19b] RUS S., BRAUN A., KIRCHBUCHNER F., KUIJPER A.: E-textile capacitive electrodes: Fabric or thread: Designing an e-textile cushion for sitting posture detection. In *Proceedings of the 12th ACM International Conference on PErvasive Technologies Related to Assistive Environments* (New York, NY, USA, 2019), PETRA '19, Association for Computing Machinery, pp. 49–52. v, vi, 6, 7, 49, 69, 98, 135, 143, 145

[Rek02] REKIMOTO J.: Smartskin: An infrastructure for freehand manipulation on interactive surfaces. In *Proceedings of the SIGCHI Conference on Human Factors in Computing Systems* (New York, NY, USA, 2002), CHI '02, Association for Computing Machinery, pp. 113–120. 99

[RGPK14] RUS S., GROSSE-PUPPENDAHL T., KUIJPER A.: Recognition of bed postures using mutual capacitance sensing. In *Ambient Intelligence*, Aarts E., de Ruyter B., Markopoulos P., van Loenen E., Wichert R., Schouten B., Terken J., Van Kranenburg R., Den Ouden E., O'Hare G., (Eds.), vol. 8850 of *Lecture Notes in Computer Science*. Springer International Publishing, 2014, pp. 51–66. v, 6, 32, 33, 34, 54, 68, 72, 143

[RGPK17] RUS S., GROSSE-PUPPENDAHL T., KUIJPER A.: Evaluating the recognition of bed postures using mutual capacitance sensing. *Journal of Ambient Intelligence and Smart Environments 9*, 1 (2017), 113–127. v, 6, 32, 68, 143

[RHvW*18] RUS S., HAMMACHER F., VON WILMSDORFF J., BRAUN A., GROSSE-PUPPENDAHL T., KIRCHBUCHNER F., KUIJPER A.: Prototyping shape-sensing fabrics through physical simulation. In *Ambient Intelligence* (Cham, 2018), Kameas A., Stathis K., (Eds.), Springer International Publishing, pp. 147–161. vi, 7, 71, 72, 91, 94, 144

[RJBK18] RUS S., JOSHI D., BRAUN A., KUIJPER A.: The emotive couch - learning emotions by capacitively sensed movements. *Procedia Computer Science 130* (2018), 263 – 270. The 9th International Conference on Ambient Systems, Networks and Technologies (ANT 2018) / The 8th International Conference on Sustainable Energy Information Technology (SEIT-2018) / Affiliated Workshops. 6, 61, 69, 144

[RKF*14] RENDL C., KIM D., FANELLO S., PARZER P., RHEMANN C., TAYLOR J., ZIRKL M., SCHEIPL G., ROTHLÄNDER T., HALLER M., IZADI S.: Flexsense: A transparent self-sensing deformable surface. In *Proceedings of the 27th Annual ACM Symposium on User Interface Software and Technology* (New York, NY, USA, 2014), UIST '14, ACM, pp. 129–138. 72

[RKP*16] RENDL C., KIM D., PARZER P., FANELLO S., ZIRKL M., SCHEIPL G., HALLER M., IZADI S.: Flexcase: Enhancing mobile interaction with a flexible sensing and display cover. In *Proceedings of the 2016 CHI Conference on Human Factors in Computing Systems* (New York, NY, USA, 2016), CHI '16, ACM, pp. 5138–5150. 15

[RLFP04] RICHARDSON B., LEYDON K., FERNSTROM M., PARADISO J. A.: Z-tiles: Building blocks for modular, pressure-sensing floorspaces. In *CHI '04 Extended Abstracts on Human Factors in Computing Systems* (New York, NY, USA, 2004), CHI EA '04, Association for Computing Machinery, pp. 1529–1532. 12

[RM20] RAJCIC N., MCCORMACK J.: Mirror ritual: An affective interface for emotional self-reflection. In *Proceedings of the 2020 CHI Conference on Human Factors in Computing Systems* (New York, NY, USA, 2020), CHI '20, Association for Computing Machinery, pp. 1–13. 146

[RSBK15] RUS S., SAHBAZ M., BRAUN A., KUIJPER A.: Design factors for flexible capacitive sensors in ambient intelligence. In *Ambient Intelligence* (Cham, 2015), De Ruyter B., Kameas A., Chatzimisios P., Mavrommati I., (Eds.), Springer International Publishing, pp. 77–92. vi, 7, 63, 98, 145

[RSL14] RAMAKERS R., SCHÖNING J., LUYTEN K.: Paddle. In *Proceedings of the 32nd annual ACM conference on Human factors in computing systems - CHI '14* (New York, New York, USA, Apr. 2014), ACM Press, pp. 2569–2578. 72

[Rus13] RUS S.: Recognition of Lying Postures using Capacitive Proximity Sensing, 2013. 32

[SCHGP16] SWEENEY D., CHEN N., HODGES S., GROSSE-PUPPENDAHL T.: Displays as a material: A route to making displays more pervasive. *IEEE Pervasive Computing 15*, 3 (2016), 77–82. 72

[SD20] SHAHMIRI F., DIETZ P. H.: Sharc: A geometric technique for multi-bend/shape sensing. In *Proceedings of the 2020 CHI Conference on Human Factors in Computing Systems* (New York, NY, USA, 2020), CHI '20, Association for Computing Machinery, pp. 1–12. 27

[SDKJ14] SAHA S., DATTA S., KONAR A., JANARTHANAN R.: A study on emotion recognition from body gestures using kinect sensor. In *2014 International Conference on Communication and Signal Processing* (April 2014), pp. 056–060. 62

[Sen] SENSIMAT: Sensimat website - features. [Online; accessed 5 July 2018]. 50

[Sen17] SENSOGLOVE: Probably the best controler for virtual and augmented reality, 2017. Online, accessed: 2018-08-15. 86

[SFC*11] SHOTTON J., FITZGIBBON A., COOK M., SHARP T., FINOCCHIO M., MOORE R., KIPMAN A., BLAKE A.: Real-time human pose recognition in parts from single depth images. *Cvpr 2011* (June 2011), 1297–1304. 33

[SGB99] SMITH J. R., GERSHENFELD N., BENTON S. A.: *Electric Field Imaging*. PhD thesis, 1999. xiii, 35, 37

[Shi] SHIELDEX: Shieldex Zell RS - technical data sheet. [Online; accessed 5 July 2018]. 138

[Shn20] SHNEIDERMAN B.: Human-centered artificial intelligence: Three fresh ideas. *AIS Transactions on Human-Computer Interaction 12*, 3 (2020), 109–124. 9

[SHZ*15] SCHNEEGASS S., HASSIB M., ZHOU B., CHENG J., SEOANE F., AMFT O., LUKOWICZ P., SCHMIDT A.: Simpleskin: Towards multipurpose smart garments. In *Adjunct Proceedings of the 2015 ACM International Joint Conference on Pervasive and Ubiquitous Computing and Proceedings of the 2015 ACM International Symposium on Wearable Computers* (New York, NY, USA, 2015), UbiComp/ISWC'15 Adjunct, ACM, pp. 241–244. 87

[SJM13] STEIMLE J., JORDT A., MAES P.: Flexpad: highly flexible bending interactions for projected handheld displays. *Proceedings of the SIGCHI Conference on Human Factors in Computing Systems - CHI'13* (2013), 237–246. 72

[SKB*15] SCHMITZ M., KHALILBEIGI M., BALWIERZ M., LISSERMANN R., MÜHLHÄUSER M., STEIMLE J.: Capricate: A fabrication pipeline to design and 3d print capacitive touch sensors for interactive objects. In *Proceedings of the 28th Annual ACM Symposium on User Interface Software and Technology* (New York, NY, USA, 2015), UIST '15, Association for Computing Machinery, pp. 253–258. 27

[SKBH18] STROHMEIER P., KNIBBE J., BORING S., HORNBÆK K.: Zpatch: Hybrid resistive/capacitive etextile input. In *Proceedings of the Twelfth International Conference*

on Tangible, Embedded, and Embodied Interaction (New York, NY, USA, 2018), TEI '18, Association for Computing Machinery, pp. 188–198. 26

[SM11] STARANOWICZ A., MARIOTTINI G. L.: A survey and comparison of commercial and open-source robotic simulator software. In *Proceedings of the 4th International Conference on PErvasive Technologies Related to Assistive Environments - PETRA '11* (New York, New York, USA, May 2011), ACM Press, p. 1. 72

[SMvB*20] SARSENBAYEVA Z., MARINI G., VAN BERKEL N., LUO C., JIANG W., YANG K., WADLEY G., DINGLER T., KOSTAKOS V., GONCALVES J.: Does Smartphone Use Drive Our Emotions or Vice Versa? A Causal Analysis. In *Proceedings of the 2020 CHI Conference on Human Factors in Computing Systems* (New York, NY, USA, 2020), CHI '20, Association for Computing Machinery, pp. 1–15. 146

[SNR*15] SINGH G., NELSON A., ROBUCCI R., PATEL C., BANERJEE N.: Inviz : Low-power personalized gesture recognition using wearable textile capacitive sensor arrays. In *Pervasive Computing and Communications (PerCom), 2015 IEEE International Conference on* (March 2015). 26, 98

[SOD*20a] SUN R., ONOSE R., DUNNE M., LING A., DENHAM A., KAO H.-L. C.: Demonstration for weaving a second skin: Exploring opportunities for crafting on-skin interfaces through weaving. In *Companion Publication of the 2020 ACM Designing Interactive Systems Conference* (New York, NY, USA, 2020), DIS' 20 Companion, Association for Computing Machinery, pp. 365–368. 14

[SOD*20b] SUN R., ONOSE R., DUNNE M., LING A., DENHAM A., KAO H.-L. C.: Weaving a second skin: Exploring opportunities for crafting on-skin interfaces through weaving. In *Proceedings of the 2020 ACM Designing Interactive Systems Conference* (New York, NY, USA, 2020), DIS '20, Association for Computing Machinery, pp. 365–377. 14, 26

[SPM04] SCHWESIG C., POUPYREV I., MORI E.: Gummi. In *Proceedings of the 2004 conference on Human factors in computing systems - CHI '04* (New York, New York, USA, Apr. 2004), ACM Press, pp. 263–270. 72

[SPW07] SATOMI M., PERNER-WILSON H.: How to get what you want, 2007. Online, accessed: 2018-08-15. 86

[SSA*20] SEMERTZIDIS N., SCARY M., ANDRES J., DWIVEDI B., KULWE Y. C., ZAMBETTA F., MUELLER F. F.: Neo-noumena: Augmenting emotion communication. In *Proceedings of the 2020 CHI Conference on Human Factors in Computing Systems* (New York, NY, USA, 2020), CHI '20, Association for Computing Machinery, pp. 1–13. 146

[SSBB12] SAVVA N., SCARINZI A., BIANCHI-BERTHOUZE N.: Continuous recognition of player's affective body expression as dynamic quality of aesthetic experience. *IEEE Transactions on Computational Intelligence and AI in Games 4*, 3 (Sept 2012), 199–212. 62

[SSH*17] SCHMITZ M., STEIMLE J., HUBER J., DEZFULI N., MÜHLHÄUSER M.: Flexibles: Deformation-aware 3d-printed tangibles for capacitive touchscreens. In *Proceedings of the 2017 CHI Conference on Human Factors in Computing Systems* (New York, NY, USA, 2017), CHI '17, Association for Computing Machinery, pp. 1001–1014. 4, 27

[SSJLB14] SAGUIN-SPRYNSKI N., JOUANET L., LACOLLE B., BIARD L.: Surfaces Reconstruction Via Inertial Sensors for Monitoring, July 2014. 72, 73

[Sta02] STATISTISCHES BUNDESAMT: Zeitbudgeterhebnung (ZBE) 2001/2002, 2002. 4

[Sta16] STATISTISCHES BUNDESAMT: Analysen zur Zeitverwendung in Deutschland. Zeitverwendung von Männern und Frauen im Lebenslauf, 2016. 4

[Ste] STEELCASE: Global Posture Study. [Online; accessed 06 May 2018]. 50

[Sul19] SULLIVAN T. G. F. .: Sensor innovations transforming healthcare sector, 2019. 105

[SV99] SUYKENS J., VANDEWALLE J.: Least squares support vector machine classifiers. *Neural Processing Letters 9*, 3 (1999), 293–300. 39

[SWD*98] SMITH J., WHITE T., DODGE C., PARADISO J., GERSHENFELD N., ALLPORT D.: Electric field sensing for graphical interfaces. *IEEE Computer Graphics and Applications 18*, 3 (May 1998), 54–60. 23

[SYM*15] SANO A., YU A. Z., MCHILL A. W., PHILLIPS A. J. K., TAYLOR S., JAQUES N., KLERMAN E. B., PICARD R. W.: Prediction of happy-sad mood from daily behaviors and previous sleep history. In *2015 37th Annual International Conference of the IEEE Engineering in Medicine and Biology Society (EMBC)* (Aug 2015), pp. 6796–6799. 62

[SYS14] SHIREHJINI A. A. N., YASSINE A., SHIRMOHAMMADI S.: Design and implementation of a system for body posture recognition. *Multimedia Tools and Applications 70*, 3 (2014), 1637–1650. 54

[Tek] TEKSCAN: Body pressure measurement system. [Online; accessed 05-July-2018]. 50

[Teo13] TEODORESCU H.-N.: Textile-, conductive paint-based wearable devices for physical activity monitoring. In *E-Health and Bioengineering Conference (EHB), 2013* (2013), IEEE, pp. 1–4. 98

[Tes12] TESKE P.: *Ein Multisensor-System zur Sturzerkennung*. Master's thesis, Hochschule für angewandte Wissenschaften Hamburg, 2012. 33

[THFM15] TORRES C., HAMMOND S., FRIED J., MANJUNATH B.: Sleep Pose Recognition in an ICU Using Multimodal Data and Environmental Feedback. In *Computer Vision Systems*, vol. 9163 of *Lecture Notes in Computer Science*. Springer International Publishing, 2015, pp. 56–66. 34

[TK19] TAKAHASHI H., KIM J.: 3d printed fabric: Techniques for design and 3d weaving programmable textiles. In *Proceedings of the 32nd Annual ACM Symposium on User Interface Software and Technology* (New York, NY, USA, 2019), UIST '19, Association for Computing Machinery, pp. 43–51. 27

[TKG*15] TAN D., KUMOREK M., GARCIA A. A., MOONEY A., BEKOE D.: Projectagami. In *Proceedings of the 33rd Annual ACM Conference Extended Abstracts on Human Factors in Computing Systems - CHI EA '15* (New York, New York, USA, Apr. 2015), ACM Press, pp. 1555–1560. 72

[TPK20] TAKAHASHI H., PUNPONGSANON P., KIM J.: Programmable filament: Printed filaments for multi-material 3d printing. In *Proceedings of the 33rd Annual ACM Symposium on User Interface Software and Technology* (New York, NY, USA, 2020), UIST '20, Association for Computing Machinery, pp. 1209–1221. 146

[TR15] TRÄNKLER H.-R., REINDL L. M.: *Sensortechnik: Handbuch für Praxis und Wissenschaft*. Springer-Verlag, 2015. xiii, 17

[TRBA20] TEJADA C. E., RAMAKERS R., BORING S., ASHBROOK D.: Airtouch: 3d-printed touch-sensitive objects using pneumatic sensing. In *Proceedings of the 2020 CHI Conference on Human Factors in Computing Systems* (New York, NY, USA, 2020), CHI '20, Association for Computing Machinery, pp. 1–10. 10

[TSP01] TAN H. Z., SLIVOVSKY L. A., PENTLAND A.: A sensing chair using pressure distribution sensors. *IEEE/ASME Transactions on Mechatronics 6*, 3 (Sep 2001), 261–268. 54

[USL19] UMAIR M., SAS C., LATIF M. H.: Towards affective chronometry: Exploring smart materials and actuators for real-time representations of changes in arousal. In *Proceedings of the 2019 on Designing Interactive Systems Conference* (New York, NY, USA, 2019), DIS '19, Association for Computing Machinery, pp. 1479–1494. 146

[VBKS08] VAN LAERHOVEN K., BORAZIO M., KILIAN D., SCHIELE B.: Sustained logging and discrimination of sleep postures with low-level, wrist-worn sensors. *2008 12th IEEE International Symposium on Wearable Computers* (2008), 69–76. 34

[vdE99] VON DER EMDE G.: Active electrolocation of objects in weakly electric fish. *Journal of Experimental Biology 202*, 10 (1999), 1205–1215. xiii, 20

[vdE06] VON DER EMDE G.: Non-visual environmental imaging and object detection through active electrolocation in weakly electric fish. *Journal of Comparative Physiology A 192*, 6 (Jun 2006), 601–612. 20

[Ver] VERGE T.: CES 2020: Der Rollable TV zeigt was mit OLED möglich ist. 3

[VPS18] VOIT A., PFÄHLER F., SCHNEEGASS S.: Posture sleeve: Using smart textiles for public display interactions. In *Extended Abstracts of the 2018 CHI Conference on Human Factors in Computing Systems* (New York, NY, USA, 2018), CHI EA '18, ACM, pp. LBW133:1–LBW133:6. 15, 87

[VS17a] VADGAMA N., STEIMLE J.: Flexy: Shape-customizable, single-layer, inkjet printable patterns for 1d and 2d flex sensing. In *Proceedings of the Eleventh International Conference on Tangible, Embedded, and Embodied Interaction* (New York, NY, USA, 2017), TEI '17, Association for Computing Machinery, pp. 153–162. 15

[VS17b] VOIT A., SCHNEEGASS S.: Fabricid: Using smart textiles to access wearable devices. In *Proceedings of the 16th International Conference on Mobile and Ubiquitous Multimedia* (New York, NY, USA, 2017), MUM '17, ACM, pp. 379–385. 87

[Ž08] ŽLAJPAH L.: Simulation in robotics. *Mathematics and Computers in Simulation 79*, 4 (Dec. 2008), 879–897. 72, 73

[Wan16] WANG Q.: Designing posture monitoring garments to support rehabilitation. In *Proceedings of the TEI '16: Tenth International Conference on Tangible, Embedded, and Embodied Interaction* (New York, NY, USA, 2016), TEI '16, ACM, pp. 709–712. 72, 73, 86

[WBvO*12] WRZUS C., BRANDMAIER A. M., VON OERTZEN T., MÜLLER V., WAGNER G. G., RIEDIGER M.: A new approach for assessing sleep duration and postures from ambulatory accelerometry. *PloS one 7*, 10 (Jan. 2012), e48089. 33

[WCC14] WEN-YING CHANG, CHI-CHUN CHEN, CHIN-LUNG YANG: The applications of projected capacitive array sensing in healthcare. In *2014 IEEE International Symposium on Bioelectronics and Bioinformatics (IEEE ISBB 2014)* (Apr. 2014), IEEE, pp. 1–4. 33, 99

[Wei99] WEISER M.: The computer for the 21st century, sigmobile mob. *Comput. Commun. Rev 3*, 3 (1999), 3–11. 3

[WFG*20] WU T., FUKUHARA S., GILLIAN N., SUNDARA-RAJAN K., POUPYREV I.: Zebrasense: A double-sided textile touch sensor for smart clothing. In *Proceedings of the 33rd Annual ACM Symposium on User Interface Software and Technology* (New York, NY, USA, 2020), UIST '20, Association for Computing Machinery, pp. 662–674. 26

[WGS18] WITHANA A., GROEGER D., STEIMLE J.: Tacttoo: A thin and feel-through tattoo for on-skin tactile output. In *Proceedings of the 31st Annual ACM Symposium on User Interface Software and Technology* (New York, NY, USA, 2018), UIST '18, Association for Computing Machinery, pp. 365–378. 4, 14, 26

[WHBS16] WALLBAUM T., HEUTEN W., BOLL S., SWALLOW D.: Remotable: Sharing daily activities and moods using smart furniture. In *Studies in health technology and informatics*, vol. 229. IOS Press, 2016, pp. 345–354. 4

[WJA20] WILHELM S., JAKOB D., AHRENS D.: Human presence detection by monitoring the indoor co2 concentration. In *Proceedings of the Conference on Mensch Und Computer* (New York, NY, USA, 2020), MuC '20, Association for Computing Machinery, pp. 199–203. 11

[WKBS07] WIMMER R., KRANZ M., BORING S., SCHMIDT A.: A Capacitive Sensing Toolkit for Pervasive Activity Detection and Recognition. In *IEEE International Conference on Pervasive Computing and Communications (PerCom 2007)* (2007), IEEE Computer Society. 35

[WL81] WONG M. A., LANE T.: *A kTH Nearest Neighbour Clustering Procedure*. Springer US, New York, NY, 1981, pp. 308–311. 39

[WLB*15] WEIGEL M., LU T., BAILLY G., OULASVIRTA A., MAJIDI C., STEIMLE J.: iskin: Flexible, stretchable and visually customizable on-body touch sensors for mobile computing. In *Proceedings of the 33rd Annual ACM Conference on Human Factors in Computing Systems* (New York, NY, USA, 2015), CHI '15, ACM, pp. 2991–3000. 4

[WM14] WALSH L., MCLOONE S.: Non-contact under-mattress sleep monitoring. *Journal of Ambient Intelligence and Smart Environments 6*, 4 (2014), 385–401. 34

[WNOS17] WEIGEL M., NITTALA A. S., OLWAL A., STEIMLE J.: Skinmarks: Enabling interactions on body landmarks using conformal skin electronics. In *Proceedings of the 2017 CHI Conference on Human Factors in Computing Systems* (New York, NY, USA, 2017), CHI '17, Association for Computing Machinery, pp. 3095–3105. 14

[WQC*20] WU T.-Y., QI S., CHEN J., SHANG M., GONG J., SEYED T., YANG X.-D.: Fabriccio: Touchless gestural input on interactive fabrics. In *Proceedings of the 2020 CHI Conference on Human Factors in Computing Systems* (New York, NY, USA, 2020), CHI '20, Association for Computing Machinery, pp. 1–14. 16

[WS17a] WEIGEL M., STEIMLE J.: Deformwear: Deformation input on tiny wearable devices. *Proc. ACM Interact. Mob. Wearable Ubiquitous Technol. 1*, 2 (June 2017), 28:1–28:23. 15

[WS17b] WITHANA A., STEIMLE J.: Personalized interactive surfaces with printed electronics. In *Proceedings of the 2017 ACM International Conference on Interactive Surfaces and Spaces* (New York, NY, USA, 2017), ISS '17, Association for Computing Machinery, pp. 473–476. 4, 27

[WSC*20] WESSELY M., SETHAPAKDI T., CASTILLO C., SNOWDEN J. C., HANTON O., QAMAR I. P. S., FRASER M., ROUDAUT A., MUELLER S.: Sprayable user interfaces: Prototyping large-scale interactive surfaces with sensors and displays. In *Proceedings of the 2020 CHI Conference on Human Factors in Computing Systems* (New York, NY, USA, 2020), CHI '20, Association for Computing Machinery, pp. 1–12. 13

[WSRVL17] WOLLING F., SCHOLL P. M., REINDL L. M., VAN LAERHOVEN K.: Combining capacitive coupling with conductive clothes: Towards resource-efficient wearable communication. In *Proceedings of the 2017 ACM International Symposium on Wearable Computers* (New York, NY, USA, 2017), ISWC '17, Association for Computing Machinery, pp. 146–149. 26

[WTC*16] WANG Q., TOETERS M., CHEN W., TIMMERMANS A., MARKOPOULOS P.: Zishi: A smart garment for posture monitoring. In *Proceedings of the 2016 CHI Conference Extended Abstracts on Human Factors in Computing Systems* (New York, NY, USA, 2016), CHI EA '16, ACM, pp. 3792–3795. 4, 15, 54, 72, 73

[WTC*19] WANG G., TAO Y., CAPUNAMAN O. B., YANG H., YAO L.: A-line: 4d printing morphing linear composite structures. In *Proceedings of the 2019 CHI Conference on Human Factors in Computing Systems* (New York, NY, USA, 2019), CHI '19, Association for Computing Machinery, pp. 1–12. 146

[WTLT16] WEI Y., TORAH R., LI Y., TUDOR J.: Dispenser printed capacitive proximity sensor on fabric for applications in the creative industries. *Sensors and Actuators A: Physical 247* (2016), 239 – 246. 28

[WTZ*20] WU T.-Y., TAN L., ZHANG Y., SEYED T., YANG X.-D.: Capacitivo: Contact-based object recognition on interactive fabrics using capacitive sensing. In *Proceedings of the 33rd Annual ACM Symposium on User Interface Software and Technology* (New York, NY, USA, 2020), UIST '20, Association for Computing Machinery, pp. 649–661. 27

[XHA*13] XU W., HUANG M. C., AMINI N., HE L., SARRAFZADEH M.: ecushion: A textile pressure sensor array design and calibration for sitting posture analysis. *IEEE Sensors Journal 13*, 10 (Oct 2013), 3926–3934. 50

[XLW*16] XU X., LIN F., WANG A., HU Y., HUANG M. C., XU W.: Body-earth mover's distance: A matching-based approach for sleep posture recognition. *IEEE Transactions on Biomedical Circuits and Systems 10*, 5 (Oct 2016), 1023–1035. 54

[XMH20] XIAO R., MAYER S., HARRISON C.: Vibrocomm: Using commodity gyroscopes for vibroacoustic data reception. In *22nd International Conference on Human-Computer Interaction with Mobile Devices and Services* (New York, NY, USA, 2020), MobileHCI '20, Association for Computing Machinery. 10

[YAB19] YANG X., AURISICCHIO M., BAXTER W.: Understanding affective experiences with conversational agents. In *Proceedings of the 2019 CHI Conference on Human Factors in Computing Systems* (New York, NY, USA, 2019), CHI '19, Association for Computing Machinery, pp. 1–12. 146

[Yak19] YAKAR P.: Breathing frequency and movement detection with e-textile capacitive sensing, 2019. 98

[YKL*13] YEO W.-H., KIM Y.-S., LEE J., AMEEN A., SHI L., LI M., WANG S., MA R., JIN S. H., KANG Z., HUANG Y., ROGERS J. A.: Multifunctional epidermal electronics printed directly onto the skin. *Advanced Materials 25*, 20 (2013), 2773–2778. 14

[YOF*11a] YOUSEFI R., OSTADABBAS S., FAEZIPOUR M., FARSHBAF M., NOURANI M., TAMIL L., POMPEO M.: Bed posture classification for pressure ulcer prevention. In *2011 Annual International Conference of the IEEE Engineering in Medicine and Biology Society* (2011), pp. 7175–7178. xiii, 11, 34

[YOF*11b] YOUSEFI R., OSTADABBAS S., FAEZIPOUR M., NOURANI M., NG V., TAMIL L., BOWLING A., BEHAN D., POMPEO M.: A smart bed platform for monitoring ulcer prevention. In *2011 4th International Conference on Biomedical Engineering and Informatics (BMEI)* (2011), vol. 3, pp. 1362–1366. xiii, 11

[YRN*12] YU M., RHUMA A., NAQVI S. M., WANG L., CHAMBERS J.: A posture recognition-based fall detection system for monitoring an elderly person in a smart home environment. *IEEE Transactions on Information Technology in Biomedicine 16*, 6 (Nov 2012), 1274–1286. 33

[ZA05] ZHANG R., AKTAN E.: Design considerations for sensing systems to ensure data quality. In *Sensing Issues in Civil Structural Health Monitoring*. Springer, 2005, pp. 281–290. xiii, 17, 18

[ZBF*17] ZHOU B., BAHLE G., FÜRG L., SINGH M. S., CRUZ H. Z., LUKOWICZ P.: Trainwear: A real-time assisted training feedback system with fabric wearable sensors. In *2017 IEEE International Conference on Pervasive Computing and Communications Workshops (PerCom Workshops)* (Kona, HI, USA, March 2017), IEEE, pp. 85–87. 87

[ZCG*20] ZHANG H., CHEN Z., GUO S., LIN J., SHI Y., LIU X., MA Y.: Sensock: 3d foot reconstruction with flexible sensors. In *Proceedings of the 2020 CHI Conference on Human Factors in Computing Systems* (New York, NY, USA, 2020), CHI '20, Association for Computing Machinery, pp. 1–13. 15

[ZL20] ZHOU B., LUKOWICZ P.: Snacap: Snacking behavior monitoring with smart fabric mechanomyography on the temporalis. In *Proceedings of the 2020 International Symposium on Wearable Computers* (New York, NY, USA, 2020), ISWC '20, Association for Computing Machinery, pp. 96–100. 16

[ZLH17] ZHANG Y., LAPUT G., HARRISON C.: Electrick: Low-cost touch sensing using electric field tomography. In *Proceedings of the 2017 CHI Conference on Human Factors in Computing Systems* (New York, NY, USA, 2017), CHI '17, ACM, pp. 1–14. 13

[ZSC*16] ZHOU B., SUNDHOLM M., CHENG J., CRUZ H., LUKOWICZ P.: Never skip leg day: A novel wearable approach to monitoring gym leg exercises. In *2016 IEEE International Conference on Pervasive Computing and Communications (PerCom)* (March 2016), pp. 1–9. 54

[ZSP*95a] ZIMMERMAN T. G., SMITH J. R., PARADISO J. A., ALLPORT D., GERSHENFELD N.: Applying electric field sensing to human-computer interfaces. In *Proceedings of the SIGCHI Conference on Human Factors in Computing Systems* (New York, NY, USA, 1995), CHI '95, ACM Press/Addison-Wesley Publishing Co., pp. 280–287. 12, 21

[ZSP*95b] ZIMMERMAN T. G., SMITH J. R., PARADISO J. A., ALLPORT D., GERSHENFELD N.: Applying electric field sensing to human-computer interfaces. *Proceedings of the SIGCHI conference on Human factors in computing systems - CHI '95*, May (1995), 280–287. 22

[ZYH*18] ZHANG Y., YANG C. J., HUDSON S. E., HARRISON C., SAMPLE A.: Wall++: Room-scale interactive and context-aware sensing. In *Proceedings of the 2018 CHI Conference on Human Factors in Computing Systems* (New York, NY, USA, 2018), CHI '18, Association for Computing Machinery, pp. 1–15. 4, 12, 28, 99